The University Of Sheffield.

New Chemical Tools for the Study of Phosphohistidine

Mehul V. Makwana

April 2019

Professor R.F.W. Jackson

Doctor R. Muimo

Preface

Declaration

This dissertation records work carried out in the department of Chemistry and the department of Infection, Immunity and Cardiovascular Disease, at The University of Sheffield between May 2015 and April 2019 and is original except where acknowledgement by reference is made.

No portion of this work is being, nor has been, submitted for a degree, diploma or other qualification at any other university.

Acknowledgements

My PhD has been one of the most fun and interesting experiences. I have thoroughly enjoyed the challenges; for if things were easy then they would be boring. During times of frustration there was not a moment I thought of giving up. These 4 years have allowed me the freedom to grow as a person and learn a lot about myself. As a scientist in training, I have learned open minded perseverance and the right attitude are just as important if not more important than natural talent. These newly gained understandings and knowledge is not self-learned but was taught through example by people. Therefore, it is only right to give thanks to those who have made this journey seem an individual's effort when it was of many.

Firstly, thank you to my Mother for always supporting me throughout my life and letting me do what I want without judgement, unless it was something foolish.

A special thank you to my principal supervisor Professor Jackson. I am certain my confidence, improvement as a scientist and person came from you giving me the freedom to think open mindedly. Thank you also for taking moments out of your time in teaching me the importance of good communication and using unpredictable moments as a learning tool. It has been a privilege to be your final PhD student. I hope I can make you proud in the future.

A special thanks to my second supervisor Doctor Muimo, it is from you I learned to challenge authority. I have enjoyed discussing science and ideas for this project with you and hope to continue working with you in the future; for you seem to never be in a bad mood.

Thank you to Professor Coldham and his group for inviting me to his house for Christmas dinner, and allowing me to participate in his group meetings. Thank you to Professor Chen and her group for the yearly Christmas dinner invitations. Thank you to Mark Thompson and members of the Grasby group for their constant help. Thank you to Sandra for NMR assistance

and thank you to Bez for teaching me biological techniques. Thank you to previous members of the Jackson group. Thank you to my sister and Adrienne for getting me into back into education. Thank you, John, for playing tennis with me. Finally thank you Mariangela for simply existing.

Abstract

A τ-phosphohistidine pyrazole analogue functionalized with dibenzyl and Fmoc protecting groups was synthesized.

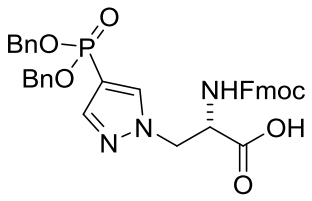

Dibenzyl Fmoc group protected pyrazolylalanine carboxylic acid τ-pHis analogue.

Based on density functional theory calculations a novel 3,4-disubstituted pyridine π-pHis analogue was also synthesized. Polyclonal antibodies were generated against both pyrazolylethylamine and 3,4-disubstituted pyridine analogues. To determine the selectivity of the antibodies two isomer-specific assays in the form of BSA τ-phosphohistidine and π-phosphohistidine conjugates were synthesized and characterized quantitively by ^{31}P NMR spectroscopy.

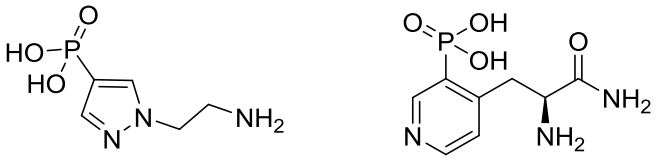

Pyrazolylethylamine τ-phosphohistidine analogue (left) and 3,4-disubstituted pyridine (right) π-phosphohistidine analogue used in antibody generation.

Antibodies generated to the pyrazole τ-phosphohistidine analogue were found to be highly selective for τ-phosphohistidine and antibodies generated to the 3,4-disubstituted pyridine π-phosphohistidine analogue were found to be highly selective for π-phosphohistidine. Both

τ- and π-phosphohistidine isomer selective polyclonal antibodies showed greater selectivity and sensitivity than the commercial pHis monoclonal antibodies in a competitive ELISA and on Western blots. The polyclonal antibodies were also used in immunoprecipitation experiments, highlighting their potential in mass spectrometry analysis.

Contents

Publications

Makwana MV, Muimo R, Jackson RFW. Advances in development of new tools for the study of phosphohistidine. Lab Invest 2017;98:291.

Abbreviations

µW: Microwave

^{1}H NMR: Proton nuclear magnetic resonance

^{31}P NMR: ^{31}Phosphorus nuclear magnetic resonance

ACLY: ATP citrate lysase

aq.: Aqueous

Arg: Arginine

Asp: Aspartic acid

ATP: Adenosine triphosphate

Bn: Benzyl

Boc: Tert-butyloxycarbonyl

BOP: Benzotriazol-1-yloxytris(dimethylamino)phosphonium hexafluorophosphate

BSA: Bovine serum albumin

CAN: Ceric ammonium nitrate

CID: Collision induced-dissociation

Cys: Cysteine

DBU: 1,8-Diazabicyclo[5.4.0]undec-7-ene

DCE: Dichloroethane

DEAD: Diethyl azodicarboxylate

DFT: Density functional theory

DMF: Dimethyl formamide

dppe: 1,2-Bis(diphenylphosphino)ethane

dppf: 1,1'-Bis(diphenylphosphino)ferrocene

DTT: Dithiothreitol

e.g.: For example

EDTA: Ethylenediaminetetraacetic acid

ELISA: Enzyme linked immunosorbent assay

Equiv.: Equivalents

ESP: Electrostatic surface potential

FBS: Fetal bovine serum

Fmoc: Fluorenylmethyloxycarbonyl

G: Glutaraldehyde

Glu Glutamic acid

Gly: Glycine

h.: Hour

HBE: Human bronchial epithelial

HCD: High energy collision dissociation

HeLa: Henrietta Lacks

HHKs: Histone H4 histidine

His: Histidine

HPLC: High performance liquid chromatography

HRP: Horseradish peroxidase

KLH: Keyhole limpet hemocyanin

LDS: Lithium dodecyl sulfate

Lys: Lysine

M: Molar

min: Minute

mM: Millimolar

MS: Mass spectrometry

NDPK: nucleoside diphosphate kinase

NMR: Nuclear magnetic resonance

p_2His: di phosphohistidine

PBS: Phosphate buffered saline

PEG: Polyethylene glycol

pHis: Phosphohistidine

pLys: Phospholysine

ppm: Parts per million

pSer: Phosphoserine

pThr: Phosphothreonine

PTM: Post translational modification

pTyr: Phosphotyrosine

RCF: Relative centrifugal force

RIPA: Radioimmunoprecipitation assay

room temp.: Room temperature

SDS: Sodium dodecyl sulfate

SDS-PAGE: Sodium dodecyl sulfate polyacrylamide gel electrophoresis

Ser: Serine

TFA: Trifluoroacetic acid

THF: Tetrahydrofuran

Thr: Threonine

TLC: Thin layer chromatography

TMB: 3,3',5,5'-Tetramethylbenzidine

TMS: Trimethylsilyl

TMSBr: Bromotrimethylsilane

TMSCl: Trimethylsilylchlroide

Tris: Tris(hydroxymethyl)aminomethane

Tris-HCl: tris(hydroxymethyl)aminomethane hydrochloride

Trt: Trityl

Tyr: Tyrosine

WB: Western blot

Xantphos: 4,5-Bis(diphenylphosphino)-9,9-dimethylxanthene

π-pHis: Pros-phosphohistidine

τ-pHis: Tele-phosphohistidine

1: Introduction

1.1: Histidine phosphorylation

Protein phosphorylation is one of the most commonly studied post-translational modifications (PTMs). In general, the phosphorylation of any amino-acid residue results in a change in charge and thus in the protein surface potential. For example, as phosphoryl groups exist mostly as a dianion under physiological conditions,[2] phosphorylation of the amino acids serine (Ser), threonine (Thr) and tyrosine (Tyr), results in a change in charge from zero to negative two. Hence, it should be of no surprise that phosphorylation affects protein conformation, protein–protein interactions, biochemical pathways and its disregulation is connected to many disease states.[3]

There are nine known phosphorylated amino-acid residues Ser, Thr, Tyr, histidine (His), lysine (Lys), arginine (Arg), aspartic acid (Asp), glutamic acid (Glu) and cysteine (Cys).[3] The hydroxy O-linked phospho-residues, phosphoserine (pSer), phosphothreonine (pThr) and phosphotyrosine (pTyr) have been extensively studied, most probably due to their relative stability in acidic conditions routinely used for analysis. By contrast, the relatively acid labile N-linked phosphoramidate, carboxy O-linked acyl phosphate and S-linked phosphorothiolate amino-acid residues (His, Lys, Arg; Asp, Glu; Cys, respectively) have been somewhat overlooked and less frequently reported. Among the phosphoramidates, phosphohistidine (pHis) is very interesting because of its unique chemical properties: first, unlike other phosphorylated residues there are two isomers of pHis; τ (tele)- and π (pros)-pHis, both of which are found in nature (Figure 1).[4,5] The pHis isomer of a protein can be identified using ^{31}P NMR and/or by chromatographic analysis of the base hydrolysate (see section 1.3).

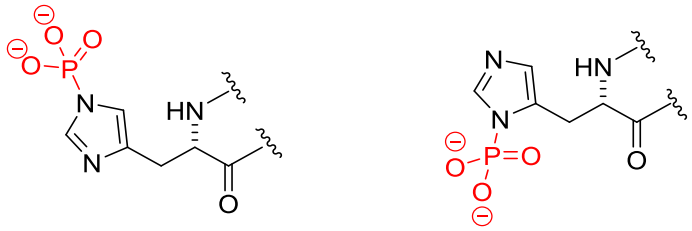

Figure 1: The two isomers of pHis, τ (tele)- and π (pros)-pHis residues found in nature existing as dianions under physiological conditions. The τ isomer is also known ε/3-pHis, and the π isomer as δ/1-pHis.

The τ- and π-pHis isomers differ in both reactivity and stability (see section 1.3). Whether these differences in reactivity and stability are mirrored in proteins is not clear at present. Conventional wisdom is that pHis serves as a high energy intermediate in the transfer of the phosphoryl group to other amino-acid residues, and molecules. Therefore, not only does pHis change the surface potential of proteins it also possesses transient transferable chemical information that can be potentially tuned depending on the isomer and environment.

His phosphorylation has been found in a number of organisms including bacteria,[6] fungi[7] and plants[8] and its major role is in cell signaling either *via* two component or multicomponent phosphorelay systems. Cell signaling via a two component phosphorelay has also been found in yeast,[7] but such processes have not yet been observed in higher eukaryotes (e.g. mammals, birds and fish).[9] The general role of pHis in prokaryotic and lower eukaryotic cells is shown in Figure 2.

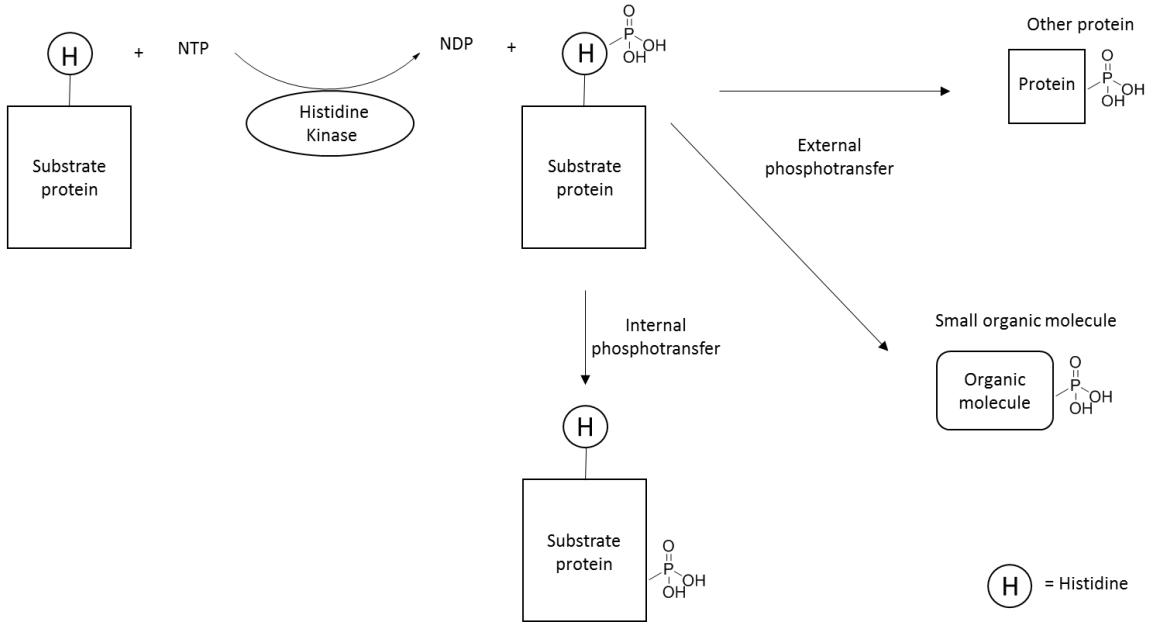

Figure 2: A simplified adopted schematic[10] showing the general role of pHis known thus far.[1]

There are nine non-metastatic (Nme) genes; Nme1-4 have nucleoside diphosphate kinase (NDPK) activity[11-13], of which NDPK-A(Nme1)[14-18] and NDPK-B(Nme2)[19-24] have been characterized as mammalian His kinases. Other mammalian His kinases exist. Evidence for histone H4 His kinases (HHKs) activity has been found in regenerating rat liver,[25-28] foetal rat and human liver,[28] human hepatocarcinoma tissue,[28] pancreatic β cells,[29,30] thymus[31] and Walker-256 carcinosarcomas,[25,32] but have not been fully characterized or purified. Interestingly, HHKs from regenerating rat liver[26] and Walker-256-carcinosarcomas[32] each phosphorylated histone H4 leading to a τ-pHis residue. In a later study, ^{31}P NMR spectroscopy suggested the presence of τ-pHis on His18 of phosphorylated histone H4 when Walker-256-carcinosarcomas were used as the kinase source.[33] However, ^{31}P NMR studies suggested the presence of π-pHis in phosphorylated histone H4 when using regenerating rat liver as the kinase source.[33] In this particular case, it is not clear which isomer of pHis is formed and on

which His residue of histone H4. Mammalian pHis phosphatases which have been characterized include: protein pHis phosphatase 1 (PHPT1);[22,34-39] Lys/His phosphatase (LHPPase);[40,41] Ser/Thr protein phosphatases (PP1/2 A/2C);[42,43] T-cell ubiquitin ligand-2 (TULA-2);[44,45] and the recently reported phosphoglycerate mutase-5 (PGAM5).[46] In each case, the relevant/corresponding gene is indicated in parenthesis. In addition, pHis phosphatase activity has been reported in rat tissue extracts but these have not been fully characterized.[47-50]

Not only is His phosphorylation predicted to be prevalent in eukaryotic proteins,[51] it has also been associated with important mammalian cellular processes (Table 1). However, the functions of many of these pHis proteins, and the pHis isomer involved, as well as associated kinases and phosphatases remain unknown.

Table 1: Known mammalian pHis proteins and the involvement of these proteins in cellular processes. In each case the relevant/corresponding gene is indicated in the parenthesis

PHis Mammalian Protein	Cellular Process
Heteromeric G protein (GNB1)[20,52,53]	G protein signaling
KCa3.1 potassium channel (KCNN4)[23,54]	Ion conductance
ATP-citrate lyase (ACLY) [14]	Cell metabolism
Histone H4 (HIST1H4A)[26,27,33]	Chromatin biology
Transient receptor potential vanilloid-5 (TRPV5) [22]	Urinary Ca^{2+} excretion regulation
Phosphoglycerate mutase 1 (PGAM1) [55-58]	Glycolysis
P-selectin (SELP)[59]	Blood platelet activation
Annexin A1 (ANXA1)[60]	Ca^{2+} dependent phospholipid-binding protein
Thymidylate synthase (TYMS)[61]	N-methylenetetrahydrofolate assisted C(5)-methylation of dUMP
Glucose-6-phosphatase (G6PC3)[62,63]	Glucose homeostasis
Nicotinamide phosphotransferase (NAMTP) [64]	Reforming nicotinamide adenine dinucleotide (NAD+) from nicotinamide
Prostatic acid phosphatase (ACPP)[65,66]	Prostate cell growth regulation

1.2: Chemistry of phosphohistidine

The chemistry of pHis was first studied by Hultquist *et al.*[67,68] and has been covered extensively in a review by Attwood *et al*.[69] In summary, pHis residues contain a weak phosphoramidate bond with the phosphoryl group being most susceptible to hydrolysis when the imidazole nitrogen is protonated (Scheme 1).[67,68] Hence, the rate of hydrolysis of pHis is dependent on pH. The respective pK_a values of the imidazole nitrogen suggests hydrolysis can occur even under physiological conditions (pK_a 7.3 for protonated π-pHis at 46 °C[68] and pK_a 6.4 for proteonated τ-pHis at 25 °C[67]).

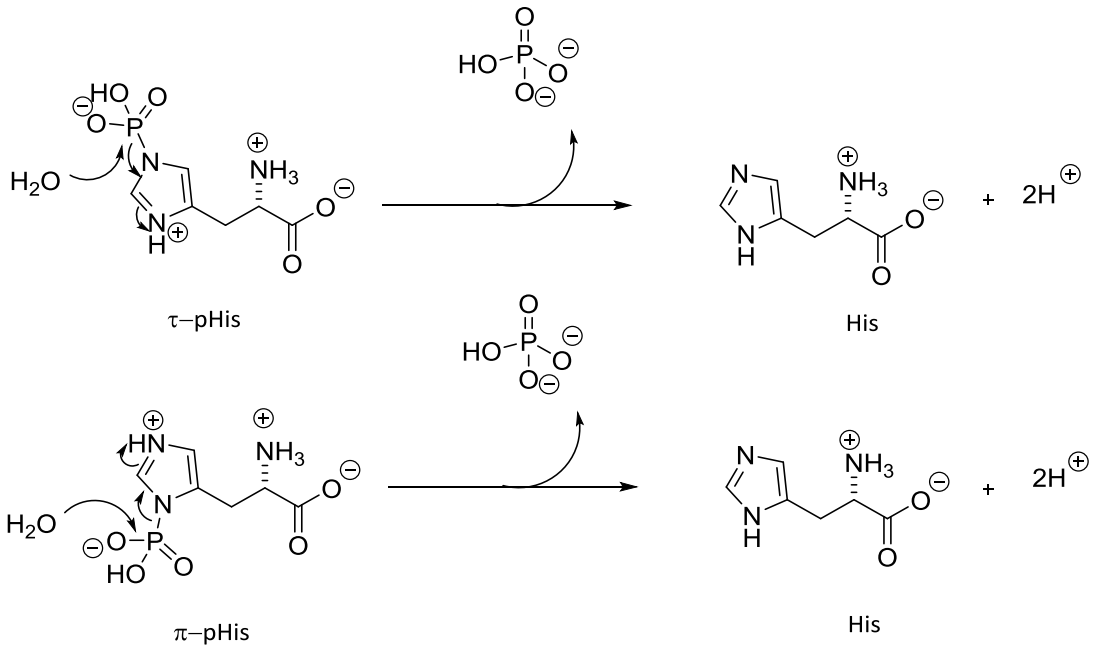

Scheme 1: Hydrolysis of the protonated τ- and π-pHis to His and phosphate under physiological conditions.

It is important to note that pHis pK_a values have been found to vary depending on salts in solution. Gassner *et al.* found π- and τ-pHis to have a pK_as of 7.74 and 6.88, respectively, from the titration of the reaction mixture of His with potassium phosphoramidate adjusted to pH 7.2 at 25 °C.[70]

Hultquist studied the decomposition of τ-pHis over the pH range 2–5, by following the decrease in absorbance of τ-pHis, and the hydrolysis of π-pHis over the pH range 2–11 by following the increase in absorbance of His, each at 46 °C (Figure 3).[68] Both isomers decompose more rapidly at low pH and, at all pHs measured, π-pHis was less stable than τ-pHis. Unlike τ-pHis, the rate constant for dephosphorylation of π-pHis decreases smoothly between pH 2 and 4, and remains approximately constant over the pH range 4–6; above pH 6 (~ pK_a of imidazole nitrogen of π-pHis) to pH 9 the rate constant decreases slowly again before a further decrease above pH 9, which is approximately the pK_a of the amine (~ 9.6).[67-69] Nonetheless, the data clearly show both π-His (pH 9–11, 46 °C)[68] and τ-pHis (pH 8–10, 80.5 °C)[67] are stable in solution for extended periods provided the right conditions are used. Hence, application of pHis standards in experiments such as enzyme linked immunosorbent assay (ELISA), chromatography and dot blots with protein conjugates, or any other test where a pHis standard is needed, should be possible.

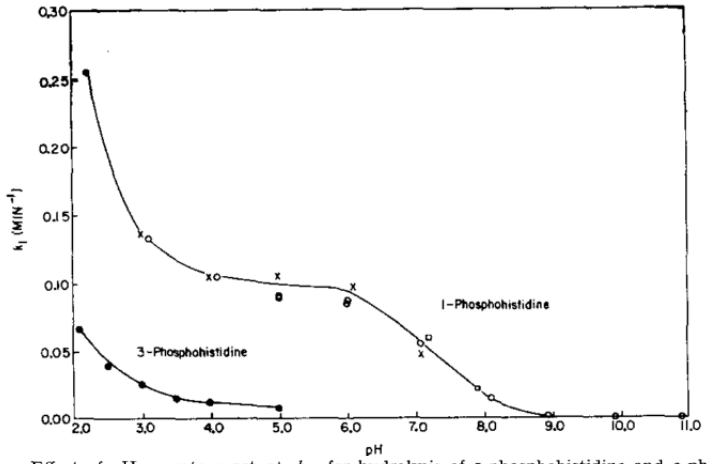

Fig. 7. Effect of pH on rate constant, k_1, for hydrolysis of 1-phosphohistidine and 3-phosphohistidine at 46°. ○—○, rates of hydrolysis of 1-phosphohistidine in 0.05 M phosphate–0.05 M citrate–0.05 M borate buffers as determined from appearance of free histidine; ×—×, in 0.05 M citrate–0.05 M phosphate buffers as determined from decrease in absorbance at wavelengths ranging from 228 to 234 mμ; □—□, in 0.05 M borate as determined from decrease in absorbance at 228 mμ; ●—●, 3-phosphohistidine in 0.05 M citrate–0.05 M phosphate buffers as determined by decrease in absorbance at 233 mμ.

Figure 3: τ- and π-pHis rate constant versus pH. Fig. 7. was taken from Hultquist's 1966 paper "The preparation and characterization of phosphorylated derivatives of histidine" Copyright © license approved by Elsevier publishing group (see appendix).[68]

Within a small neutral peptide (Gly-pHis-Gly) Lecroisey *et al.* found the π-pHis residue to be less stable than the τ-pHis residue in the same position, consistent with Hultquist's findings.[71] Whether the relative stability of π- and τ-pHis residues in this case could be explained by pKa alone is questionable (in the absence of the primary amine) because it is not known to what extent the peptide backbone affects pHis stability. Furthermore, a denatured pHis protein where tertiary interactions are absent may have a hydrolysis half-life that differs from that in the tertiary structure.[71,72] For example, the enzyme NDPK has a His residue within its active site, which interacts with a nearby Glu residue assisting in the isomer selective phosphorylation to form a π-pHis residue, but this interaction is absent in the denatured state.[73,74] Hence, procedures where denaturants are used such as Western blots must take this into account. Another important factor to consider in any procedure involving pHis is the type/concentration of salts present in solution. For example, the calcium salt of π-pHis was found to be very unstable relative to the sodium salt of π-pHis.[68] Thus, each protein phosphorylated on a His residue will likely have a unique half-life under a defined set of conditions and as such, meaningful half-life comparisons can only be made between pHis proteins using normalized conditions.

An important question to be addressed is: does π-pHis isomerize to τ-pHis or vice versa under any conditions, because this will have implications for methods used to study pHis? A good place to start to address the question of isomerization is the work by Hultquist *et al.* who reported the synthesis, stability and transferable nature of the phosphoryl group on each pHis isomer.[67,68]

Reaction of His with potassium phosphoramidate **1** in H_2O gives both isomers of pHis, as well as the di phosphorylated (p_2His) residue (Scheme 2). The pHis isomers were separated using

anion exchange chromatography as either lithium, potassium[67] or sodium salts[68] after desalting. By following the progress of the reaction by electrophoresis, it was established that π-pHis formed rapidly before gradually decomposing, accompanied by the formation of τ-pHis and p_2His. Similar, observations were made in ^{1}H NMR studies by Gassner *et al.* where phosphorylation with potassium phosphoramidate **1** (pH 7.2, 25 °C) resulted in initial rapid formation of π-pHis (maximum at ~ 10 min), then p_2His (maximum at ~ 60 min), both of which subsequently decomposed, accompanied by a gradual increase in τ-pHis.[70] The observation that π-pHis forms more rapidly initially is consistent with the major tautomer (τ protonated nitrogen) of His present in H_2O (Scheme 2).[75]

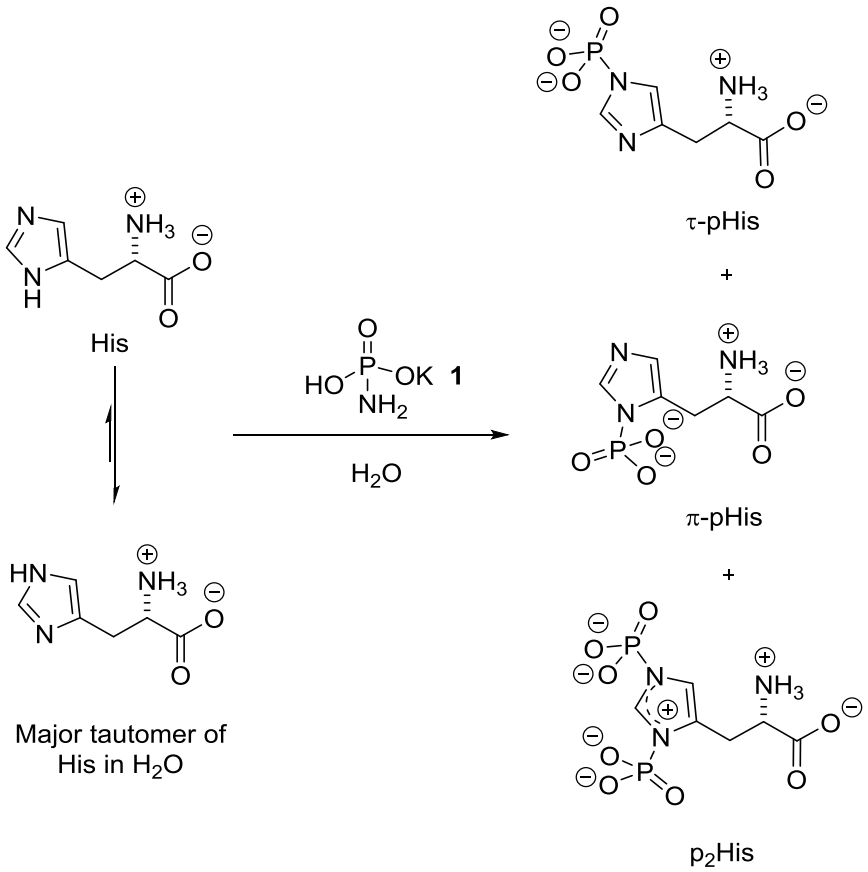

Scheme 2: Synthesis of τ-pHis, π-pHis and p_2His by reaction of His with potassium phosphoramidate **1** in H_2O.

Hultquist carried out a series of experiments to understand phosphoryl transfer in pHis (Scheme 3). Phosphoryl transfer reactions (1–8) suggest that the phosphoryl group of pHis can be donated to the imidazole nitrogen of His or α-N-acetyl-His. Comparison of (1) and (5), with (7) and (8) suggests that π-pHis has a more labile phosphorus nitrogen (P-N) bond compared with τ-pHis. Reactions (2) and (4) also show there is a preferential transfer of the π-phosphoryl group of p_2His to form τ-pHis.

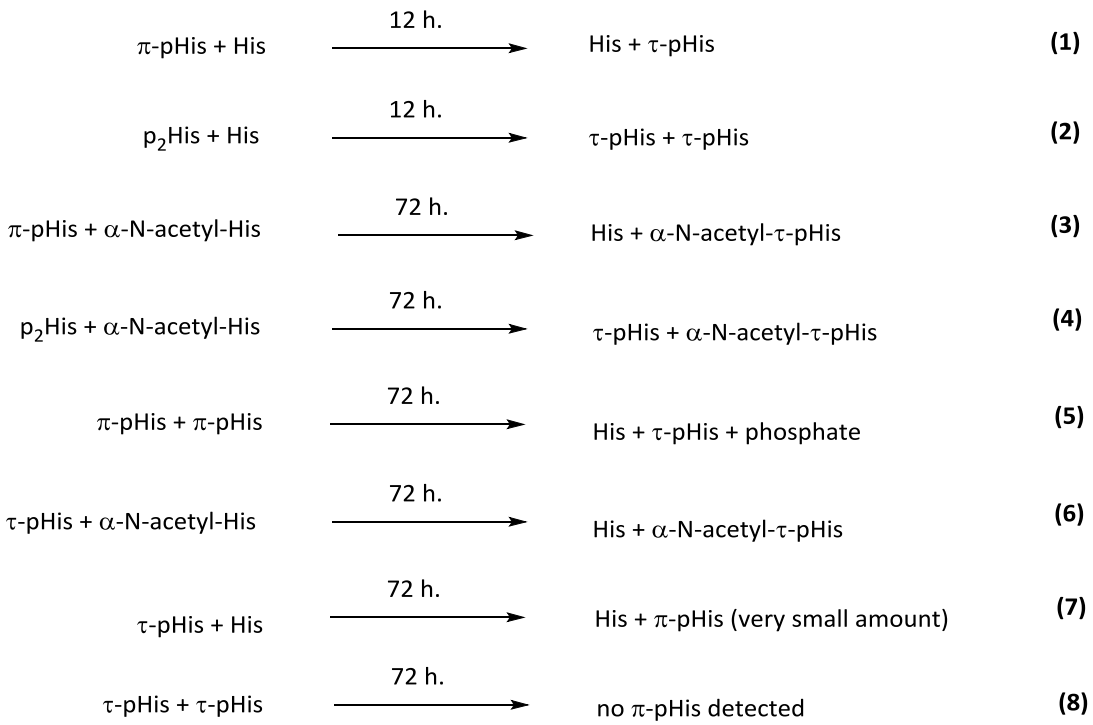

Scheme 3: Phosphoryl transfer reactions of τ-pHis, π-pHis and p_2His as donors and His and a-N-acetyl-His as acceptors in 0.1 M Tris, pH 8.5 at 4 ˚C.[67]

Importantly, reactions (1), (5) and (7) show that one isomer of pHis can undergo conversion to the other isomer, but only via a bimolecular reaction with His. Although this can be viewed as isomerization, it is in fact a bimolecular process and strictly not a unimolecular isomerization as has been inferred to occur under certain conditions, both for pHis and pHis

residues (Scheme 4).[76-80] Indeed, Hultquist himself avoided the term isomerization and defined reactions (1), (5) and (7) as conversion of one isomer to the other.[68] It is unlikely unimolecular isomerization is occurring under acidic conditions because the hydrolysis of π-pHis (1 M HCl, 49 °C)[68] and τ-pHis (0.5 M HCl, 48.5 °C)[67] followed first-order rate kinetics.

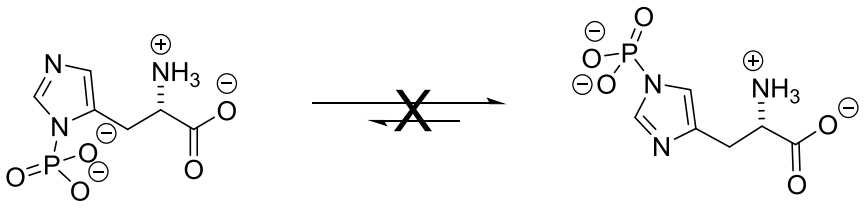

Scheme 4: Inferred unimolecular isomerization of π-pHis to τ-pHis and vice versa that does not occur.

Concerning the question of isomerization of pHis residues in proteins, Lecroisey *et al*. found using ^{31}P NMR spectroscopy only the π-pHis residue in autophosphorylated Dictyostelium NDPK (25 °C, 50 mM Tris-HCl, 10% D_2O, pH 8.1) and in the denatured state after treatment with 9 M urea (*vide supra*).[71] Similarly, Williams *et al.* observed only τ-pHis by ^{31}P NMR spectroscopy in ATP citrate lyase (ACLY) from rat liver (50 mM Tris-HCl, 14% D_2O, pH 8.4) both for the functioning enzyme and when denatured with 1% SDS and 1% β-mercaptoethanol.[81] Wagner and Vu, found that upon base hydrolysis (3 M KOH, 120 °C, 100 min) of [γ^{32}P] adenosine triphosphate (ATP) phosphorylated rat liver NDPK, only π-pHis was detected in the hydrolysate by thin layer chromatography (TLC) analysis against the reference compound.[14] In the same study, only τ-pHis was detected by TLC from the base hydrolysate of (^{32}P) phosphorylated rat adrenal ACLY.[14] These results show that in these specific examples, isomerization of the pHis residue does not occur.

By contrast in an early study of phosphorylated human erythrocytic NDPK by Walinder, phospholysine (pLys) and both isomers of pHis were found in the base hydrolysate after chromatographic separation of the phosphoamino acids.[82] However, ^{31}P NMR spectroscopy,[71] X-ray crystallography (showing only the π imidazole nitrogen is available for phosphorylation),[73,74] and base hydrolysate data,[14] have shown that NDPK is autophosphorylated by ATP on a specific His residue to form the π-pHis residue exclusively. Similarly, ACLY has been found to be phosphorylated by NDPK or ATP to form τ-pHis only, both by ^{31}P NMR spectroscopy and in the base hydrolysate.[14,83] So why the discrepancy with the results from Walinder? It may be that the phosphoryl group of one isomer of pHis was transferred either directly to another His residue giving the other pHis isomer (Scheme 3, reaction (1) and (7)), or to a Lys residue (nitrogen lone pairs are known to accept the phosphoryl group from phosphoramidate containing compounds),[84,85] which then subsequently phosphorylated His under the particular experimental and analysis conditions used.

Although, in this introduction, the focus has been on possible pHis isomerization on ACLY and NDPK, there are other examples of pHis-containing proteins, which have been characterized by ^{31}P NMR spectroscopy, or X-ray crystallography which show no evidence of isomerization (E.g. histone H4,[33] succinyl-CoA synthase[72] and phosphocarrier protein HPr[70]).

1.3: Detection of phosphohistidine

There are many ways to detect pHis and extensive reviews on the subject exist.[76,79,86] However, in the context of this work, some of the most important methods will be discussed briefly. Detection of pHis residues using antibodies will be discussed in section 1.5. ^{31}P NMR spectroscopy is a useful spectroscopic method to detect pHis residues but requires large amounts of purified sample. Nonetheless, it is one of the methods that allows pHis isomer distinction against pHis standard chemical shifts. In some cases, the local peptide sequence of the pHis residue is required to generate reference chemical shifts of π- and τ-pHis residues within a sequence and this is not always known. For example, Lecroisey *et al*. found that the ^{31}P NMR chemical shifts of phosphorylated NDPK did not match any known τ-pHis or π-pHis ^{31}P NMR chemical shifts.[71] The chemical shifts of the pHis residue also differed in the native (−2.72 ppm) and denatured state (−4.20 ppm) (see section 1.2 for conditions).[71] However, π-His phosphorylated peptide (Glu-pHis-Gly, known phosphorylated sequence of NDPK) matched the denatured state chemical shift, which was used as a reference.[71] Another consideration when characterizing pHis by ^{31}P NMR is pH because there are three states the phosphoryl group can exist in; as the phosphonic acid, monoanion and dianion, which will affect chemical shifts.[70] Usually basic conditions (pH >8), which stabilize pHis are used, where the phosphoryl group exists as a dianion.[2]

The approach used by Wagner and Vu, for detecting either π- or τ-pHis from the base hydrolysate of pHis proteins by TLC against pHis standards seems encouraging because of the method simplicity.[14] However, Wagner and Vu used radioactive [γ^{32}P]ATP to phosphorylate the protein samples and protein base hydrolysate was analyzed by TLC and autoradiography. On the other hand, detection of τ-pHis in the base hydrolysate of enzymatically

phosphorylated histone H4 using high performance liquid chromatography (HPLC) against pHis standards has been reported.[87] The method of base hydrolysis, although useful, cannot give any direct information about the site of His phosphorylation or the presence of multiple pHis residues in the protein.

Mass spectrometry (MS) has been used in the detection of phosphorylated amino acid residues, including phosphorylated His residues.[76] MS generally uses acidic eluents in chromatographic separation of enzymatically digested peptides before analysis, conditions, which are not suitable for pHis-containing proteins; changing the eluent to basic or neutral solution decreases the resolution and sensitivity.[88] However, mildly acidic conditions (0.5% aqueous acetic acid) have proved successful so long as the contact time is kept to a minimum.[89] Aqueous formic acid (0.1%) has also been used as an eluent.[90,91]

One of the challenges with MS analysis is how to eliminate false positives when analyzing pHis data. For example, Gonzalez-Sanchez *et al*. found phosphorylation of the peptide DAPAHDAKD with potassium phosphoramidate **1** resulted in exclusive His phosphorylation, which was confirmed by collision-induced dissociation (CID) tandem MS.[76] The same peptide analyzed by nano-ultraperformance liquid chromatography nano-electrospray ionization MS, eluted with 50 mM ammonium acetate and then loaded under acid conditions (pH 2) gave two distinct peaks. One peak was identified as the His phosphorylated peptide (DAPAp**H**DAKD) and the other as the phosphorylated aspartate peptide (DAPAHp**D**AKD).[76] In later work Gonzalez-Sanchez *et al*. found using low energy CID in a Paul-type ion trap peptide, FVIAFILp**H**LVK could form a dimer in the gaseous phase and transfer one of the pHis phosphoryl groups to lysine residue to give doubly phosphorylated peptide FVIAFILp**H**LVp**K**.[92] This also raises the question what other amino acid residues can the pHis phosphoryl group

be transferred to in MS experiments? However, what is clear is that false positives could be an issue in pHis proteomic MS analysis using certain techniques.

Nevertheless, Oslund *et al*. observed a characteristic TRIPLET fingerprint decomposition pattern of pHis residues (neutral losses of 98, 80 and 116 Da) in CID MS analysis of various pHis-containing peptides, and claimed this TRIPLET fingerprint decomposition was a specific marker for pHis which could differentiate it from other phosphorylated residues.[91] On the contrary, Hardman *et al.* found only a ~8 % (ptmRS >75 %) of His phosphorylated tryptic peptides from Henrietta Lacks (Hela) cells to have the TRIPLET loss which was not exclusive for pHis but also observed with pSer and pThr containing peptides.[90] In a later study Potel *et al*. showed that the protonated pHis immonium cation mass ion could be used to differentiate pHis from other phosphorylated residues.[93,94]

Many of the pHis detection methods described so far require an effective enrichment and purification strategy, as well as a selective phosphorylation method. This can be quite tricky if the protein of interest requires a pHis kinase for phosphorylation because the pHis kinase may be unknown or will also have to be isolated and phosphorylated. Lapek *et al*. has developed an MS method for the direct analysis of a whole cell lysate, which helps preserve acid labile modifications by using a buffer mixture including ammonium bicarbonate between pH 2.5 and 5 (adjusted with formic acid) in the chromatography before MS analysis. Twenty pHis phosphopeptides were identified but the authors argue that the buffer system limits the analysis to peptide sequences possessing an intrinsic positive charge.[88] Traditional methods avoid this by using more acidic conditions to positively charge the peptide, but this is undesirable with acid labile phosphorylated residues. Despite MS being a powerful tool for the analysis of PTMs, it cannot give any direct information about the pHis isomer present,

which is an important requirement. Thus, a variety of complementary detection methods is needed.

1.4: Enrichment of phosphohistidine

The most common ways to enrich a phosphoprotein and phosphopeptides use an immobilized metal affinity column (IMAC), an immobilized metal oxide column or an immobilized phospho-selective antibody.[95] Phospho-selective antibodies are generally more useful when investigating a particular phosphorylated amino-acid residue.[96] Enrichment of pHis-containing proteins using IMAC has been met with some success but has its limitations.[95]

Muimo *et al*. enriched His phosphorylated proteins from sheep trachea membrane fractions using iron (III) affinity columns.[60] Upon discovering the protein being bound to the iron (III) affinity column was Annexin A1, a calcium (II) chelating agent was introduced to assist binding of membrane associated proteins. However, both conditions were found to be inefficient pHis enrichment methods. Napper e*t al*. used copper (II) in what they describe as the selective enrichment of pHis-containing HPr protein from *E.coli*.[97] However, this technique is limited to peptides. These two examples suggest IMAC can be used to enrich pHis samples but requires optimization to avoid the acidic conditions typically used to release the bound pHis proteins from the resin, which destroys pHis residues and reduces efficiency.

Potel *et al.* found that the efficiency of iron (III) affinity columns could be improved in the enrichment of pHis peptides by reducing procedure temperature and contact time with the acidic eluents.[93] Alternatively, Hardman *et al.* demonstrated that strong anion exchange chromatography could be used to enrich pHis peptides and the bound pHis peptides could be dissociated from the resin with a pH 8.0 triethylammonium phosphate gradient.[90]

1.5: Phosphohistidine analogues and antibodies

Antibodies have been extensively used in the detection and enrichment of phosphorylated peptide/proteins, namely pTyr, pSer and pThr.[96] The development of pTyr antibodies in the late 80s led to a boom in the research field which arguably led to the discovery of the drug Gleevec. Gleevec is a protein kinase inhibitor used to treat leukaemia and other malignancies.[98-100] Among the detection methods which have been used to detect phosphorylated amino-acid residues, such as MS, NMR spectroscopy, radiolabelling (^{32}P) and dyes, antibodies hold the most potential. Antibodies allow for rapid non-invasive detection (can be used *in vivo* and *in vitro*), with high sensitivity (up to femtomolar detection[101]) and can be used in enrichment (perhaps most importantly because nearly all the detection methods discussed require a reliable enrichment process before analysis) from whole-cell lysates.[102] None of the other methods mentioned above has these three characteristics in combination and furthermore antibodies do not have many of the disadvantages associated with other techniques (see section 1.3 and 1.4) so long as they are selective for a particular antigen or target. There have not been any reports in which pHis has been used successfully to generate selective antibodies, most likely due to its labile nature.

Many authors have reported potential pHis analogues and one of the first approaches was to substitute one of the oxygens of the phosphoryl group for a sulfur atom to give thiophosphorylhistidine **2**, a more stable derivative of pHis (Figure 4).[103] There are no reports of analogue **2** in the generation of pHis antibodies. An antibody was raised against the thiophosphorylhistidine derivative **3** but the antibody so raised could not distinguish pHis from other phosphoamino acids.[104,105] Pirrung *et al*. reported the preparation of malonate **4**

and fluoromalonate **5** derivatives of His as τ-pHis analogues but no biochemical studies using these analogues have been reported.[106]

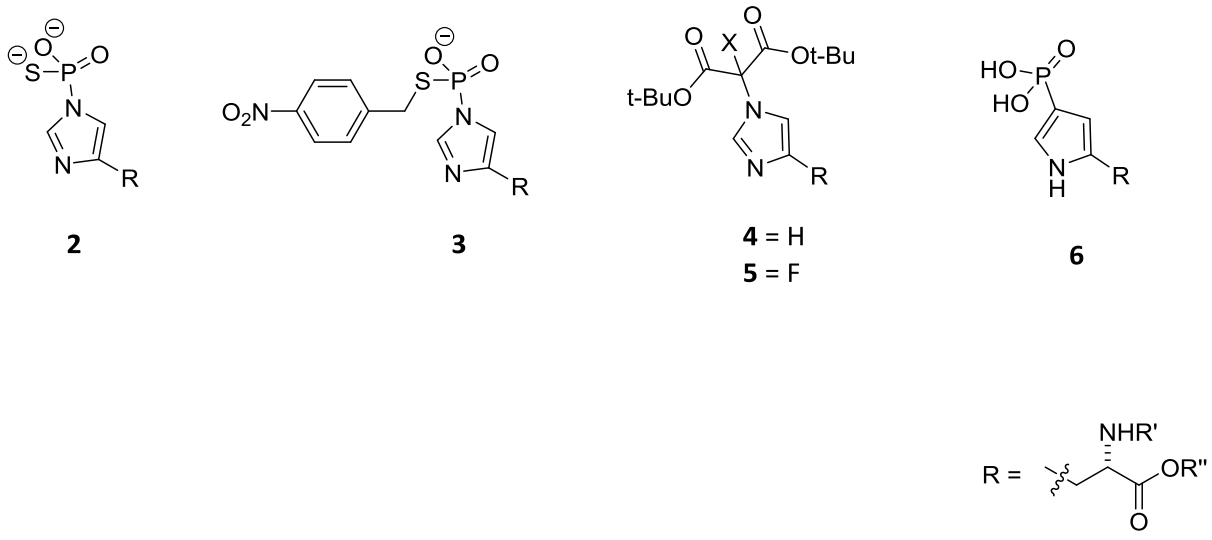

Figure 4: Some early proposed analogues of pHis.

Schenkels *et al*. reported the synthesis of phosphofurylalanine **9** while also proposing phosphopyrrole **6** as a potential non-hydrolysable τ-pHis analogue (Scheme 5).[107] Phosphofurylalanine **9**, was synthesized in five steps, by alkylation of furan **7** with Boc-protected diethyl aminomalonate to give compound **8**. The desired compound **9** was then synthesized in three further steps which involved acidic decarboxylation, and enzymatic resolution. Use of the free amino-acid phosphofurylalanine **9** as an epitope gave antibodies that detected the antigen, and not pHis.[108] Similarly, Schenkels' proposed phosphopyrrole **6** as a pHis analogue which was later synthesized by Attwood *et al.,* but the polyclonal antibodies raised against this epitope detected only the analogue and not pHis.[69]

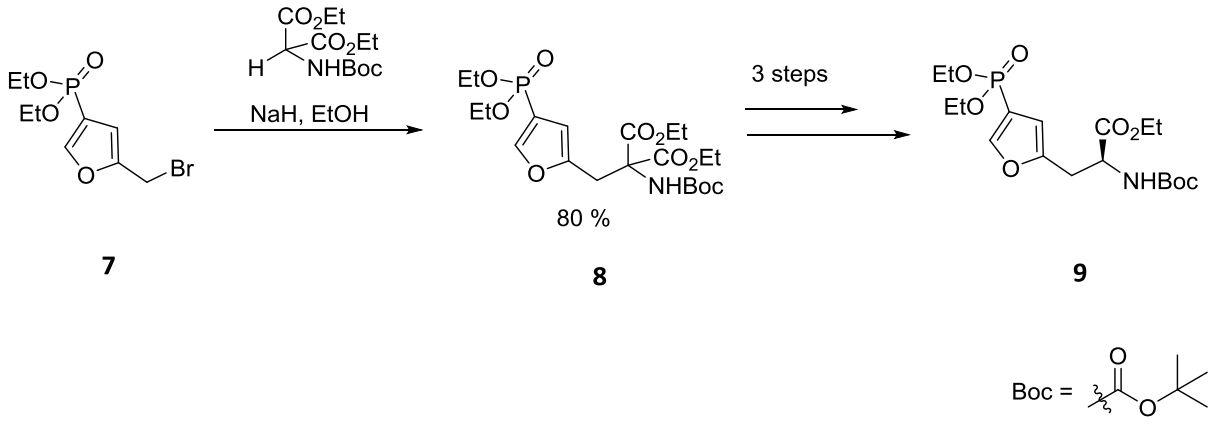

Scheme 5: Synthetic route to proposed furan pHis analogue **9**.[107]

Following Schenkels' proposal of phosphofurylalanine **9** as a potential pHis analogue Lilley *et al*. synthesized phosphothiophene **16** (Scheme 6).[109] The phosphorus-carbon bond was formed by Hirao cross-coupling of 3-bromothiophene **10**, with diethyl phosphite. Electrophilic iodination of thiophene **11** and subsequent Negishi cross-coupling of iodothiophene **12** with zinc reagent **13** gave the protected thiophene amino acid **14** in good yield. The desired product **16** was then accessible after a two-step deprotection.

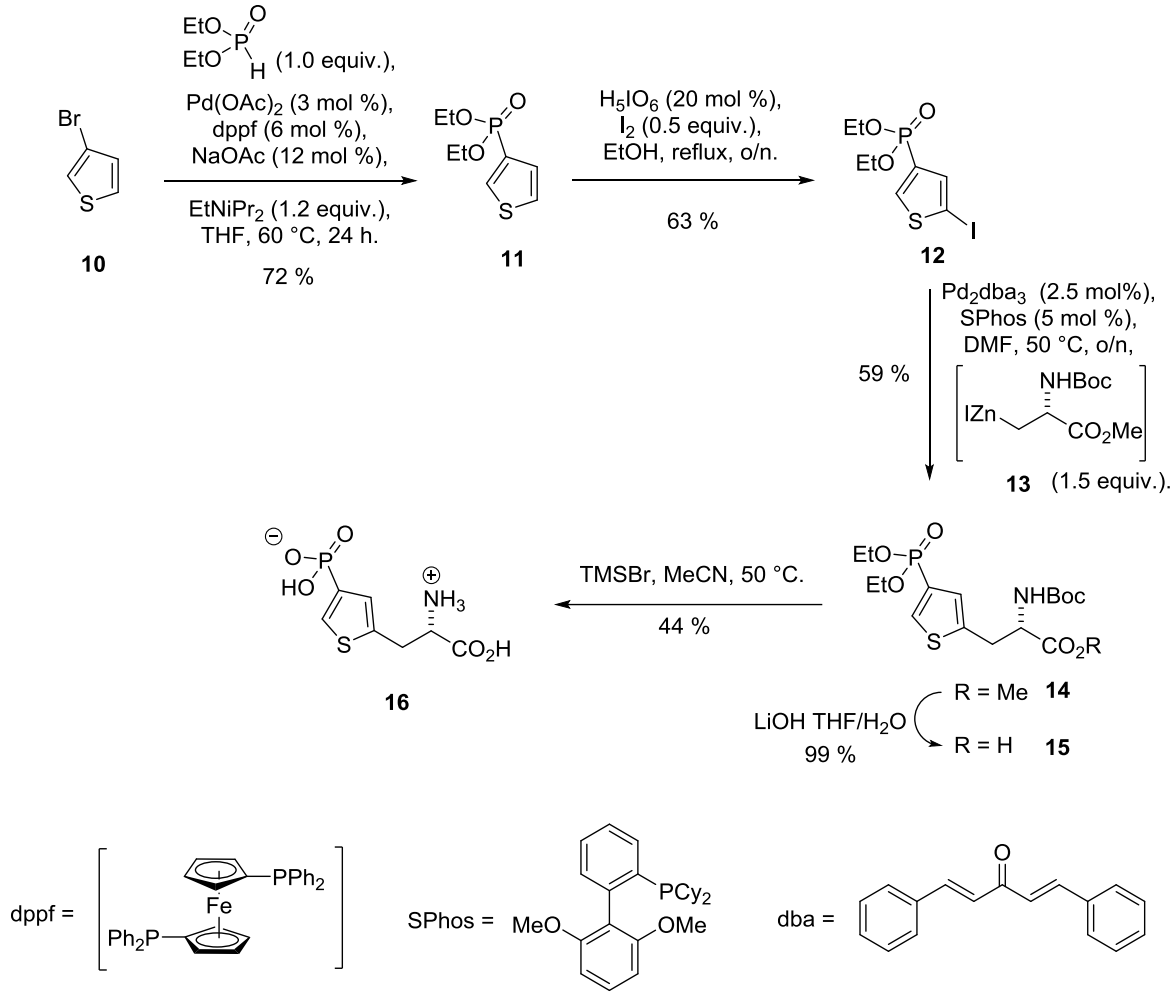

Scheme 6: Synthesis of 4-phosphothiophen-2-yl alanine **16**.[109]

Thiophene **16** was conjugated to keyhole limpit hemocyanin (KLH) using glutaraldehyde and administered into a rat. The affinity purified polyclonal antibodies were found to be highly selective for pTyr but did not detect pHis. The phosphopyrrole **6**, the free amino-acid phosphofurylalanine **9,** and phosphothiophene **16** antibody generation results suggested that retaining the nitrogen with a lone pair of electrons relative to the phosphoryl group as present in pHis is necessary. In addition, replacement of the labile phosphorus nitrogen bond with a non-hydrolyzable phosphorus carbon bond is probably essential.

1.5.1: Triazole phosphohistidine analogues

Kee *et al*. synthesized triazolylalanine analogues **19** and **21** as τ-and π-pHis analogues, respectively (Scheme 7).[110] Density functional theory (DFT) calculations on the unprotected residue of triazolylalanine **19** suggested a close structural match to τ-pHis but with an observable difference in electrostatic surface potential (ESP) around the extra nitrogen and lone pair of electrons.[80,111] Triazolylalanine **19** was accessed from the reaction of azidoalanine **17**, with diethyl ethynylphosphonate **18** using click chemistry. Alternatively, conversion of the azidoalanine **17** into the benzyl ester **20**, followed by ruthenium catalysed dipolar cycloaddition with ethynylphosphonate **18** gave azide **21**.

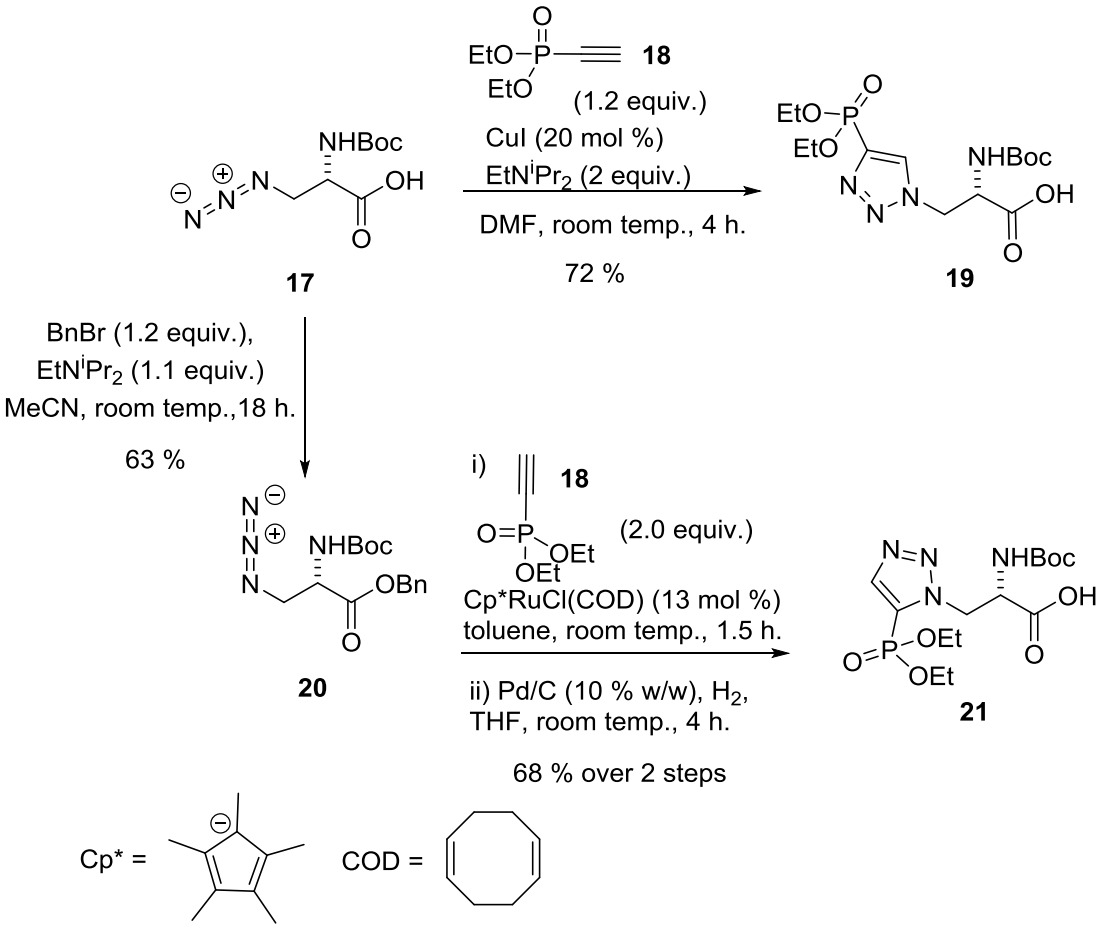

Scheme 7: Synthesis of Boc diethyl protected triazolylalanine carboxylic acid **19** and **21**.[110]

Both analogues **19** and **21** were incorporated into peptides via Boc solid phase peptide synthesis (SPPS) to give peptides **22** and **23** respectively (Scheme 8).[110] Peptide **22** was conjugated to protein KLH and used to generate antibodies. The polyclonal antibodies were found to cross-react with pHis substituted peptide **22** as assessed by dot blots but no other pHis peptides, highlighting the selectivity of the antibodies for peptide **22**. However, one of the three immunized rabbit antibodies, namely Rb.#3 antibodies showed significant cross-reactivity with the pTyr substituted peptide **22** (see supplementary Figure S4 in reference) suggesting that the triazolyl moiety in peptide **22** may not be an optimal analogue of pHis.[110]

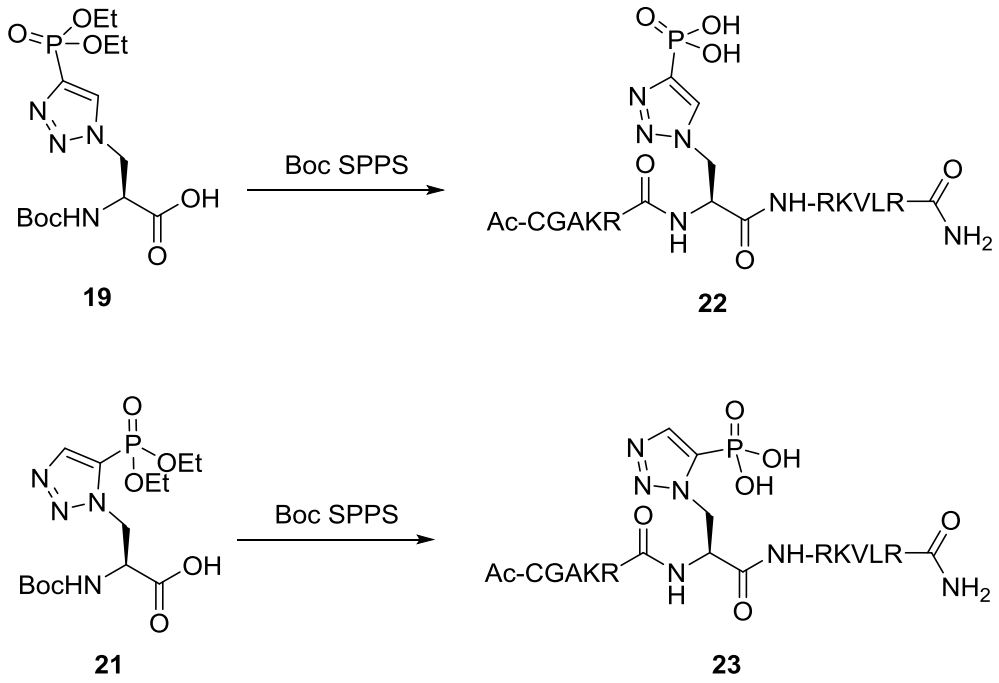

Scheme 8: Incorporation of Boc diethyl protected triazolylalanine **19** and **21** into peptides via Boc SPPS.[110]

Inspired by the earlier work on the generation of pTyr antibodies using the hapten[112] alone, Kee *et al*.[80] used the triazolylethylamine **24** conjugated to KLH via a linker to give a much simpler epitope for use in immunization (Figure 5). The affinity purified antibodies were used

to detect pHis in various known peptides where phosphorylation sites vary widely, including histone H4, bacterial His kinase, KinB, and the *E.Coli* metabolic enzyme I (PtsI) and PpSA, illustrating its sequence independence.[80] However, control experiments to assess the selectivity of the antibody against other phosphorylated amino acids/peptides showed significant cross-reactivity with pTyr as observed by ELISA and dot blots (see Supplementary Figure 3 in reference).[80]

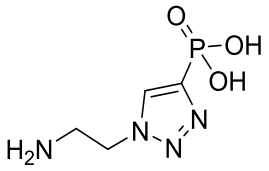

24

Figure 5: Triazolylethylamine **24** pHis analogues.[80]

These results suggest that the phosphotriazolyl residue of compound **24** has a hybrid functionality for both pHis and pTyr in antibody generation, perhaps similar to the azobenzene reported in the 1980s.[113] Despite the limitations, Kee *et al*. study has demonstrated that pHis analogues alone could be effective as epitopes.

Phosphonates protected as Bn groups have been shown to have a general applicability in Fmoc SPPS.[114] McAllister *et al.*, reported the synthesis of dibenzyl Fmoc protected triazolylalanine **25**, and which was incorporated into peptides using Fmoc SPPS strategy (Figure 6).[115] Fuhs *et al*. made use of McAllister's report and synthesized both dibenzyl Fmoc protected triazolylalanine **25** and **26** and incorporated them in neutral peptides libraries (Figure 6 and 7).[77]

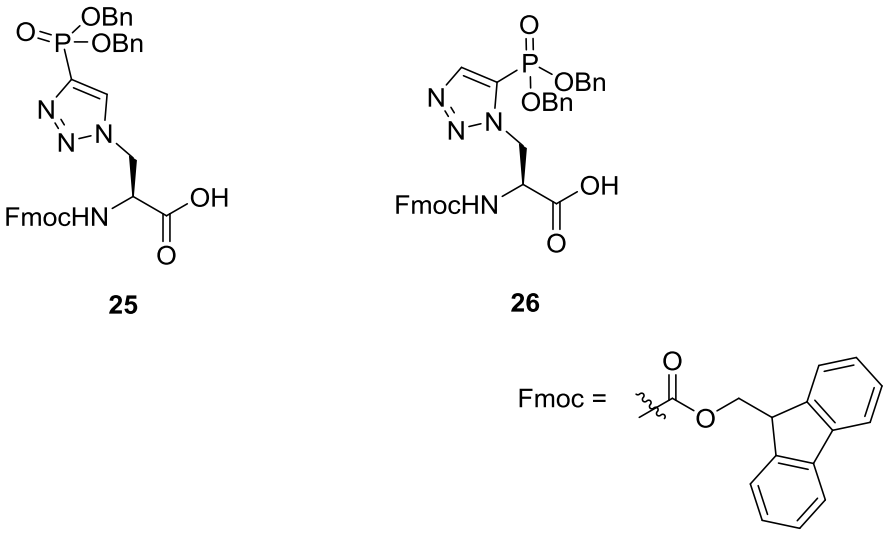

Figure 6: Dibenzyl Fmoc protected triazolylalanine carboxylic acid **25** and **26** pHis analogues.[77,115]

Fuhs *et al*. took peptide libraries **27** and **28** conjugated to KLH and generated polyclonal antibodies (Figure 7). The antibodies were tested by dot blots/immunoblots against **27** and **28**, pTyr peptides and two protein targets as standards, His phosphorylated NME1/NME2 and PGAM, which contain a π-pHis or a τ-pHis residue, respectively. Analysis by immunoblots showed the polyclonal antibodies raised against triazole peptides **28** recognized phosphorylated PGAM, whereas the polyclonal antibody raised against triazolyl peptides **27** recognized, in a complementary way, phosphorylated NME1. The triazolyalanine residue **27** has been proposed as a mimic of π-pHis by Kee *et al*. but was not used in antibody generation (*vide supra*).[110] Monoclonal antibodies raised with peptides **28** recognized peptides containing residue **28** but not residue **27** on dot blots, and vice versa for **27**.

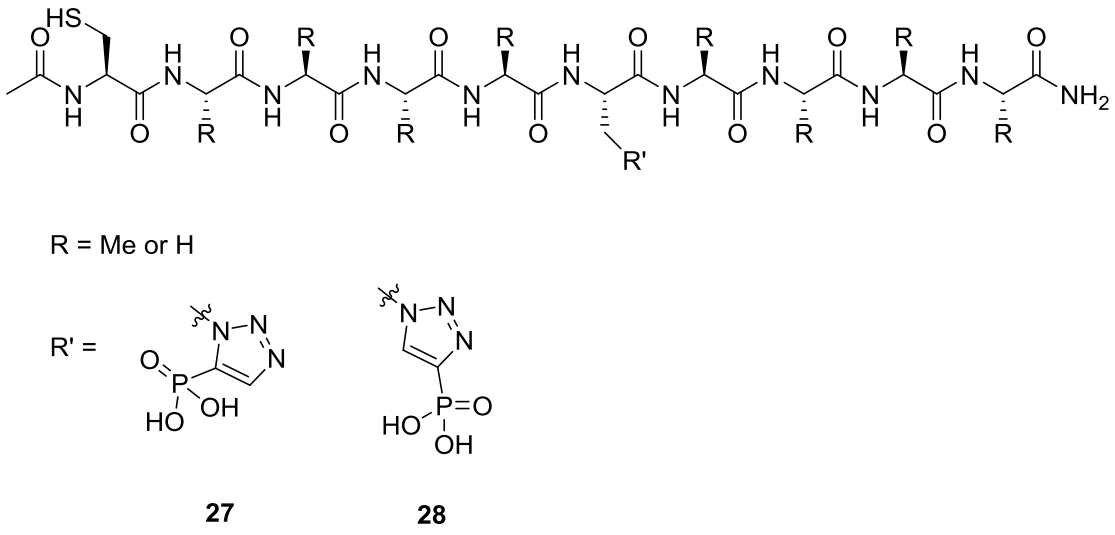

Figure 7: Triazolyl containing peptides **27** and **28** used to generate pHis antibodies.[77]

The monoclonal antibodies were used in Western blots of many mammalian whole-cell lysates and in pHis protein enrichment.[77] Fuhs *et al.* found significant overlap of π-and τ-pHis proteins binding to all monoclonals in the enrichment data. It is important to point out that in the initial report by Kee *et al*.[110] the use of Histone H4 peptide **22** gave peptide sequence dependent polyclonal antibodies and their later method using triazolylethylamine **24** gave cross reactive polyclonal antibodies for pHis and pTyr.[80] Evaluation of potential interaction between pHis and pTyr binding domains indicated that peptides containing triazole residue **28** (as replacement for pTyr) are capable of strongly binding to the prototypical pTyr binding Grb2 SH2 domains.[116] However, this result apparently contradicted a previous study that showed that τ-pHis could not substitute for pTyr in high-affinity binding of peptides to pTyr binding Grb2 SH2 domains.[117] It is worth noting that peptides containing a pHis substitution were not considered in the experimental setup by McAllister *et al*.[116] As such, it is possible that the Grb2 SH2 binding observed resulted from the ability of triazole residue **28** to mimic both pTyr and pHis. Thus, their results are in line with data from antibody generation using

the triazolylethylamine **24** (*vide supra*) and supports the notion that triazole residue **28** has a hybrid functionality for both pHis and pTyr.[80] Furthermore, the peptide sequence dependent antibodies generated to Histone H4 peptide **22** cross-reacted with pTyr substitution (*vide supra*).[110] This indicates that peptides containing triazole residue **28** may not be entirely suitable as tools to raise pHis peptide sequence dependent antibodies.

1.5.2: Imidazole phosphohistidine analogues

Based on Vliet's ESP calculations, the unprotected imidazole phosphonate **33** residue closely mimics the τ-pHis residue (Scheme 9). [118] Hence, Vliet proposed building block **33** as a τ-pHis analogue. Imidazole **33** was synthesized in fifteen steps using aza-Wittig chemistry. Azide **29**, accessed in eight steps, was coupled to aspartic acid **30** which gave compound **31**. Subsequent intramolecular aza-Wittig reaction of **31** using 1,2-bis(diphenylphosphino)ethane (dppe) led to imidazoline **32**. Base induced aromatization of imidazoline **32**, and subsequent trityl and Fmoc protection gave building block **33**.

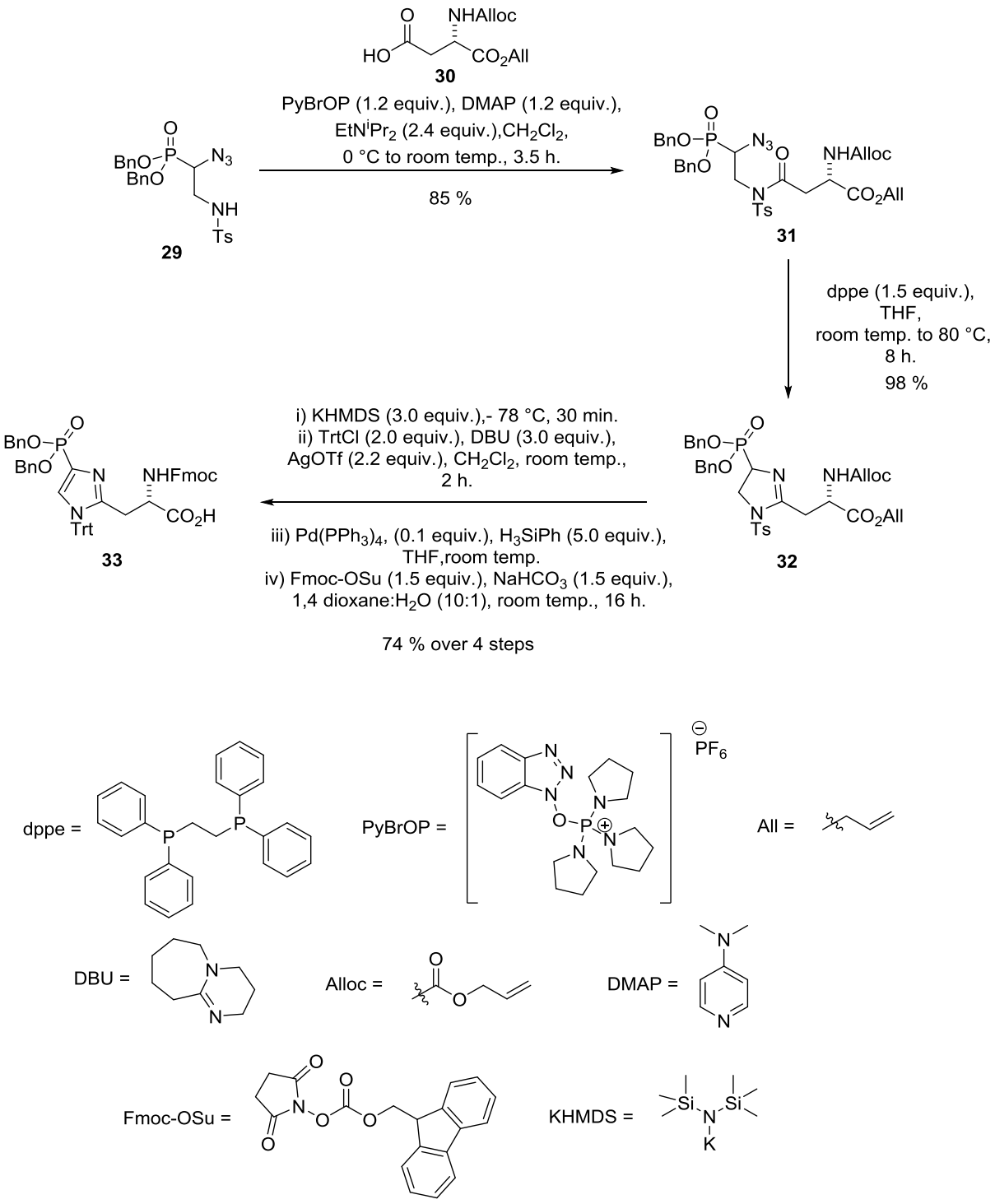

Scheme 9: Fifteen step Aza-Wittig synthesis of dibenzyl Fmoc trityl protected imidazolylalanine carboxylic acid **33**[118] Synthesis of azide **29** is not shown.

Building block **33** was incorporated into peptide **34** (based on the sequence of histone H4) and peptide **35** (containing a polyethylene glycol (PEG) linker) using Fmoc SPPS (Figure 8).[118] Peptides **34** and **35** were conjugated to KLH and used as immunogens to immunize rabbits. On dot blots, affinity purified polyclonal antibodies generated with peptide **34** detected pHis substituted peptide **34** and not the unphosphorylated counterpart. These antibodies also detected histone H4 and various other unidentified protein on Western blots of mouse hepacyte nuclear protein fractions. Affinity purified polyclonal antibodies generated with peptide **35** detected pHis substituted peptide **35** and not the unphosphorylated counterpart. Experiments to assess the selectivity of both polyclonal antibodies for pHis over other phosphorylated amino acids were not reported.

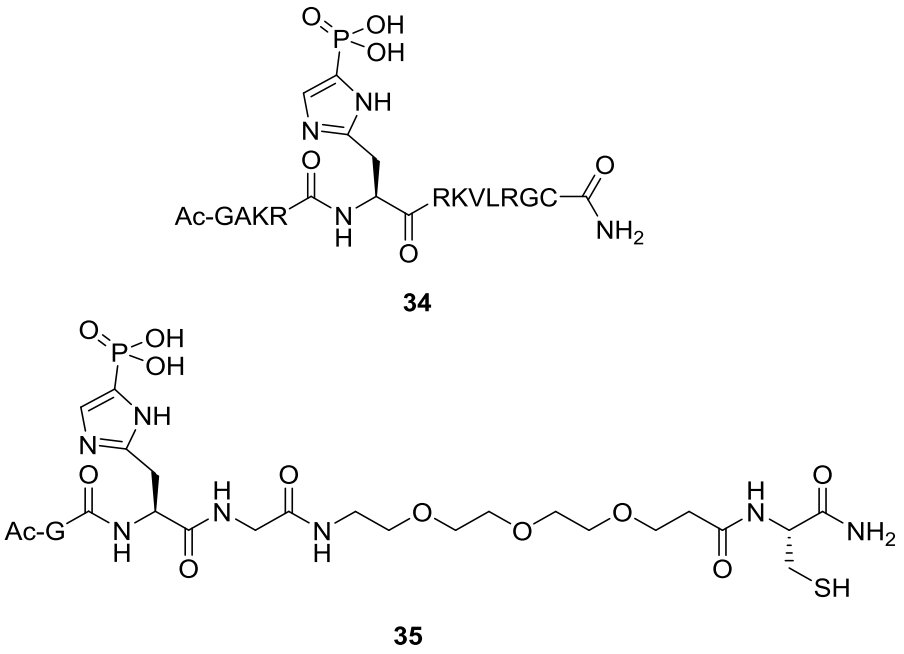

34

35

Figure 8: Peptides **34** and **35** synthesized Fmoc SPPS using building block **33** .[118]

In a follow up study Eerland *et al*. designed and synthesized sulphonamide **43** as a sulphonamide-based transition state analogue of enzymatic pHis dephosphorylation (Scheme

10).[119] Reaction of imidazole **36**, with chlorosulfonic acid, followed by treatment with thionyl chloride gave compound **37**. Compound **37** was then converted into sulphonamide **38**, by nucleophilic displacement with 2,4-dimethoxybenzylamine. Regioselective protection with a trityl group to give **39** allowed in turn for subsequent regioselective iodination to give iodoimidazole **40**. Negishi cross coupling of iodoimidazole **40** with zinc reagent **41** was next investigated.[120] Significant catalyst screening and optimization was required and, 10 mol % XPhos to 5 mol % tris(dibenzylideneacetone)dipalladium(0) was found to be the most effective ligand in the synthesis of imidazole **42**. The methyl ester of compound **42** was cleaved with trimethyltin hydroxide (Me_3SnOH) which gave the desired building block **43** for use in peptide synthesis. The analogue was successfully incorporated into peptides, but efforts to use these peptides as pHis phosphatase inhibitors, or as baits to pull down pHis-binding proteins, were not unsuccessful.[121]

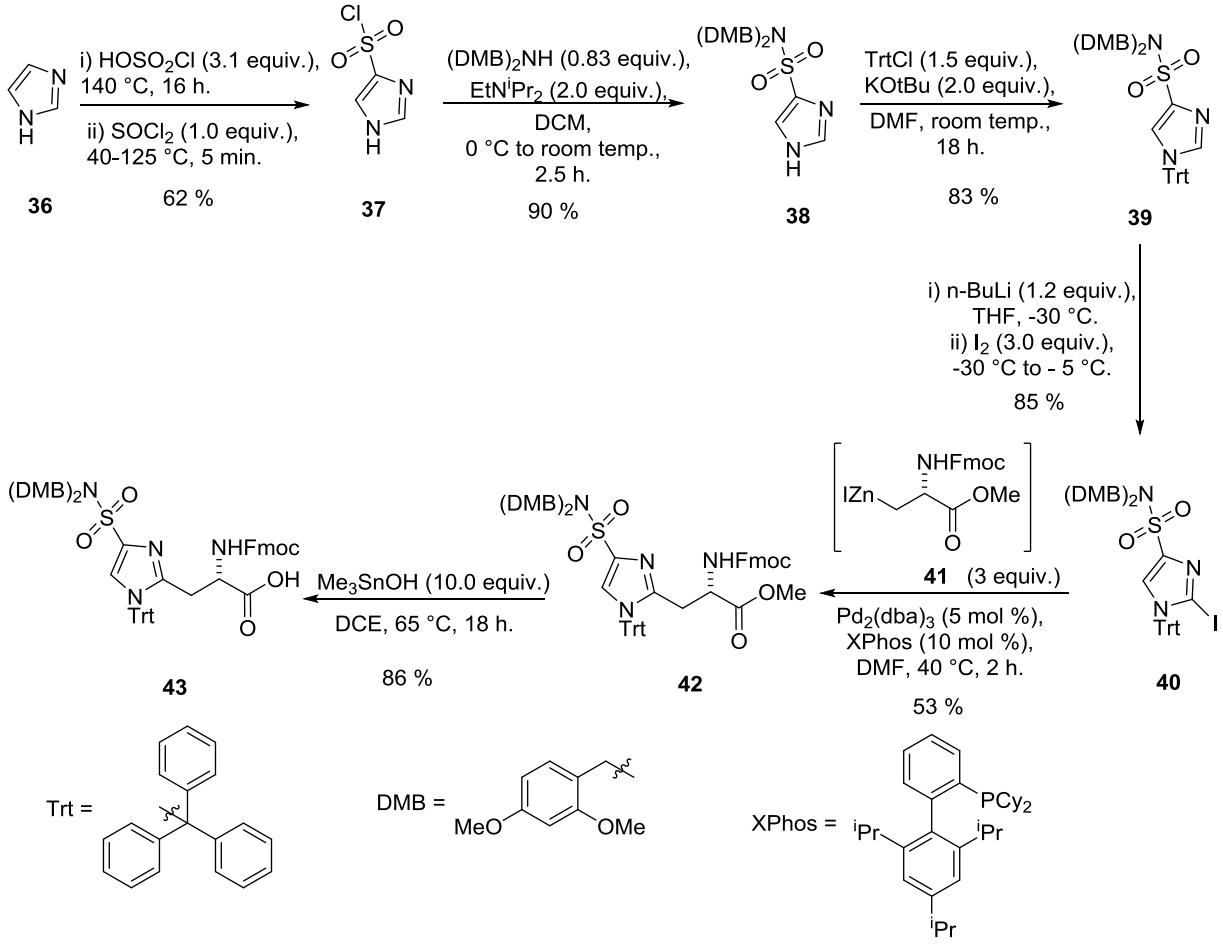

Scheme 10: Synthesis of sulphonamide-based pHis transition state building block **43**.[121]

A synthesis for imidazole building block **33** involving a Negishi cross coupling step was first proposed and initiated by Vliet.[118] Vliet began with 1-trityl-4-iodoimidazole **44** which underwent a metal halogen exchange with isopropylmagnesium chloride lithium chloride complex (Scheme 11). The resulting Grignard reagent was quenched with bis(diethylamino)phosphine chloride to give phosphoramidate **45**.[118] Tetrazole catalyzed substitution with benzyl alcohol, and oxidation, gave imidazole phosphonate **46**.

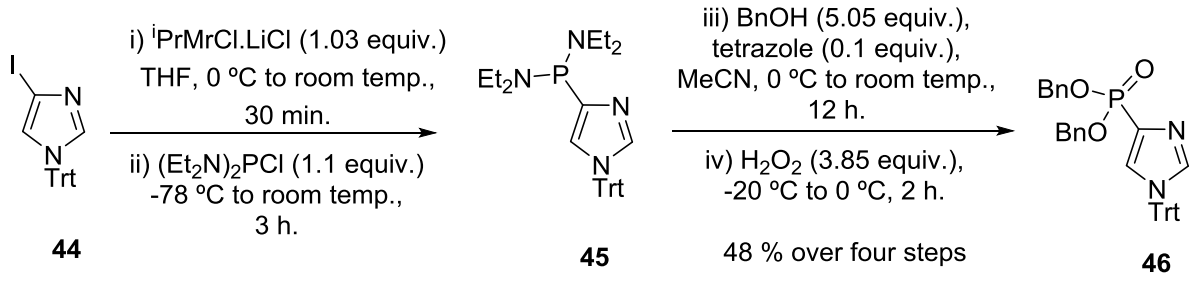

Scheme 11: Vliet's four step one pot synthesis of imidazole phosphonate **46**.[118]

Vliet found deprotonation of imidazole **46** using n-BuLi at -30 ºC followed by a iodine quench gave the regioisomer **47** (Scheme 12).[118,121] Vliet's efforts to Negishi cross couple iodo imidazole **47** with zinc reagent **41** failed, perhaps due to the steric bulk surrounding the iodine carbon aromatic bond. In the follow up study, Eerland rationalized that these conditions favored lithiation in the 5 position which was the thermodynamic product. However, the kinetic lithiated product (2-position) was accessible by deprotonating imidazole **46** at -100 ºC and using the bulky base t-BuLi for 2 minutes, before quenching with iodine to give regioisomer **48** (Scheme 12). Distinguishing between isomers **47** and **48** was made difficult by the similar ^{1}H NMR chemical shifts and J values of 7.60 ppm (2.6 Hz) and 7.43 ppm (0.8 Hz) respectively.

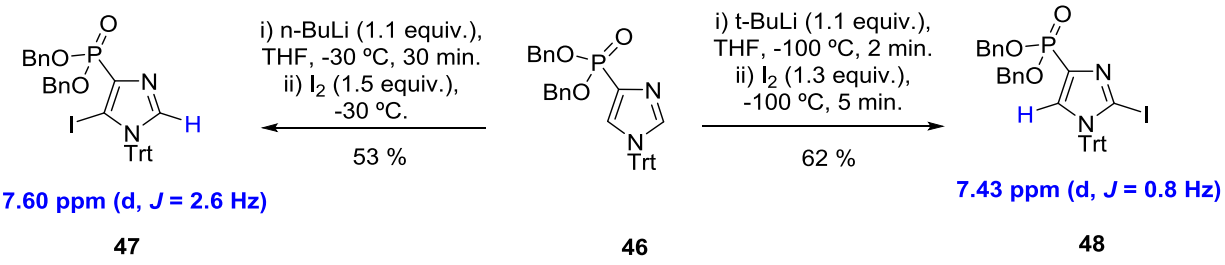

Scheme 12: Synthesis of iodo imidiazole isomers **47**[118] and **48**[121] from **46**.

Vliet implied that Eerland successfully carried out the Negishi reaction between imidazole **46** and zinc reagent **41**, citing "and the reaction went to completion;" and "unpublished results manuscript in preparation" but this does not appear to have been published yet (Scheme 13).[118] Despite Eerland using building block **33** for peptide synthesis in his PhD work he gave no further details on the synthesis of building block **33** apart from citing Vliet's thesis.[121]

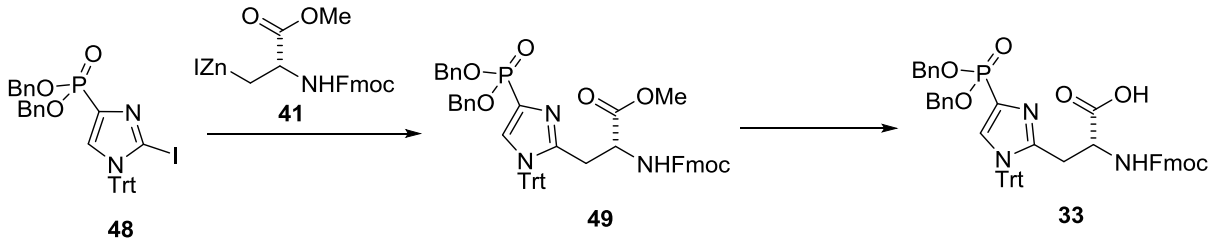

Scheme 13: Vliet's claimed Negishi synthesis of Fmoc dibenzyl trityl protected imidazolylalanine carboxylic acid **33** by Eerland.[121]

1.5.3: Pyrazole phosphohistidine analogues

Owing to the limitations of the triazole residue **28** Lilley *et al*. reported the synthesis of pyrazolylalanine **56** (Scheme 14)**.** [122] Synthesis began with the ring opening of Boc-β-lactone **50** using 4-iodopyrazole **51** to give carboxylic acid **52**. The carboxyl group of pyrazole **52** was esterified to give pyrazole **53**, which subsequently underwent a Hirao cross coupling reaction. The protected pyrazolyl alanine **54** was deprotected in two steps to give pyrazolylalanine **56.** Pyrazolylalanine **56** was conjugated to KLH via a glutaraldehyde linker and used as an immunogen to raise antibodies.

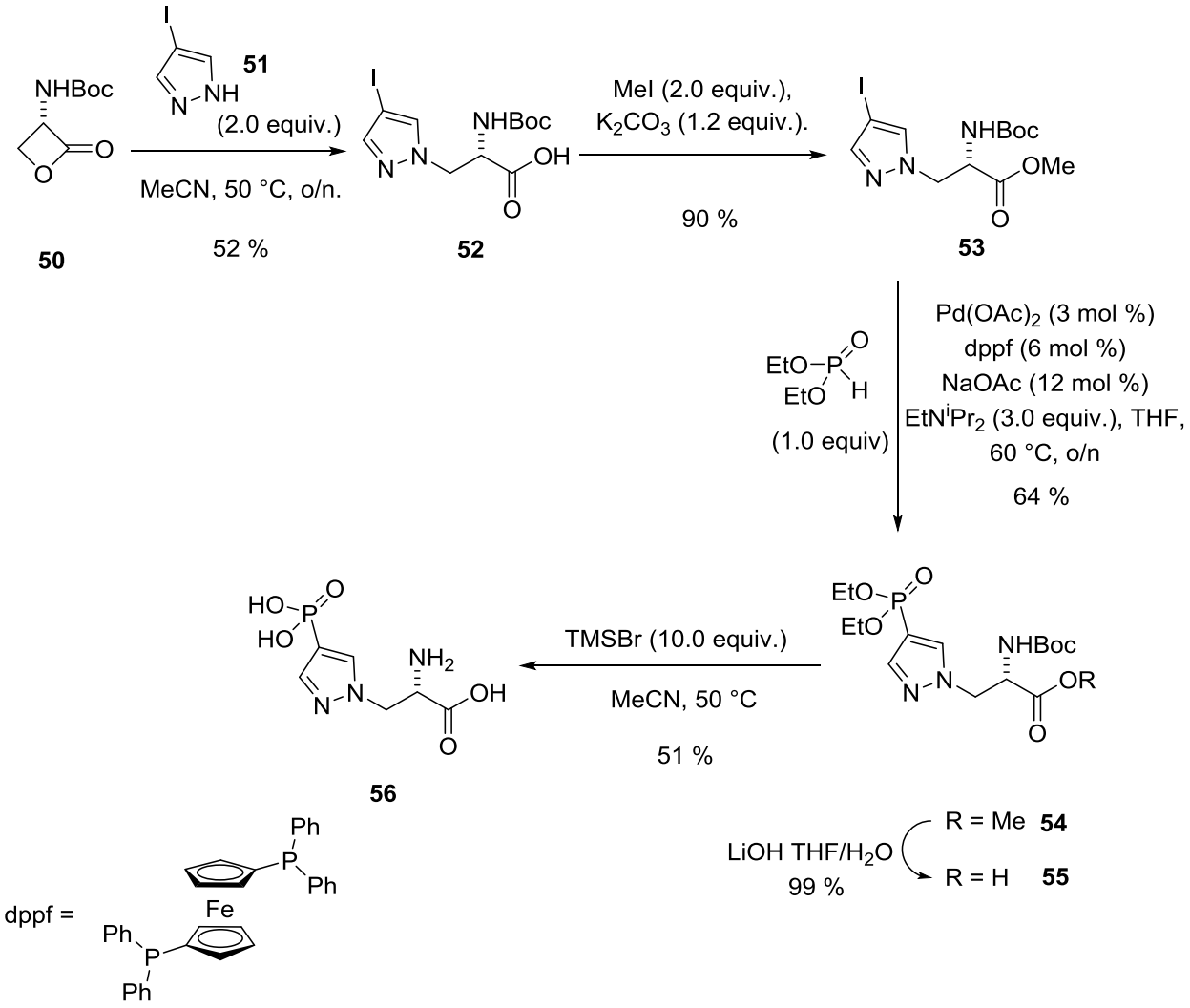

Scheme 14: Synthesis of pyrazolylalanine **56**.[122]

The affinity purified polyclonal antibodies raised with the pyrazole amino acid **56** were found to detect pHis selectively over pTyr, on dot blots, immunoblots and ELISA against BSA phosphorylated amino acid conjugates as standards.[122] The purified polyclonal antibodies were used to detect His phosphorylated proteins Gβ and both NDPK-A/B after immunoprecipitation from human bronchial epithelial (HBE) cells.

In addition, to the synthesis shown in Scheme 14, Lilley was able to synthesise pyrazole carboxylic acid **55** using a more convergent route (Scheme 15, unpublished work).[1] Synthesis

began with the Boc protection of 4-iodopyrazole **51** to pyrazole **57**. This was followed by a Hirao cross-coupling of pyrazole **57** with diethyl phosphite which gave phosphonate **58** in moderate yields. Removal of the Boc protecting group gave phosphonate **59** and a subsequent ring opening reaction with Boc β-lactone **50** gave the desired Boc diethyl pyrazolylalanine **55**.

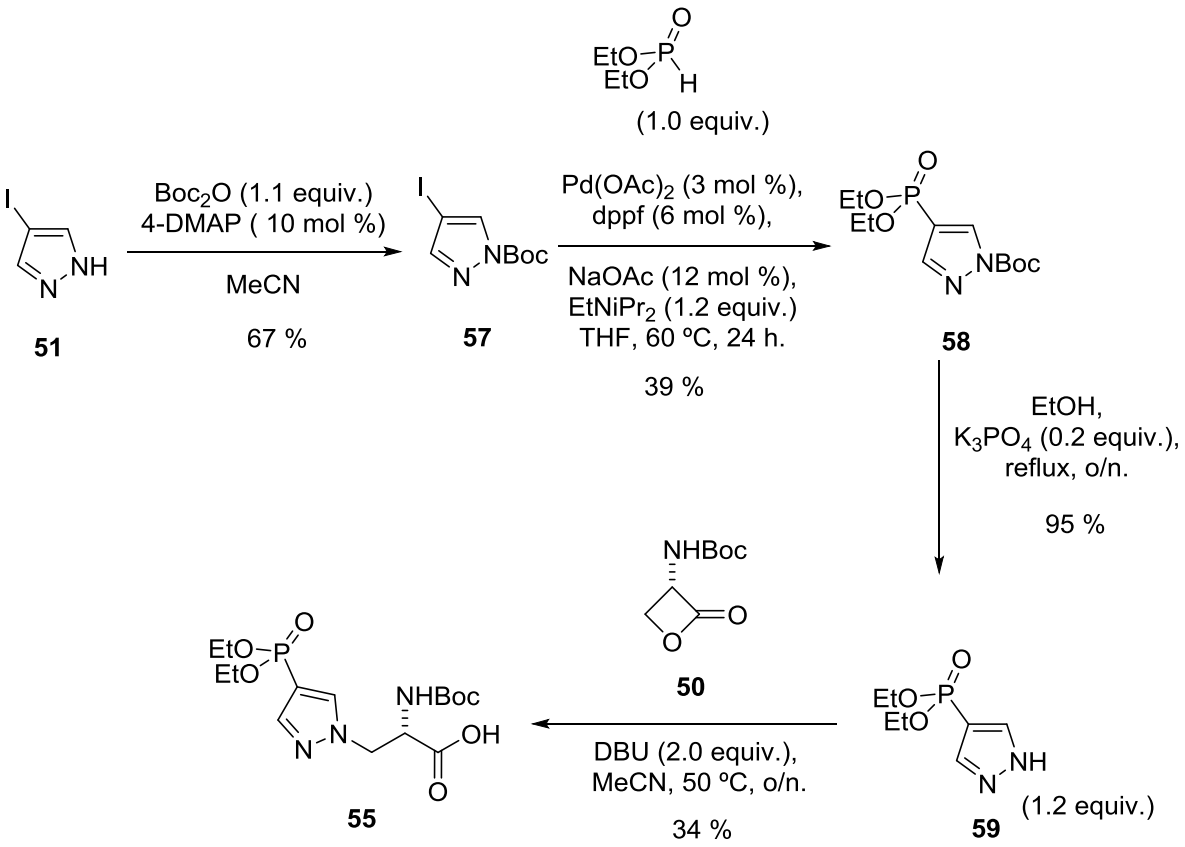

Scheme 15: Alternative synthesis to Boc diethyl protected pyrazolylalanine carboxylic acid **55**.[1]

During the same time Kee *et al.* reported pyrazolylethylamine **61** as a second-generation τ-pHis analogue (Scheme 16).[111] DFT calculations by Kee *et al.* show that the pyrazole analogue **61** residue resembles the τ-pHis residue both structurally and electronically.[111] Pyrazole analogue **61** was synthesized from the displacement reaction between bromoethylamine **60**

and pyrazole **59**. Subsequently, the protecting groups were removed using acidic conditions to give the pyrazolylethylamine **61**.

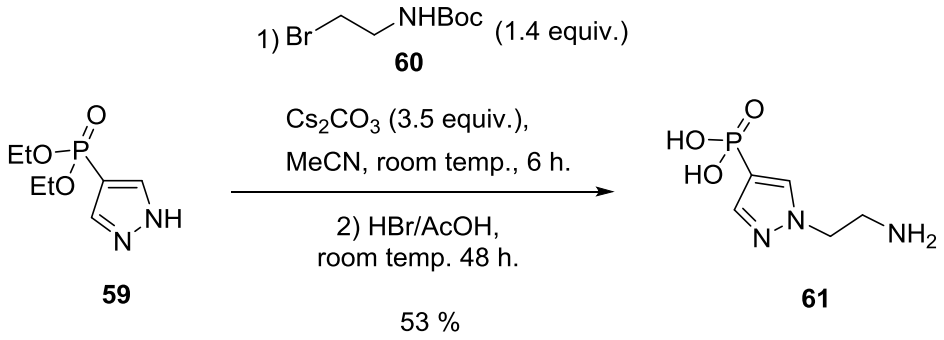

Scheme 16: Synthesis of pyrazolylethylamine **61**.[111]

Affinity purified polyclonal antibodies raised to pyrazole analogue **61** conjugated to KLH via a glutaraldehyde linker were found to selectively detect pHis over pTyr, as assessed by ELISA against His phosphorylated bovine serum albumin (BSA) and phosphorylated amino-acid conjugates. The purified polyclonal antibodies were used to detect various *in vitro* His phosphorylated proteins including PGAM1, mammalian histone H4 and PtsI.

The pyrazole ethylamine analogue **61** has also been independently synthesised by a Jackson group Erasmus student, P. Niesobski (Scheme 17).[123] Synthesis began with the formation of a carbon nitrogen bond via a S_N2 type reaction between pyrazole **51** with iodoethylamine **62** in the presence of potassium carbonate. Subsequently modified Hirao cross-coupling conditions between iodopyrazole **63** and diethyl phosphite gave phosphonate **64** in good yield. Phosphonate **64** was globally deprotected using TMSBr. The crude mixture was purified by a previous member of Jackson group, M. Thompson, using ion exchange chromatography which gave the desired pyrazolylethylamine **61** in high purity. Subsequently M. Thompson conjugated pyrazole ethylamine **61** to KLH via glutaraldehyde, and the conjugate was used as

an immunogen to immunise sheep. The isolated crude antiserum was stored away at – 20 °C and awaits purification and characterisation.

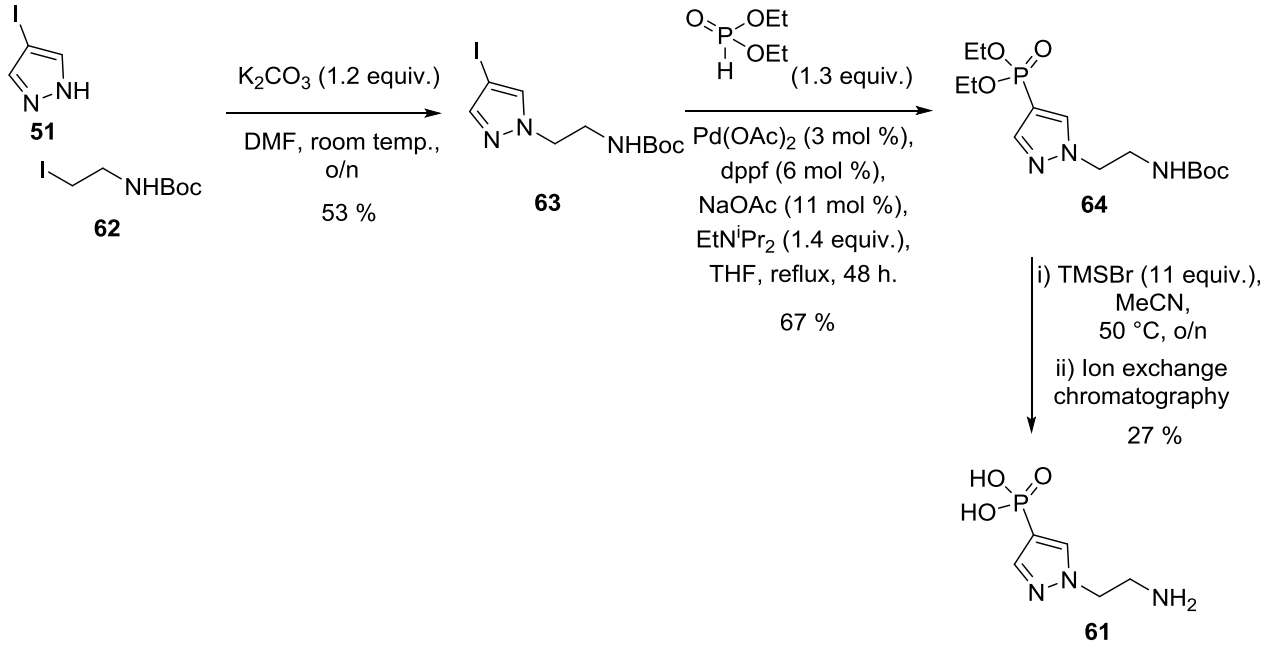

Scheme 17: Synthesis and purification of of pyrazolylethylamine **61** by previous Jackson group member, P. Niesobski and M.Thompson.[123]

1.5.4: Pyridine phosphohistidine analogues

In his PhD study Lilley (unpublished work) also synthesised 2, 4-disubstituted pyridine **68** (Scheme 18) and 2, 5-disubstituted **72** as pHis analogous (Scheme 19).[1] The synthesis of 2, 4-disubstituted pyridine **68** began with the Hirao cross coupling of 2-chloro-4-iodo-pyridine **65** with diethyl phosphite. The resulting phosphonate **66** underwent a Negishi cross coupling with zinc reagent **13** to give pyridine **67**. Global acidic deprotection gave the desired analogue **68** as the hydrochloride salt. The 2,4-disubstituted pyridine **68** was conjugated to KLH via glutaraldehyde and used as an immunogen to immunise a rat. The affinity purified polyclonal

antibodies gave selective pHis antibodies, as assessed by dot blots against BSA phosphorylated amino acid conjugates as standards.[1]

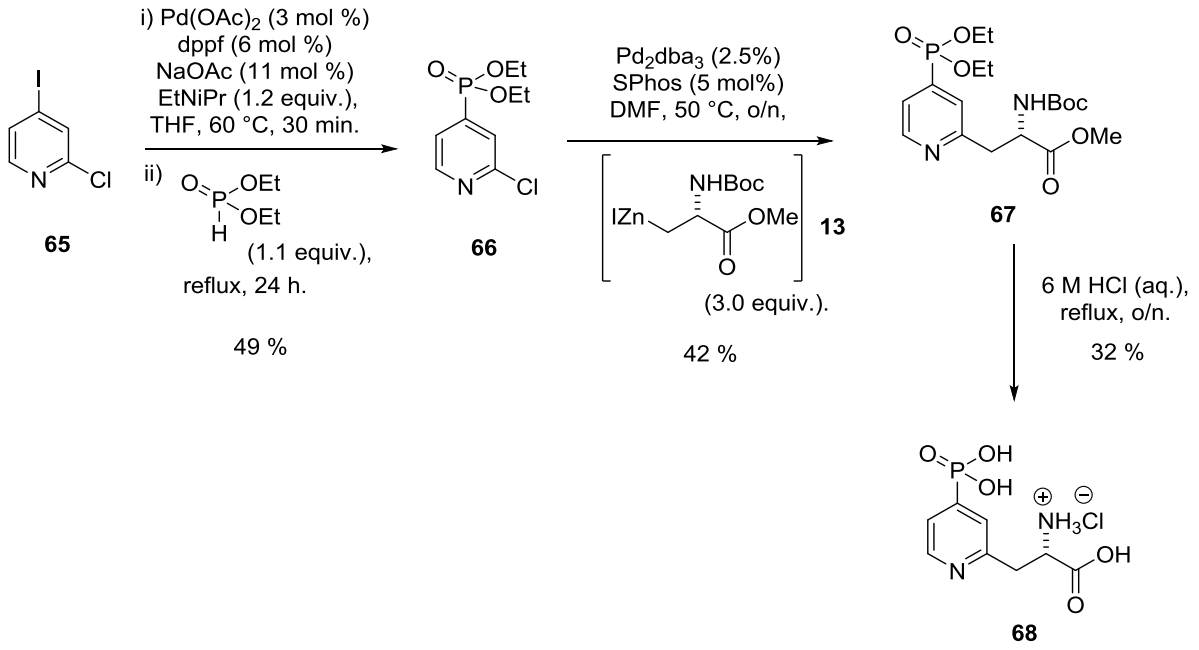

Scheme 18: Synthesis of 2,4-disubstitued pyridine hydrochloride salt **68**.[1]

Synthesis of the 2,5-disubstituted pyridine **72** began with the Negishi cross-coupling of zinc reagent **13** with 2,5-bromodipyridine **69** (Scheme 19).[1] Hirao cross coupling of pyridine **70** with diethyl phosphite gave pyridine **71**, which was globally deprotected using 6 M HCl (aq.) to give the desired compound **72** as the hydrochloride salt. As with 2,4-disubstituted pyridine **68**, 2,5-disubstituted pyridine **72** was conjugated to carrier protein KLH via glutaraldehyde, which was used as a immunogen to immunise a rat. The affinity purified polyclonal antibodies were found to strongly detect pHis and weakly His on dot blots against BSA phosphorylated amino acid conjugates as standards. A subsequent affinity depletion with His gave antibodies that only detected 2,5-disubstituted pyridine **72** and not pHis or His.

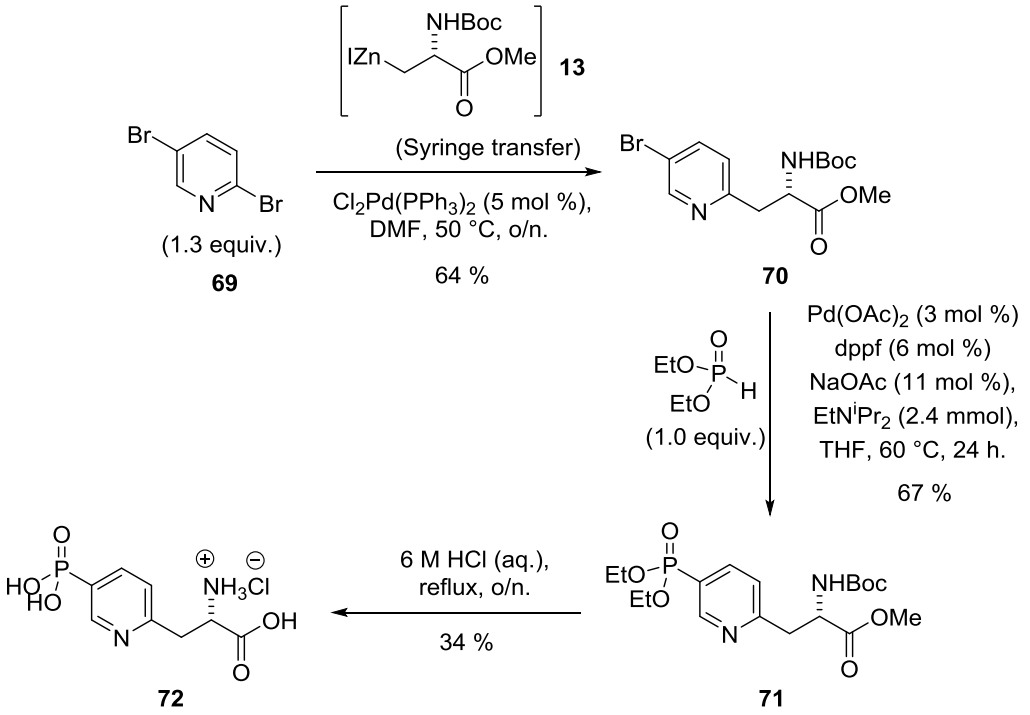

Scheme 19: Synthesis of 2,5-disubstituted pyridine hydrochloride salt **72**.[1]

1.6: Electrostatic surface potential maps and density calculations

Theoretical calculations on molecular structure and electron distribution can give a chemist further validation of a proposal (mechanism, structure etc). Mapped electrostatic surface potentials (ESP) provide a visual representation of structure and charge distribution.[124] Such representations are useful for this project because they give an insight in to what the immune system is likely exposed to during an immune response.

The representations in this section are a result of DFT calculations performed by University of Sheffield theoretical chemistry emeritus Professor B. T. Pickup. For reasons of tractability, the calculations were carried out on the amino acid side chains replaced with a methyl group. The program Gaussian 2009 was used on the phosphonate dianions, the likely ionic state under physiological conditions, using the B3LYP density functional, a large basis set (aug-cc-pVTZ)

suitable for anions, and with PCM to model an aqueous environment. The geometry of each molecule was carefully optimized, and an electron density contour of 0.004 was chosen on which to map the ESP, since this value closely matches the Connelly molecular surface which is often used to map ESPs.[125] The colour red represents a region of negative ESP, and the colour green represents a region of neutral ESP on the mapped ESPs.

1.6.1: τ-pHis analogue side chain calculations

It was assumed the molecular recognition was based on molecular shape/structure and electrostatic interaction. Mapped ESPs on model compounds **73**, **74**, **75** and **76** show (Figure 9 middle row) that the triazole **75** and pyrazole **76** are structurally similar to τ-pHis side chain **73**. However, in the mapped ESPs of side chains **73**, **74**, **75** and **76**, the dianion of the phosphonate dominates the representations and identifying subtler distinguishing features is made difficult. Professor Pickup found that the electrostatic potential field could be better understood by showing more completely the variation of ESP itself. The ESP surface isocontours were drawn at a value of -0.284 au (equivalent to -748.3 kJ mol^{-1}) since this was found to give information that accurately discriminated between the different models. The orange regions signify ESP values of exactly -0.285 au, whilst values of ESP inside the orange regions have ESP values that are more negative. The ESP contour diagrams are shown below the mapped ESPs in Figure 9.

From the ESP isocontours it was clearer that the triazole model **75** negative region of ESP was more similar to that of the pTyr model **74** and did not have two separate region of negative ESP seen with the τ-pHis model **73**. Therefore, the calculations suggest the triazole residue **75** is a hybrid analogue of both τ-pHis and pTyr, whereas the pyrazole model **76** has two

separate regions of negative ESP separated by a sp^2 carbon hydrogen bonds bearing a positive ESP, analogous to the τ-pHis model **73**.

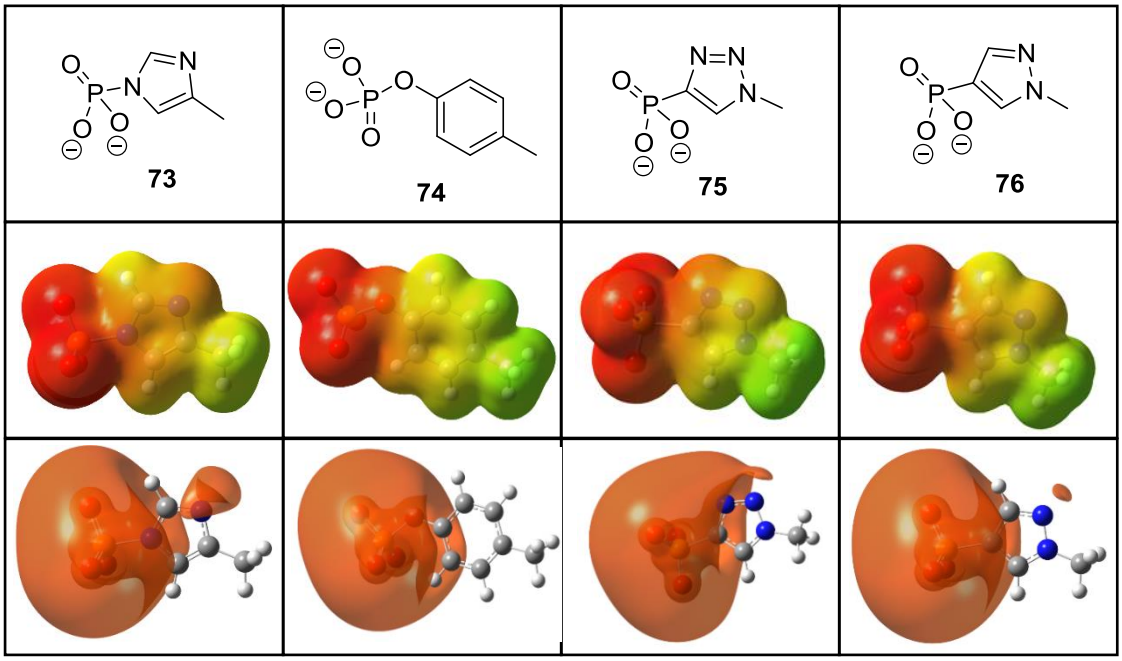

Figure 9: Comparison of mapped ESP surfaces (middle row) and ESP surfaces (contours drawn at a potential of -0.285 au, bottom row) for model compounds τ-pHis **73**, pTyr **74**, triazole **75** and pyrazole **76**.

ESP surface isocontours on model side chain thiophene **78** closely resemble the pTyr model **74** (Figure 10) rationalizing why antibodies raised to Jackson's/Muimo's thiophene **16** (Scheme 6, page 20) were highly selective for pTyr. This would also explain why antibodies generated to Schenkel's side chain furan **77**, which is structurally and electronically similar to thiophene **78** and pTyr **74** did not detect pHis. These results also suggest that despite the structural similarities of furan **77** and thiophene **78** to τ-pHis **73**, having negative ESP regions that closely resembles τ-pHis **73** is likely essential. On the other hand, having generated selective antibodies for the 6 membered aromatic ring pTyr, using a 5 membered heteroaromatic phosphothiophene ring (side chain **78**) suggests some flexibility in the

aromatic ring size is possible for generating phosphoamino aromatic selective antibodies (*vide infra*).

ESP surface isocontours of thiazole **79**, oxazole **80**, and imidazole **81** show negative ESP regions similar to τ-pHis **73** (Figure 10). According to the ESP surface calculations, imidazole **81** appears to be the optimal mimic of τ-pHis **73** whilst thiazole **79** and oxazole **80** are comparable to pyrazole **76**. The other tautomer of imidazole **81** was calculated to be substantially higher in energy (16.6 kJ mol^{-1}), probably due to electrostatic repulsion between the nitrogen lone pair of electrons and phosphonate dianion.

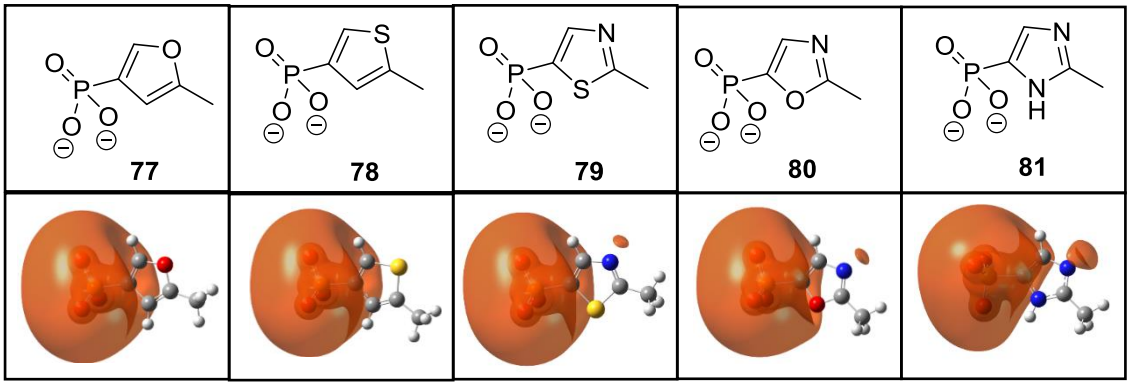

Figure 10: ESP surfaces (contours drawn at a potential of -0.285 au, bottom row) for model compounds furan **77**, thiophene **78**, thiazole **79**, oxazole **80**, and imidazole **81**.

To date, five membered aromatic rings, that have been proposed as τ-pHis analogues, which has had some success in the generation of pHis antibodies have taken the general form **83** (Figure 11). Where the τ-pHis residue **82** atoms colored in red have been preserved in the analogue residue **83** and the phosphoramidate bond has been replaced with a phosphorus carbon bond.

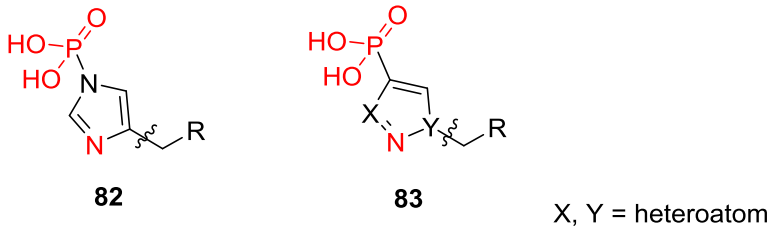

Figure 11: General form of five membered aromatic rings **83**, that have been proposed as τ-pHis analogues, and have had some success in the generation of pHis antibodies.

Lilley has previously used 2,5-disubstituted pyridine **68** and 2,4-disubstituted pyridine **72** in the generation of pHis antibodies (see section 1.5.4). ESP isocontours of models 2,5-disubstituted pyridine **84**, 2,4-disubstituted pyridine **85** have two regions of negative ESP as seen in τ-pHis **73** (Figure 12). These calculations together with Lilley's encouraging pHis antibody generation results using 2,5-disubstituted pyridine **68** and 2,4-disubstituted pyridine **72** show that some flexibility in the aromatic ring size is possible if the electron distribution is similar to pHis. Hence, in addition to the ESP isocontours of models 2,5-disubstituted pyridine **84**, and 2,4-disubstituted pyridine **85**, calculations on a new 3,5-disubstituted pyridine **85** model, also look promising.

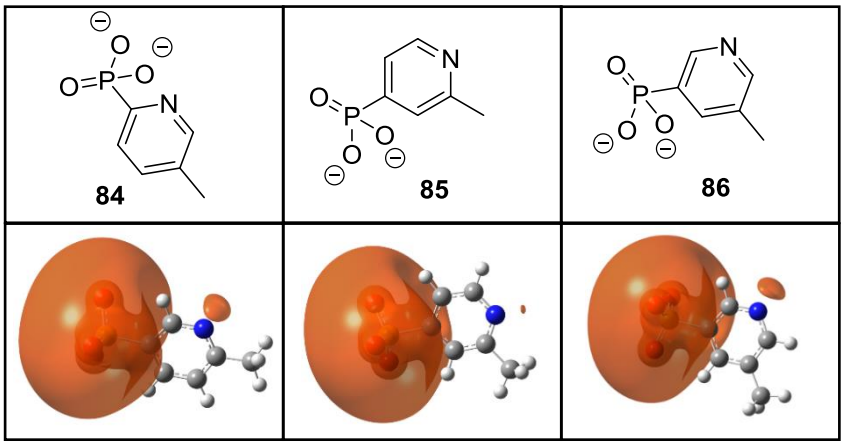

Figure 12: ESP surfaces (contours drawn at a potential of -0.285 au, bottom row) for model compounds 2,5-disubstituted pyridine **84**, 2,4-disubstituted pyridine **85**, and 3,5-disubstituted pyridine **85**.

1.6.2: π-pHis analogue side chain calculations

To date, the only stable π-pHis analogue reported has been the triazolylalanine **21**.[110] Comparison of model π-pHis **87** and triazole **88** ESP surface isocontours reveal an additional negative region in the ESP present in triazole **88** arising from the nitrogen lone pair of electrons next to the methyl group (Figure 13). Substitution of this nitrogen with a carbon hydrogen bond gives imidazole **89**; a better mimic of π-pHis **87**. Moreover, the 3,4-disubstituted pyridine **90** also looks promising.

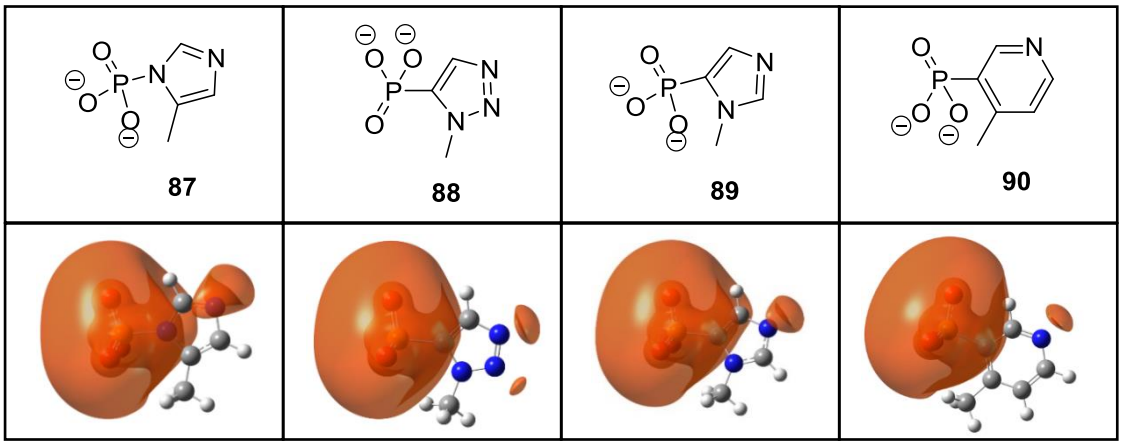

Figure 13: ESP surfaces (contours drawn at a potential of -0.285 au, bottom row) for model compounds π-pHis **87**, triazole **88**, imidazole **89**, and 3,4-disubstituted pyridine **90**.

2: Aim

The aim of the project was to synthesise building block **91**; a known pyrazole τ-pHis analogue with protecting groups suitable for Fmoc SPPS.

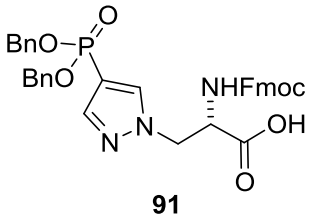

91

Pyrazole τ-pHis building block

The other aim of the project was to revisit the synthesis of 2,4-disubstituted pyridine of **92** and synthesise newly identified 3,5-disubstituted pyridine **93** and imidazole **94** τ-pHis analogues.

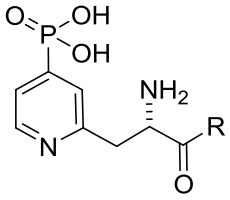

92

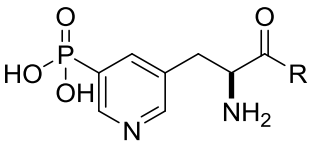

93

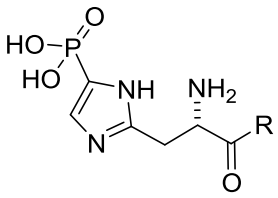

94

R = OH, or NH_2

π-pHis analogues

Furthermore, the plan was to synthesise the complementary 3,4-disubstituted pyridine **95** and imidazole **96** π-pHis analogues.

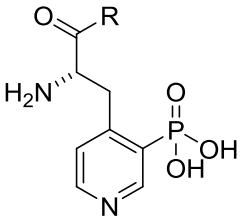

95

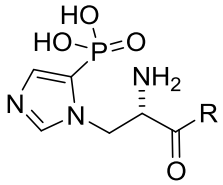

96

R = OH, or NH_2

τ-pHis analogues

The final aim of the project was to use the analogues in antibody generation and purify the antisera; including the antiserum previously generated with pyrazolylethylamine **61**. The purified antibodies would be used in immunological methods, such as ELISA, Western blot, and immunoprecipitation.

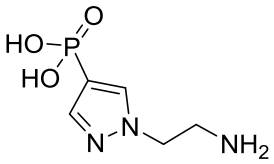

61

Uncharacterised antiserum previously generated to pyrazolylethylamine 61

3: Results and Discussion

3.1: Chemistry

3.1.1: Synthesis of Fmoc dibenzyl pyrazolylalanine carboxylic acid

In two independent studies, the pyrazole side chain **76** (Figure 9) has been reported in the successful generation of selective pHis rabbit polyclonal antibodies (see section 1.5.3).[111,122] This suggests it has chemical properties similar to pHis. Hence, the synthesis of the pyrazolylalanine **91** suitable for Fmoc SPPS was an important priority for the project. Within a peptidic environment the pyrazole analogue could potentially be used in the generation of peptide/protein selective antibodies, or to study protein-protein/protein-peptide interactions, and even biochemical pathways.

To have an amino acid suitable for Fmoc SPPS, the N^{α}-amine of an amino acid must be Fmoc protected.[114] Usually when the amino acid possesses a phosphoaromatic residue, such as pTyr, dibenzyl or phosphoramidate protection of the phosphoryl group has proved successful in Fmoc SPPS procedures.[114] McAllister *et al*. synthesized and successfully incorporated dibenzyl Fmoc protected triazolylalanine **25** into peptides (Figure 14).[115] Since dibenzyl Fmoc protected triazolylalanine **25** only differs from the proposed dibenzyl Fmoc protected pyrazolylalanine **91** by one nitrogen atom, it was thought the dibenzyl protecting groups that have been effective for the phosphoryl group of triazolylalanine **25** in Fmoc SPPS would also be effective for pyrazolylalanine **91** in Fmoc SPPS.

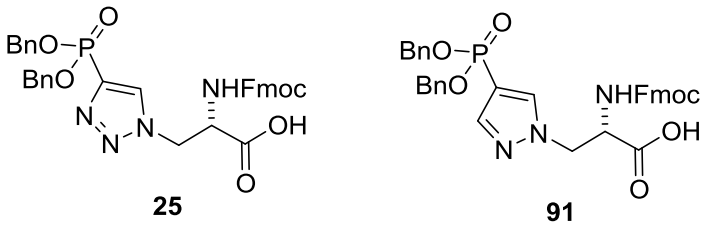

Figure 14: Previously used dibenzyl Fmoc protected triazolylalanine carboxylic acid **25** in Fmoc SPPS and proposed τ-pHis dibenzyl Fmoc protected pyrazolylalanine carboxylic acid **91**.

The Hirao cross-coupling reaction is a useful reaction in the formation of aryl phosphonates.[126] Dibenzyl aromatic compounds are potentially challenging compounds to synthesise using the Hirao cross coupling reaction because the benzyl groups are prone to dealkylation by halide anions; a by-product of the reaction. To our knowledge there has been only one report of a Hirao cross coupling reaction between dibenzyl phosphite and a haloaromatic. Kalek *et al*. was able to rapidly cross couple bromobenzene **97** with dibenzyl phosphite under microwave to give phosphonate **98** in good yield (Scheme 20).[127]

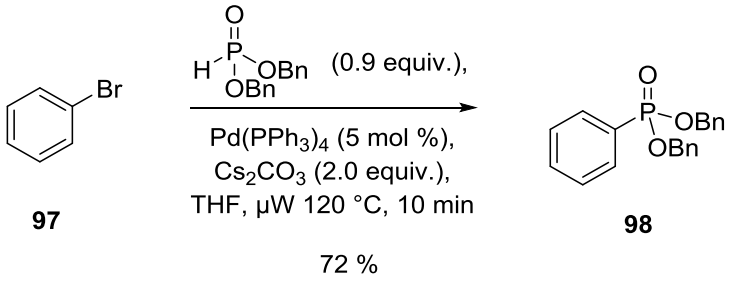

Scheme 20: The Hirao cross coupling synthesise of dibenzyl phosphonate **98**.[127]

There are examples of 2-iodopyrazole derivatives being used in Hirao cross coupling reactions. Lilley has shown that iodopyrazole **53** and **57** can undergo Hirao cross coupling with diethyl phosphite (Schemes 14 and 15, pages 33-34), while Tran *et al.* has reported the Hirao

cross coupling of protected iodopyrazole **99** with diethyl phosphite to give phosphonate **100** (Scheme 21).[128] Even though the Hirao cross coupling conditions used by Lilley (Scheme 14 and 15, pages 33-34) and Tran *et al*. (Scheme 21) are similar there is a considerable difference in the yields and reaction time. These differences may be explained by the different ligands used. Lilley used the ligand 1,1'-ferrocenediyl-bis(diphenylphosphine) (dppp) and Tran *et al*. used 4,5-bis(diphenylphosphino)-9,9-dimethylxanthene (Xantphos). During the ligand screen Tran *et al*. reported a considerable compromise in yields when dppf was used.[128] It is not clear if this is due to Xantphos (108 °) having a larger bite angle than dppf (99 °) or an electronic effect, but Xantphos seems to be the superior ligand for 2-iodopyrazole type subtrates.[129]

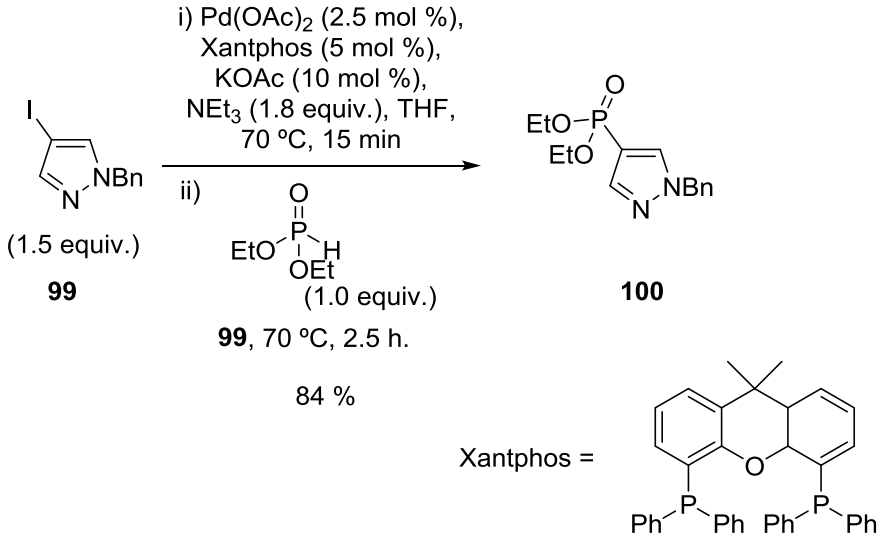

Scheme 21: Hirao cross-coupling of iodopyrazole **99** with diethyl phosphite to give phosphonate **100**.[128]

Lilley's synthesis routes to diethyl Boc protected pyrazolylalanine **55** (Scheme 14 and 15, pages 33-34) can be used as potential guides in the retrosynthetic analysis of dibenzyl Fmoc protected pyrazolylalanine **91**. Lilley's more convergent route in the synthesis of diethyl Boc protected pyrazolylalanine **55** included a step in which diethyl pyrazole phosphonate **59** underwent a ring opening reaction with Boc β-lactone **50** in the presence of base 1,8-

diazabicyclo[5.4.0]undec-7-ene (DBU) (Scheme 15, page 35).[1] Using the less convergent synthesis of diethyl Boc protected pyrazolylalanine **55** (Scheme 14, page 34) would likely require additional protection and deprotection steps after the β-lactone ring opening reaction with iodopyrazole **51**.

Hence, the retrosynthetic analysis begins with functional group interconversion (FGI) of dibenzyl Fmoc protected pyrazolylalanine **91** to compound **101** (Scheme 22). A disconnection between the nitrogen carbon bond gives the pyrazole anion synthon **102** and alanine beta cation **103**. A plausible synthetic equivalent for the pyrazole anion synthon **102** is phosphonate **104** which can be taken back to dibenzyl phosphite and pyrazole **108**. There are a few potential alanine beta cation **103** synthetic equivalents, and based on literature precedent β-lactone **105**[1] and serine **106**[130] (*vide infra*) have been selected to be most suitable for the synthesis of dibenzyl Fmoc protected pyrazolylalanaine **91**.

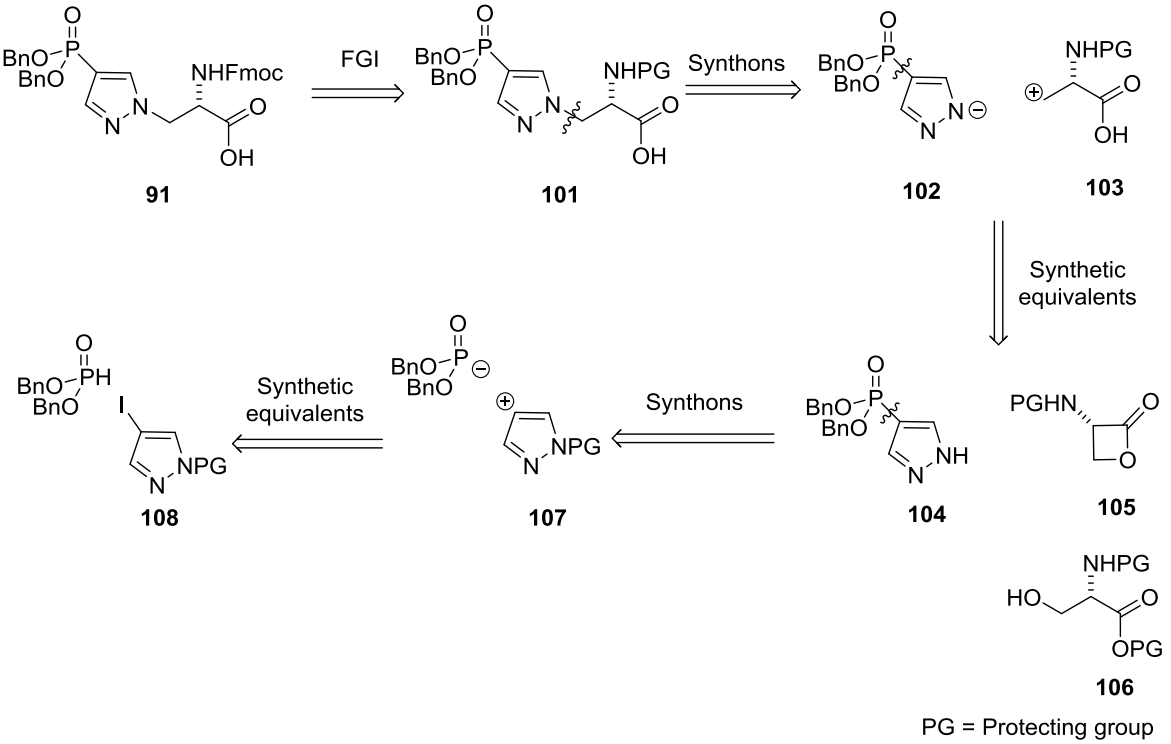

91 **101** **102** **103** **104** **105** **106** **107** **108**

Scheme 22: Retrosynthetic analysis of dibenzyl Fmoc protected pyrazolylalanine carboxylic acid **91**.

3.1.1.1: Synthesis of dibenzyl pyrazole phosphonate

Before attempting any Hirao cross coupling reactions on iodopyrazole **51** type derivatives, iodopyrazole **51** needed to be first synthesised (Scheme 23). Following a literature method, the electrophilic iodination of pyrazole **109** was carried out in the presence of 0.6 equiv. of iodine and ceric ammonium nitrate (CAN) as the oxidant which gave pyrazole **51** in near quantitative yield (Scheme 23).[131] This reaction could be performed on a multigram scale without a compromise in yield.

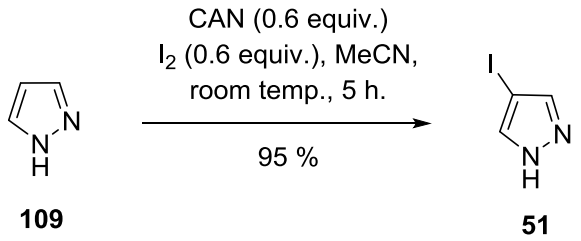

109 **51**

Scheme 23: Iodination of pyrazole **109**.

To show in principle iodo aromatics are suitable in Hirao cross coupling reactions with dibenzyl phosphite, a model reaction between iodobenzene **110** and dibenzyl phosphite was carried out following Kalek *et al.* procedure (Scheme 24, b).[127] Phosphonate **98** was isolated in a comparable yield of 74 %, to the 72 % reported by Kalek *et al*. with bromobenzene **97** (Scheme 20).[127] However, when pyrazole **51** was used under these conditions the reaction failed to give any of the desired product **104** (Scheme 23, b) and pyrazole **51** was recovered. Changing the base from caesium carbonate to trimethylamine gave no product **104**.

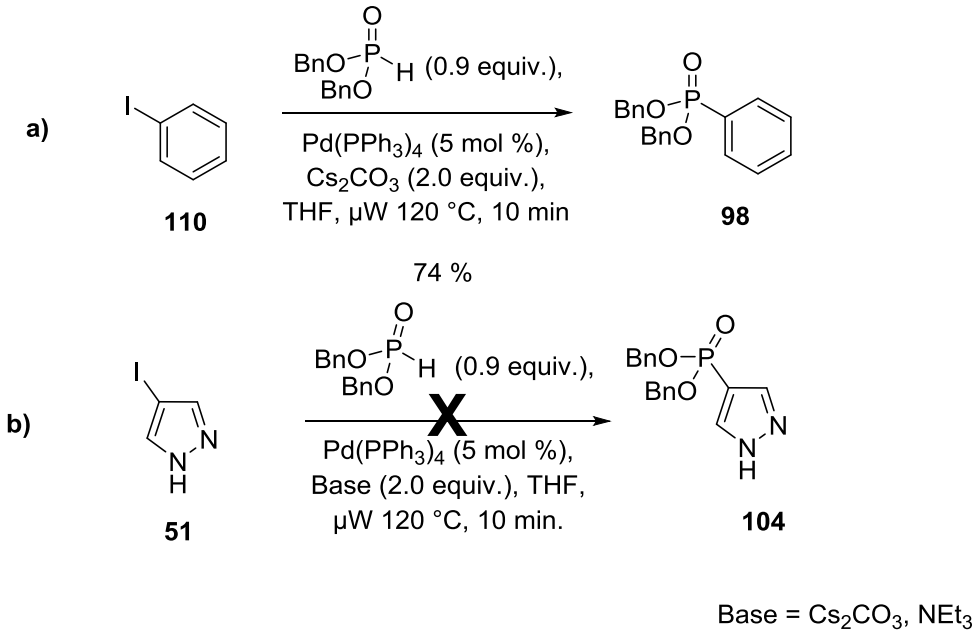

Scheme 24: a) Hirao cross-coupling reaction of iodobenzene **110** with dibenzyl phosphite; **b**) attempted synthesis of dibenzyl pyrazole phosphonate **104**.

3.1.1.2: Boc β-lactone synthesis

Tran *et al*. has previously shown that Xantphos is an excellent ligand in the Hirao cross coupling reaction involving protected pyrazole substrates (Scheme 21).[128] Application of Tran *et al*. reaction conditions on unprotected iodopyrazole **51** and dibenzyl phosphite gave the desired phosphonate **104** in moderate yields (Scheme 25, and Table 2). The crude NMR spectrum indicated extensive monobenzylated pyrazole by the presence of a benzyl methylene chemical shift at 4.94 ppm. It was thought by increasing the catalyst loading, and changing to a bulkier base, N,N-diisopropylethylamine (EtN^iPr_2) from triethylamine, debenzylation by the iodide anion could be suppressed. An increased phosphonate **104** yield of 60 % was obtained after monitoring the consumption of iodopyrazole **51** by TLC. Halving the catalyst loading decreased yields. A 49 % yield was obtained under reflux. It may be

possible to carry out the reaction at lower temperatures, which could allow for lower reagent equivalence and catalyst loading but further optimization was not pursued.

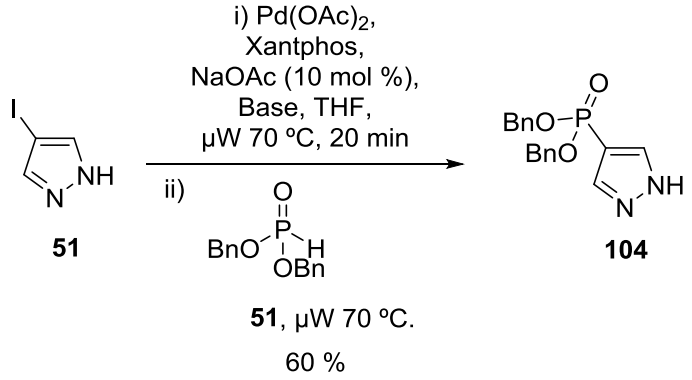

Scheme 25: Synthesis of dibenzyl pyrazole phosphonate **104**.

Table 2: Condition used in the synthesis of dibenzyl pyrazole phosphonate **104** outlined in Scheme 25.

Dibenzyl phosphite (equiv.)	Base (equiv.)	$Pd(OAc)_2$ (mol %)	Xantphos (mol %)	Coupling time (min)	Obtained yield (%)
1.0	NEt_3 (1.8)	2.5	5	150	38
2.2	EtN^iPr_2 (2.0)	10	20	45	60

Lilley *et al*. synthesised diethyl Boc protected pyrazolylalanine **55** from the ring opening reaction of diethyl pyrazole phosphonate **59** with Boc β-lactone **50** which required the base DBU (Scheme 15, page 34). The ring opening reaction between dibenzyl pyrazole phosphonate **104** and Boc β-lactone **50** following Lilley's reaction conditions gave dibenzyl Boc protected pyrazolylalanine **111** in 28 % yield (Scheme 26); comparable to the diethyl Boc protected pyrazolylalanine **55** yield of 34 % (Scheme 15, page 34). Though both Boc and phosphoryl benzyl esters can be removed with trifluoroacetic acid (TFA),[115] selective Boc

deprotection was achieved with TFA in dichloromethane (DCM)[132] and subsequent Fmoc protection[133] gave the desired product **91** in good yield.

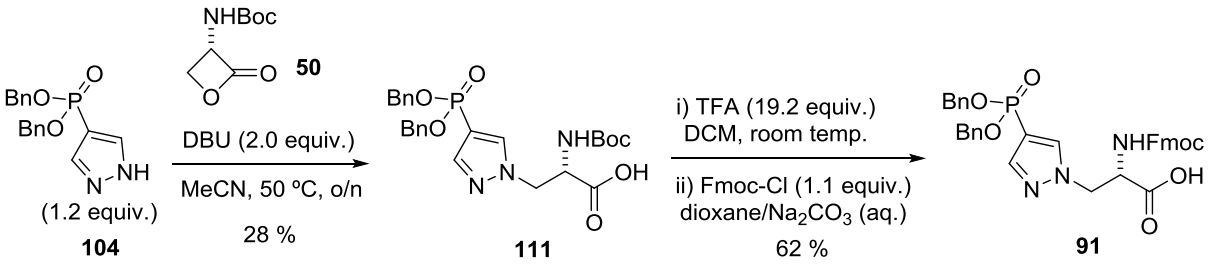

Scheme 26: Synthesis of dibenzyl Fmoc protected pyrazolylalanine carboxylic acid **91**.

Despite the successful synthesis of dibenzyl Fmoc protected pyrazolylalanine **91**, the synthesis shown in Scheme 26 was not synthetically satisfactory. The synthesis of Boc β-lactone **50** can be poor yielding on a large scale, and due to its unstable nature, it can degrade during purification. In addition, the key ring opening reaction of Boc β-lactone **50** with dibenzyl pyrazole phosphonate **104** gave a low yield. Hence, alternative routes were explored.

3.1.1.3: β-lactone salt synthesis

Vederas has previously shown that pyrazole **109** can undergo a ring opening reaction with β-lactone salt **112** to give amino acid **113** (Scheme 27).[134] Such a reaction is useful because the resulting amino acid amine can be subsequently derivatised. Whether dibenzyl pyrazole phosphonate **104**, is a reactive enough nucleophile to undergo a ring opening reaction with β-lactone salt **112** would have to be seen. However, since the β-lactone **112** is a bench stable and easily accessible compound,[134-136] the reaction between β-lactone salt **112** and dibenzyl pyrazole phosphonate **104** was thought to be worth an attempt.

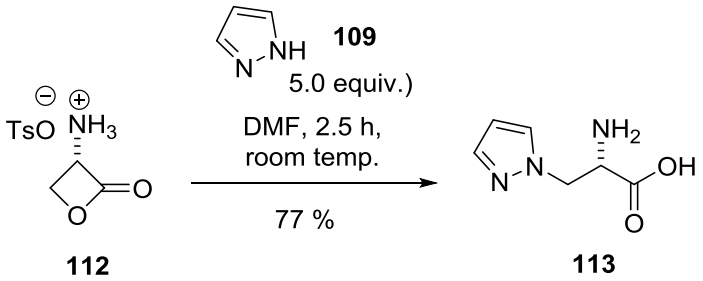

Scheme 27: Synthesis of pyrazole amino acid **113**.[134]

The synthesis of β-lactone salt **112** began with the N protection of L-serine **114** using the reagent trityl chloride following a "one pot" synthesis procedure reported by Barlos *et al*. (Scheme 28).[137] L-serine **114** was globally protected with trimethylsilyl chloride (TMSCl) to form silyl **115** *in situ*. Treatment with methanol selectively removed the N-protected trimethylsilyl (TMS) group and the resulting amine **116** was N-trityl protected to give compound **117**. A final treatment with excess methanol gave the desired N-trityl protected L-serine **118**.

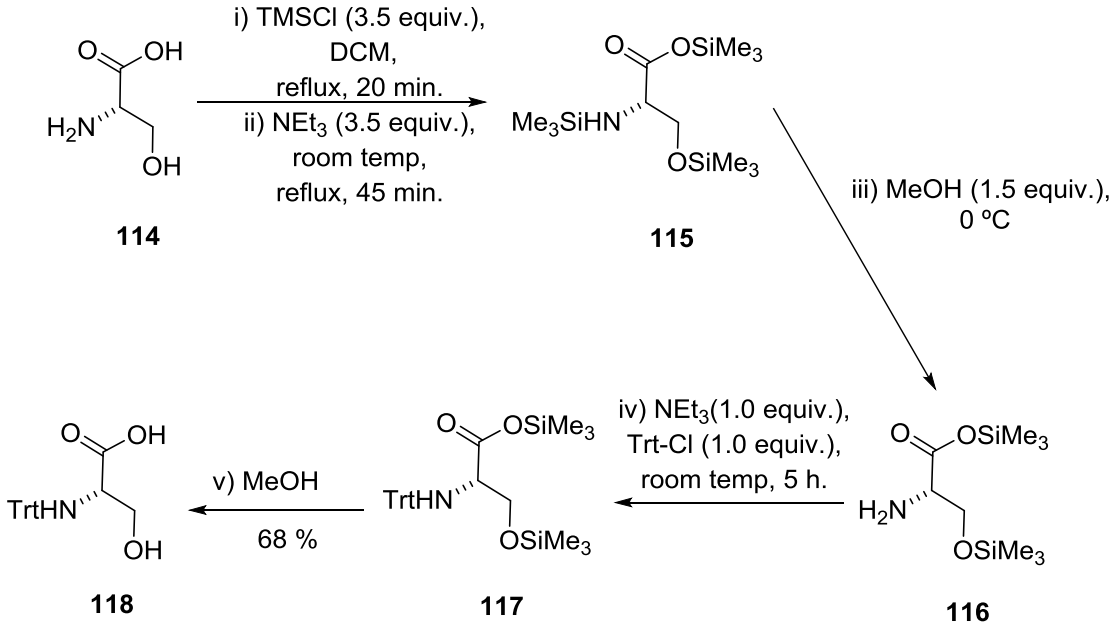

Scheme 28: One pot synthesis of N-trityl protected L-serine **118.**

N-trityl protected L-serine **118** was cyclised using a benzotriazol-1-yloxy)tris(dimethylamino)phosphonium hexafluorophosphate (BOP)-mediated ring closure to form trityl β-lactone **119** following reported procedures (Scheme 29).[134-136] Unlike Boc β-lactone **50**,[138] trityl β-lactone **119** was much more stable[136] and the synthesis was higher yielding. Treatment of trityl β-lactone **119** with TFA in the presence para-toluenesulfonic acid gave the β-lactone salt **112** in excellent yield. Both steps were reproducible on a gram scale.[134,135]

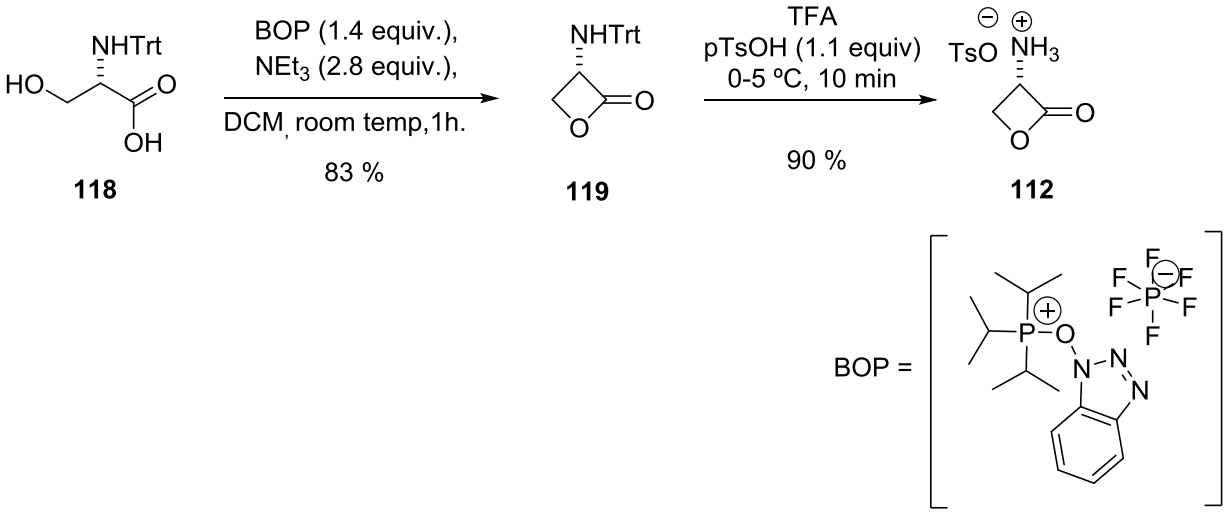

Scheme 29: Two step synthesis of β-lactone salt **112** from N-trityl protected L-serine **118**.

Unlike pyrazole **109** in Scheme 27 dibenzyl pyrazole phosphonate **104** did not undergo a ring opening reaction with β-lactone salt **112** to give amino acid **120** (Scheme 30, and Table 3). Increasing the temperature to 50 ^{o}C and/or adding base DBU gave the same result. Only pyrazole **104** was recovered after cation exchange chromatography. The presence of the electron withdrawing phosphoryl group in dibenzyl pyrazole phosphonate **104** would suggest it is a weaker nucleophile than pyrazole **109**. Furthermore, the ring opening reaction between dibenzyl pyrazole phosphonate **104** (Scheme 26) and diethyl pyrazolyl phosphonate **59**

(Scheme 15, page 35) with Boc β-lactone **50** required the strong base DBU. DBU deprotonates dibenzyl pyrazole phosphonate **104** and diethyl pyrazolyl phosphonate **59** giving a stronger nucleophile which can then react with Boc β-lactone **50.**

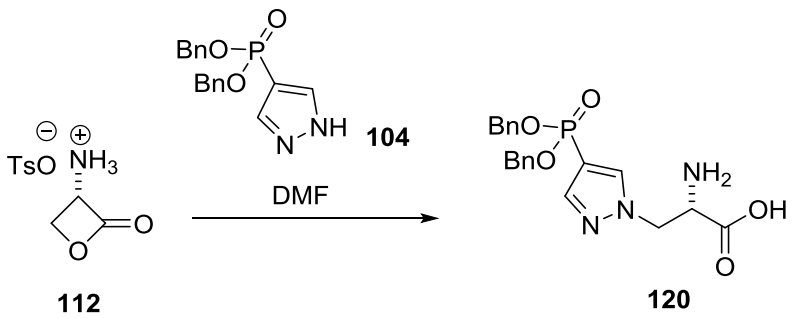

Scheme 30: Ring opening reaction between β-lactone salt **112** and dibenzyl pyrazole phosphonate **104**.

Table 3: Conditions used in the reaction between dibenzyl pyrazole phosphonate **104** and β-lactone salt **112** outlined in Scheme 30.

Temp	Time	DBU (equiv.)	Compound 104 (equiv.)	Yield (%)
Room temp.	o/n	0	5	0
50 °C	o/n	0	5	0
Room temp.	2.5 h.	1	5	0
Room temp.	2.5 h.	6	5	0
Room temp.	2.5 h.	1	1	0
50 °C	2.5 h.	6	5	0

In the reaction between β-lactone salt **112** and dibenzyl pyrazole phosphonate **104**, DBU will first deprotonate the more acidic ammonium cation of β-lactone salt **112** rather than the dibenzyl pyrazole phosphonate **104** to give β-lactone **121** which then presumably polymerises or degrades (Scheme 31). The realisation that dibenzyl pyrazole phosphonate **104** was not a

suitable nucleophile for β-lactone salt **112**, prompted the search for another synthetic route for dibenzyl Fmoc protected pyrazolylalannine **91**.

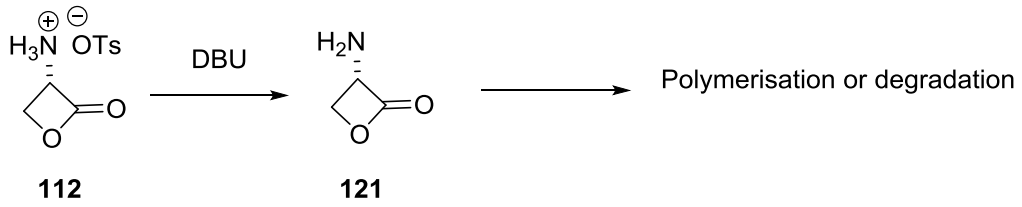

Scheme 31: Proposed preferential deprotonation of β-lactone salt **112** by DBU and assumed degradation of β-lactone **121**.

3.1.1.4: Mitsunobu synthesis

The Mitsunobu reaction is a useful method for forming carbon oxygen, carbon nitrogen and carbon sulphur bonds. Krenk *et al*. synthesised compound **123** in good yield from the reaction of protected L-serine **122** and phenol under Mitsunobu conditions (Scheme 32).[130,139] The Mitsunobu reaction usually requires the pronucleophile to have $pK_a < 11$.[139] The pk_a of pyrazole **109** is 20.4[140] which would suggest that it is an non ideal pronucleophile. However, the pK_a of dibenzyl pyrazole phosphonate **104** will have a lower pK_a than pyrazole **109** due the presence of the electron withdrawing phosphoryl group and is potentially a suitable pronucleophile for the Mitsunobu reaction.

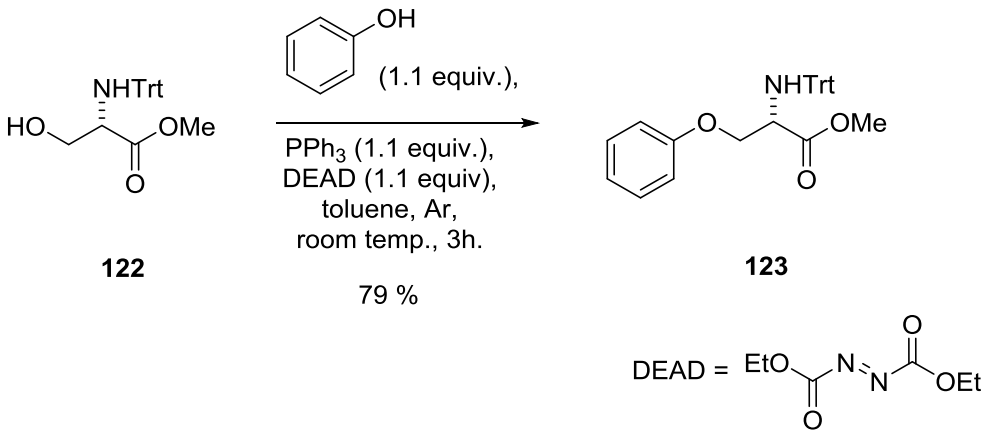

Scheme 32: The Mitsunobu synthesis of compound **123.**[130]

Following literature sources, the synthesis of protected L-serine **122** began with the esterification of L-serine **114** using acetyl chloride as the acid source and methanol (Scheme 33).[141] The hydrochloride salt **124** was subsequently N-trityl protected to give L-serine **122** in moderate yields.[142] Under similar Mitsunobu conditions as Scheme 32 dibenzyl trityl protected pyrazolylalanine **125** was synthesised in good yield. Initial exploration of this approach was carried out by an undergraduate project student, Kiera Bailey, under my supervision; the results reported are my own, however. The trityl group of dibenzyl trityl protected pyrazolylalanine **125** was selectively removed using TFA and then N-Fmoc protected to give dibenzyl Fmoc protected pyrazolylalanine **126**. The final methyl ester hydrolysis was not carried out but treatment with trimethyltin hydroxide[143] (see Scheme 10, page 30) is expected to give the desired dibenzyl Fmoc protected pyrazolylalanine carboxylic acid **91**.

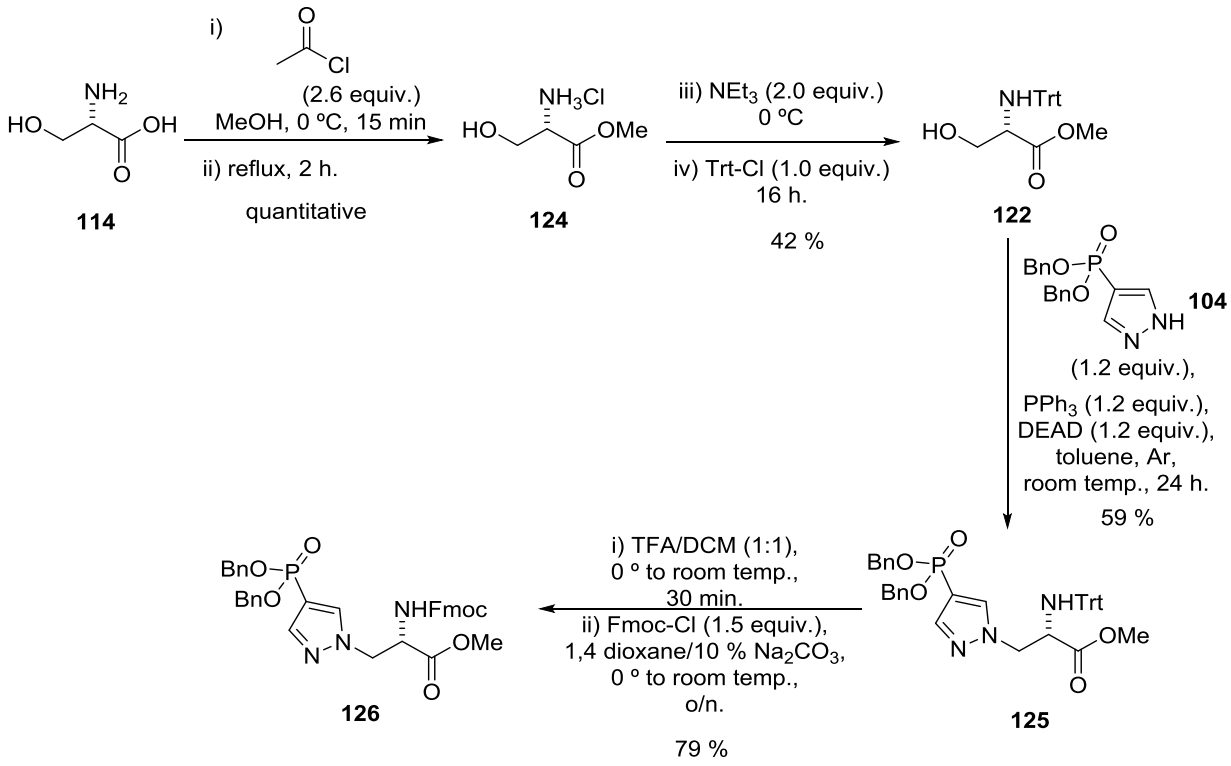

Scheme 33: Synthesis of dibenzyl Fmoc protected pyrazolylalanine **126** using a Mitsunobu step.

3.1.2: Synthesis of pyridine τ- and π-pHis analogues

pHis analogues, pyrazolylalanine **56** and pyrazolylethylamine **61** bearing the phosphopyrazolyl residue have proved to be useful in the generation of pHis antibodies (see section 1.5.3). On the other hand, Lilley has used the 2,4-disubstituted pyridine **68** and 2,5-disubstituted pyridine **72** in the generation of pHis antibodies, suggesting the phosphopyridyl moiety has potential as a pHis analogue (see section 1.5.4). According to the ESP isocontour calculations, the 3,5-disubstituted pyridine model **86** (Figure 12, page 42) has a more negative ESP on the pyridine nitrogen than the pyrazole model **76** nitrogen and is more similar to the nitrogen of the τ-pHis model **76** (Figure 9, page 40). Whilst the 3,4-substituted pyridine model **90** does not have the additional negative ESP region seen in the triazole model **88** and has negative ESP regions similar to the π-pHis model **87** (Figure 13, page 43).

Furthermore, the chemistry used in the synthesis of 2,4-disubstituted pyridine **68** and 2,5-disubstituted pyridine **72** (Scheme 18 and 19) will be applicable in the synthesis of 3,5-disubstituted pyridine amino acid **127** and 3,4-disubstituted pyridine amino acid **129**, making these pHis analogues rapidly accessible (Figure 15). 3,5-Disubstituted pyridine amino amide **128** and 3,4- disubstituted pyridine amino amide **130** will also be pursued because in earlier work the primary amides have worked well in the generation of selective phospho residue antibodies.[111,112,144]

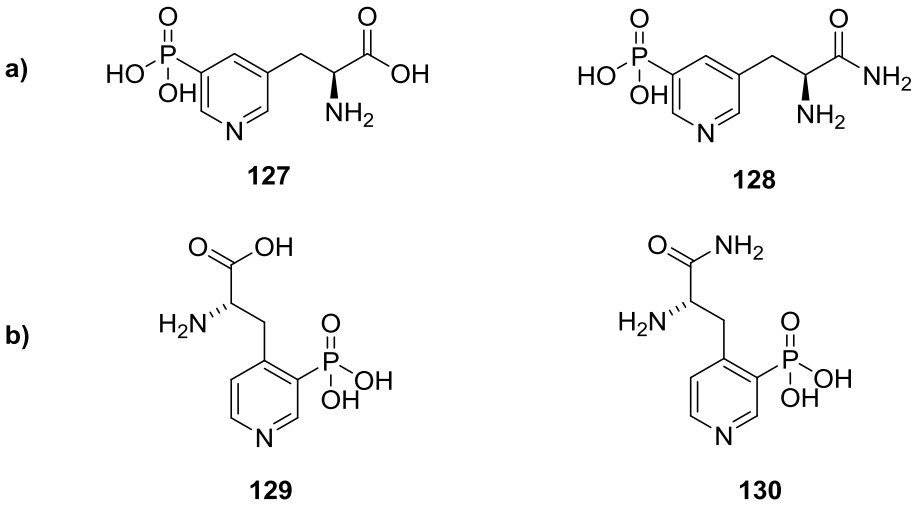

Figure 15: Pyridine pHis analogues proposed for synthesis: **a**) τ-pHis analogues, 3,5-disubstituted pyridine amino acid **127** and 3,5-disubstituted pyridine amino amide **128**; **b**) π-pHis analogues, 3,4-disubstituted pyridine amino acid **129** and 3,4-disubstituted pyridine amino amide **130**.

A general retrosynthetic analysis of phosphopyridine amino acids/amides is shown in Scheme 34, where the order of phosphorus carbon and carbon carbon bond formation can be altered depending on the starting dihalogenated pyridine. The type of halogen atom and its position in the pyridine ring will determine the most reactive position and the order the phosphoryl group is introduced by Hirao reaction or the alanine group by the Negishi reaction.[120] Hence, the starting dihalogenated pyridine must be carefully chosen.

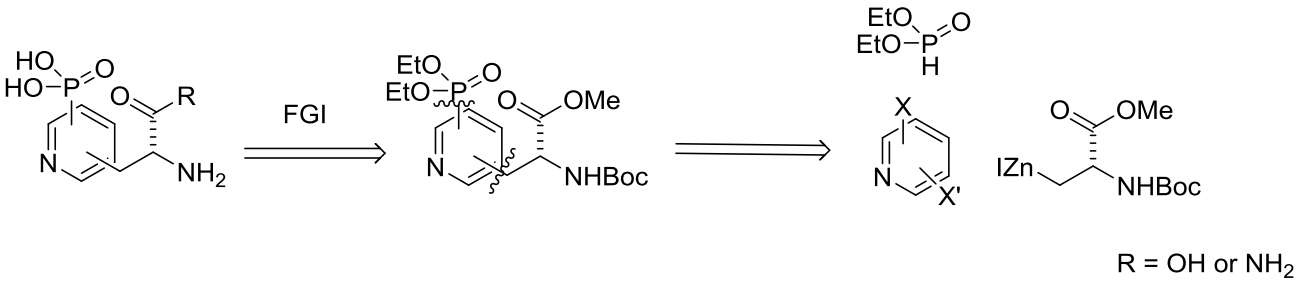

Scheme 34: General retrosynthesis of disubstitutted phosphopyridine amino acids/amino amides**.**

Protected iodoalanine **131** can be synthesised on a multigram scale and is the compound used to make zinc reagent **13** (Scheme 35).[141,145] Protected iodoalanine **131** can then undergo zinc insertion with activated zinc. Activated zinc refers to using chemical or mechanical means to release zinc from zinc covered in zinc oxide. In this work Huo's method of iodine activation[146] which has previously worked well with protected iodoalanine **131**[147] was used.

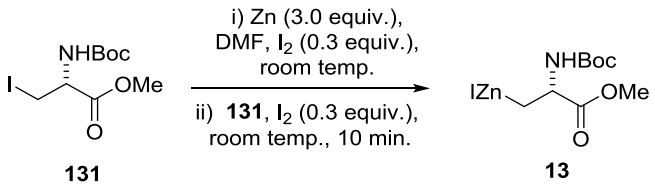

Scheme 35: Zinc insertion into protected iodoalanine **131** to form zinc reagent **13**.

3.1.2.1: Synthesis of 2,4-disubstituted pyridine

The 2,4-disubstituted pyridine **68** has been previously synthesised by Lilley (Scheme 18, page 37) and gave promising pHis antibodies (see section 1.5.4). In the preparation for the synthesis of the newly identified 3,5-disubstituted pyridine amino acid **127** and 3,4-disubstituted pyridine amino acid **129,** the synthesis of 2,4-disubstituted pyridine **68** was revisited (Figure 16). In addition, in the preparation for the synthesis of 3,5-disubstituted pyridine amino amide **128** and 3,4- disubstituted pyridine amino amide **130**, the 2,4-disubtituted pyridine amino amide **132** was also pursued.

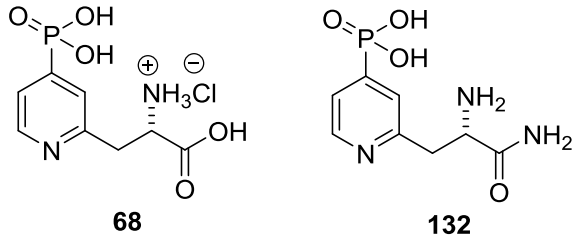

68 **132**

Figure 16: Revisiting the synthesis of 2,4-disubstituted pyridine **68** and the synthesis of 2,4-disubstituted pyridine amino amide **132.**

The synthesis of 2,4-disubstituted pyridine **67** began with the Hirao cross coupling of 2-chloro-4-iodopyridine **65** with diethyl phosphite which gave diethyl 2-chloropyridine phosphonate **66** in 36 % yield (Scheme 36) and was lower than the 49 % yield reported by Lilley (Scheme 18, page 37). This may have been due to an old sample of 2-chloro-4-iodopyridine **65** used**.** Di phosphorylation was not observed in the crude ^{1}H NMR spectrum. Negishi cross coupling of diethyl 2-chloropyridine phosphonate **66** with 2 equivalents of zinc reagent **13** gave 2,4 disubstituted pyridine **67** in an increased yield of 61 % compared to the 42 % reported by

Lilley who used 3 equivalents of zinc reagent **13** (Scheme 18, page 37). The increased yield may have been a result of syringe transferring the zinc reagent **13** away from excess zinc which could otherwise potentially react with diethyl 2-chloropyridine phosphonate **66**, and then transferring the zinc reagent **13** into the flask containing diethyl 2-chloropyridine phosphonate **66**.

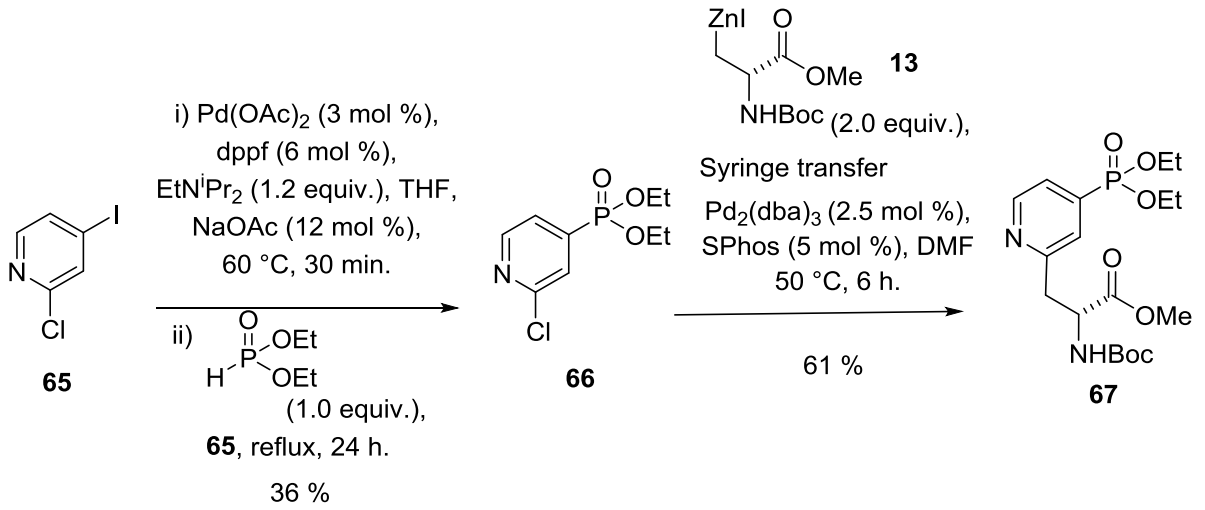

Scheme 36: Synthesis of 2,4-disubstituted pyridine **67**.

2,4-Disubstituted pyridine **67** was deprotected using a two-step procedure, first by ester hydrolysis using lithium hydroxide and a subsequent treatment with TMSBr (Scheme 37). The crude was purified by silica gel chromatography to give the 2,4-disubstituted pyridine amino acid **133**. The corresponding 2,4-disubstituted amino amide **132** was synthesised by amidation with ammonia and a subsequent treatment with TMSBr.

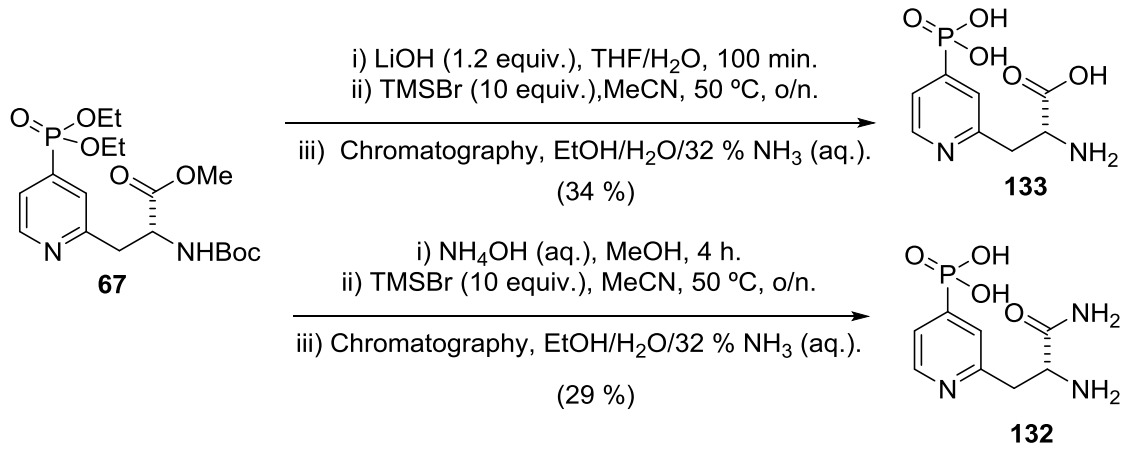

Scheme 37: Synthesis of 2,4-disubstituted pyridine amino acid **133** and 2,4-disubstituted pyridine amino amide **132.**

3.1.2.2: Synthesis of 3,5-disubstituted pyridine

Zon *et al*. have reported the synthesis of pyridine **135** by Hirao cross coupling using diethyl phosphite, 3,5-dibromopyridine **134** and a tetrakis(triphenylphosphine)palladium(0) catalyst (Scheme 38).[148] The study reported UV, ^{31}P NMR, IR and elemental analysis data for diethyl 3-bromopyridine phosphonate **135** but no ^{1}H NMR, ^{13}C NMR, and MS. Following their experimental procedure, a 26 % yield was obtained compared to the 43 % reported.[148]

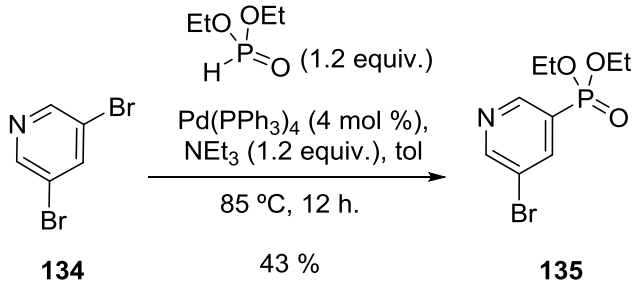

Scheme 38: Zon *et al*. Hirao cross coupling synthesis of diethyl 3-bromopyridine phosphonate **135**.[148]

However, a higher yield of 45 % was obtained when applying the Hirao cross coupling conditions used in the synthesis diethyl 3-chloropyridine **66** (Scheme 36) with a palladium(0) dppf ligand complex (Scheme 39). Bis phosphorylation was expected because diethyl 3-bromopyridine phosphonate **135** is more reactive than 3,5-dibromopyridine **134**. The crude ^{1}H NMR spectrum suggested the presence of some bis phosphorylated pyridine (1:5 bis:mono) from additional aromatic chemical shifts at 8.50 ppm (triplet of triplets) and 9.12 ppm (multiplet). Negishi cross coupling of halogenated pyridines with zinc reagent **13** have typically worked well in the presence of bis(triphenylphosphine)palladium chloride.[120] Negishi cross coupling of diethyl 3-bromopyridine phosphonate **135** with zinc reagent **13** using bis(triphenylphosphine)palladium chloride gave the desired 3,5 disubstituted pyridine **136** in good yield.

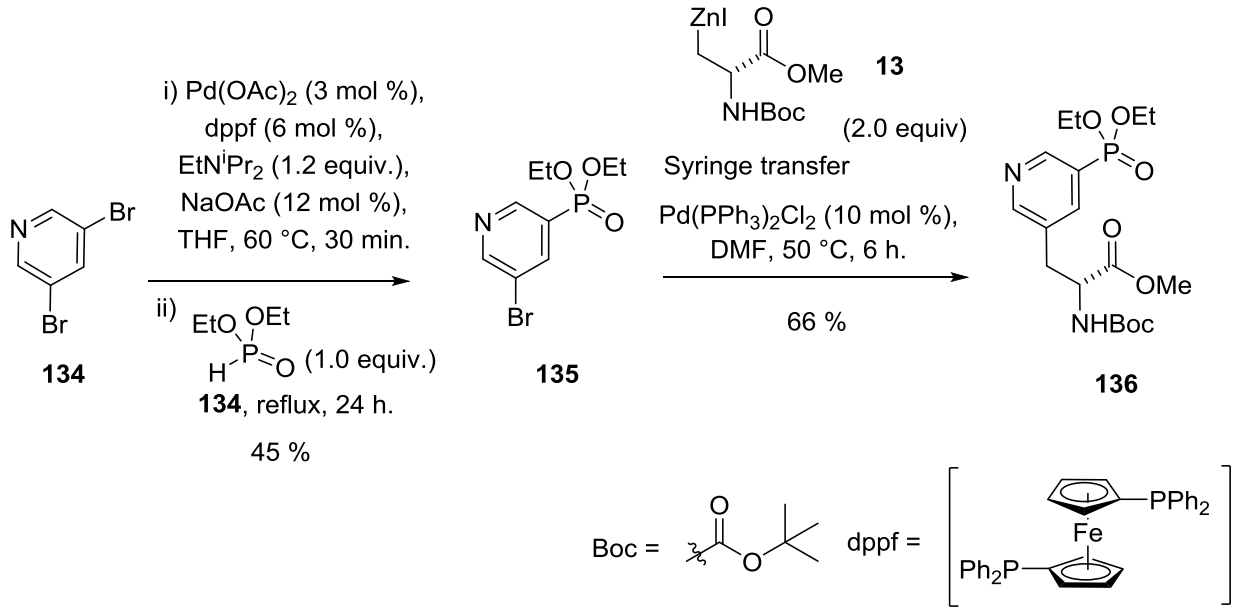

Scheme 39: Synthesis of 3,5-disubstituted pyridine **136**.

3,5-Disubstituted pyridine **136** was globally deprotected by refluxing in aqueous 6 M hydrochloric acid, and the desired 3,5-disubstituted pyridine amino acid **127** was isolated after chromatographic purification (Scheme 40). Treatment of 3,5-disubstituted pyridine **136** with ammonia and subsequently with TMSBr gave the desired 3,5-disubstituted pyridine amino amide **128** after chromatographic purification.

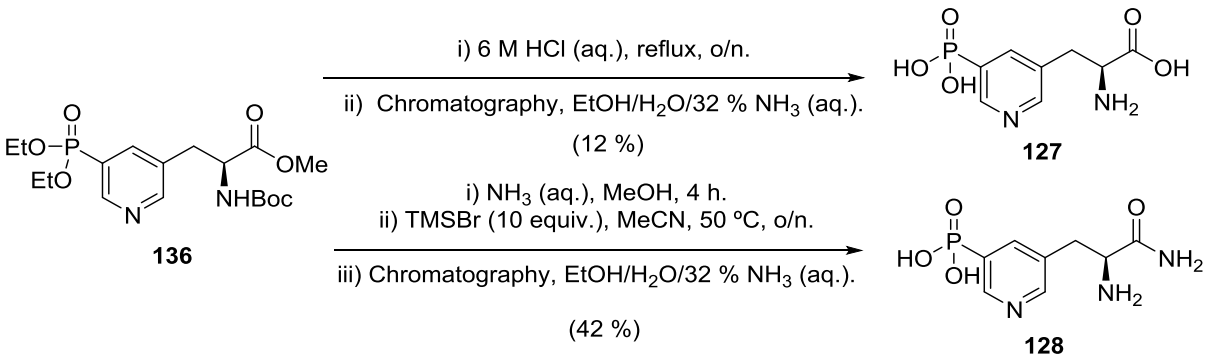

Scheme 40: Synthesis of 3,5-disubstituted pyridine amino acid **127** and3,5-disubstituted pyridine amino amide **128.**

3.1.2.3: Synthesis of 3,4-disubstituted pyridine

3,4-Disubstituted pyridine **137** has been shown in Negishi cross coupling reactions to react selectively at the four position and then subsequently in the three position using palladium chemistry.[149] Negishi cross-coupling of zinc reagent **13** with 3,4-dibromopyridine **137** gave diethyl 3-bromopyridine phosphonate **138** in good yield (Scheme 41). There was a significant upfield shift of the 5-position aromatic proton of diethyl 3-bromopyridine phosphonate **138** from 7.61 ppm in 3,4-dibromopyrdine **137** to 7.19 ppm, suggesting substitution had occurred in the four position. Neither the three or bis substitution was observed in the crude ^{1}H NMR spectrum. 3,4-Disubstituted pyridine **139** was synthesised in low yields (~5 %) from diethyl 3-bromopyridine phosphonate **138** using the Hirao cross coupling conditions described in

Scheme 40**.** Guilard *et al*. had reported Hirao cross coupling which gave good yields on ortho substituted pyridines,[150] noticeably, ethanol was used as the solvent and triphenylphosphine (PPh_3) as the palladium ligand. On application of these conditions with diethyl 3-bromopyridine phosphonate **138**, 3,4 disubstituted pyridine **139** was isolated 55 % yield (Scheme 41).

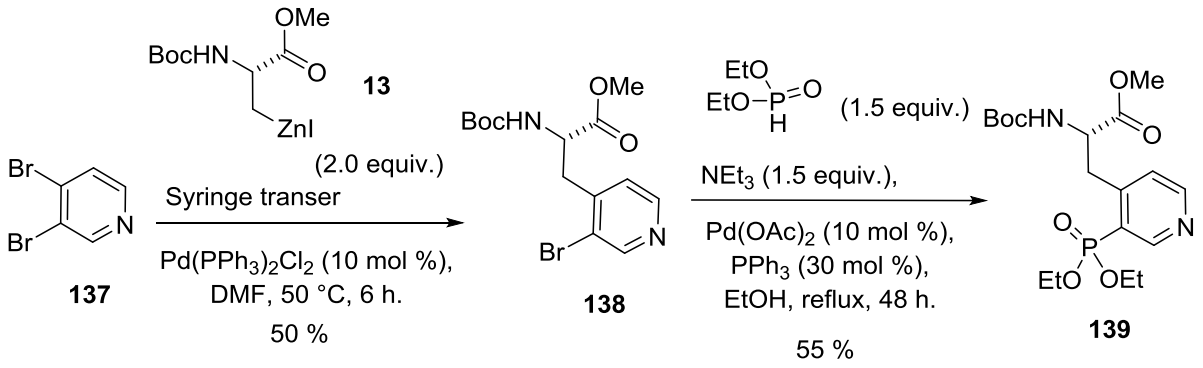

Scheme 41: Synthesis of 3,4-disubstituted pyridine **139**.

The same conditions used in the deprotection and amidation of 3,5-disubstituted pyridine **136** (Scheme 40) were used on 3,4-disubstituted pyridine **139** (Scheme 42). 3,4-Disubstituted pyridine **139** was globally deprotected by refluxing in aqueous 6 M hydrochloric acid, and desired 3,4-disubstituted pyridine amino acid **129** was isolated after chromatographic purification. Treatment of 3,4-disubstituted pyridine **139** with ammonia and subsequently with TMSBr gave the desired 3,4-disubstituted pyridine amino amide **130** after chromatographic purification.

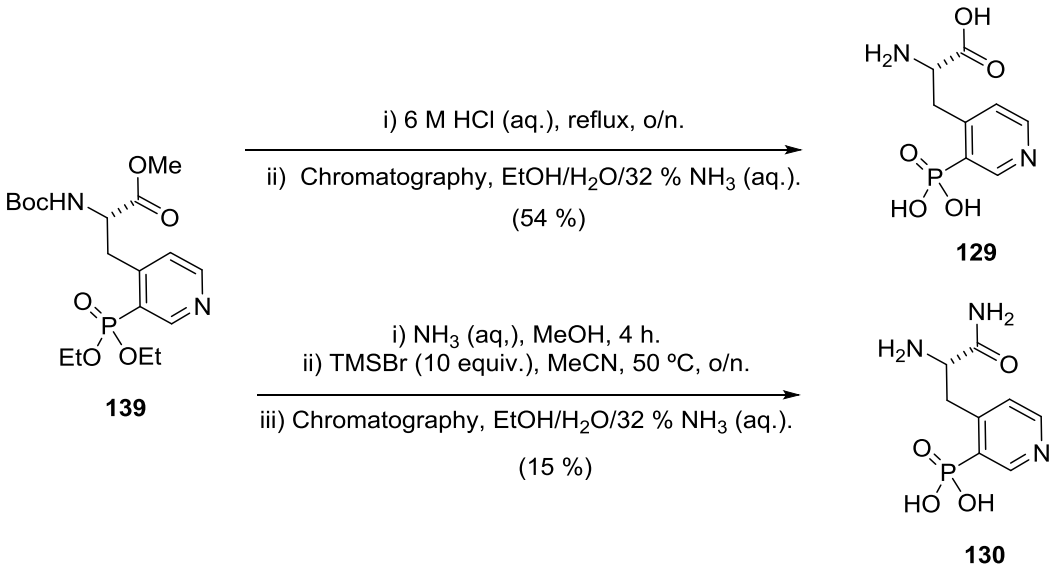

Scheme 42: Synthesis of 3,4-disubstituted pyridine amino acid **129** and 3,4-disubstituted pyridine amino amide **130.**

3.1.3: Pyrazole and 3,4-disubstituted pyridine competitors

Pyrazolylethylamine **61** and 3,4-disubstituted pyridine amino amide **130** (Figure 17) were found to give highly selective τ-pHis and π-pHis antibodies respectively (see section 3.2). As described in section 1.5, antibodies can be used in a range of immunological techniques, with one of the most important being in sample enrichment. In preparation for using τ-pHis and π-pHis antibodies in the enrichment of pHis protein, complementary chemical tools need to be synthesised.

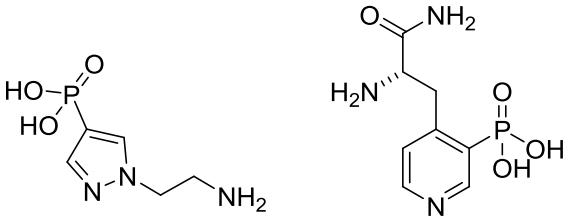

Figure 17: Selective τ-pHis and π-pHis antibodies generated to pyrazolylethylamine **61** and 3,4-disubstituted pyridine amino amide **130** respectively (see section 3.2).

During a sample enrichment there comes a point where the pHis protein/peptides bound to the antibody must be dissociated. The most common method of dissociation is treatment with 0.1 M glycine at pH 2.2. These conditions are not suitable for pHis as they would rapidly hydrolyse pHis residues. Having a compound which could be used to compete for the pHis antibody binding site was important if gentle elution method was to be applied. Using pHis as a competitor is not suitable because the pHis phosphoryl group of pHis can be transferred to other His residues, which could give rise to false positives (see section 1.2).

The best antibody binding site competitors would be the compounds used to generate the pHis antibodies, in this case pyrazolylethylamine **61** and 3,4-disubstituted pyridine amino amide **130**. However, both pyrazolylethylamine **61** and 3,4-disubstituted pyridine amino amide **131** have amine groups which could potentially dephosphorylate pHis,[84] furthermore synthesising them on a multi milligram scale would not be practical. A pyrazole with a n-butyl tail, pyrazole **140** was envisaged as an acceptable replacement as a competitor for pyrazolylethylamine **61**, in which the amine has been replaced with an ethyl group. A n-butyl chain in the four position of 3,4-disubstituted pyridine **130** as in pyrazolylbutane **140** was desirable but introducing a n-butyl chain in the 4 position is a potentially challenging prospect

using Negishi cross coupling reactions. As a compramise a truncated 4-methyl 3-phosphopyridine was identified as a replacement competitor for 3,4-disubstituted pyridine amino amide **141**.

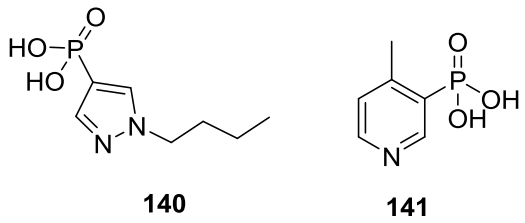

140 **141**

Figure 18: Pyrazole competitor **140** and pyridine competitor **141**.

3.1.3.1: Synthesis of pyrazolylethylamine

Pyrazolylethylamine **61** has been previously synthesised by the Jackson group (Scheme 17) and used as an epitope in antibody generation. However, the antiserum isolated has not yet been purified but stored away at -80 ^{o}C. Therefore, in the preparation for purification of the antiserum and the synthesis of pyrazolylbutane **140**, it was necessary to have pyrazolylethylamine **61** in hand for potential use in assays.

Mukai reported the synthesis of diethyl pyrazole phosphonate **59** from the Hirao reaction of iodopyrazole **51** with diethyl phosphite.[151] Kee *et al*. also followed Mukai's procedure in the synthesis of diethyl pyrazole phosphonate **59** (Scheme 16, page 35).[111] However, in our hands the reaction gave none of the desired product. The experimental procedure described using 10 mL ethanol for a 0.29 mmol scale reaction, which can be considered dilute for palladium assisted reactions. Therefore, it was assumed the stated ethanol volume was incorrect and reducing the ethanol volume to 1 mL gave product **59** in near quantitative yields (Scheme 43). There is no clear explanation for the large discrepancy in the yield by Mukai (47 %)[151] and our near quantitative result.

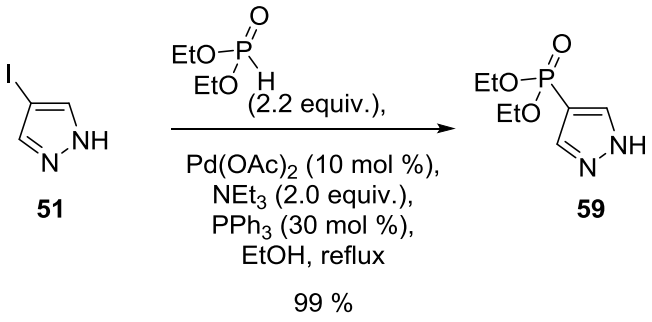

Scheme 43: Synthesis of diethyl pyrazole phosphonate **59**.

Hydrobromide salt **142** was N-Boc protected to give Boc bromoethylamine **60** (Scheme 44)**.** In our hands, following Scheme 16 (page 36), the displacement reaction of bromoethylamine **60** with diethyl pyrazole phosphonate **59** followed by treatment with a 33 % (wt/wt) hydro bromic acid/acetic acid mixture gave only trace amounts of product **61**. ^{1}H NMR analysis of the partially purified mixture suggested the presence of mono phosphate ester. Kee *et al*. did not specify whether the concentration of HBr used for the deprotection was 33 % (wt/v) or 33 % (wt/wt) and 33 % (wt/wt) HBr was assumed. Upon treatment of the crude reaction product between diethyl pyrazole phosphonate **59** and with Boc bromoethylamine **60** with TMSBr in MeCN, the desired product **61** was isolated after chromatographic purification. The low yield was partly due to efforts made to isolate a highly pure sample and the sub-optimal deprotection conditions used.

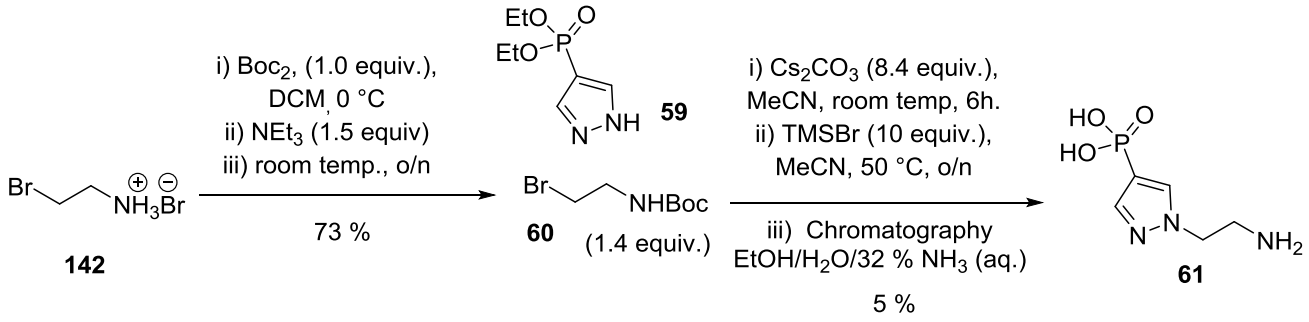

Scheme 44: Synthesis of pyrazolylethylamine **61**.

3.1.3.2: Synthesis of pyrazolylbutane

The synthesise of pyrazolyl **140** began with the displacement reaction between bromobutane **143** and diethyl pyrazole phosphonate **59** to give the intermediate product **144** (Scheme 45). After treatment of pyrazole **144** with TMSBr, and chromatographic purification, the pyrazolylbutane **140** was isolated in 78 % yield. The final yield of pyrazolylbutane **140** is noticeably higher than the yields of pyrazolylethylamine **61** (Scheme 44). The low yield of pyrazolylethylamine **61** was unlikely to have been caused by differences in the electrophile (Boc bromobutane **143** and bromoethylamine **60**), but possibly because the protected intermediate **144** was isolated in Scheme 45 which was not done in Scheme 44, where the crude intermediate was carried forward without purification.

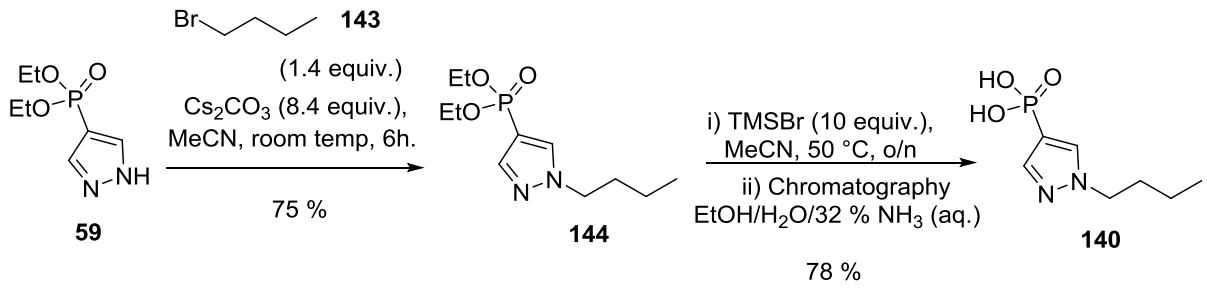

Scheme 45: Synthesis of pyrazolylbutane **140**.

3.1.3.3: Synthesis of 3-methylpyrdine phosphonate

Commercially available 4-methyl-3-bromopyridine **145** was chosen as the starting material in the synthesis of 3-methylpyridine phosphonate **141** (Scheme 46). It was thought that Hirao cross coupling conditions which had worked well in the synthesis of 3,4-disubstituted pyridine **139** (Scheme 41, page 67) could be used on 4-methyl-3-bromopyridine **145**. Indeed, 4-methyl-3-bromopyridine **145** was converted into the diethyl 3-methylpyridine phosphonate **146** by the Hirao cross coupling reaction, which was subsequently deprotected with TMSBr to give the desired product **141.**

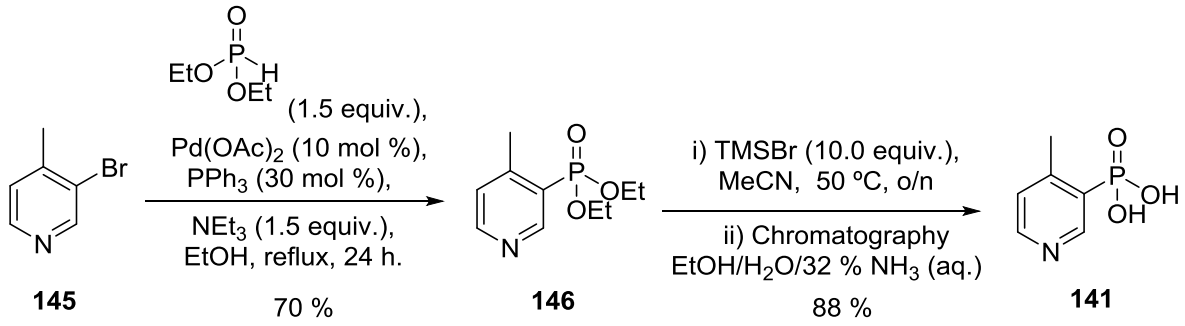

Scheme 46: Synthesis of 3-methylpyridine phosphonate **141**.

3.1.4: Synthesis and purification of τ- and π-pHis

Unlike, pSer, pThr and pTyr, neither pHis isomer is commercially available and pHis standards must be synthesized. The most commonly used phosphorylating agent for His residue is potassium phosphoramidate **1** which gives a mixture of of τ- and π- and p_2His (Scheme 47). The challenge lies in the purification of each isomer without inducing isomer conversion and decomposition. Ion exchange chromatography works well but is poorly yielding,[68,152] whilst other methods do not give salt free products.[70] On the other hand, purification by silica gel

chromatography gives adequate separation, is moderately yielding and both isomers can be isolated salt free.[153]

Potassium phosphoramidate **1** was synthesised following Kee *et al*., with slight modifications (Scheme 47).[80] This method was previously adopted from Wei *et al*.[152] Phosphorus oxychloride **148** was added dropwise to a solution of 10 % (v/v) aqueous ammonia at 4 °C. Significant decomposition to inorganic phosphate (~20 % contamination of final product) was observed if the ammonia solution was not precooled on ice. The ammonium hydrogen phosphoramidate synthesised in the first step was deprotonated in step two with aqueous 50 % (w/v) potassium hydroxide to give potassium phosphoramidate **1**, isolated by precipitation.

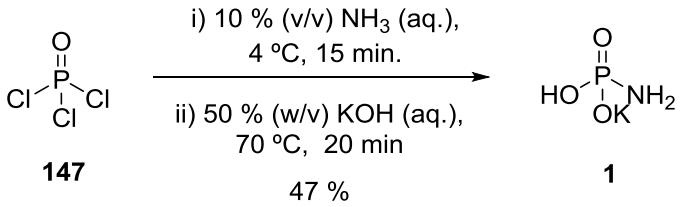

Scheme 47: Synthesis of potassium phosphoramidate **1**.

A time course spectroscopic study for the phosphorylation of His by potassium phosphoramidate under the conditions used has not been previously reported (Scheme 48). In order isolate optimal amounts of π-pHis, it was important to find the time of maximum π-pHis concentration which is known to undergo conversion to τ-pHis during the course of the reaction.[68]

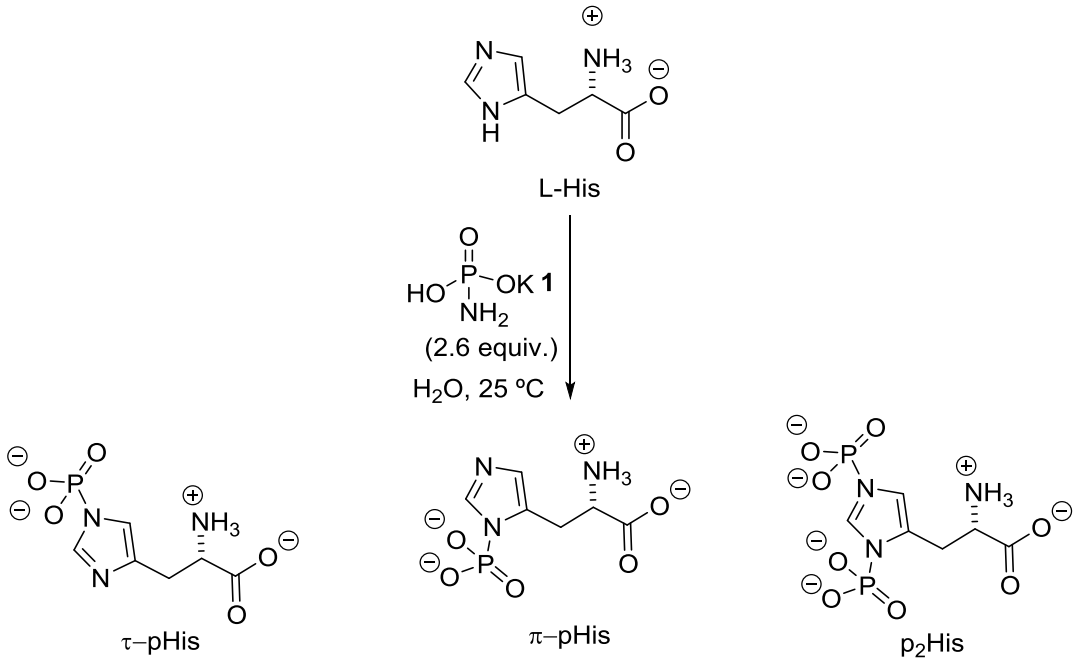

Scheme 48: Reaction of L-His with potassium phosphoramidate **1.**

^{31}P NMR was chosen as the spectroscopic method of choice due to the simplicity of the spectra produced. A spectrum was taken approximately every 20 minutes for 20 hours (Figure 19). Multiple stacked spectra display of p_2His, τ-pHis and π-pHis as a function of time is shown in Figure 19. As the reaction proceeds there is a noticeable upfield change in the chemical shift of both τ- and π-pHis, and a minor upfield change for p_2His. At first it was thought this change was due to a change in pH; however, in 1 M Tris buffer, pH 7.0 near identical ^{31}P NMR profiles were observed. The ^{31}P NMR peak areas (relative to a minor unchanging peak at 13.22 ppm, carried forward from the synthesis of potassium phosphoramidate **1**) of τ-pHis, π-pHis, p_2His, phosphate, and potassium phosphoramidate were plotted against time (Figure 20). After ~8 hours the concentration of τ-pHis had reached an approximate steady state and remained at this level for 20 hours. Whilst the concentrations of π-pHis and p_2His rapidly increased (*vide infra* for details) and then slowly reduced but stayed far below τ-pHis concentrations.

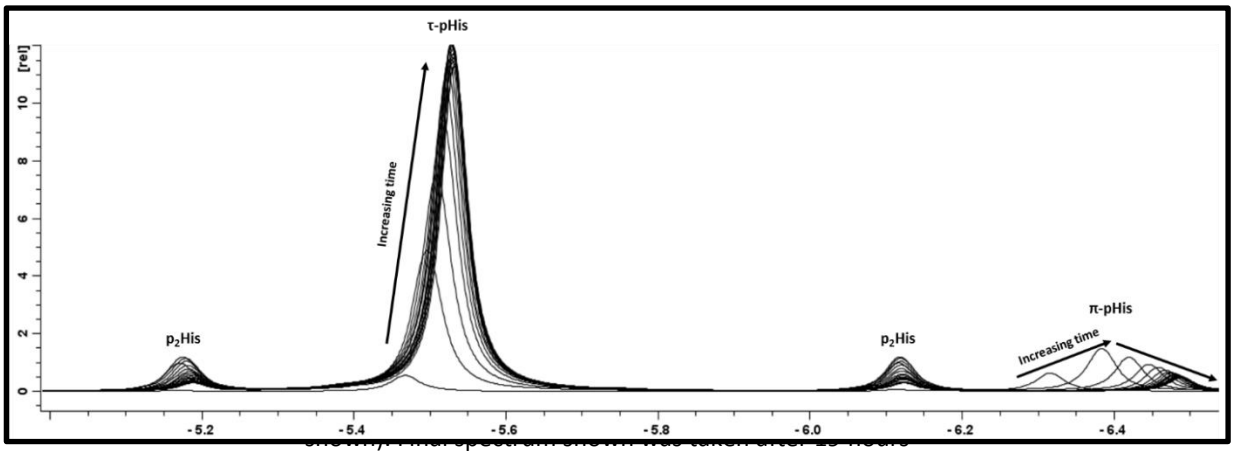

Figure 19: Multiple stacked spectra display time course ^{31}P NMR spectra of p_2His, τ-pHis and π-pHis chemical shifts from the phosphorylation of His (0.36 M) with potassium phosphoramidate **1** (0.93 M) in H_2O (near identical profiles were observed in D_2O). A spectrum was taken at 25 °C approximately every 20 min (not all spectra are shown).

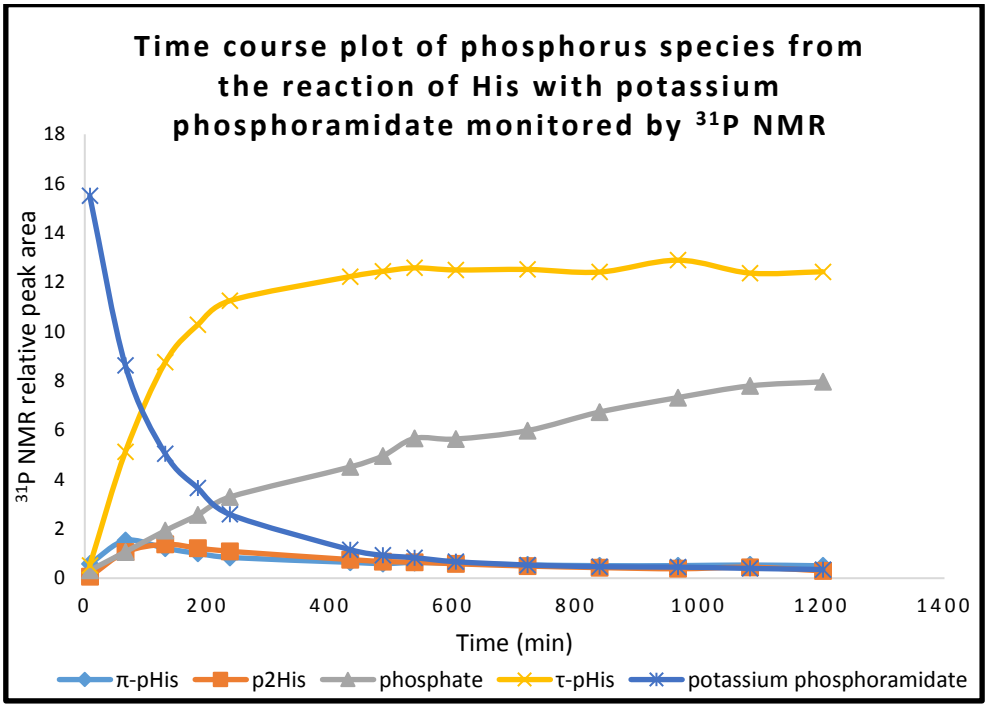

Figure 20: A time course plot of phosphorus species (π-pHis, p_2pHis, τ-pHis, phosphate, potassium phosphoramidate) from the reaction of His (0.36 M) with potassium phosphoramidate **1** (0.93 M) in D_2O monitored by ^{31}P NMR chemical shift peak area. A spectrum was taken at 25 °C approximately every 20 min (not all spectra are shown).

To purify and isolate τ-pHis, Attwood's method of silica gel chromatography using a gradient solvent system of 32 % (wt/wt) aqueous ammonia, water and ethanol was chosen.[153] Using this method, τ-pHis and π-pHis were found to have similar retention factors (τ-pHis elutes after π-pHis).[153] Hence, to minimise τ and π-pHis mixtures coeluting a reaction time of 16 hours was used. At this time point relative π-pHis concentrations are minimal and τ-pHis concentration are near maximal. Unlike Attwood, the combined eluent fractions after concentration under reduced pressure were not lyophilised (which caused extensive decomposition) but reduced to a volume where conversion to π-pHis was not observed by ^{1}H NMR spectroscopy. This required controlled conditions where the pH was maintained at 12 using 2 M aqueous sodium hydroxide (NaOH) to suppress decomposition to phosphate and His as the ammonia was removed. The τ-pHis yield (27 %) was determined using an internal standard (dioxane).

Figure 20 shows that the time taken to reach maximal π-pHis concentration is much faster than that of τ-pHis. To optimise π-pHis yields it was important to determine a more accurate time of maximal π-pHis concentration. The time course spectroscopic study was therefore repeated, with spectra taken at 2.5 minutes intervals (Figure 21 and 22). Between 40 and 50 minutes was found to be the maximum π-pHis concentrations (Figure 22). The π-pHis yield (2 %) was determined using an internal standard (dioxane).

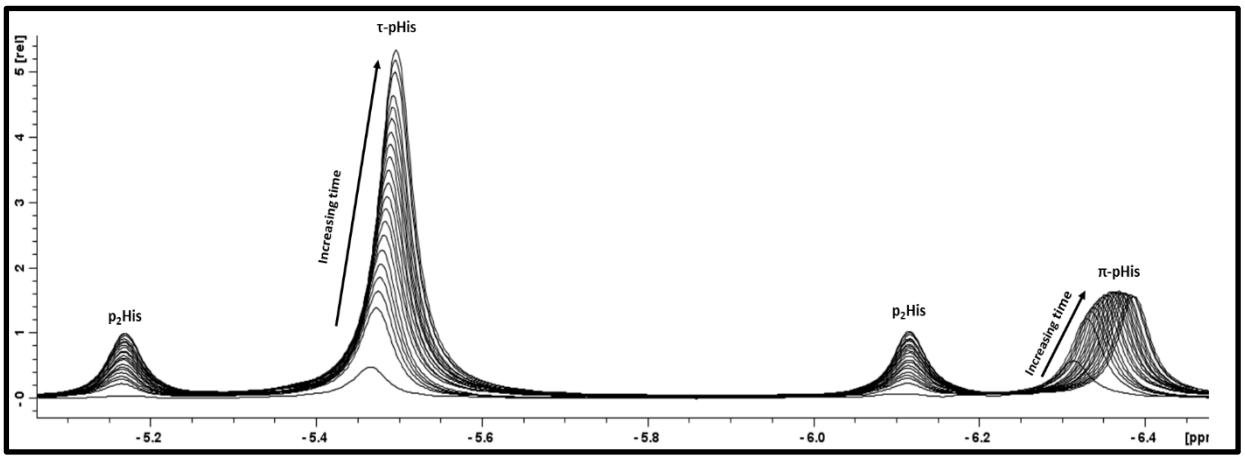

Figure 21: Multiple display time course ^{31}P NMR spectra of p_2His, τ-pHis and π-pHis chemical shifts from the phosphorylation of His (0.36 M) with potassium phosphoramidate **1** (0.93 M) in H_2O (near identical profiles were observed in D_2O). A spectrum was taken at 25 °C approximately every 2.5 min (not all spectra are shown).

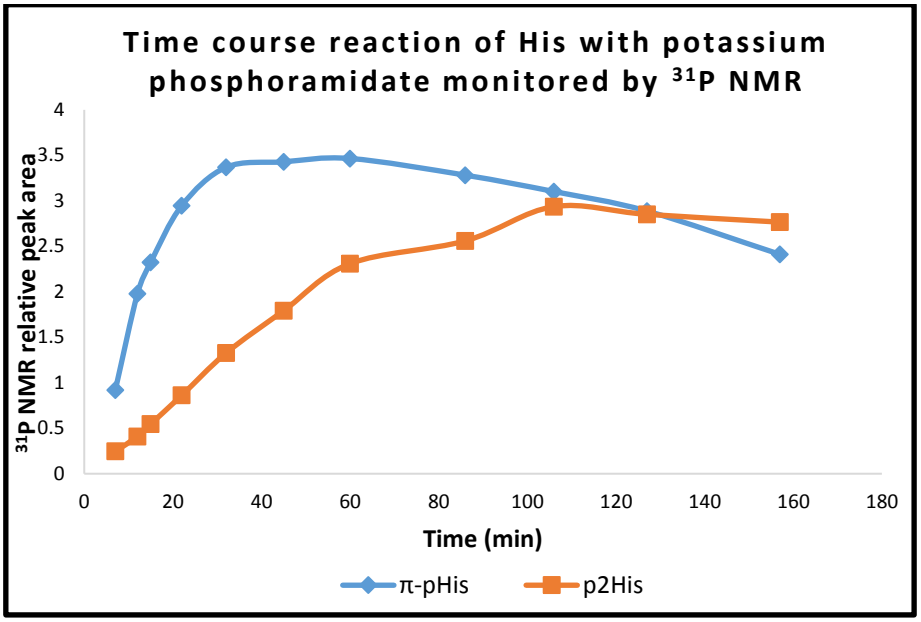

Figure 22: A time course plot of phosphorus species (π-pHis, and p_2pHis) from the reaction of His (0.36 M) with potassium phosphoramidate **1** (0.93 M) in H_2O monitored by ^{31}P NMR chemical shift peak areas. A spectrum was taken at 25 °C approximately every 2.5 min (not all spectra are shown). There was a 6 min delay between mixing of reagents and the first spectrum.

3.2: Biology

3.2.1: Assay synthesis and characterisation

With key compounds in hand the second phase of the project could begin. Both commercial monoclonal τ- and π-pHis antibodies (those generated by Fuhs *et al*.,[77] see section 1.5.1) and those published in the literature have not been used in experiments using assays which give a clear assessment of their selectivity.[77,111,122] Therefore, it was essential to have assays which could be used to confidently assess pHis antibody selectivity, including the ability to selectively detect both π- and τ-pHis. One approach would be to use known pHis proteins containing either the τ- or the π-pHis residue. However, the disadvantage of using a protein as a standard is the influence of the protein's structure or local peptide environment on antibody binding. In addition, from a practical point of view, protein biosynthesis, selective His phosphorylation, and assay verification can be lengthy and expensive process. As such, we opted to adopt a different and simpler strategy that avoids the complexity of the protein structure and local peptide environment. A simple assay would be to have a protein conjugated to the amino acid of interest via a linker. τ- and π-pHis conjugates that have been distantly characterised show have not been synthesised by the group previously and would be valuable general assays in determining the selectivity of the antibodies generated.[122]

Amino acids His, pSer, pThr, pTyr, τ-pHis and π-pHis were conjugated via the amino group to the many available surface Lys residues of BSA using the linker glutaraldehyde (G).[154] The intermediate imines formed were reduced with sodium borohydride, and unreacted compounds were dialysed out (Scheme 49), 0.1 M $NaHCO_3/Na_2CO_3$, pH 10.8 buffer was used as the dialysis buffer for the pHis conjugates, whilst phosphate buffered saline (PBS), pH 7.4 was used for all the other conjugates.

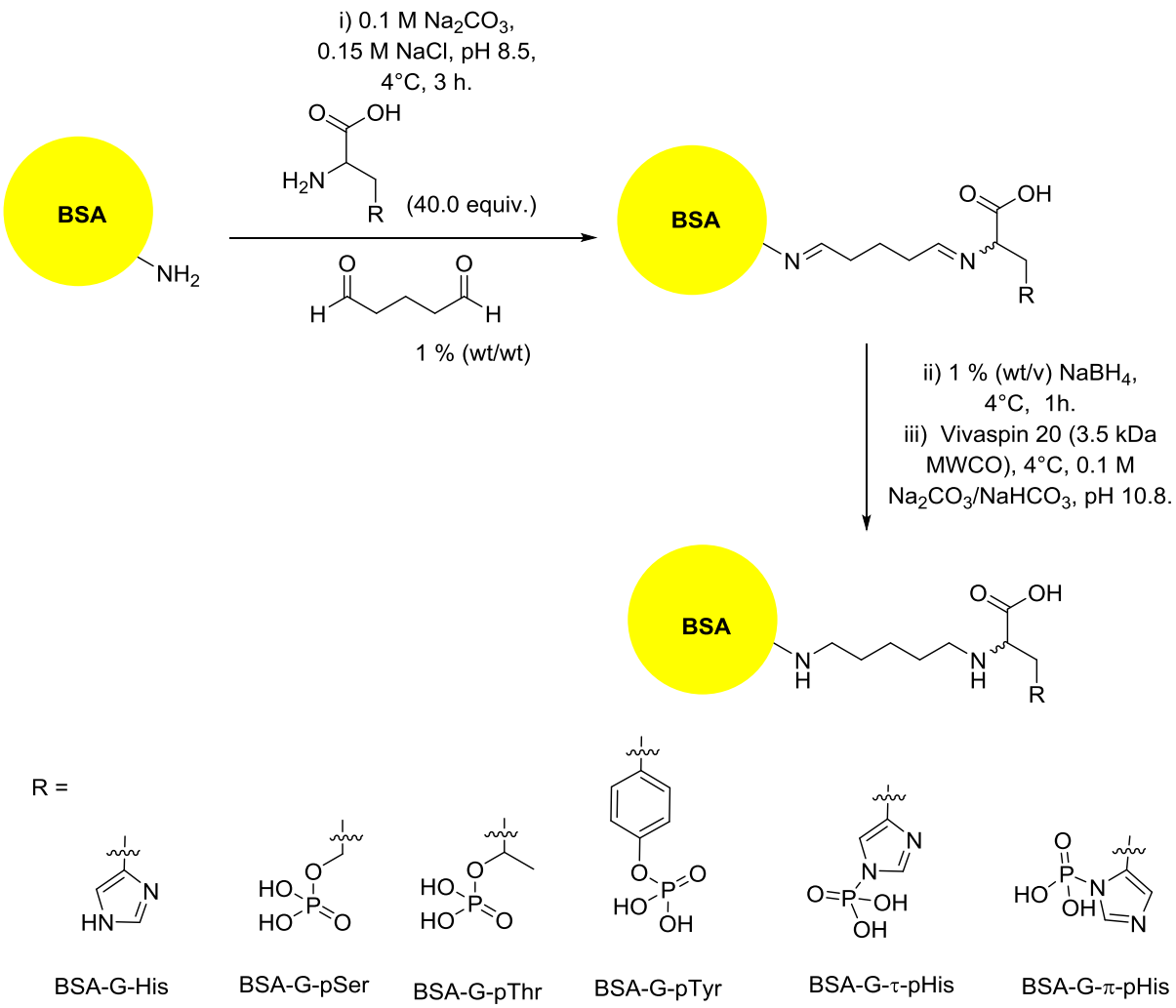

Scheme 49: Synthesis of protein conjugates; BSA-G-His, BSA-G-pSer, BSA-G-pThr, BSA-G-pTyr, BSA-G-π-pHis, BSA-G-τ-pHis. G = Glutaraldehyde linker.

It was important to show that τ-pHis and π-pHis was conjugated to BSA. ^{31}P NMR spectroscopy has previously been used to good effect to detect His phosphorylated residues in proteins and differentiate between pHis isomers.[71] The ^{31}P NMR spectrum will also show if any unimolecular isomerism of pHis residues was occurring as claimed in some reports (see section 1.2).[76-79]

A ^{31}P NMR chemical shift of -4.78 ppm (lit.[70] -4.55 ppm, pH 11.8) was observed for τ-pHis in a solution of ~pH 12, which was close to the chemical shift of-4.86 ppm for the BSA-G-τ-pHis conjugate in a 0.1 M $NaHCO_3/Na_2CO_3$, pH 10.8 buffer (Figure 23). For π-pHis, a chemical shift of -5.61 ppm solution of ~pH 12 was observed (lit.[70]-5.37, pH 11.8) and a corresponding chemical shift of -5.63 ppm for the BSA-G-π-pHis conjugate in a 0.1 M $NaHCO_3/Na_2CO_3$, pH 10.8 buffer (Figure 24). A mixture of the pHis isomers and BSA-G-pHis conjugates shows similar chemical shifts to the individual pHis isomers and BSA-G-pHis conjugates (Figure 25). There was no evidence to suggest the presence of π-pHis in the BSA-G-τ-pHis conjugate and no τ-pHis chemical shift was found in the BSA-G-π-pHis, so it was concluded that pure isomer samples had been synthesised.

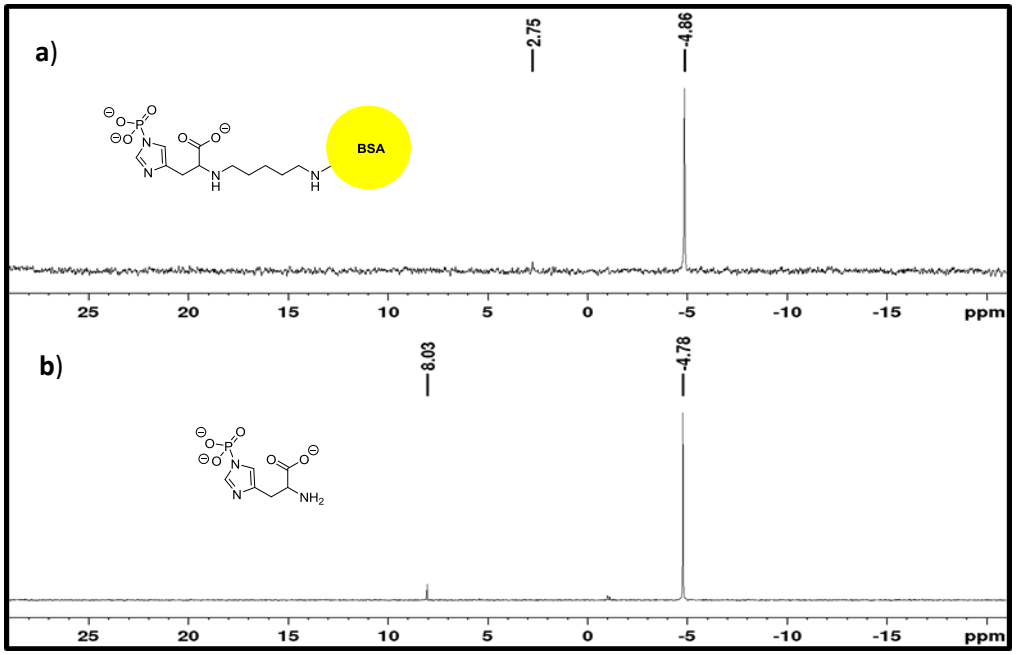

Figure 23: ^{31}P NMR of: **a**) BSA-G-τ-pHis (32 mg/mL) in 10 % (v/v) deuterium oxide, 0.1 M $NaHCO_3/Na_2CO_3$ pH 10.8 buffer, the minor peaks at 2.75 ppm is phosphate; **b**) τ-pHis (4.9 mg/mL) in basic solution (~pH 12, basified with 10 M KOH (aq.).The minor peak at 8.03 ppm is an unknown impurity present in potassium phosphoramidate **1**.

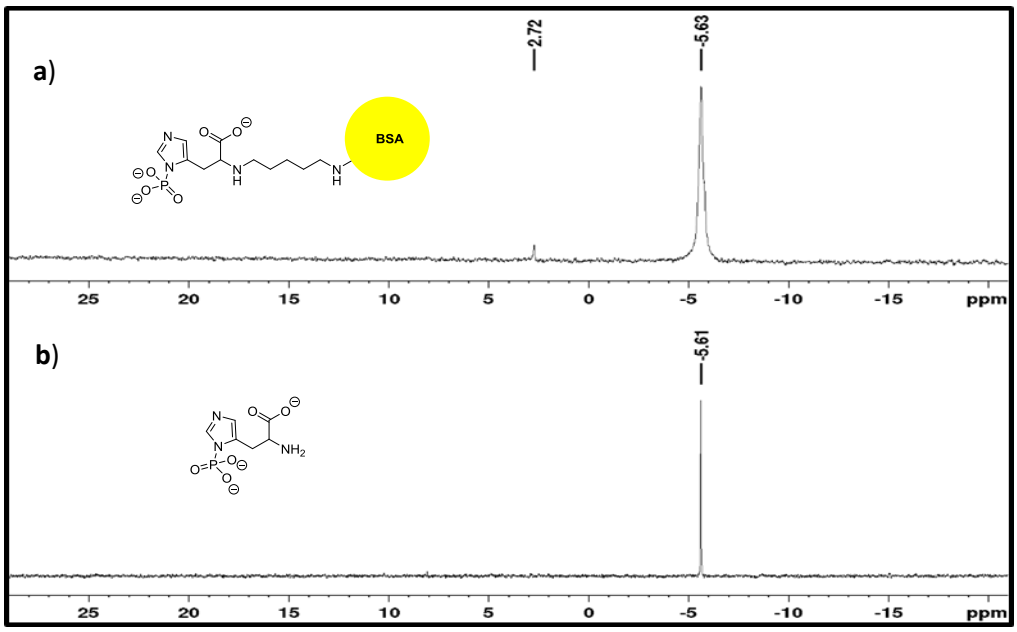

Figure 24: ^{31}P NMR of: **a**) BSA-G-π-pHis (40 mg/mL) in 10 % (v/v) deuterium oxide, 0.1 M $NaHCO_3/Na_2CO_3$pH 10.8 buffer, the minor peak at 2.72 ppm is phosphate; **b**) π-pHis (1.43 mg/mL) in basic solution ~pH 12, basified with 10 M KOH (aq.).

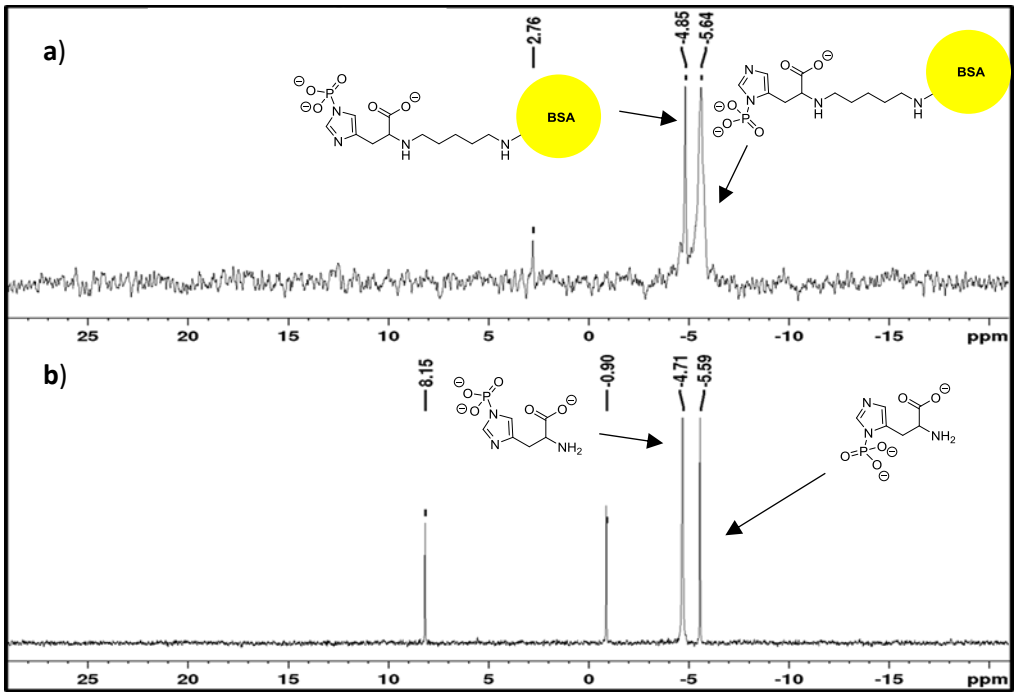

Figure 25: ^{31}P NMR of: **a**) a mixture of BSA-G-π-pHis and BSA-G-τ-pHis in 10 % (v/v) deuterium oxide, 0.1 M $NaHCO_3/Na_2CO_3$ pH 10.8 buffer, the minor peak at 2.75 ppm is phosphate; **b**) π-pHis and τ-pHis in basic solution ~pH 12, basified with 10 M KOH (aq.), the peak at 8.15 ppm and -0.90 is an unknown impurity present in potassium phosphoramidate **1**.

BSA-G-pTyr was also analysed by ^{31}P NMR spectroscopy, and the phosphorus chemical shift of the amino acid at 0.28 ppm in a solution of ~pH 12 was close to that of the conjugates (0.05 ppm) in 0.1 M $NaHCO_3/Na_2CO_3$, pH 10.8 buffer (Figure 26).

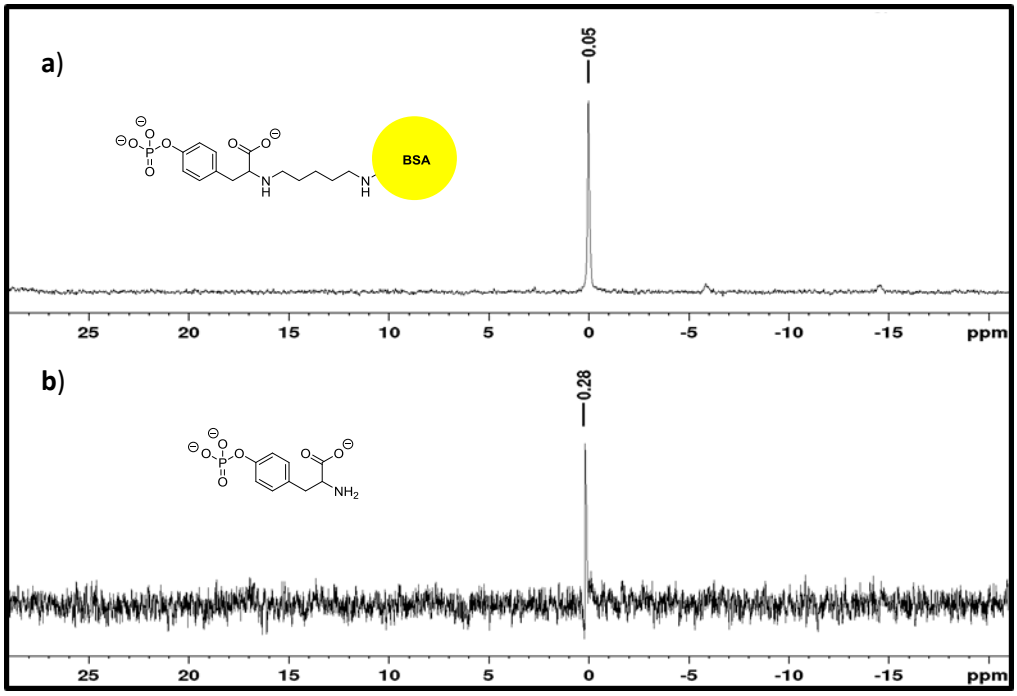

Figure 26: ^{31}P NMR of: **a**) BSA-G-pTyr (34 mg/mL) in 10 % (v/v) deuterium oxide, 0.1 M $NaHCO_3/Na_2CO_3$ pH 10.8 buffer; **b**) pTyr in basic solution ~pH 12, basified with 10 M KOH (aq.).

The average number of phosphorylated amino acids conjugated per BSA was then determined using triphenylphosphine oxide as an internal standard (Table 4). The results in Table 4 shows that the efficiency of amino acid conjugation can vary; with conjugation in BSA-G-pTyr > BSA-G-π-pHis > BSA-G-τ-pHis. One of the factors contributing to the differences in conjugation efficiency between pHis and pTyr conjugates will be the differences in stability between pHis and pTyr in the conjugation buffer (0.1 M Na_2CO_3, 0.15 M NaCl, pH 8.5) and reaction conditions. However, this does not explain the differences in conjugation between BSA-G-τ-pHis, and BSA-G-π-pHis which at first sight is inconsistent with the fact the π-pHis is less stable than τ-pHis. A potential explanation could be that the π-pHis residues of BSA-G-π-pHis are

conformationally orientated inwards and are interacting with BSA, making it less susceptible to hydrolysis, this could also explain why the BSA-G-π-pHis chemical shift is broader than the BSA-G-τ-pHis chemical shift (Figure 25). However, after dialysis both BSA-G-τ-pHis and BSA-G-π-pHis were found to be stable for weeks (> 6) at room temperature and for months at -80 ^{o}C in 0.1 M $NaHCO_3/Na_2CO_3$, pH 10.8 buffer.

Table 4: The average number of τ-pHis, π-pHis or pTyr conjugated to BSA-G-τ-pHis, BSA-G-π-pHis and BSA-G-pTyr.

Sample	Average number per BSA	Relative amounts
BSA-G-τ-pHis	0.27, τ-pHis	1
BSA-G-π-pHis	1.70, π-pHis	6.3
BSA-G-pTyr	2.44, pTyr	9.0

To evaluate the approximate molecular weight distribution, the conjugates were first treated with Laemmli sample buffer. Laemmli sample buffer contains glycerol to increase the sample density, a blue dye for visibility, ethylenediaminetetraacetic acid (EDTA), dithiothreitol (DTT) to reduce protein disulphide bonds, and sodium dodecyl sulphate (SDS) to denature the proteins all in a Tris buffer, at pH 8.0. The samples were resolved using a 12 % (wt/v) sodium dodecyl sulfate polyacrylamide gel (SDS-PAGE) (Figure 27). The gel was then stained with Coomassie stain to visualise the proteins. On comparison to the BSA lane, the conjugate stains suggest an approximately even distribution of monomers, dimers, trimers and higher conjugates. This was contrary to matrix assisted laser desorption/ionization mass spectrometry data previously used method[122] which suggested mostly monomers. However, it is likely the higher molecular weight conjugates did not ionize, decomposed, or fragmented upon ionization in matrix-assisted laser desorption/ionization.

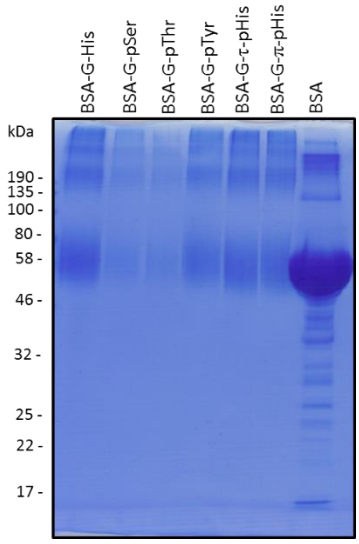

Figure 27: Coomassie stained 12 % (wt/v) SDS-PAGE of BSA-G-His, BSA-G-pSer, BSA-G-pThr, BSA-G-pTyr, BSA-G-π-pHis, and BSA-G-τ-pHis. 5 μg of protein loaded per well. Image taken using a scanner.

3.2.2: Competitive ELISA

Lilley[1,122] and Kee *et al*.[80,111] used sandwich ELISA to assess the relative selectivity of pHis antibodies over other phosphorylated amino acids (Scheme 50). Lilley's sandwich ELISA procedure began with the coating of the ELISA plate wells with the BSA-G-amino acid conjugates (columns A-L, Scheme 50). The unoccupied sites in the well were then blocked with gelatin followed by a wash. Then the pHis antibody was added (rows 1-8, Scheme 50), and any unbound antibody was washed away. A secondary antibody conjugated to the enzyme horseradish peroxidase (HPR) selective for the primary antibody was added and the unbound antibody was washed away. To quantitate the relative detection of BSA-G-amino acid conjugate 3,3',5,5'-tetramethylbenzidine (TMB) was added which was catalytically oxidised by HRP in the presence of hydrogen peroxide (Scheme 51).[155] The reaction was then stopped with 1 M sulphuric acid. The yellow solution was spectroscopically probed by taking

the absorbance at 450 nm. The larger the absorbance correlates with more primary antibody bound to the BSA-G-amino acid conjugate.

To minimise bias in the sandwich ELISA it is important to have BSA conjugates of similar molecular weight and epitope number. Controlling the latter is made difficult because of the instability of pHis residues (and difference in stability between τ-pHis and π-pHis residues) in the neutral buffers (PBS, pH 7.4) and temperatures (37 ^{o}C) used.

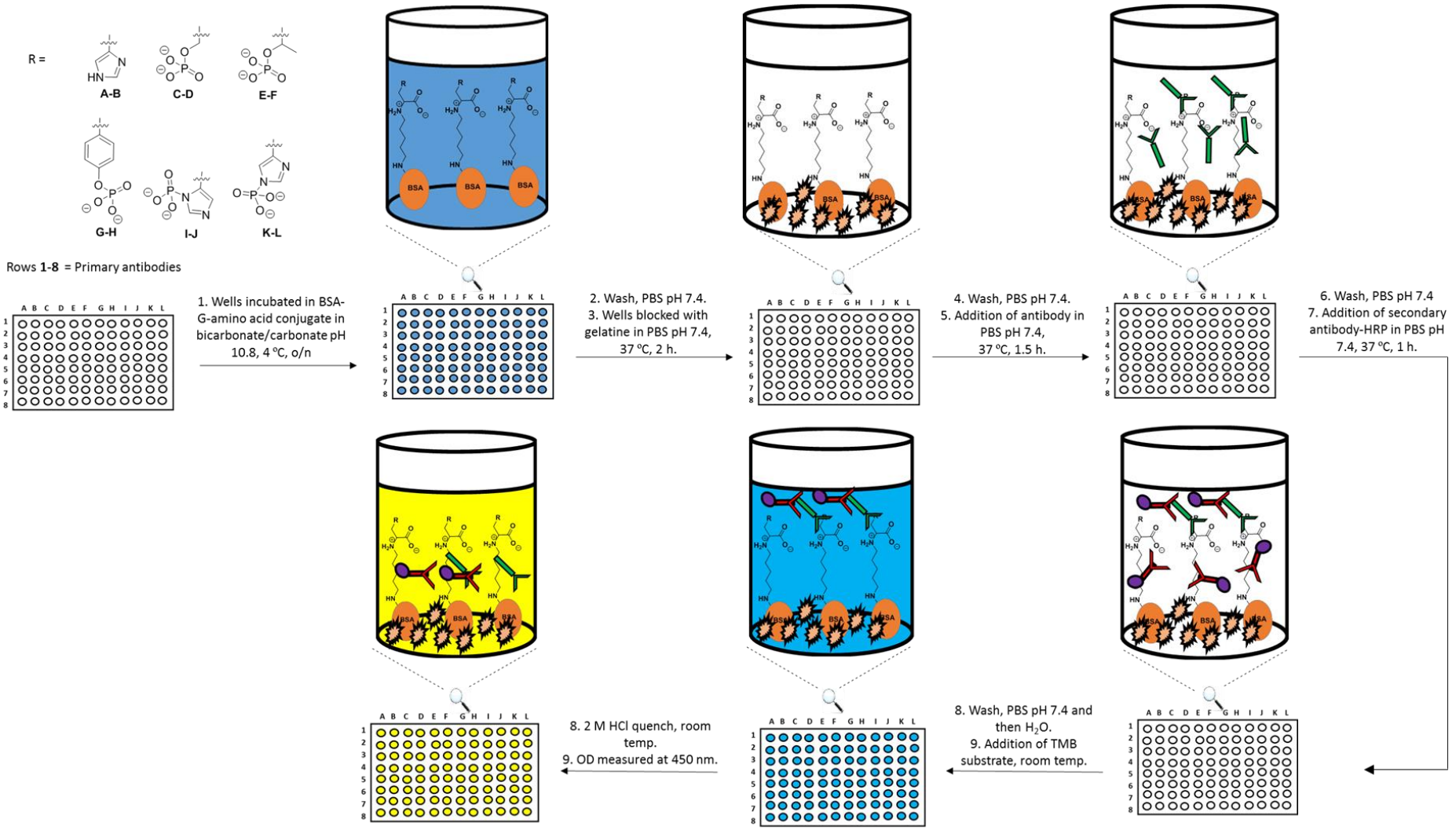

Scheme 50: Previously used sandwich ELISA procedure for pHis antibodies. Note these other studies did use individual BSA-G-π-pHis and BSA-G-τ-pHis conjugates.[1] They have been included here for illustrative purposes

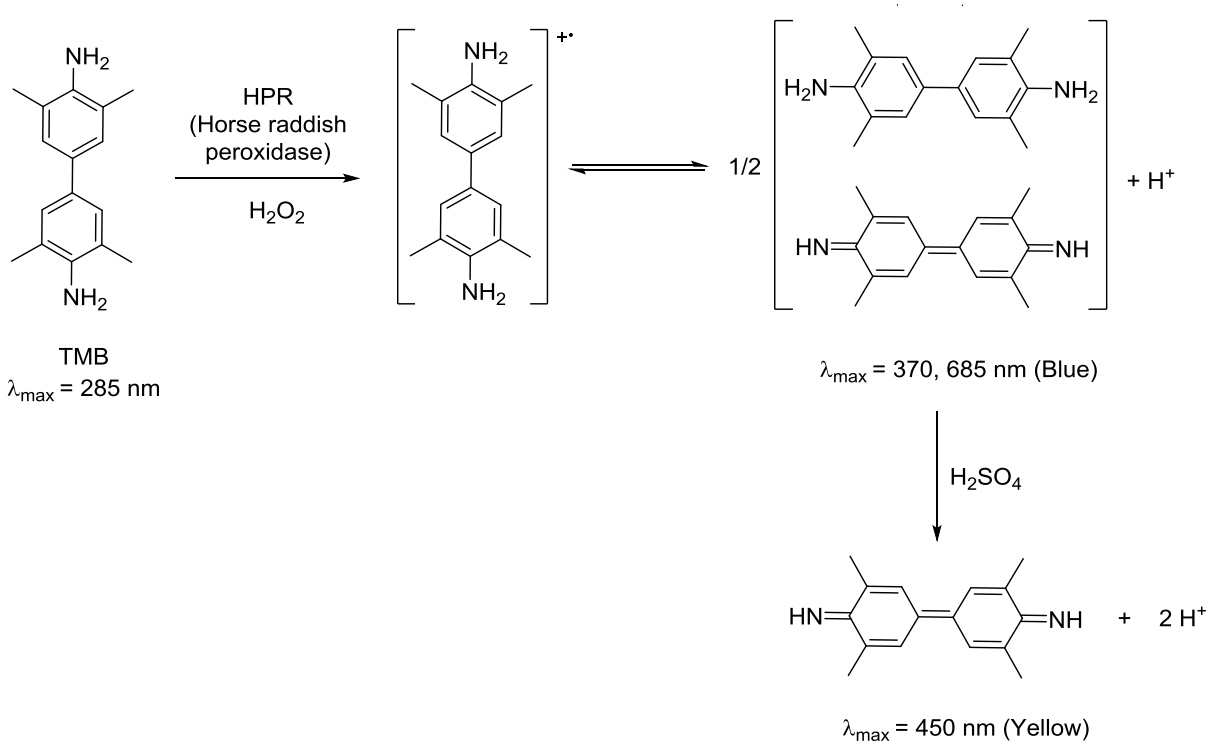

Scheme 51: Oxidation of TMB by H_2O_2 followed quenching with 2 M sulphuric acid.[155]

It was thought using an assay such as a competitive ELISA which is not dependent on individual BSA-G-amino acid conjugates, would give more informative pHis antibody selectivity results. In an competitive ELISA, a known quantity of a competitor (in this assay His, pSer, pThr, pTyr, π-pHis, and τ-pHis, Scheme 51) is pre-equilibrated with the pHis antibody before transferring to an ELISA plate, with wells coated with BSA-G-pHis (either τ- or π-pHis) conjugate. After incubation, the wells are washed and the secondary antibody and well development follows the same steps used in the sandwich ELISA (Scheme 52). A reduction in absorbance relative to the control well absorbance suggests the presence of competition.

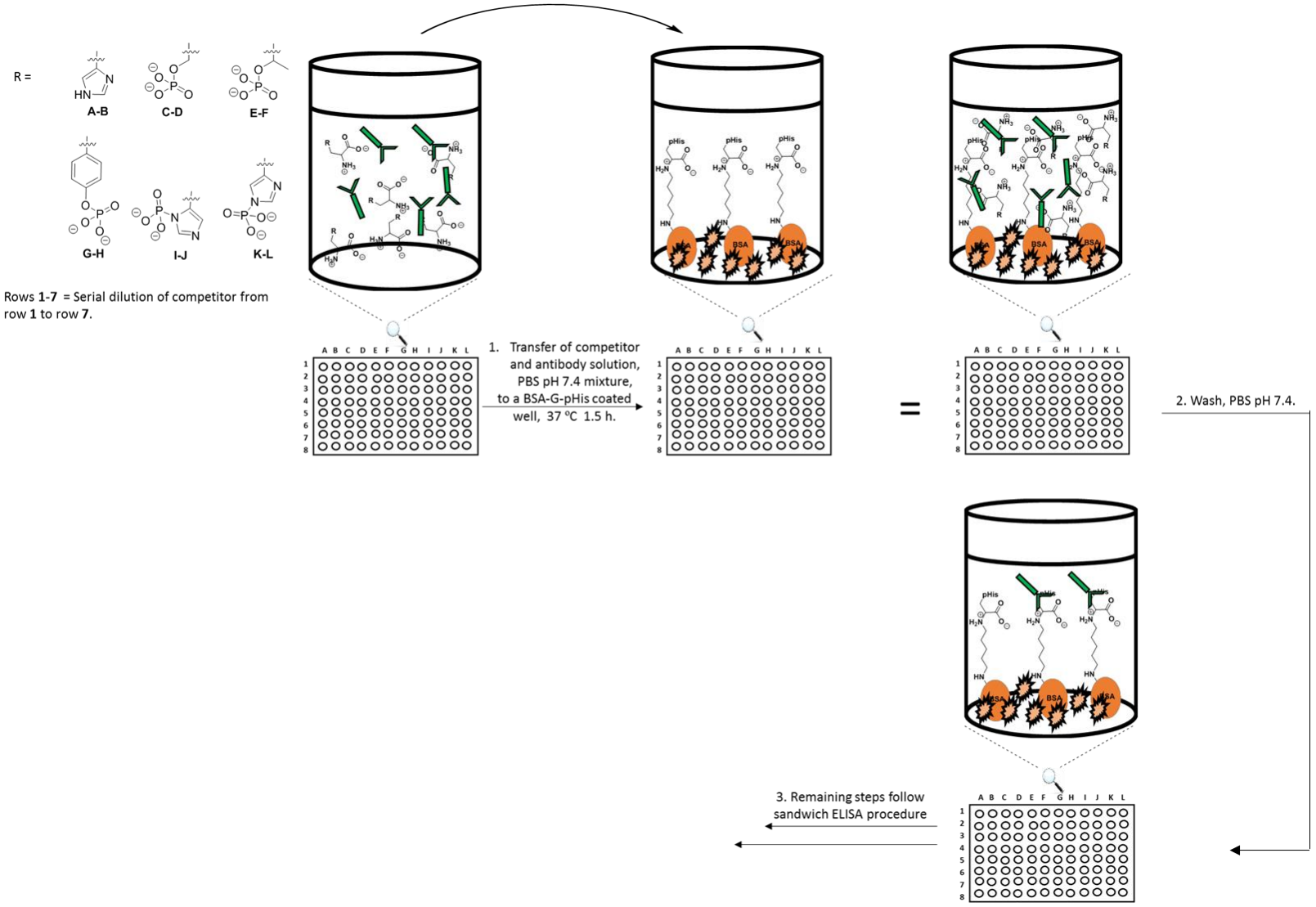

Scheme 52: Proposed competitive ELISA procedure for pHis antibodies.

Fuhs *et al*. reported the generation and use of pHis monoclonal antibodies SC56-2 (raised using peptide **88**, page 25 and claimed to be specific for the τ-pHis residue) and SC1-1/SC50-3 (raised using peptide **27**, page 25 and claimed to be specific for the τ-pHis residue) but no clear data on the antibody selectivity or sensitivity was included.[77] Since both these antibodies were commercially available, this therefore gave us a good opportunity as proof of concept, to test the proposed competitive ELISA.

The competitive ELISA of monoclonal antibody SC56-2 gave a profile which suggested the antibody was not specific for τ-pHis but in fact selective for the π-pHis residue (Figure 28). No competition was observed when using 1/1000 (v/v) antibody dilution. Only when the antibody concentration was increased to 1/500 (v/v) antibody dilution was a minor change seen. However, the interpretation of the result was unclear. On Western blot (WB) of human bronchial epithelial (HBE) cell lysate, a cell line known to contain pHis proteins, a 1/100 (v/v) antibody dilution of SC56-2 weakly detected low molecular weight proteins, highlighting the poor sensitivity of this monoclonal antibody (see section 3.2.7.1, for Western blot conditions). As controls, the lysates were treated with acid or base to destroy or preserve pHis. respectively.

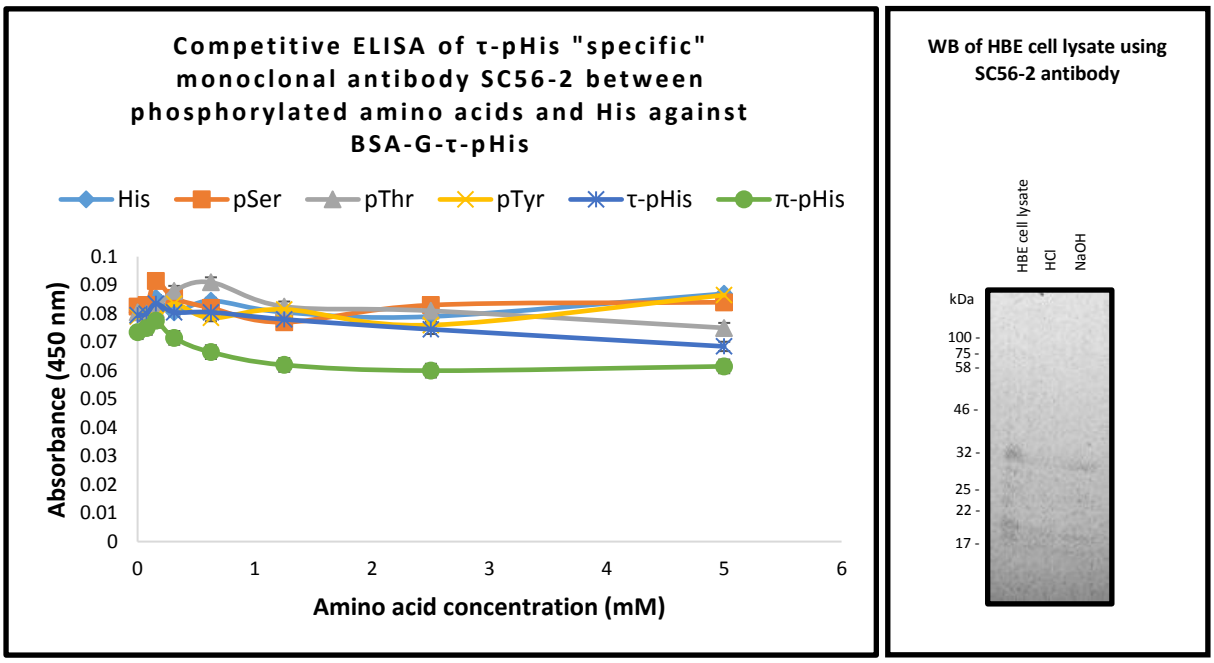

Figure 28: Left: competitive ELISA of commercial monoclonal antibody SC56-2 (1/500 (v/v) dilution) with His, pSer, pThr, pTyr, τ-pHis, and π-pHis against BSA-G-τ-pHis. Right: Western blot (WB) (1/100 (v/v) antibody dilution) of 100 µg HBE protein cell lysate, treated with HCl to pH 3 at 90 ^{o}C for 15-45 min and with NaOH, (0.1 M final concentration) at room temp. in modified sample buffer. The membranes were visualised using Bio-Rad ChemiDoc™ XRS+, 3600 sec exposure. Error bars show the standard error of the mean (N = 2).

However, monoclonal antibodies SC1-1 and SC50-3 at a 1/1000 (v/v) dilution gave ELISA assay profiles which suggested the clones are selective for the π-pHis residue below ~1 mM competitor concentration as claimed (Figure 29). However, they are not specific for the π-pHis as claimed because at higher competitor concentrations there is general recognition of phosphorylated amino acid residues. On Western blot of HBE cell lysate only a few low molecular weight pHis proteins were detected (1/1000 (v/v) antibody dilution).

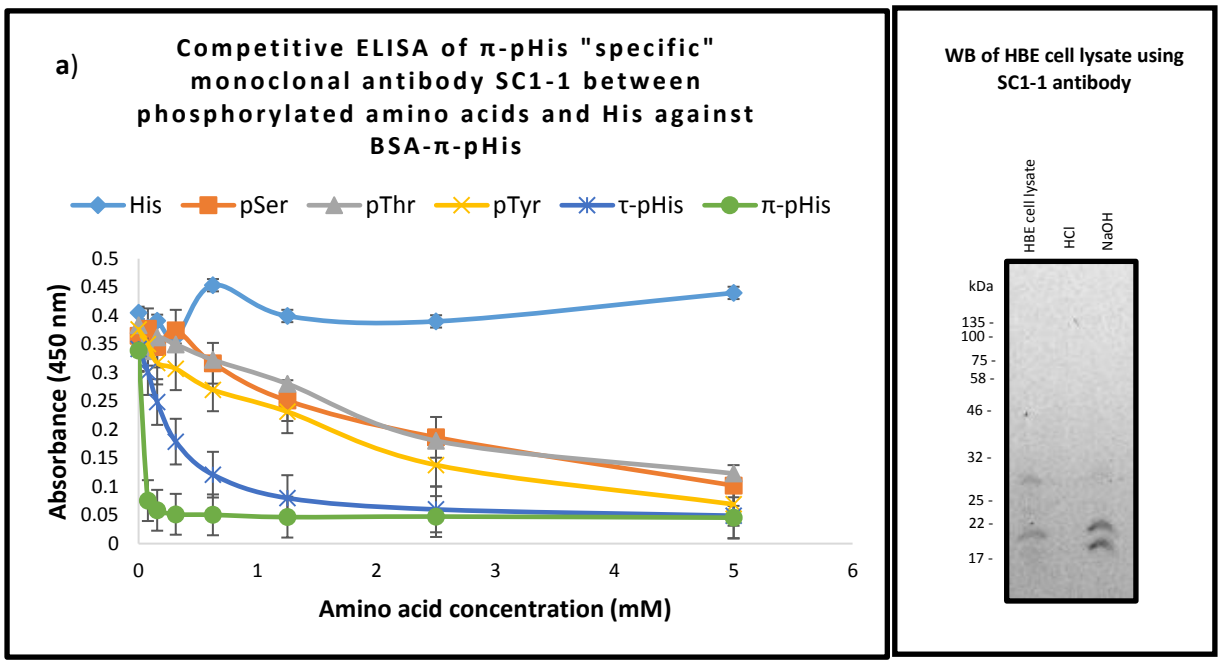

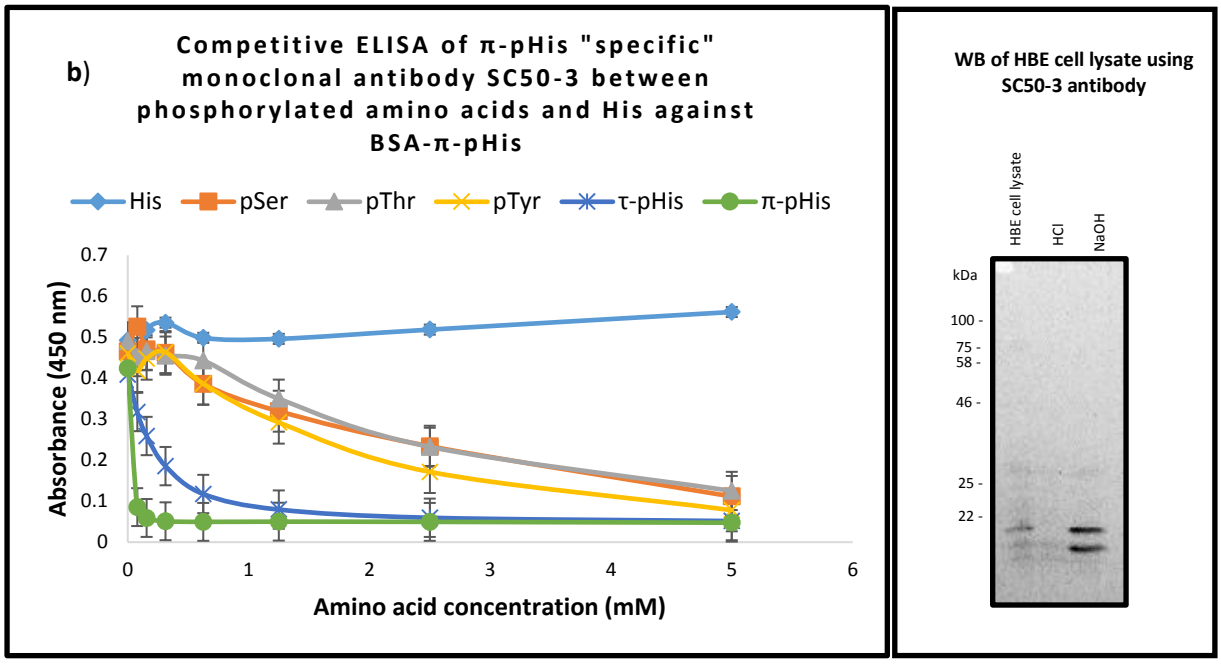

Figure 29: Characterisation of commercial π-pHis "specific" monoclonal antibody: **a**) SC1-1; **b**) SC50-3. Left: competitive ELISA (1/1000 (v/v) antibody dilution) with His, pSer, pThr, pTyr, τ-pHis, and π-pHis against BSA-G-π-pHis. Right: Western blot (WB) (1/1000 (v/v) antibody dilution) of 100 µg HBE protein cell lysate, treated with HCl to pH 3 at 90 ^{o}C for 15-45 min and with NaOH, (0.1 M final concentration) at room temp. in modified sample buffer. The membranes were visualised using Bio-Rad ChemiDoc™ XRS+, 3600 sec exposure. Error bars show the standard error of the mean (N = 2)

3.2.3: Immunogen synthesis

The analogues themselves are too small to be used on their own to elicit an immune response and generate antibodies. Analogues can be conjugated to large protein such as BSA or KLH to give a hapten which can be used as an immunogen. KLH, a 5000 kDa protein, has a proven track record as a good epitope carrier in antibody generation.[154] Glutaraldehyde was chosen as the linker because antibodies independent of the peptide environment and selective for the τ- or π-pHis residue were the project goal.

Analogues **127-130** and **61** (Figure 30) were conjugated to KLH using condition 1; (Scheme 53 and Table 5) which are similar to the conditions used in Scheme 49 (page 81).[154] A Jackson group member (Mark Thompson) had previously synthesised pyrazole immunogen **148** using condition 2 and the antiserum generated to this immunogen had been stored at -20 ^{o}C. Hence, pyrazole immunogen **148** synthesised using conditions 1 was not used for immunisation but to compare conjugation condition efficiencies. In addition, due to the high cost of immunisation, not all analogues synthesised were prepared for immunisation. 2,4-disubstituted pyridine amino acid **133** and 2,4-disubstituted pyridine amino amide **132** (see section 3.1.2.1) were not used in immunisaton.

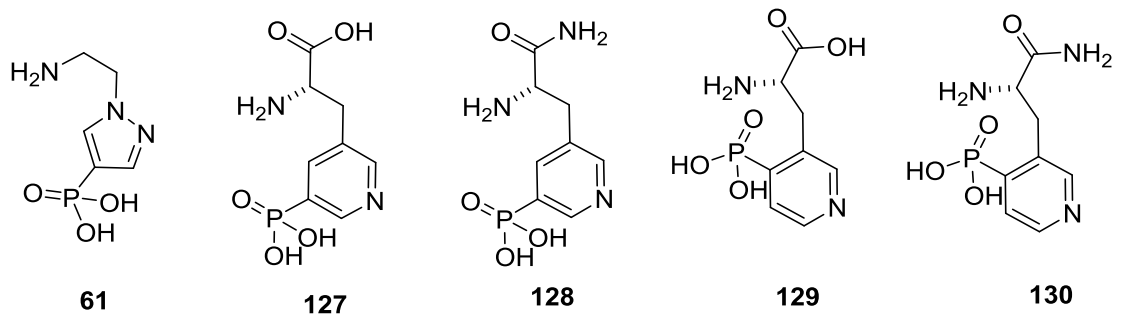

Figure 30: pHis analogues.

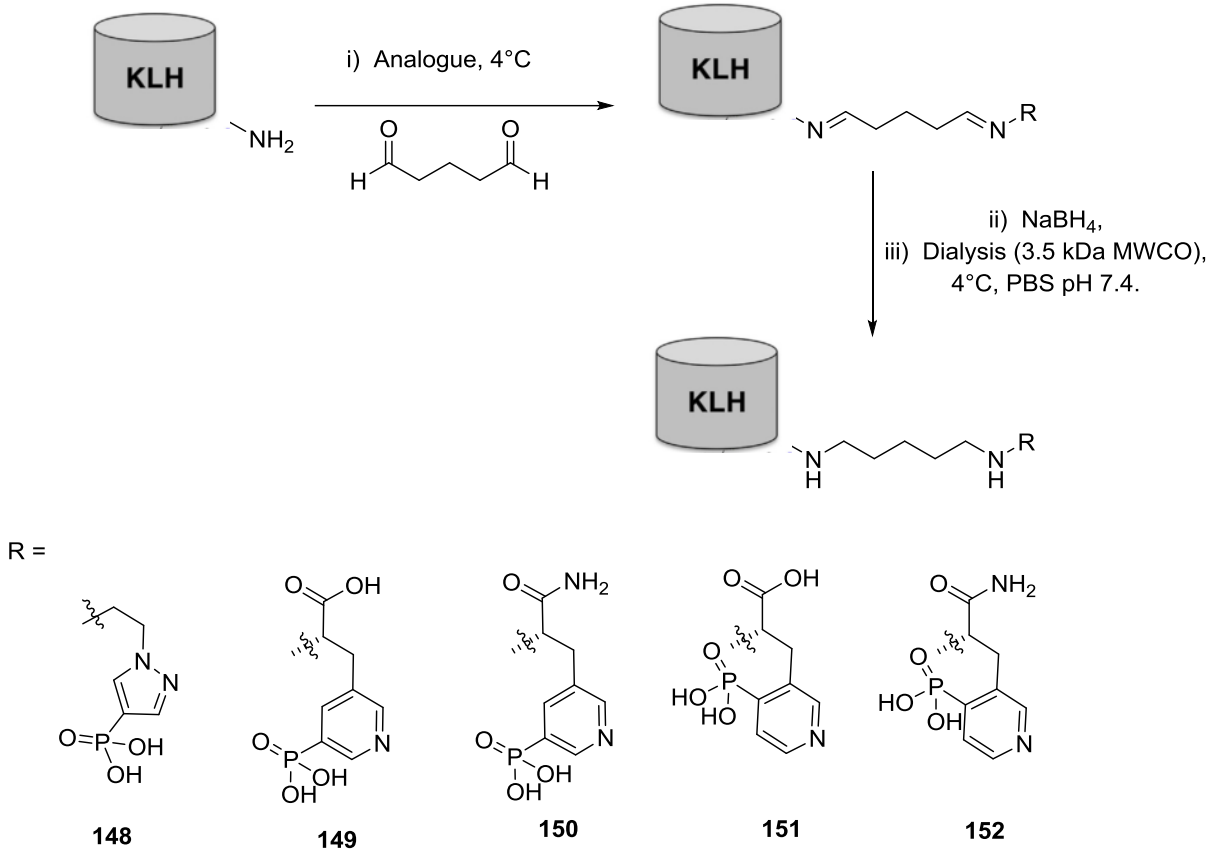

Scheme 53: General synthesis of immunogens **148**-**152**.

Table 5: Condition used for the conjugation of pHis analogues **127-130** and **61** to KLH using glutaraldehyde.

Condition	KLH (mg/mL)	Amine (equiv.)	Glutaraldehyde % (wt/wt)	Buffer	Time (h.)	$NaBH_4$ % (wt/v)	Analogous
1	2	2000	1	0.15 M NaCl 0.1 Na_2CO_3 pH 8.5	1	1 (1h.)	**127-130** and **61**
2	21	39000	1	31	o/n	0.1 (o/n)	**61**

In a post immunisation study, ^{31}P NMR analysis of pyrazole immunogen **148** synthesised using condition 2 gave a relatively sharp peak at 5.02 ppm (Figure 31). Furthermore, when pyrazole immunogen **148** synthesised using condition 1 was compared to pyrazole immunogen **148**

synthesised using condition 2, ~22 times more pyrazolylethylamine **61** was found to be conjugated to KLH. The calculation was determined from taking peak integration ratios of both samples using normalised protein concentrations. Time did not permit absolute quantitation using an internal standard to confirm the conjugation differences and average conjugation number per KLH protein.

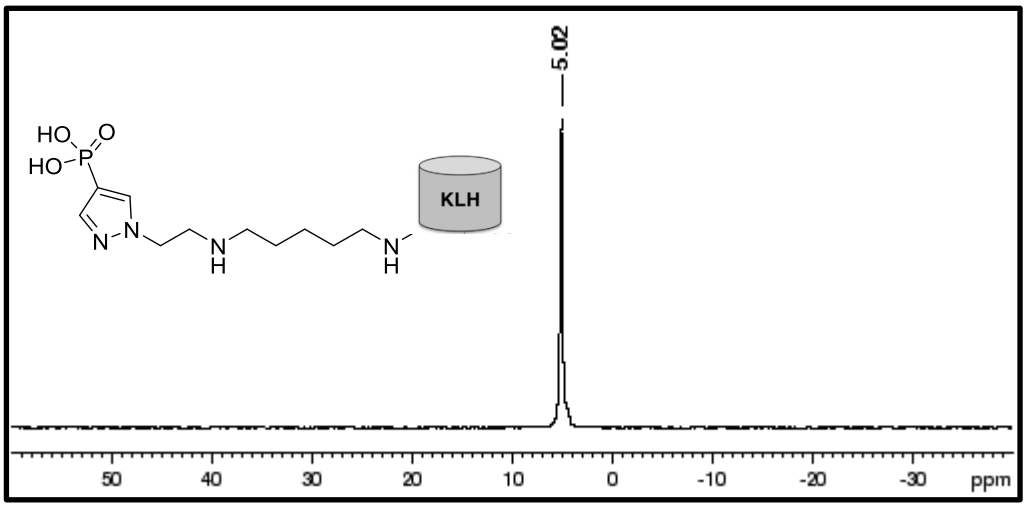

Figure 31: ^{31}P NMR of immunogen **148** (3.4 mg/mL) synthesised using condition 2 in 10 % (v/v) D_2O, 0.1 M $NaHCO_3/Na_2CO_3$ pH 10.8 buffer.

Pyrazole immunogens **148** (conditions 1 and 2) were resolved by SDS-PAGE (TGX gradient gel 5-20 %) and the gel was Coomasie stained (Figure 32). Comparison of the Pyrazole immunogens **148** (condition 1) lane with the KLH lane shows the presence of higher molecular weight conjugates (dimers, trimers etc). Whereas, pyrazole immunogen **148** (condition 2) lane has a similar profile to KLH. However, the profile of pyrazole immunogen **148** (condition 2)* synthesised by Mark Thompson (the sample used for immunisation) shows very high

molecular weight conjugates (see top of lane) which is not seen in the pyrazole immunogen **148** profile (condition 2), despite both conjugates being synthesised using conditions 2. It is not clear why this has occurred but may be due to the different forms of KLH used. KLH is commercially available as a lyophilised powder and as a solution. Excluding pyrazole immunogen **148** (condition 2)*, for the ^{31}P NMR study (Figure 31) and SDS-PAGE analysis (Figure 32) the immunogen were synthesised with lyophilised KLH powder as it was cheaper than KLH in solution. However, all conjugates used for immunisation were prepared using KLH in solution.

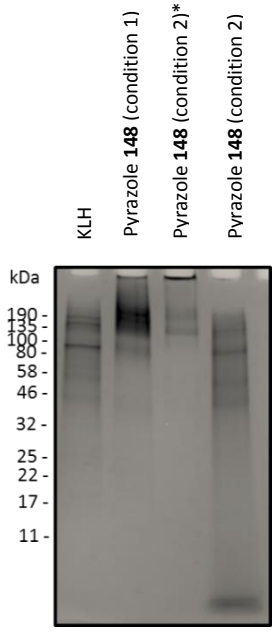

Figure 32: Coomassie stained Bio-Rad TGX gradient gel (4-20 %) of pyrazole immunogen **148** (condition 1), **148** (condition 2)* and **148** (condition 2). 50 µg loaded per well, after treatment with Laemmli sample buffer. The gel was visualised using a Bio-rad Gel Doc EZ imaging system. See Table 5 for conditions. *Pyrazole immunogen **148** was synthesised by a previous member of the Jackson group (Mark Thompson) using condition 2 and for immunisation.

3.2.4: Immunisation of Sheep and antiserum assessment

The immunogens **148**-**152** were administered into individual sheep (Figure 33). Bleeds were collected on a monthly basis prior to boost injections, two boost injections were given. Each bleed was processed to remove unwanted cells and the sterile antiserum was assessed by ELISA against BSA-G-pHis conjugates (Figure 35-38). Comparison of the pre-immune bleed with bleeds 1-3 suggested that all immunogens **148**-**152** had elicited an immune response and generated polyclonal antibodies which could detect BSA-G-pHis. Sheep S976D (Figure 34) gave a stronger response following boost injections for bleeds 2 and 3 whilst all the other sheep did not show much change from bleed 1.

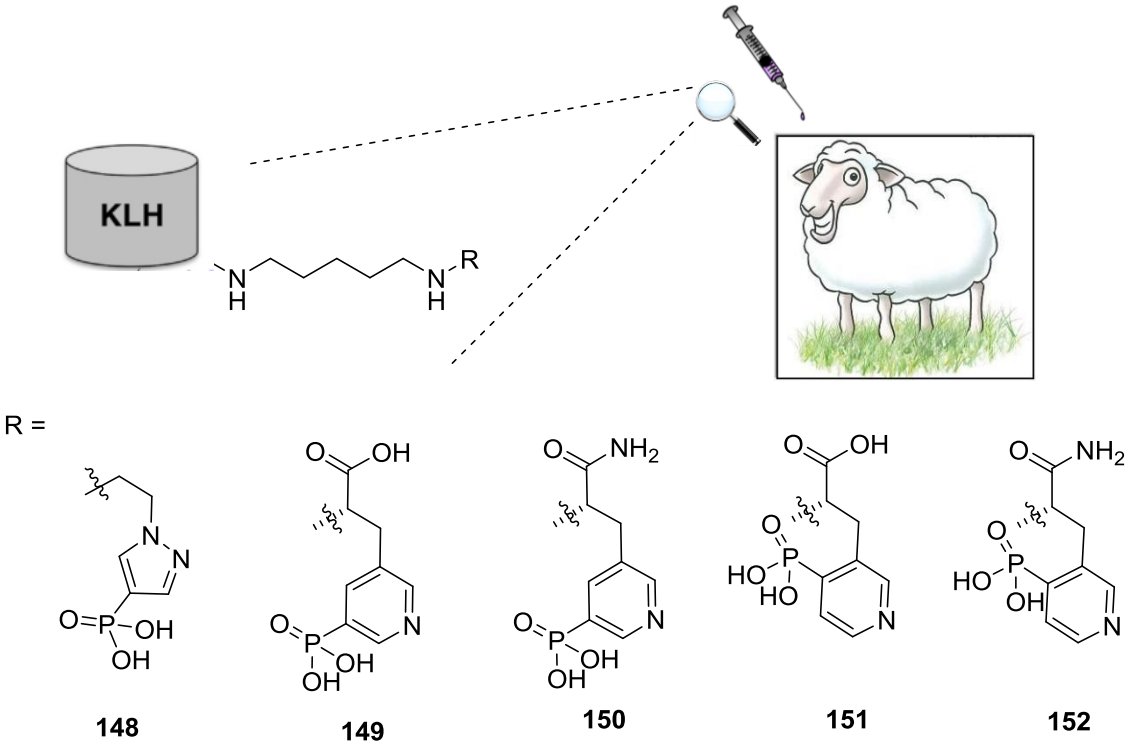

Figure 33: Immunisation of sheep with KLH conjugates **148-152**.

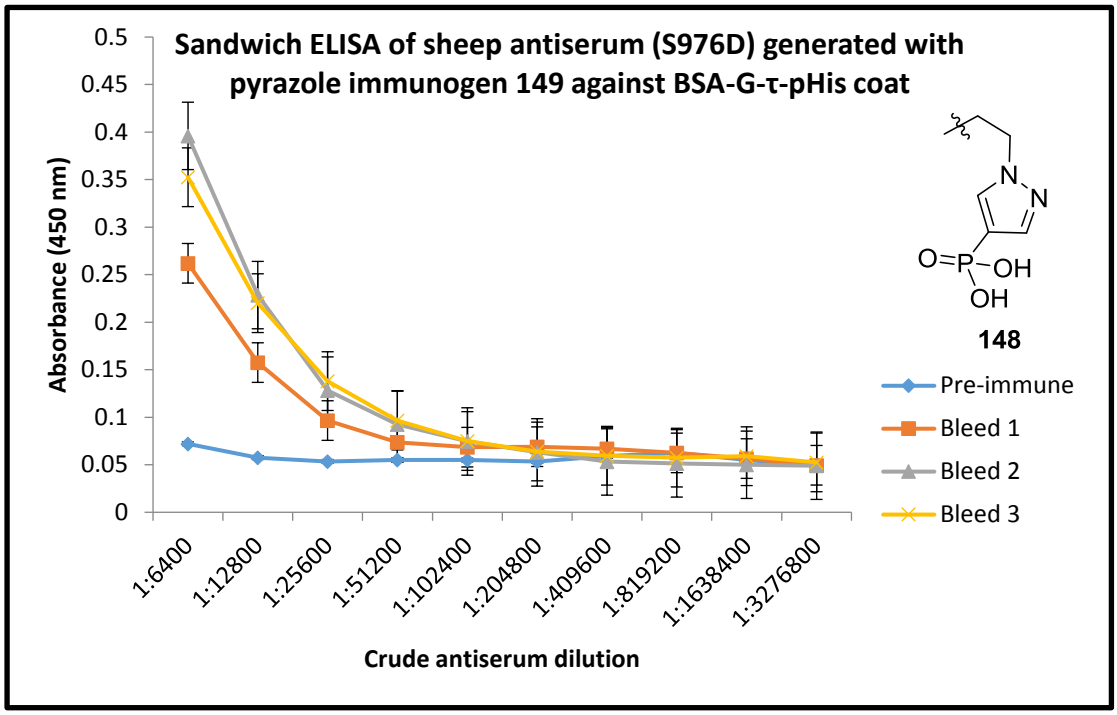

Figure 34: Sandwich ELISA against BSA-G-τ-pHis of serially diluted sheep antiserum S976D, pre-immune and bleed 1-3 after immunisation with pyrazole immunogen **148**. Error bars show the standard error of the mean (N = 2).

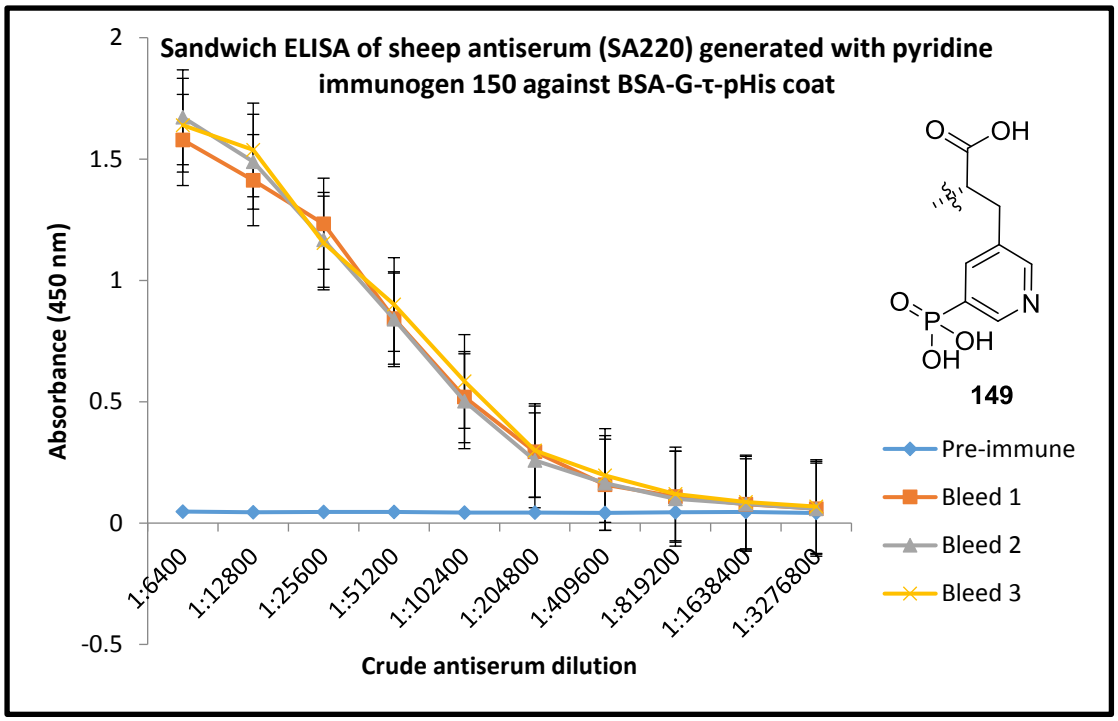

Figure 35: Sandwich ELISA against BSA-G-τ-pHis of serially diluted sheep antiserum S976D, pre-immune and bleed 1-3 after immunisation with pyridine immunogen **149**. Error bars show the standard error of the mean (N = 2).

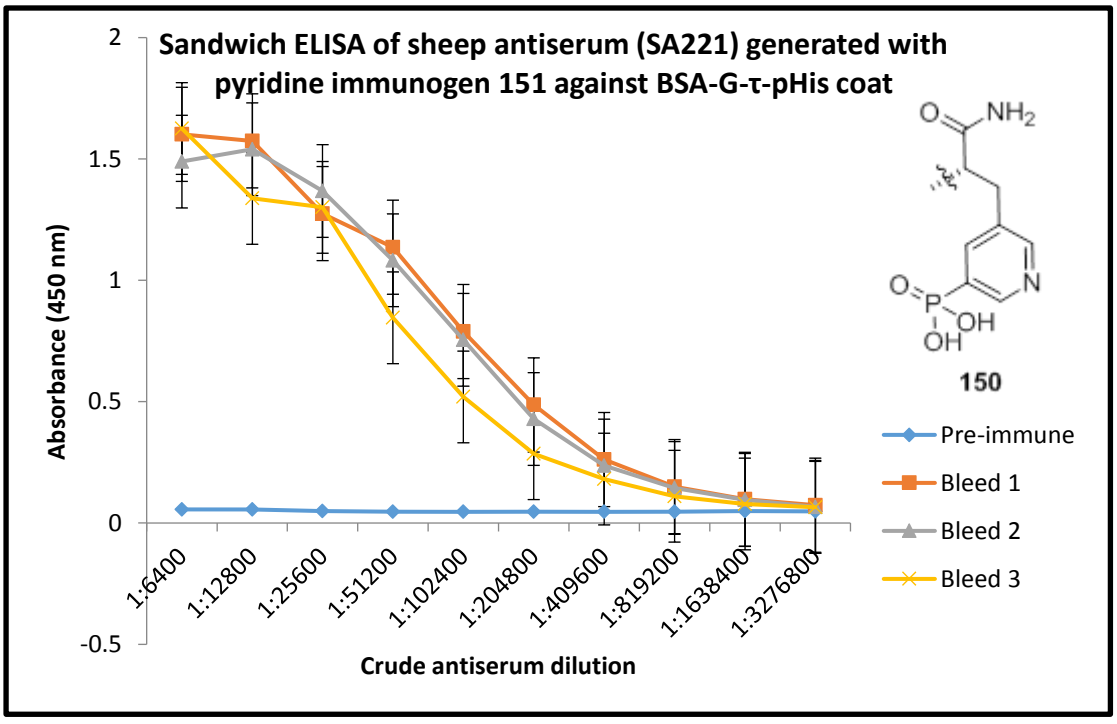

Figure 36: Sandwich ELISA against BSA-G-τ-pHis of serially diluted sheep antiserum S976D, pre-immune and bleed 1-3 after immunisation with pyridine immunogen **150**. Error bars show the standard error of the mean (N = 2).

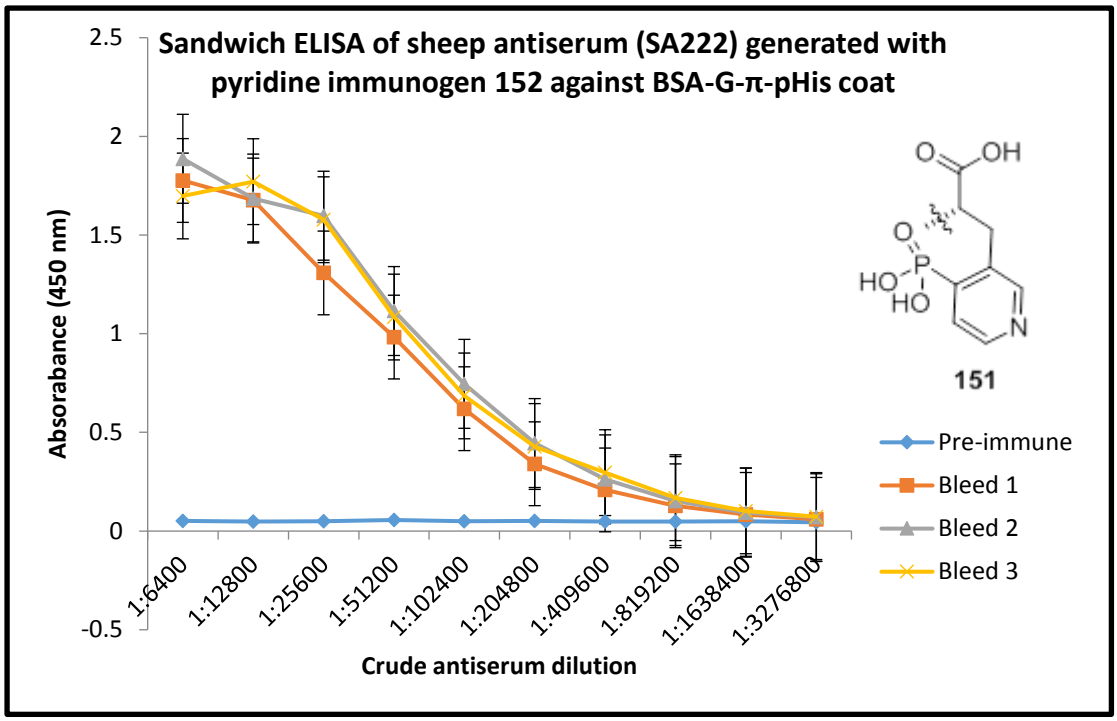

Figure 37: Sandwich ELISA against BSA-G-π-pHis of serially diluted sheep antiserum S976D, pre-immune and bleed 1-3 after immunisation with pyridine immunogen **151**. Error bars show the standard error of the mean (N = 2).

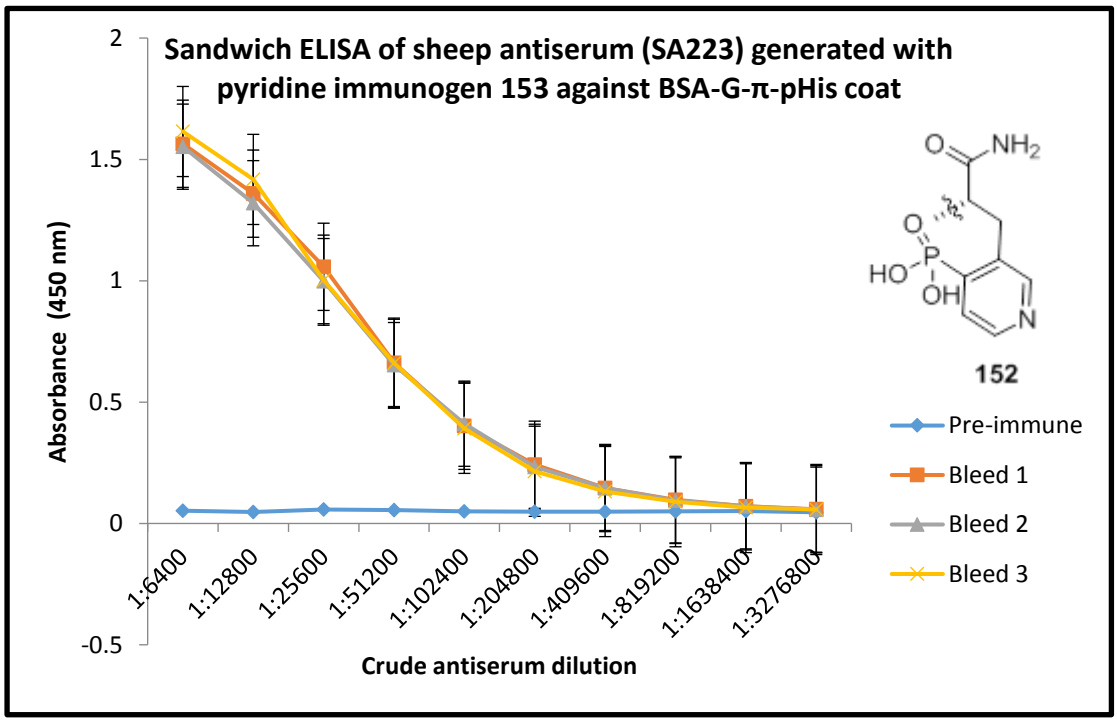

Figure 38: Sandwich ELISA against BSA-G-π-pHis of serially diluted sheep antiserum S976D, pre-immune and bleed 1-3 after immunisation with pyridine immunogen **152**. Error bars show the standard error of the mean (N = 2).

As a crude assessment, bleed 3 (B3) of sheep S976D-B3, SA220-B3, SA221-B3, SA222-B3, SA223-B3 were analysed by dot blots against BSA conjugates (Figure 39). For sheep S976D-B3 1 µg of each BSA conjugate was blotted on to the membrane, whereas for the other dot blots, BSA-G-τ-pHis, BSA-G-π-pHis and BSA-G-pTyr were blotted by equal phosphorus loading. All antiserum dot blots show similar profiles and all weakly detect BSA-G-His, suggesting the presence of some antibodies for the glutaraldehyde linker and general aromatic group. The increase in detection for BSA-linker-pTyr conjugates, suggests the presence of generic aromatic and phosphoryl group antibodies. The detection intensity for BSA-G-pHis conjugates was promising but further tests were needed to assess pHis isomer selectivity. At longer exposure times all BSA conjugates are detected without being distinguishable (data not shown).

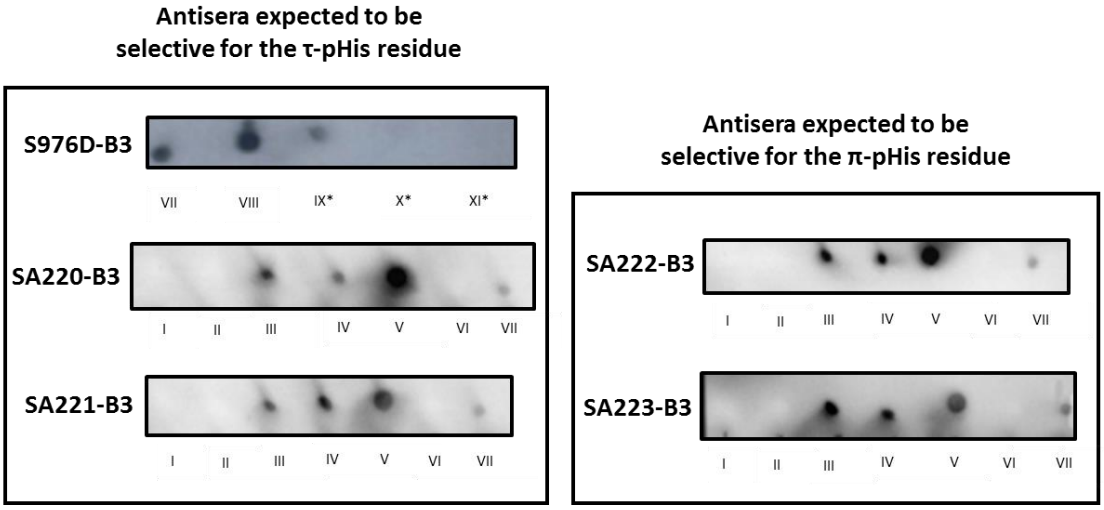

Figure 39: Left: dot blots of sheep antisera S976D-B3, SA220-B3, SA221-B3. Right: dot blots of sheep bleed 3 antiserums SA222-B3, and SA223-B3. I = BSA-G-pSer, II = BSA-G-pThr, III = BSA-G-pTyr, IV = BSA-G-π-pHis, V = BSA-G-τ-pHis, VI = BSA, VII = BSA-G-His, VIII = BSA-G-pHis, IX* = BSA-BS3-pTyr, X* = BSA-BS3-pSer, or XI* = BSA-BS3-pThr. BSA-G-τ-pHis, BSA-G-π-pHis and BSA-G-pTyr analysed by ^{31}P NMR and equal phosphorus loadings were used. The membranes were visualised using Bio-Rad ChemiDoc™ XRS+, 20 sec exposure. *Commercially sourced BSA BS3 linked phosphoamino acid conjugate and 1 µg of conjugate was blotted.

3.2.5: Sheep antiserum purification and assessment by ELISA

The usual practice of isolating selective antibodies from a polyclonal antiserum is to affinity purify with the epitope of interest. The dot blot data suggested the presence of unwanted glutaraldehyde and pTyr detecting antibodies. Previously when attempting to isolate pHis antibodies, an affinity depletion with a sepharose BSA-G-pTyr conjugate resin to remove cross-reactive antibodies preceded an affinity purification with a sepharose BSA-G-pHis conjugate resin.[1,122] To begin with, sheep antiserum S976D-B3 generated to pyrazole immunogen **148** was chosen to develop the purification strategy because the group has had some previous experience with antisera generated using a similar epitope.[122] The sandwich ELISA flow through (FT) fraction suggested that affinity depletion of antiserum S976D-B3 (2 mL) improved the selectivity of the antiserum for pHis (Figure 40). Noticeably, the sandwich ELISA absorbance intensities of IN for BSA-G-amino acid conjugates did not match the dot blot assay profiles (Figure 39), despite these two assays being similar. This may be because saturating amounts of IN was used. Additionally, the ELISA method does not allow absorbances to be taken at different exposure times with the substrate without repeating the whole experiment. The Wash (W1) fraction suggests there are some weakly bound pHis antibodies to the sepharose BSA-G-pTyr conjugate resin. However, the pHis selectivity was not as expected because the epitope (pyrazole **61**) used to generate antiserum S976D-B3 was designed to generate τ-pHis selective antibodies and not π-pHis selective antibodies observed in this ELISA test. To access what was bound to the sepharose BSA-G-pTyr conjugate resin, the resin was treated with 0.1 M Gly, pH 2.2 buffer to extract any bound proteins. The solution was then rapidly neutralised with 1.0 M Tris, pH 9.0 buffer. The ELISA profile of the extracted (E1 (Gly)) and IN fractions are similar but interpreting the result was made difficult because

denaturing extractions conditions were used and later it was found that these antibodies were sensitive to these conditions (*vide infra*).

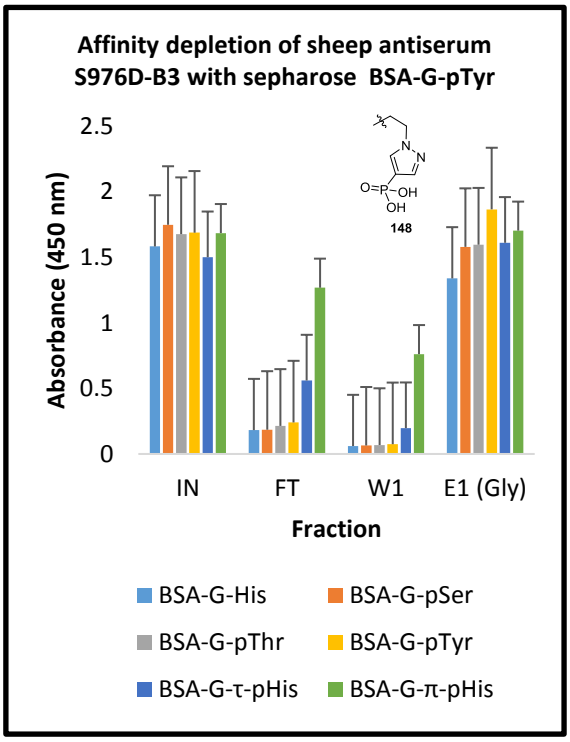

Figure 40: Sandwich ELISA of affinity depleted sheep S976D-B3 antiserum using sepharose BSA-G-pTyr conjugate resin. IN = input sheep S976D-B3 antiserum; FT = Flow through, fraction after incubation in with a sepharose BSA-G-pTyr conjugate resin; W1 = wash of sepharose BSA-G-pTyr conjugate resin with 25 mM Tris base, 150 mM NaCl, pH 7.4; E1 (Gly) = extraction of sepharose BSA-G-pTyr conjugate resin with 0.1 M Gly pH 2.2 followed by rapid neutralisation with 1.0 M Tris, pH 9.0 buffer. The ELISA plate was coated with a 1 µg/mL of BSA-G-amino acid conjugates, not checked by ^{31}P NMR. Error bars show the standard error of the mean (N = 2).

The FT fraction (Figure 40) indicated the presence of either cross reactive pHis antibodies or of mixture of τ- and π-pHis selective antibodies. A sepharose BSA-G-τ-pHis conjugate resin was used in an attempt to isolate these τ-pHis antibodies by an affinity purification (Figure

41). When 0.1 M Gly, pH 2.2, (followed by rapid neutralisation of the flow through with 1.0 M Tris, pH 9.0 buffer) was used to release the bound antibodies from the sepharose BSA-G-τ-pHis conjugate resin, the antibodies lost their selectivity for pHis on sandwich ELISA (data not shown). However, selective pHis antibodies were competitively dissociated from the resin using pHis.

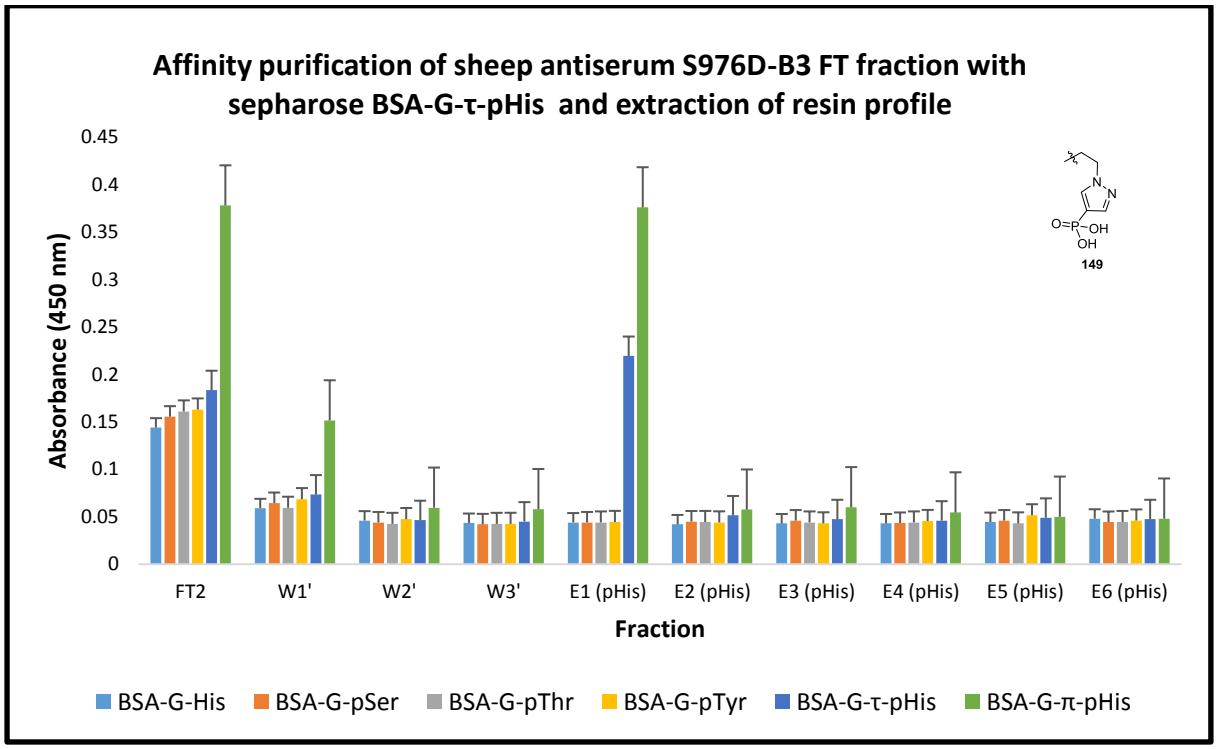

Figure 41: Sandwich ELISA of affinity purified sheep S976D-B3 FT fraction using a sepharose BSA-G-τ-pHis conjugate resin to; FT2 = Flow through 2, sample after incubation in with a sepharose conjugated to BSA-G-τ-pHis; W1'-W3' = washing of sepharose BSA-G-τ-pHis conjugate resin with 25 mM Tris, 150 mM NaCl, pH 7.4; E1 (pHis)-E6 (pHis) = competitive extraction of sepharose BSA-G-pTyr conjugate resin with 25 mM Tris base, 150 mM NaCl, 200 µg/mL pHis, pH 7.4. The ELISA plate was coated with a 1 µg/mL of BSA-G-amino acid conjugates, not checked by ^{31}P NMR. Error bars show the standard error of the mean (N = 2).

Despite successful isolation of selective pHis antibodies, the recovery was very low and the selectivity of the fraction E1 (pHis) in Figure 41 remained similar to FT fraction in Figure 40. Hence, to maximise recovery an affinity depletion purification strategy was chosen for antiserum S976D-B3. A 2mL sample of sheep antiserum S976D-B3 was affinity depleted with a sepharose BSA-G-pTyr conjugate resin (Scheme 54 and Figure 42) as previously in Scheme 40. The FT fraction was further affinity depleted with a sepharose BSA-G-π-pHis conjugate resin to give fraction FT2 which had a similar sandwich ELISA profile to FT. However, the sandwich ELISA in Figure 42 did not use normalised phosphorus loadings of BSA-G-pTyr, BSA-G-π-pHis, and BSA-G-τ-pHis but equivalent protein concentrations.

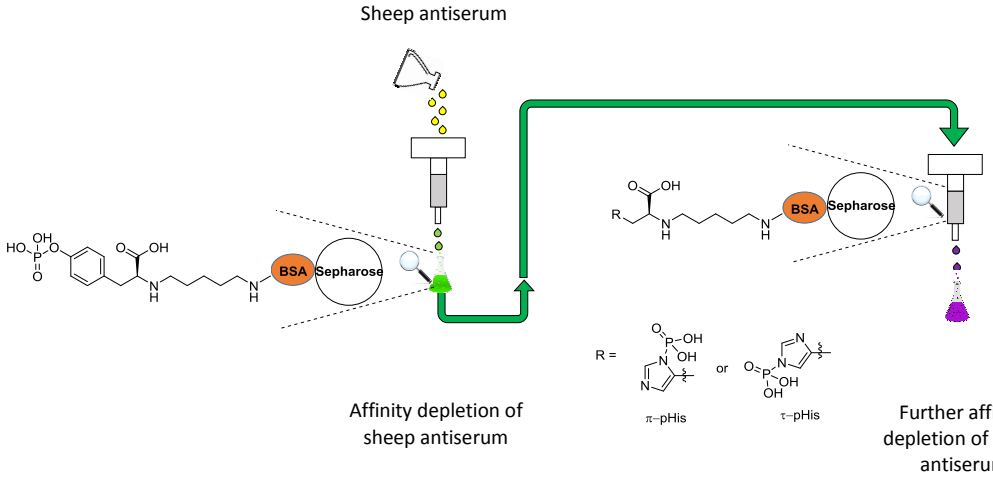

Scheme 54: A general schematic outlining the sequential affinity depletion steps for sheep antisera S976D-B3, SA220-B3, SA221-B3, SA222-B3, SA223-B3.

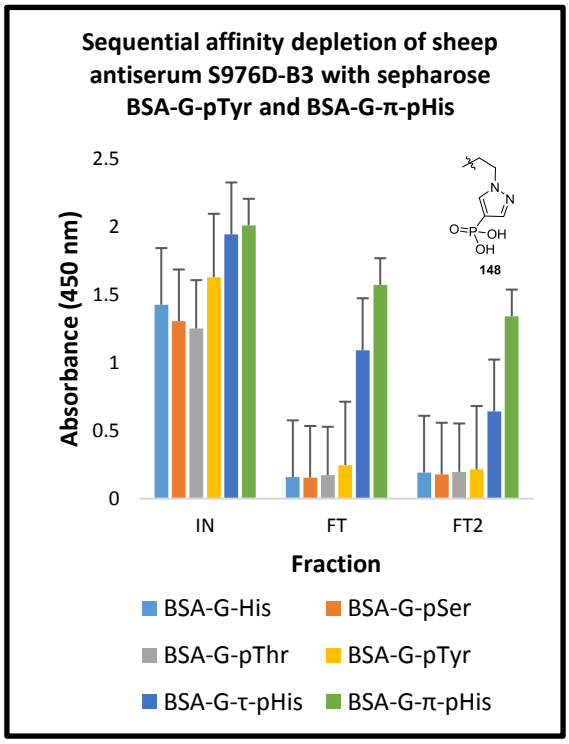

Figure 42: Sandwich ELISA of affinity depleted antiserums S976D-B3. IN = Input; starting antiserum. FT = Flow through; fraction after affinity depletion with a sepharose BSA-G-pTyr conjugate resin. FT2 = Flow through 2; fraction after a further affinity depletion with a sepharose BSA-G-π-pHis conjugate resin. The ELISA plate was coated with a 1 µg/mL of BSA-G-amino acid conjugates, not checked by ^{31}P NMR. Error bars show the standard error of the mean (N = 2).

The sequential affinity depletion strategy (Scheme 54) used to purify antiserum SA976D-B3 was also applied to antisera SA220-B3 and SA221-B3 generated to pyridine immunogens **149**, and **150** respectively. There was a significant improvement in selectivity for pHis on sandwich ELISA for both affinity depleted antisera on comparison of the IN fraction to the FT fraction (Figure 43). Both antisera showed further improvement in selectivity for BSA-G-τ-pHis following an affinity depletion of fraction FT with a sepharose BSA-G-π-pHis conjugate resin.

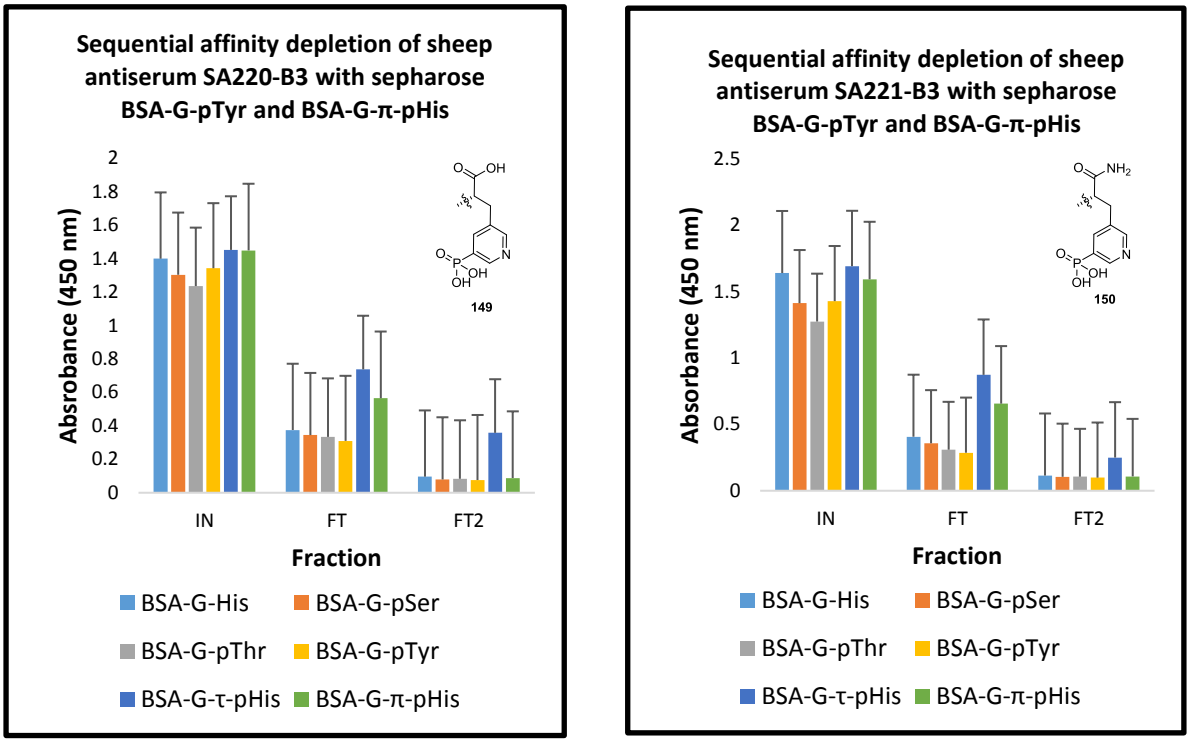

Figure 43: Sandwich ELISA of affinity depleted antisera SA220-B3 (right), and SA221-B3 (left). IN = Input; starting antiserum. FT = Flow through; fraction after affinity depletion with a sepharose BSA-G-pTyr conjugate resin. FT2 = Flow through 2; fraction after a further affinity depletion with a sepharose BSA-G-π-pHis conjugate resin. BSA-G-pTyr, BSA-G-π-pHis, and BSA-G-τ-pHis were analysed by ^{31}P NMR and normalised phosphorus loadings of these three conjugates was used. Error bars show the standard error of the mean (N = 2).

Likewise, antisera SA222-B3, and SA223-B3 generated to pyridine immunogens **151** and **152** respectively showed an improved selectivity for pHis after affinity depletion with sepharose BSA-G-pTyr conjugate resin, on comparison of the IN fraction to the FT fraction. An increase in selectivity for BSA-G-π-pHis was observed for both FT2 fractions after a further affinity depletion of the FT fractions with sepharose BSA-G-τ-pHis conjugate resin (Figure 44).

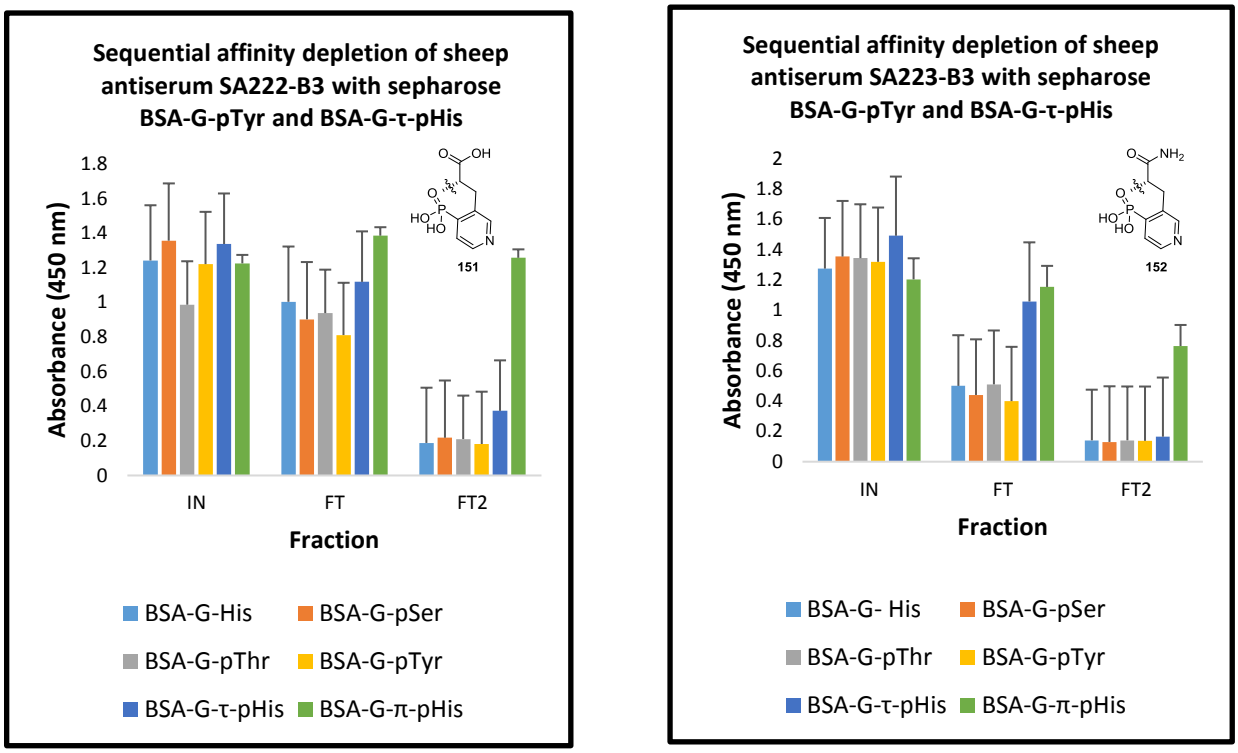

Figure 44: Sandwich ELISA of affinity depleted antiserums, SA222-B3 (right), and SA223-B3 (left). IN = Input; starting antiserum. FT = Flow through; fraction after affinity depletion with a sepharose BSA-G-pTyr conjugate resin. FT2 = Flow through 2; fraction after a further affinity depletion with sepharose BSA-G-τ-pHis conjugate resin. BSA-G-pTyr, BSA-G-π-pHis, and BSA-G-τ-pHis were analysed by ^{31}P NMR and normalised phosphorus loadings of these three conjugates was used. Error bars show the standard error of the mean (N = 2).

On competitive ELISA, fraction FT2 from the affinity depleted antiserum S976D-B3 (Figure 42), gave an ELISA profile which suggested the presence of selective τ-pHis antibodies (Figure 45). This was contrary to the sandwich ELISA result (Figure 42) but likely accurate because analogue **61**, which was proposed as a τ-pHis analogue was used as the epitope.

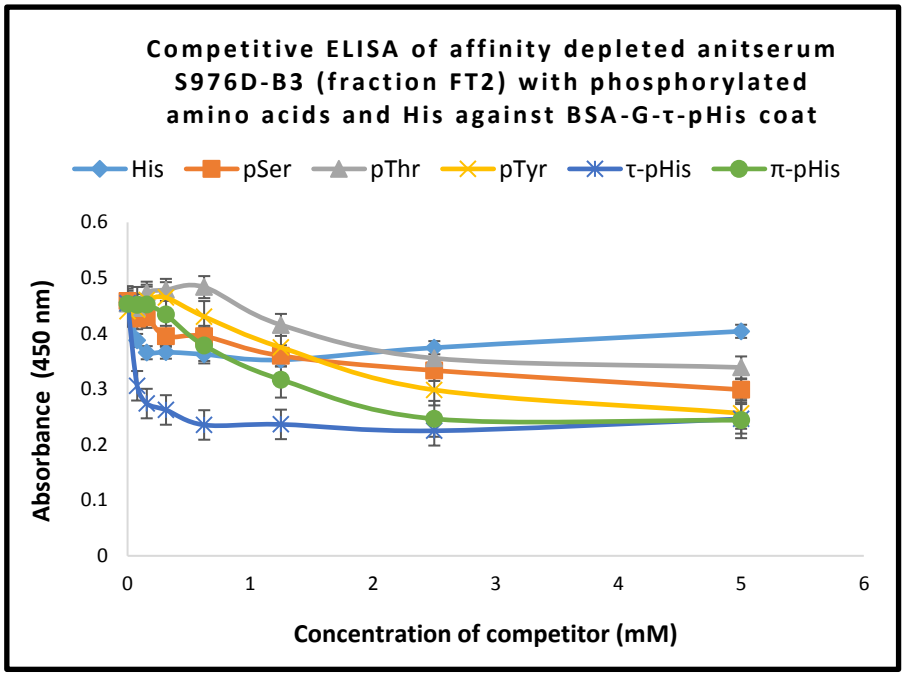

Figure 45: Competitive ELISA of affinity depleted antiserum S975D-B3 (fraction FT2, see Figure 42), with His, pSer, pThr, pTyr, π-pHis, and τ-pHis against BSA-G-τ-pHis (20 µg/mL) analysed by ^{31}P NMR. 1/18 (v/v) antiserum dilution. Error bars show the standard error of the mean (N = 2).

Competitive ELISA of fraction FT2 (Figure 43) from affinity depleted antisera SA220-B3 (Figure 46) and SA221-B3 (Figure 47) suggested the presence of selective π-pHis antibodies; which appeared inconsistent with the sandwich ELISA results (Figure 43). Close examination of ESP surface of side chain **86** and **90** show two side chains with very similar regions of ESP (Figure 48). The larger pyridine ring size (compared to the imidazole ring) could give it enough spatial freedom to be a mimic of π-pHis and not τ-pHis or both.

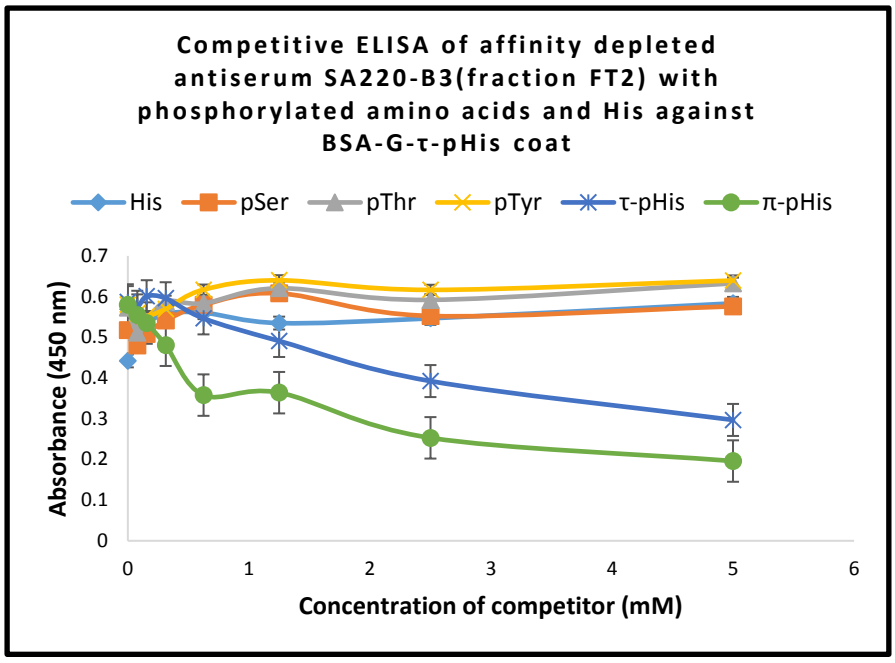

Figure 46: Competitive ELISA of affinity depleted antiserum, SA220-B3 (fraction FT2, see Figure 43) with His, pSer, pThr, pTyr, π-pHis, and τ-pHis against BSA-G-τ-pHis (20 µg/mL) analysed by ^{31}P NMR. 1/70 (v/v) antiserum dilution. Error bars show the standard error of the mean (N = 2).

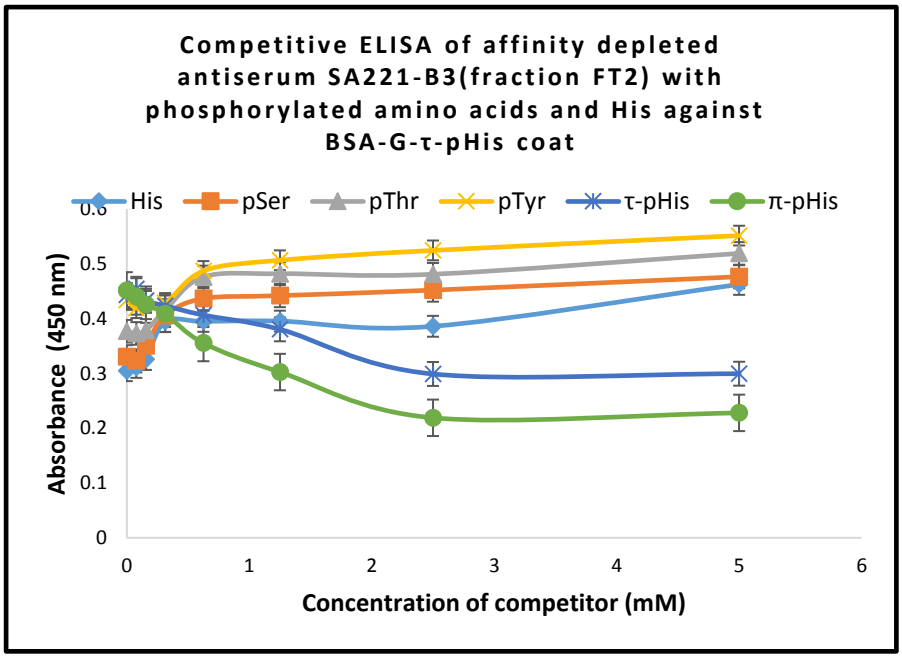

Figure 47: Competitive ELISA of affinity depleted antiserum SA221-B3 (fraction FT2, see Figure 43), with His, pSer, pThr, pTyr, π-pHis, and τ-pHis against BSA-G-τ-pHis (20 µg/mL) analysed by ^{31}P NMR. 1/50 (v/v) antiserum dilution. Error bars show the standard error of the mean (N = 2).

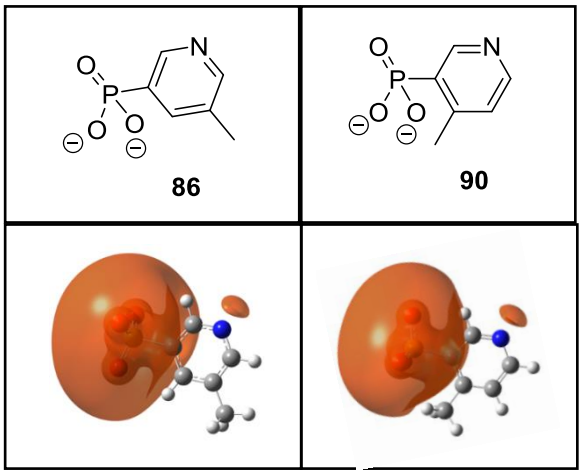

Figure 48: ESP surfaces (contours drawn at a potential of -0.285 au, bottom row) for model compounds 3,5-disubstituted pyridine **86**, and 2,4-disubstituted pyridine **90**.

The competitive ELISA of fraction FT2 (Figure 44) from affinity purified antisera SA222-B3 (Figure 49) and SA223-B3 (Figure 50) showed that both fractions were selective π-pHis antibodies. There was no significant difference in the competitive ELISA profiles of the affinity depleted antiserum SA220-B3 (Figure 46) generated with the 3,5-disubstituted pyridine amino acid immunogen **149** and the affinity depleted antiserum SA221-B3 (Figure 47) generated with 3,5-disubstituted pyridine amino amide immunogen **150**. On the other hand, the competitive ELISA profiles of affinity depleted antiserum SA222-B3 (Figure 49) generated with 3,4-disubstituted amino acid immunogen **151** suggest these antibodies are more cross reactive for pTyr and less selective for π-pHis than affinity depleted antiserum SA223-B3 (Figure 50) generated with 3,4-disubstituted pyridine amino amide **152**.

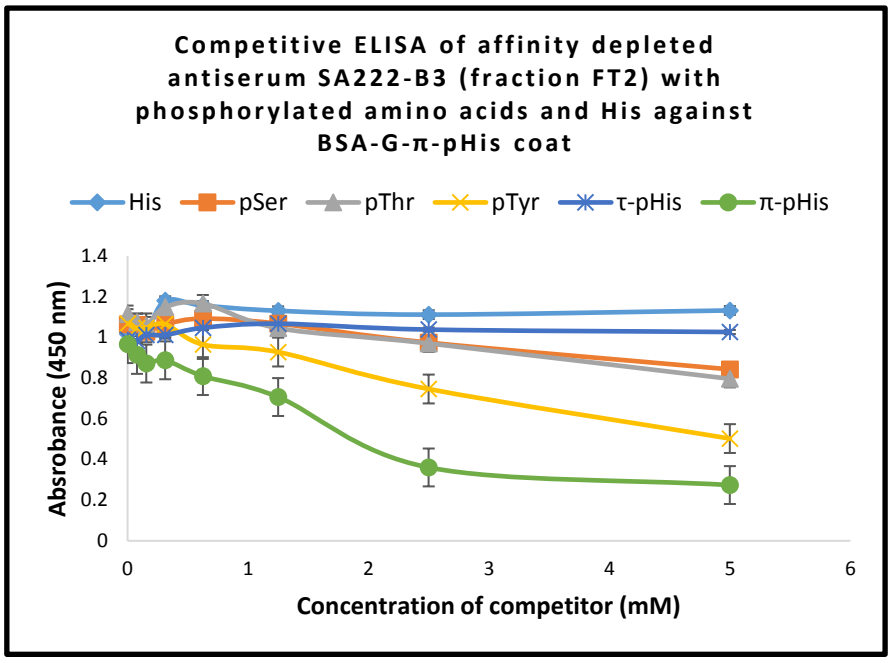

Figure 49: Competitive ELISA of purified antiserums, SA222-B3 (fraction FT2, see Figure 44), with His, pSer, pThr, pTyr, π-pHis, and τ-pHis against BSA-G-π-pHis (20 µg/mL) analysed by ^{31}P NMR. 1/70 (v/v) antiserum dilution. Error bars show the standard error of the mean (N = 2).

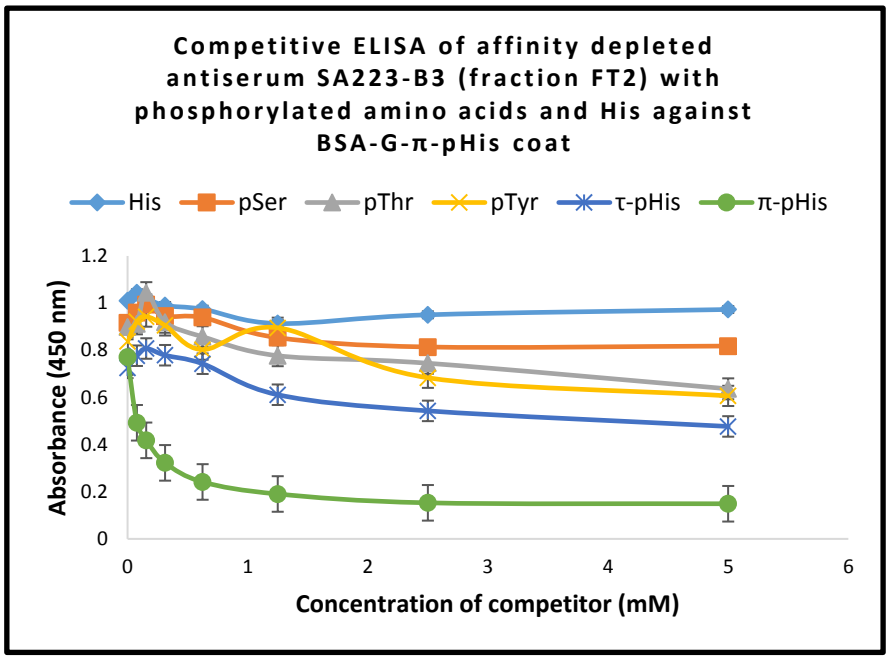

Figure 50: Competitive ELISA of purified antiserums SA223-B3 (fraction FT2, see Figure 44) with His, pSer, pThr, pTyr, π-pHis, and τ-pHis against BSA-G-π-pHis (20 µg/mL) analysed by ^{31}P NMR. 1/70 (v/v) antiserum dilution. Error bars show the standard error of the mean (N = 2).

3.2.6: Large scale purification and characterisation of sheep antiserum S967D-B3

On competitive ELISA, fraction FT2 of affinity depleted sheep antisera S976D-B3 (Figure 45) and SA223-B3 (Figure 50) seemed most promising. However, larger quantities of purified polyclonal antibody from both antisera was required to find suitable conditions for use in biological techniques such as Western blot and immunoprecipitation Hence, a large-scale purification of both antiserums was needed.

In a linear scale up, 35 mL of sheep antiserum S976D-B3 was affinity depleted as before with sepharose BSA-G-pTyr conjugate resin (Figure 51). Comparison of the sandwich ELISA of the IN and FT fractions show that the sepharose BSA-G-pTyr conjugate resin effectively removed undesired antibodies; specifically, those which recognised the glutaraldehyde linker and those that were cross-reactive for pTyr residues. The fractions W1-W6 suggested the presence of selective π-pHis polyclonal antibodies which were weekly bound to the sepharose BSA-G-pTyr conjugate resin. It was thought that by competitive dissociation with π-pHis, a more selective antibody for π-pHis could be obtained. Next to maximize antibody recovery, the sepharose BSA-G-pTyr conjugate resin was further competitively dissociated with τ-pHis. Antibody fractions showing similar selectivity, W3-W6, E1-E4(π-pHis) + W7-W9, and E1-E4(τ-pHis) + W10-W11 were labelled as antibody 3(τ), 4(τ) and 5(τ) respectively.

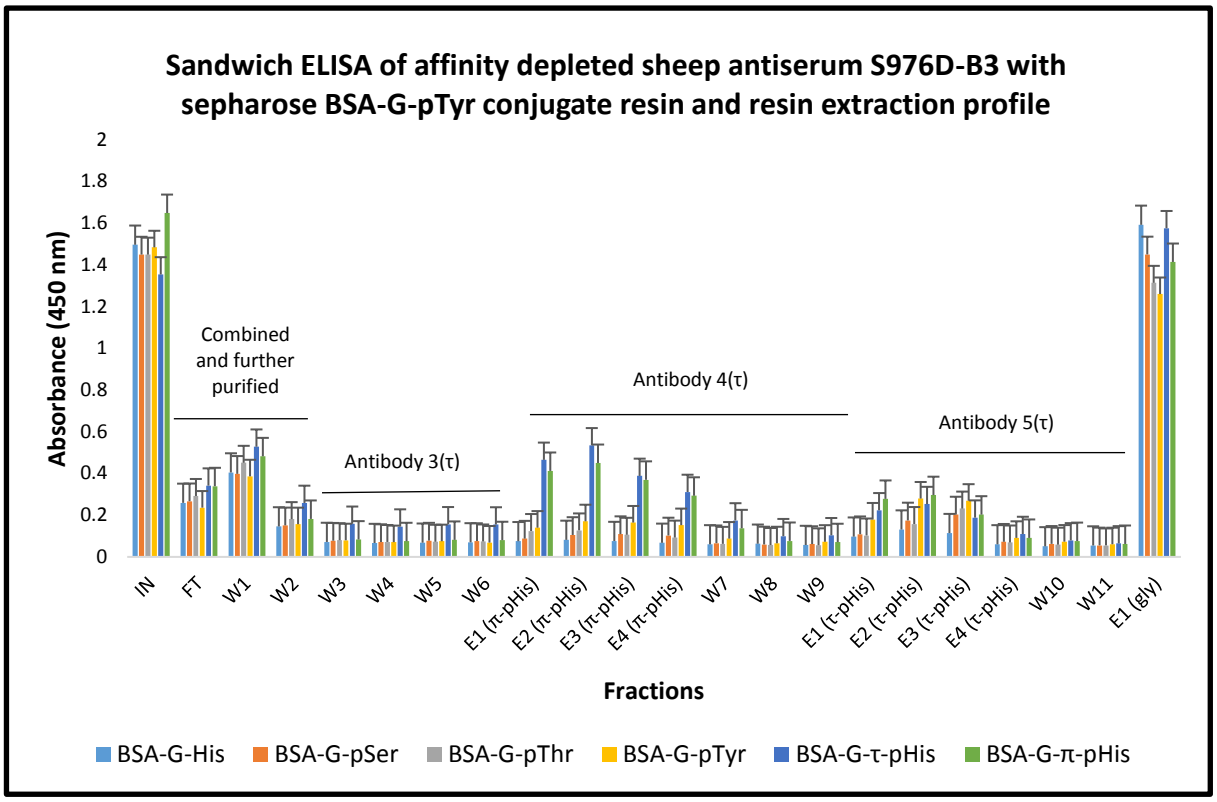

Figure 51: Sandwich ELISA of sheep antiserum S976D-B3 affinity depleted with sepharose BSA-G-pTyr conjugate resin. FT = Flow through, after incubation in with a sepharose BSA-G-pTyr conjugate resin. W1-W11 = washing of sepharose BSA-G-pTyr conjugate resin with 25 mM Tris base, 150 mM NaCl, pH 7.4. E1-E4 (pHis) = competitive extraction of sepharose BSA-G-pTyr conjugate resin with 25 mM Tris base, 150 mM NaCl, 200 µg/mL τ- or π-pHis, pH 7.4. E1 (gly) = extraction of sepharose BSA-G-pTyr conjugate resin with 0.1 M Gly pH 2.2 followed by rapid neutralisation with 1.0 M Tris, pH 9.0. BSA-G-τ-pHis, BSA-G-π-pHis and BSA-G-pTyr assays were analysed by ^{31}P NMR and equal phosphorus loadings were used. Error bars show the standard error of the mean (N = 2).

FT, W1 and W2 fractions from Figure 51 were combined and further affinity depleted with a sepharose BSA-G-π-pHis conjugate resin (Figure 52). ELISA showed there was no was improvement in selectivity for τ-pHis. The fractions FT2-W1' and W2'-W4'were combined and labelled antibody 1(τ) and 2(τ) respectively.

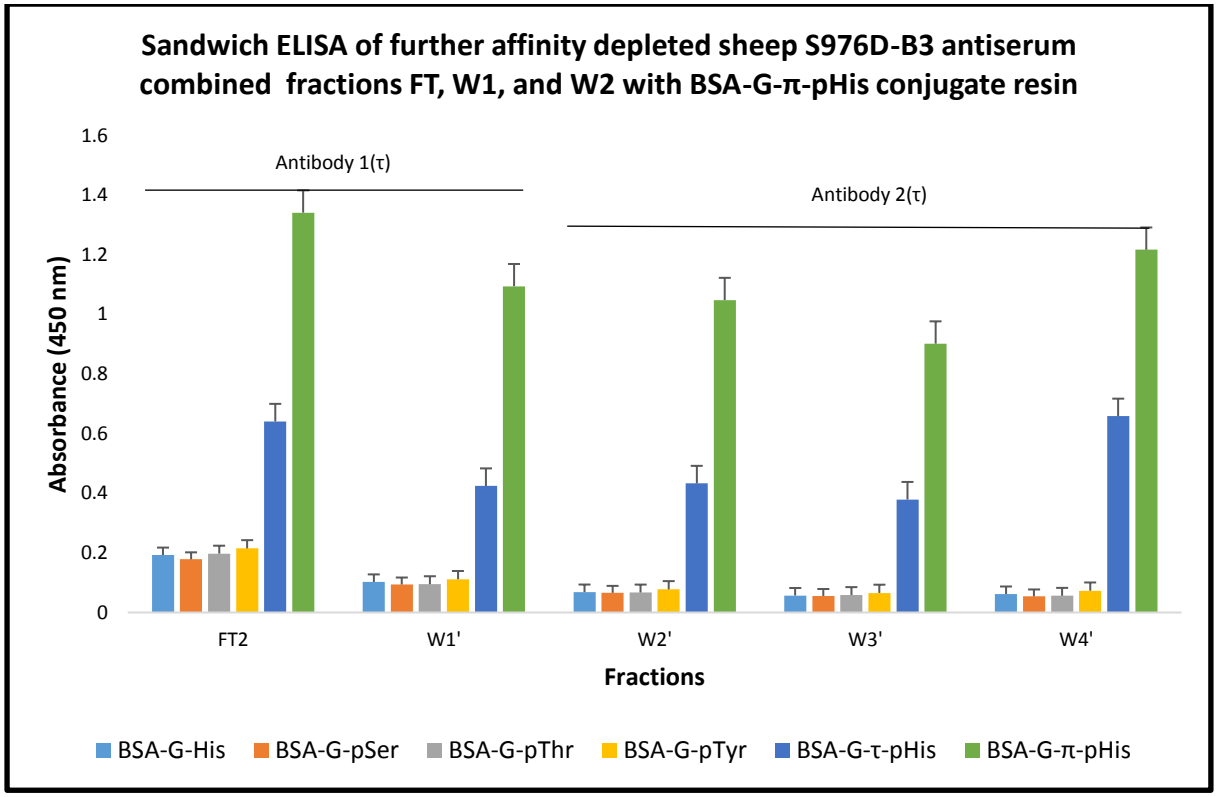

Figure 52: Sandwich ELISA of further affinity depleted sheep S976D-B3 combined antiserum fractions FT, W1 and W2 (Figure 51). FT2 = Flow through, after incubation in with a sepharose conjugated to BSA-G-π-pHis. W1'-W4' = washing of sepharose BSA-G-π-pHis conjugate resin with 25 mM Tris base, 150 mM NaCl, pH 7.4. The ELISA plate was coated with a 1 µg/mL of BSA-G-amino acid conjugates, not checked by ^{31}P NMR. Error bars show the standard error of the mean (N = 2).

As described in section 3.2.2, a competitive ELISA uses only one BSA-G-amino acid conjugate to coat the ELISA plate surface and a quantifiable amount of amino acid as a competitor. Before further analysis of the fractions by competition ELISA, antibodies 1(τ)-5(τ) and BSA-G-τ-pHis conjugate were subjected to titer ELISA experiments to determine optimal antibody and conjugate concentrations (absorbance value close to 1). The competitive ELISA profiles of antibody 1(τ), 2(τ), 3(τ) 4(τ) and 5(τ) show that at low concentrations all antibodies were highly selective for τ-pHis over π-pHis and is consistent with selectivity that would be

expected from polyclonal antibodies raised with pyrazole analogue **61** (Figure 53-57). The ELISA profiles also suggest phospho amino acid residue detection at higher competitor concentrations which would be expected for polyclonal antibodies. Importantly, overcoming the challenge of generating selective τ-pHis antibodies over pTyr was achieved here, and the polyclonal antibody selectivity was much greater than the commercially available monoclonal antibody (Figure 28, page 92).

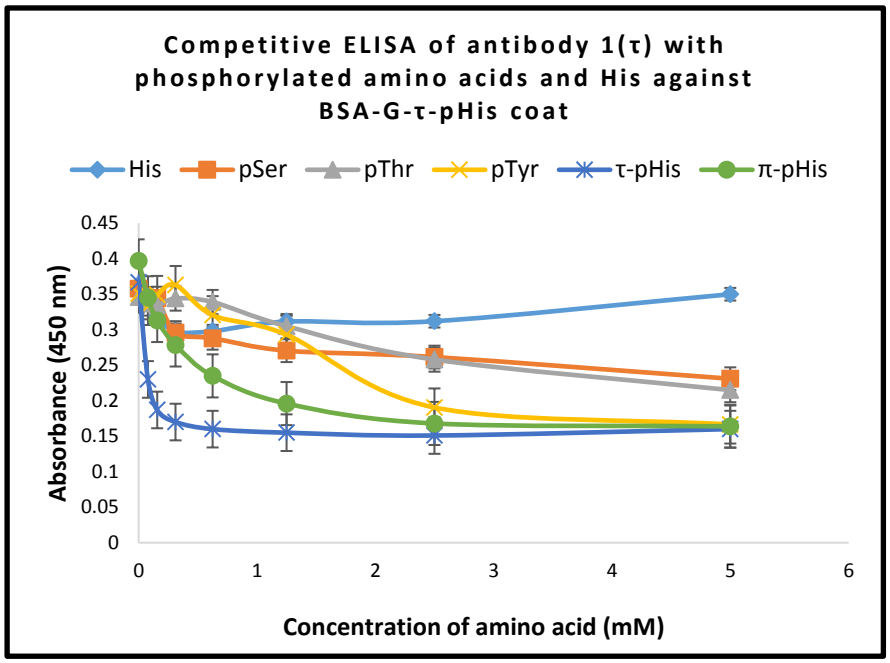

Figure 53: Competitive ELISA of antibody 1(τ) (combined antibody fractions FT2, W1' see Figure 52) with His, pSer, pThr, pTyr, τ-pHis, and π-pHis against BSA-G-τ-pHis (20 µg/mL) analysed by ^{31}P NMR. Error bars show the standard error of the mean (N = 2).

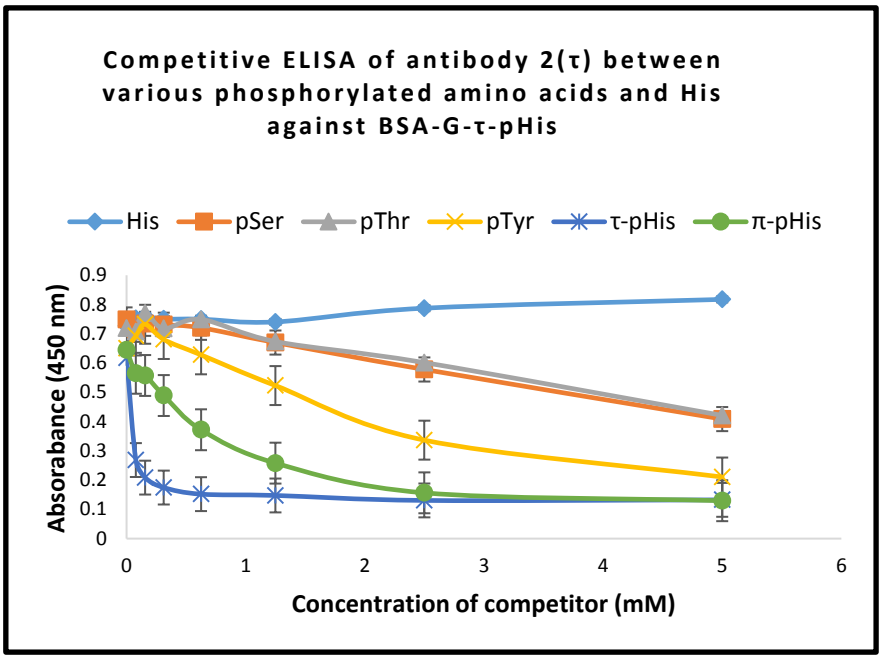

Figure 54: Competitive ELISA of antibody 2(τ) (combined antibody fractions W2'-W4'see Figure 52) with His, pSer, pThr, pTyr, τ-pHis, and π-pHis against BSA-G-τ-pHis (20 µg/mL) analysed by ^{31}P NMR. Error bars show the standard error of the mean (N = 2).

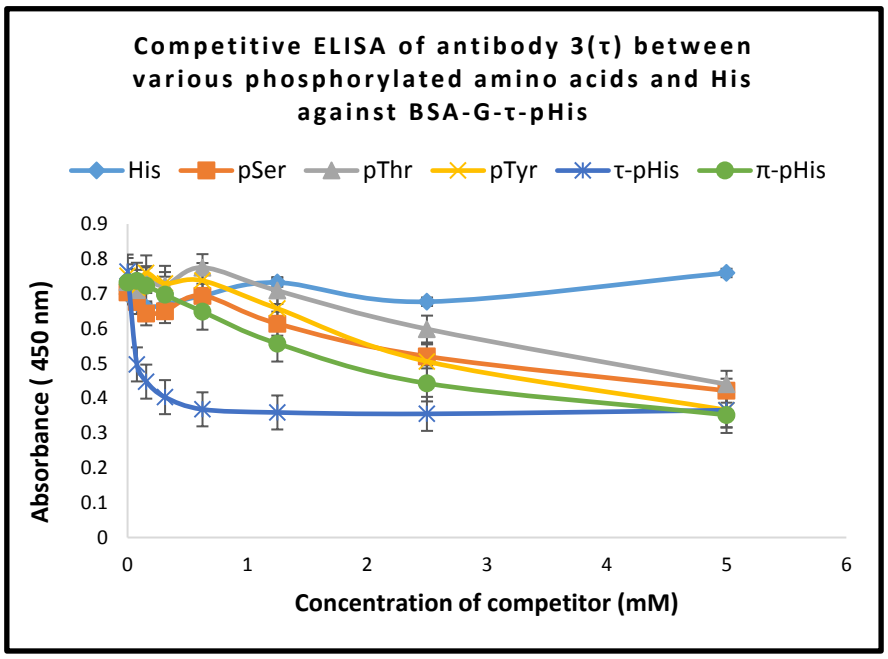

Figure 55: Competitive ELISA of antibody 3(τ) (combined antibody fractions W3-W6 see Figure 51) with His, pSer, pThr, pTyr, τ-pHis, and π-pHis against BSA-G-τ-pHis (20 µg/mL) analysed by ^{31}P NMR. Error bars show the standard error of the mean (N = 2).

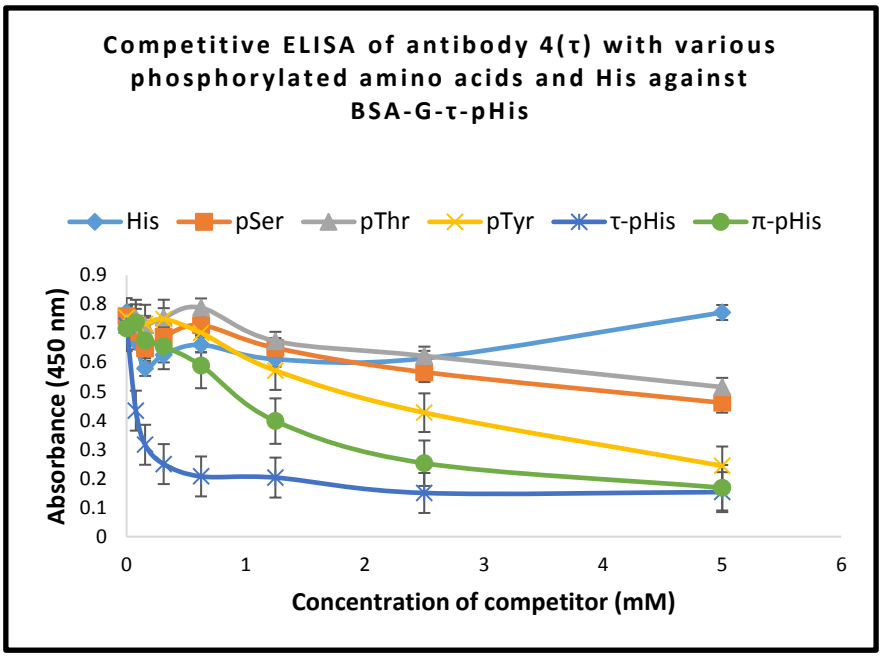

Figure 56: Competitive ELISA of antibody 4(τ) (combined antibody fractions E1-E4 (π-pHis), and W7-W9 see Figure 51) with His, pSer, pThr, pTyr, τ-pHis, and π-pHis against BSA-G-τ-pHis (20 µg/mL) analysed by ^{31}P NMR. Error bars show the standard error of the mean (N = 2).

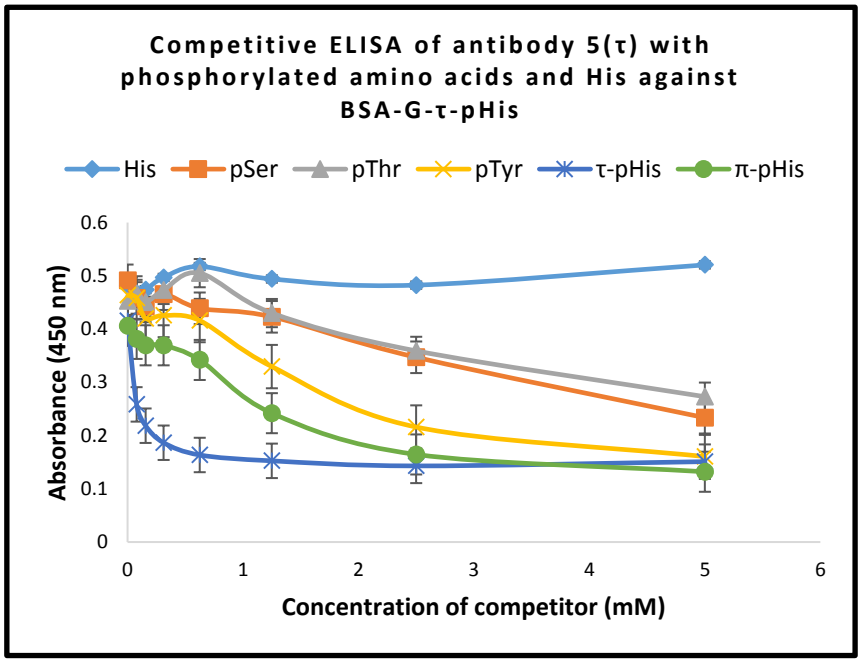

Figure 57: Competitive ELISA of antibody 5(τ) (combined antibody fractions E1-E4 (τ-pHis), and W10-W11 see Figure 51) with His, pSer, pThr, pTyr, τ-pHis, and π-pHis against BSA-G-τ-pHis (20 µg/mL) analysed by ^{31}P NMR. Error bars show the standard error of the mean (N = 2).

To stop microbial growth, the antibodies 1(τ)-5(τ) were buffer exchanged into 0.1 M Tris-Gly, 150 mM NaCl, 0.05 % (wt/v) NaN_3, pH 7.4 buffer. The antibodies were found to retain their selectivity on competitive ELISA between pH 6.5-8.8 at room temperature and could be snap frozen (freeze thaw cycles were avoided to minimise antibody damage) for long term storage at -80 ^{o}C. After a few weeks at 4 ^{o}C antibody 1(τ) was found to have formed a precipitate. Presumably this unknown substance was a protein carried forward in the antiserum because antibody 1(τ) was affinity depleted. As a precaution, every time antibody 1(τ) was needed an aliquot was centrifuged to pellet the precipitate and the supernatant was used for experiments.

3.2.6.1: Use of τ-pHis antibodies in Western blot

Considerable optimisation of the general Western blot procedure was required before good signal to background was observed. To achieve this, it was important to stabilise pHis residues in cell lysates until to the end of the Western blot procedure. The radioimmunoprecipitation assay (RIPA) lysis buffer previously used by the group for studying phosphorylated amino acids included: 150 mM NaCl (for protein solubilisation), 0.5 % sodium deoxycholate (for membrane protein solubilisation), 1 % Triton X-100 (cell lysis and protein solubilisation), and 0.1 % SDS (cell lysis and protein solubilisation); Roche complete protease inhibitor cocktail, and a 1 mM 4-(2-aminoethyl)benzenesulfonyl fluoride (irreversible protease inhibitor); 10 mM sodium fluoride (phosphatase inhibitor), 5 mM sodium orthovanadate (phosphatase inhibitor), 10 mM sodium pyrophosphate (phosphatase inhibitor), and 50 mM Tris, pH 8.0 (as the buffer). The majority of the RIPA lysis buffer components are suitable for pHis but the primary amine, 4-(2-aminoethyl)benzenesulfonyl fluoride, which could potentially dephosphorylate pHis, was omitted, and the buffer pH was raised to 9. The phosphatase inhibitors in the lysis buffer are general mimics of the phosphoryl group and it was thought

they would also competitively inhibit His phosphatases. This modified RIPA lysis buffer was also advantageous because it precipitates the DNA which can interfere with protein resolution in SDS-PAGE and solubilizes membrane proteins unlike many other lysis buffers.

In a Western blot procedure, proteins from a whole cell lysate are separated (or resolved) by molecular weight using SDS-PAGE before being blotted onto a membrane such as polyvinylidene difluoride (PVDF) or nitrocellulose. For good protein separation, cell lysate are treated with a Laemmli sample buffer (typical composition: 2 % (wt/v) SDS, 10 % (v/v) glycerol, 5 % (v/v) 2-mercaptoethanol, 0.002 % (wt/v) bromphenol blue, 63 mM Tris HCl, pH 6.8) at 95 ^{o}C for up to 10 minutes to denature and reduce disulphide bonds before SDS-PAGE. Such conditions would be expected to destroy pHis. Unlike SDS, lithium dodecylsulphate (LDS) effectively denatures proteins at low temperature (< 15 ^{o}C)[156] and DTT is a more effective reducing agent than 2-mercaptoethanol. Substituting these two reagents, and raising the pH and adding other minor alterations gave a sample buffer with the following composition: 2 % (w/v) LDS, 8 % (w/v) glycerol, 0.004 % (w/v) bromophenol blue, 10 mM EDTA, 100 mM DTT, 60 mM Tris, pH 9.0 which was effective at low temperature. It was necessary to immerse the gel electrophoresis tank in ice during the transfer step to minimise loss of pHis. This is because during the transfer step of the Western blot, the resolved proteins in the gel need to be electro blotted onto a PVDF membrane. During this step the transfer buffer, which contains methanol can get hot and increase the rate of pHis destruction.

Once the proteins had been blotted onto the PVDF membrane, the unoccupied sites needed to be blocked. Milk contains a mixture of proteins (albumins, and immunoglobulins and caseins) and is commonly used as a blocker in a buffer at a 5 % (wt/v) concentration for these purposes. However, the protein casein is known to be Ser phosphorylated, making milk a non-

ideal blocking agent for phosphor antibodies. BSA has been successfully used as a blocking protein with phospho antibodies but is expensive. In this work we found that 0.2 % (v/v) gelatin from cold water fish skin gave excellent Western blot profiles with the pHis antibodies and very little background.

There was a significant number of pHis proteins detected in the Western blot of the HBE cell lysate when probed with the isolated τ-pHis polyclonal antibodies (Figure 58) compared to the commercial monoclonal pHis antibody (Figure 28, page 92) after 3599 seconds of exposure visualised using Bio-Rad ChemiDoc™ XRS+. The Western blot profiles between pHis antibodies 1(τ)–5(τ) are similar (low molecular weight proteins) with some variations in the detection of high molecular weight proteins. There may also be many more pHis proteins in the HBE lysate which are of low abundance and may not have been detected by the antibodies because of degradation during the Western blot procedure. As controls the HBE lysate was treated with acid or base.[77,122] Precipitation was observed when using previously reported acid treatment of the HBE lysate (0.1 M HCl and 60 ^{o}C).[122] Acidifying with aqueous HCl to ~pH 3 in the modified sample buffer and then heating at 90 ^{o}C between 30-45 minutes gave no precipitation. Under these conditions pSer, pThr, and pTyr are known to be stable and a reduction/abolishment in the Western blot signal would not be expected as observed.[45] Base treatment (1 M NaOH, 37 ^{o}C, 18-20 h.) is known to decompose pSer and pThr.[85] However, later it was found that the base treatment (0.1 M NaOH, room temp., 15-45 min) used on the HBE cell lysate was probably not vigorous enough to eliminate the phosphoryl groups of pSer/pThr.

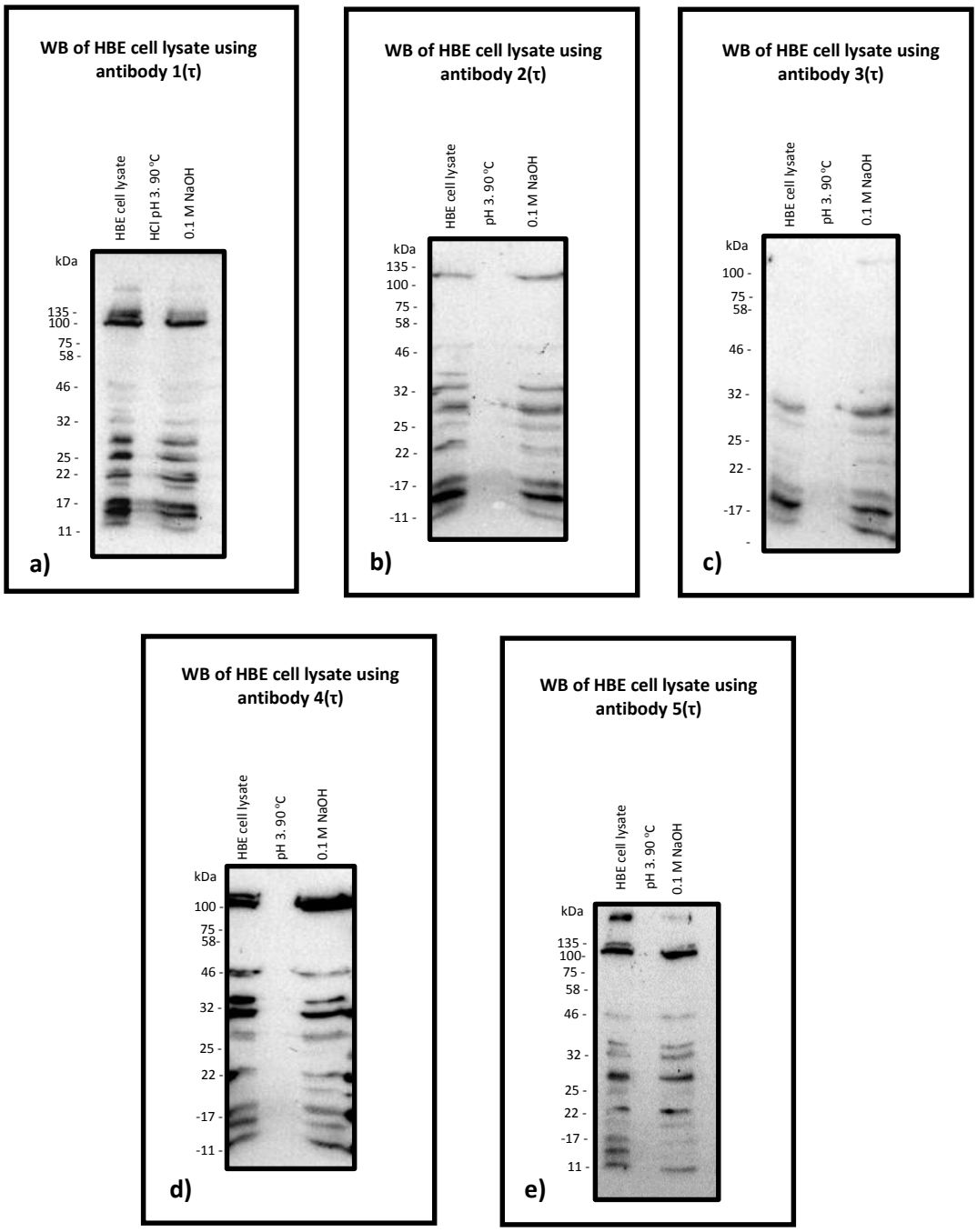

Figure 58: Western blot (WB) of 100 µg HBE protein cell lysate, treated with HCl to pH 3 at 90 °C for 15-45 min and with NaOH, (0.1 M final concentration) at room temp. in modified sample buffer. The membranes were visualised using Bio-Rad ChemiDoc™ XRS+, 3600 second exposure: **a**) 1(τ), 1/18 (v/v) antibody dilution; **b**) 2(τ), 1/4 (v/v) antibody dilution; **c**) 3(τ), 1/8 (v/v) antibody dilution; **d**) 4(τ), 1/12 (v/v) antibody dilution; **e**) 5(τ), 1/8 (v/v) antibody dilution.

3.2.6.2: Immunoprecipitation using τ-pHis antibody

It was important to demonstrate that the pHis antibodies could be used in the enrichment of pHis proteins from a whole cell lysate. Of the five τ-pHis antibodies, antibody 1(τ) was available in the largest quantities. However, since antibody 1(τ) was an affinity depleted antibody, it was possible small quantities of other proteins were still present. Protein G is a non-covalent binding immunoglobulin G binding (IgG) protein[157] and has been used to selectively bind IgGs prior to immunoprecipitation of proteins/peptides. Protein G is commercially available conjugated to a beaded form of agarose known ad sepharose. Protein G sepharose is advantageous because as a conjugate it can still be used to bind IgG and pull-down proteins but since the protein G sepharose is insoluble in aqueous solvents, isolation of the pulled down proteins is possible (Scheme 55).

HBE cell lysate with and without pH reduction and heat treatment was incubated with proteins G sepharose bound to pHis antibody 1(τ) (Scheme 55). The unbound material was washed away, and the bound pHis proteins were dissociated from the antibody using pyrazolylbutane **140** in 50 mM Tris buffered saline, pH 8.5. To remove any undissociated proteins, the resin was treated with 0.1 M Gly, pH 2.0 (as a denaturant) and immediately neutralised with 1 M Tris-HCl, pH 8.0.

As a control it was necessary to find conditions that would destroy pHis in the HBE lysate before immunoprecipitation. Commonly used pHis dephosphorylation conditions of acid and heat treatment on the HBE lysate (in modified RIPA buffer) caused protein precipitation. Protein precipitation was also observed with hydroxylamine, a chemical known to dephosphorylate pHis.[122] A denaturing lysis buffer with the following composition: 6 M Urea, 30 mM Octyl-β-D-glucopyranoside, Roche complete protease inhibitor cocktail, 0.1 M

Na_2CO_3/$NaHCO_3$, pH 10 was found decrease the extent of pHis when the solution pH was reduced to pH 7 and heated at 60 ^oC for 30 minutes.

An aliquot from each sample from the immunoprecipitation experiment was resolved by SDS page and blotted on to PVDF membranes (Figure 59). The blotted proteins were stained with colloidal gold which is as sensitive (ng) as the silver stain.[158] Colloidal gold is advantageous because it does not involve a complicated work flow or use toxic reagents such as silver nitrate used in the silver stain. To show that the proteins being pulled down were pHis proteins, a Western blot was carried out in parallel using the pHis antibody 1(τ).

The colloidal gold stained membranes suggest on average fewer proteins were pulled down when the HBE lysate was heated (60 ^oC) at pH 7. The untreated HBE lysate, has more intense protein bands on Western blot probed with pHis antibody 1(τ) than the acid/heat treated sample. This confirmed that many of the proteins pulled down from the HBE lysate are likely His phosphorylated. The colloidal gold stained lane (0.1 M Gly pH 2.0) shows that the competitor did not dissociate all the bound proteins. There are also additional protein bands < 25 kDa, and > 135 kDa in this lane which are not seen in the competitor lanes. If these additional proteins are His phosphorylated, the low pH used to dissociate them probably destroyed the pHis modification and hence they are not detected in the Western blot.

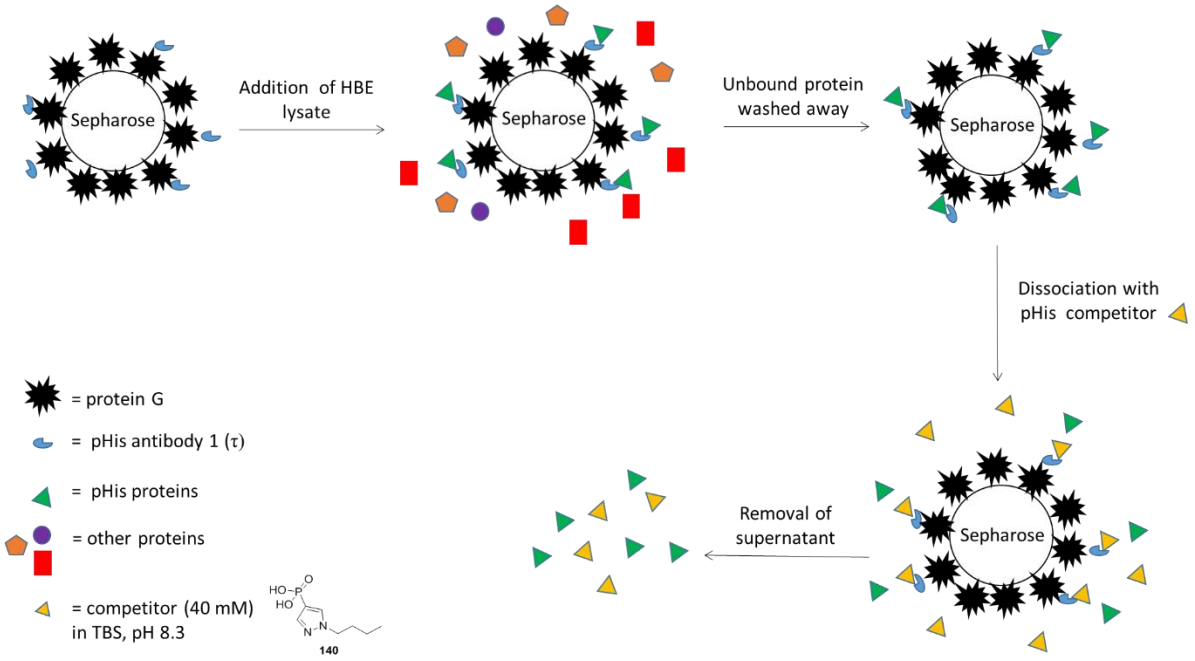

Scheme 55: Overview schematic of the immunoprecipitation experimental procedure used to pull down pHis proteins from the HBE lysate using pHis antibody 1(τ) bound to protein G sepharose.

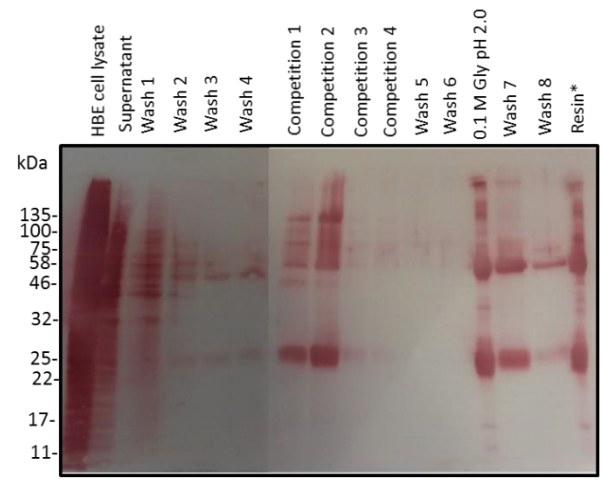

Colloidal gold stained PVDF membrane

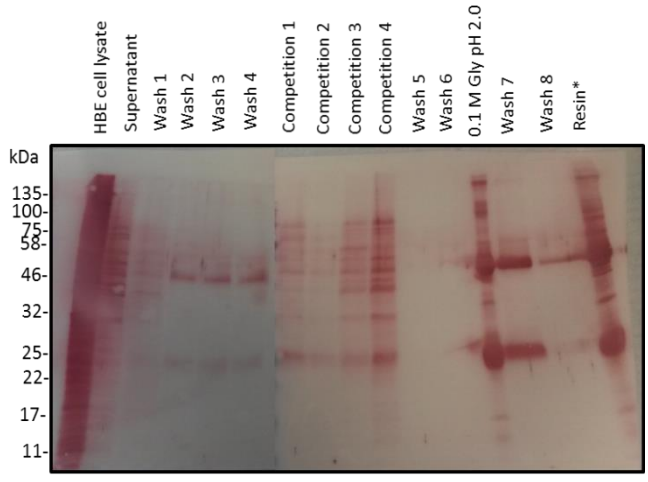

Colloidal gold stained PVDF membrane. Acid treated

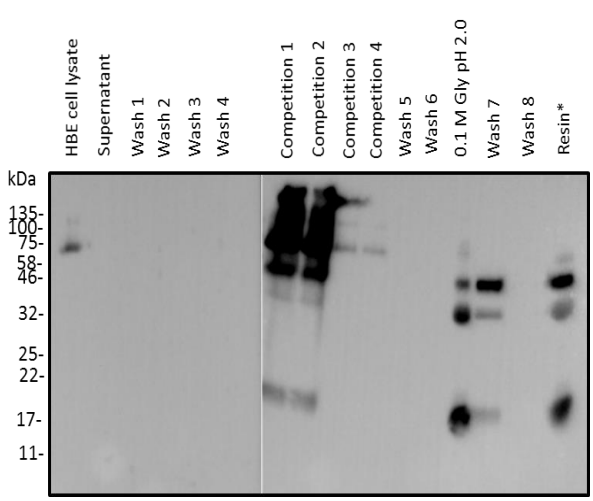

WB probed with pHis antibody 1(τ)

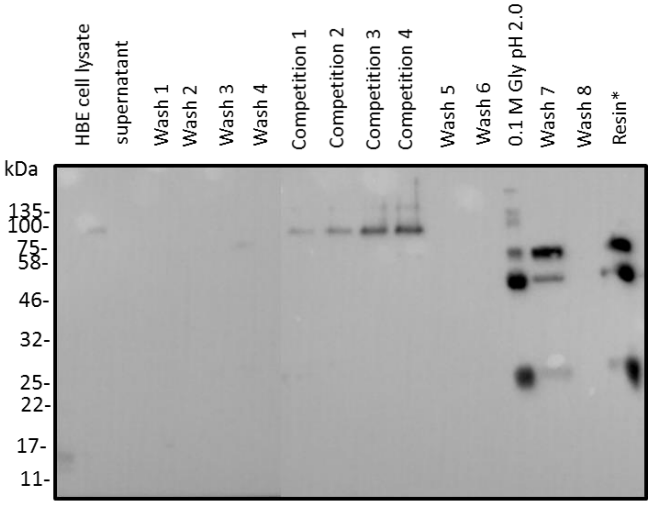

WB probed with pHis antibody 1(τ). Acid treated

Figure 59: Immunoprecipitation of HBE cell lysate using pHis antibody 1(τ) bound to protein G sepharose experiment samples. Upper membranes: proteins stained with colloidal gold. Lower membranes: Western blot (WB) with pHis antibody 1(τ); the membranes were visualised using Bio-Rad ChemiDoc™ XRS+, 49 sec exposures. Membranes on the left: Untreated HBE cell lysate. Membranes on the right: HBE cell lysate pH reduced to 7.0 and heated at 60 ^{o}C for 30 min before immunoprecipitation. *Sepharose protein G after immunoprecipitation experiment.

On Western blot (Figure 58), many low molecular weight (<32 kDa) pHis proteins were detected from the HBE whole cell lysate pHis with antibody 1(τ). However, these low molecular weight proteins were not observed from the IP experiments using pHis antibody 1(τ). In a Western blot procedure, proteins are denatured, and the antibody detects a residue in a peptidic environment. In an immunoprecipitation experiment non-denaturing buffers are used for antibody compatibility and proteins will retain some or all of their tertiary structure. The pyrazole **61** analogue used to generate these pHis antibodies were specifically designed to give peptide sequence independent selective τ-pHis antibodies. It may be that the pHis residue for some of these pHis proteins was unavailable for antibody binding due to the protein structure (e.g. buried in a pocket or sterically hindered). Another potential explanation could that excess HBE lysate to antibody was used, and the particular pHis proteins which were pulled down out competed the other pHis proteins because they were more strongly binding to pHis antibody 1(τ). Alternatively, some of HBE lysate pHis proteins did not strongly bind the pHis antibody 1(τ) and were not pulled down or they weakly bound the pHis antibody 1(τ) and were lost in the wash

In a preliminary MS study, the proteins pulled down with pHis antibody 1(τ) were resolved by SDS-PAGE. The gel was stained with InstantBlue™ Coomasie stain and the stained protein bands were cut out. The gel pieces were treated with trypsin and the digested proteins were extracted from the gel and analysed by MS. This work was carried out by Adelina Acosta Martin, whilst I shadowed her in the sample preparation. A total of 608 proteins was identified, including, ATP citrate lyase (ACLY),[83] and Histone H4 (HIST1H4);[33] two known proteins which have τ-pHis residues. However, the site of pHis modification was only detected for 5 proteins, none of which have been previously known to have pHis (Table 6).

The 5 pHis sites detected from the pulled down HBE lysate proteins using the pHis antibody 1(τ) is low compared to the 187 pHis sites detected by Hardman *et al.*, who enriched pHis peptides from HeLa cells using strong ion exchange chromatography.[90] However the sample preparation conditions that we used to prepare the pulled down HBE lysate proteins involved prolonged exposure to acidic solutions and increased temperatures (37 ^{o}C), over an extended period (2 days). It is quite possible that these conditions destroyed the pHis modification in many cases so they were not detected by MS. Pulling down pHis peptides rather than pHis proteins using the τ-pHis antibodies and using conditions that stabilise pHis would be expected to increase the number of pHis sites detected in future MS experiments.

Table 6: New His phosphorylated proteins detected by MS from HBE lysate immunoprecipitated with pHis antibody 1(τ). H in bold is the His residues with pHis.

Peptide	Protein	Gene
WRVSLDVN**H**FAPDELTVK	Heat shock protein beta-1	HSPB1
FHINI**H**ILK	TNF receptor-associated factor 6	TRAF6
IR**H**HIYVLNQVDHFR	Beta-1,4-galactosyltransferase 7; Xylosylprotein 4-beta-galactosyltransferase	B4GALT7
GCSGLTAHLAI**H**TEK	Zinc finger protein 528	ZNF528
M**H**VKKYLLK	Amiloride-sensitive sodium channel subunit beta	SCNN1B

3.2.7: Large scale purification and characterisation of sheep antiserum SA223-B3

Having both isomer selective pHis (τ-pHis and π-pHis) antibodies is necessary for the study of pHis containing proteins. Importantly, isomer selective pHis antibodies can give information on the likely pHis isomer present in a sample from relatively quick and cheap experiments such as Western blots. Hence, a large-scale purification on sheep antiserum SA223-B3 was needed to explore the use of these antibodies in biological techniques.

A sample of 16 mL of sheep antiserum SA223-B3 was affinity depleted with sepharose BSA-G-pTyr conjugate resin (Figure 60). As with sheep antiserum SA223-B3, sandwich ELISA of the IN and FT fractions show that the sepharose BSA-G-pTyr conjugate resin effectively removed undesired antibodies. The resin was then first competitively dissociated with τ-pHis because the small-scale affinity purification sandwich ELISA (Figure 44, Left) suggested the presence of τ-pHis antibodies. The resin was then competitively dissociated with π-pHis to remove any weakly bound π-pHis antibodies. Fractions W1-W4, and W5-W6, E1-E4(π-pHis), were combined and labelled pHis antibody 3(π), and 4(π) respectively.

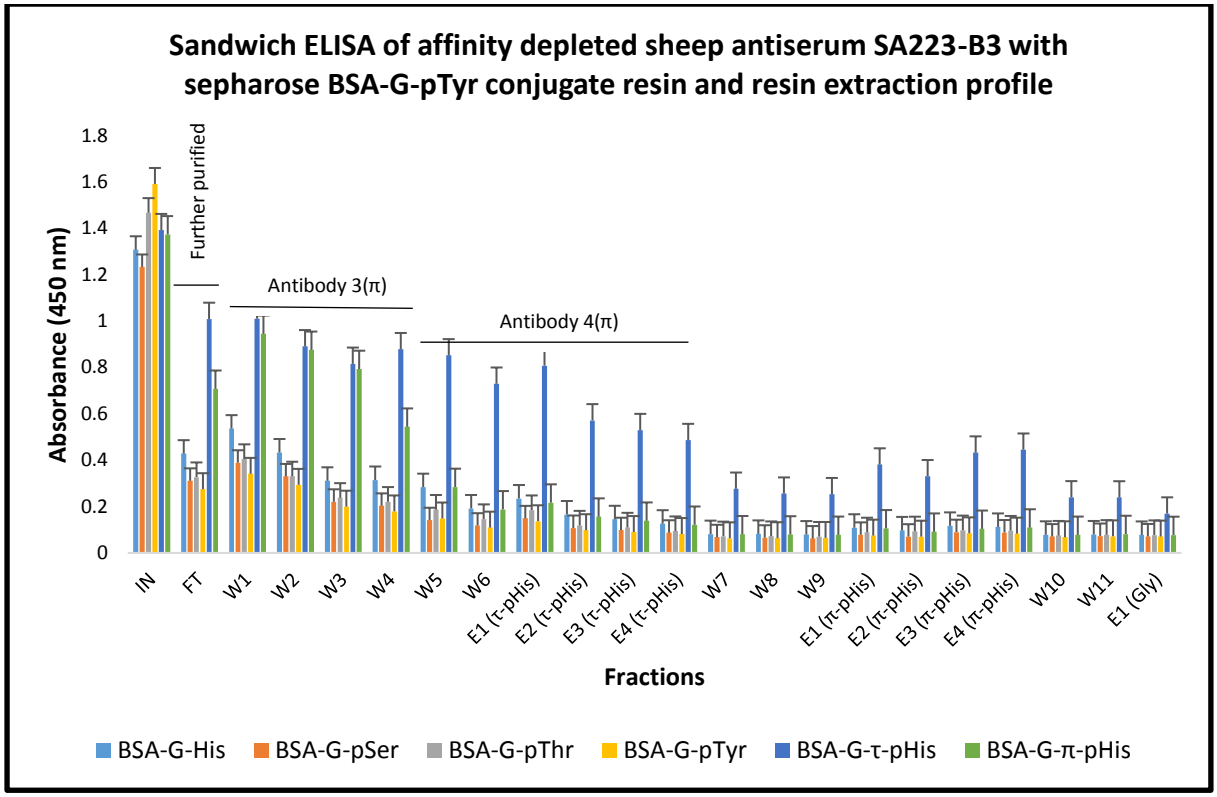

Figure 60: Sandwich ELISA of sheep antiserum SA223-B3 affinity depleted with sepharose BSA-G-pTyr conjugate resin. FT = Flow through, after incubation in with a sepharose BSA-G-pTyr conjugate resin. W1-W11 = washing of sepharose BSA-G-pTyr conjugate resin with 25 mM Tris base, 150 mM NaCl, pH 7.4. E1-E4 (pHis) = competitive extraction of sepharose BSA-G-pTyr conjugate resin with 25 mM Tris base, 150 mM NaCl, 200 µg/mL τ- or π-pHis, pH 7.4. E1 (Gly) = extraction of sepharose BSA-G-pTyr conjugate resin with 0.1 M Gly pH 2.2 followed by rapid neutralisation with 1.0 M Tris pH 9.0. BSA-G-τ-pHis, BSA-G-π-pHis and BSA-G-pTyr assays were analysed by ^{31}P NMR and equal phosphorus loadings of these three conjugates were used. Error bars show the standard error of the mean (N = 2).

The FT fraction from Figure 60 was further affinity depleted with sepharose BSA-G-τ-pHis conjugate (Figure 61) to increase the selectivity of the antiserum for π-pHis. The sandwich ELISA of the wash fractions suggested some of the pHis antibodies was weakly bound to the sepharose BSA-G-τ-pHis conjugate resin. To maximise recovery, the resin was competitively

dissociated with π-pHis and fractions FT2, W1'-W4' and E1-E4(π-pHis)' were combined and labelled antibody 1(τ) and 2(τ) respectively.

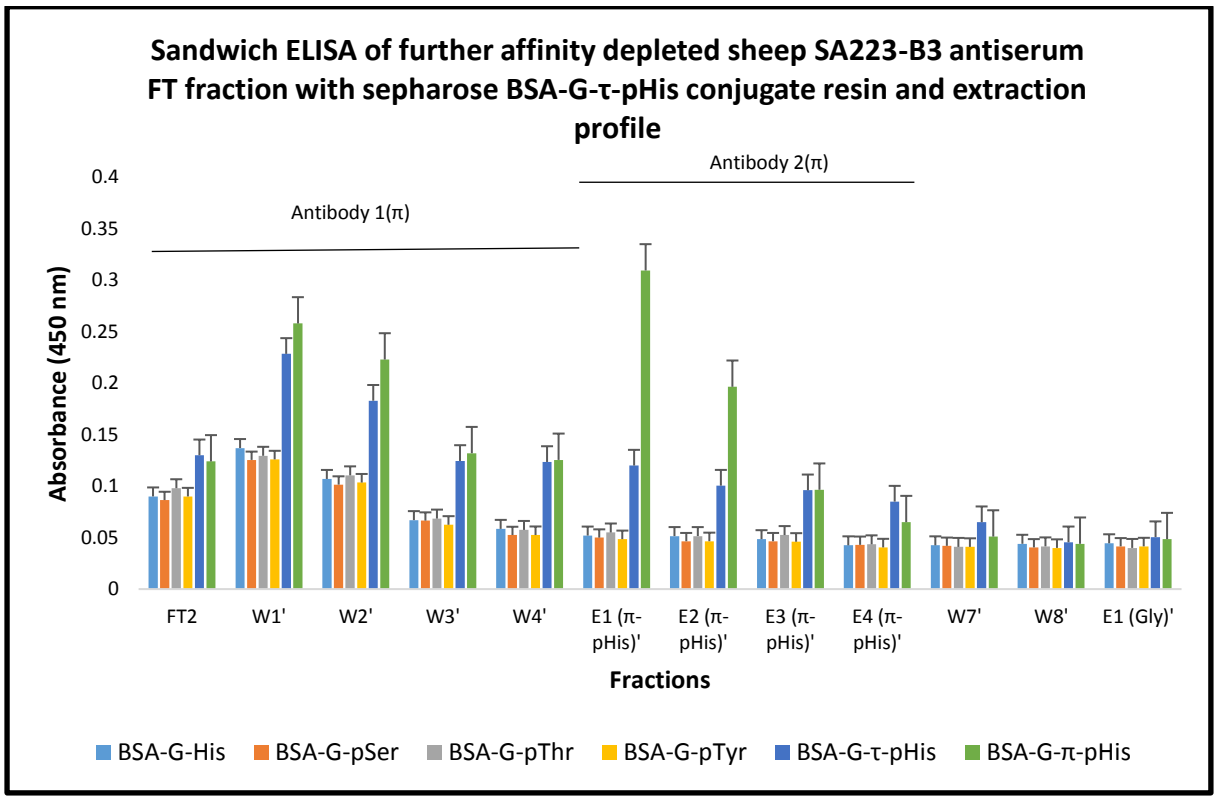

Figure 61: Sandwich ELISA of further affinity depleted sheep SA223-B3 antiserum fractions FT (Figure 60). FT2 = Flow through, after incubation in with a sepharose BSA-G-τ-pHis conjugate resin. W1'-W8' = washing of sepharose BSA-G-τ-pHis conjugate resin with 25 mM Tris base, 150 mM NaCl, pH 7.4. E1-E4 (π-pHis) = competitive extraction of sepharose BSA-G-pTyr conjugate resin with 25 mM Tris base, 150 mM NaCl, 200 µg/mL π-pHis, pH 7.4. E1 (Gly) = extraction of sepharose BSA-G-τ-pHis conjugate resin with 0.1 M Gly, pH 2.2 followed by rapid neutralisation with 1.0 M Tris pH 9.0. BSA-G-τ-pHis, BSA-G-π-pHis and BSA-G-pTyr assays were analysed by ^{31}P NMR and equal phosphorus loadings of these three conjugates were used. Error bars show the standard error of the mean (N = 2).

Note the sepharose BSA-G-τ-pHis conjugate resin used for the further affinity depletion of sheep antiserum S976D-B3 was not competitively dissociated with τ-pHis, which in hindsight

may have been worth doing (see section 3.2.6) However, at the time the purification was focused on following the small-scale procedure which had seemed promising.

The selectivity of the pHis antibodies 1(π), 2(π), 3(π) and 4 (π) was determined by competitive ELISA with His, pSer, pThr, pTyr, τ-pHis, and π-pHis as competitors against a BSA-G-π-pHis coat (Figure 62-65). All four antibodies were found to be highly selective for π-pHis over the other amino acid competitors with pHis antibody 2(π) being the most selective of the four antibodies. Overall, on competitive ELISA, the selectivity of the π-pHis antibodies 1-4(π) are superior to the to the τ-pHis polyclonal antibodies (isolated in section 3.2.6), especially at high competitor concentrations and between pHis isomers, precisely as suggested by the calculation (see section 1.6). The results here highlight that the pyridine moiety can be effective in pHis analogues.

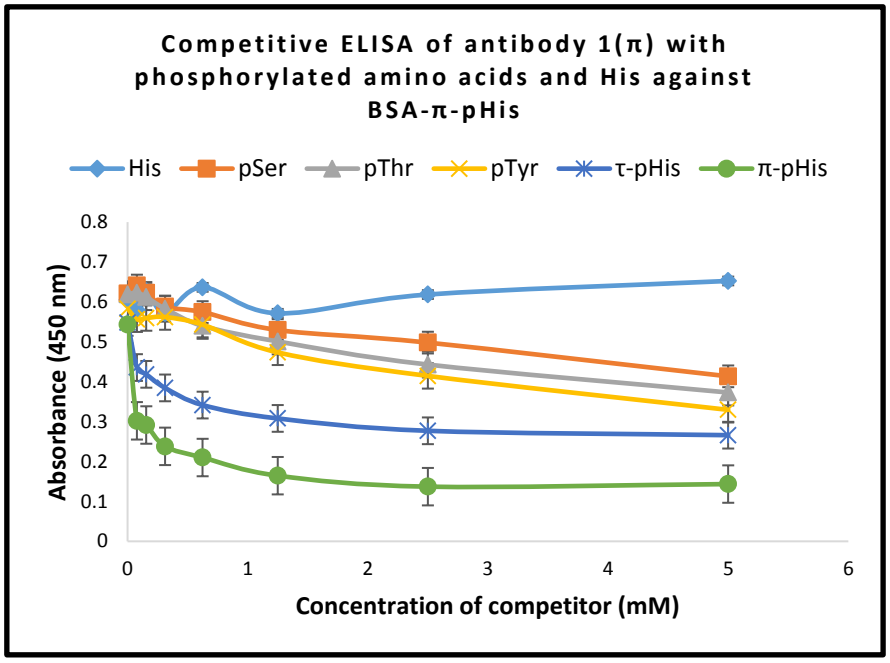

Figure 62: Competitive ELISA of antibody 1(π) (combined fraction FT2 and W1'-W4', see Figure 61) with His, pSer, pThr, pTyr, τ-pHis, and π-pHis against BSA-G-π-pHis (20 µg/mL) analysed by ^{31}P NMR. Error bars show the standard error of the mean (N = 2).

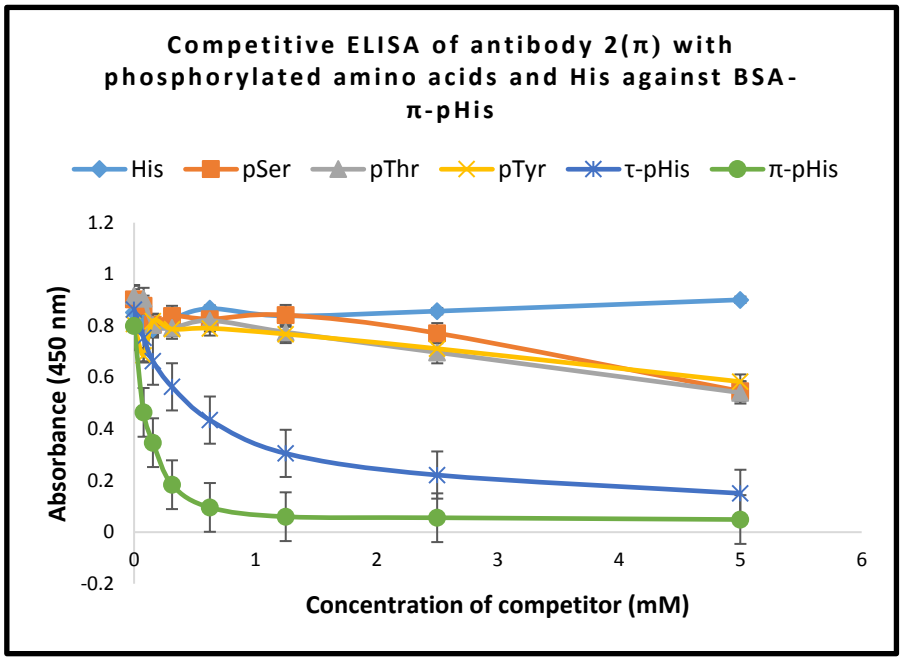

Figure 63: Competitive ELISA of antibody 2(π) (combined fraction E1-E4 (π-pHis)', see Figure 61) with His, pSer, pThr, pTyr, τ-pHis, and π-pHis against BSA-G-π-pHis (20 µg/mL) analysed by ^{31}P NMR. Error bars show the standard error of the mean (N = 2).

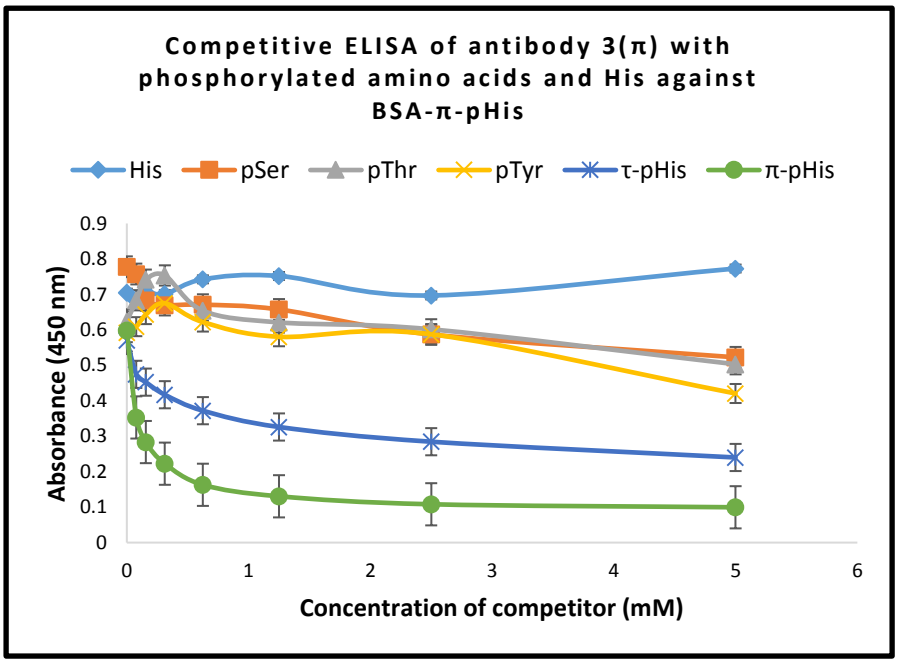

Figure 64: Competitive ELISA of antibody 3(π) (combined fraction W1-W4, see Figure 60) with His, pSer, pThr, pTyr, τ-pHis, and π-pHis against BSA-G-π-pHis (20 µg/mL) analysed by ^{31}P NMR. Error bars show the standard error of the mean (N = 2).

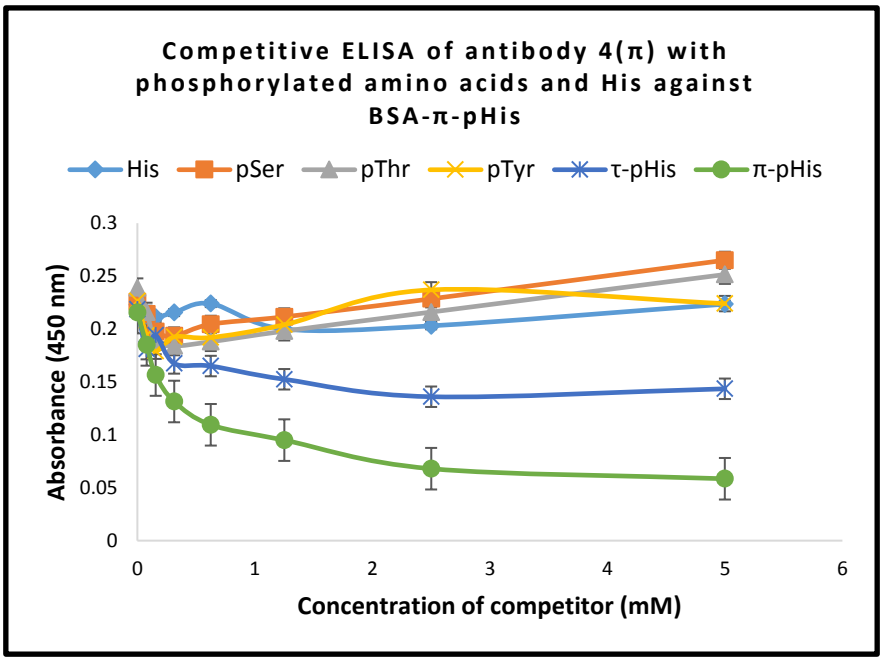

Figure 65: Competitive ELISA of antibody 4(π) (combined fraction W5-W6, E1-E4(τ-pHis) see Figure 60) with His, pSer, pThr, pTyr, τ-pHis, and π-pHis against BSA-G-π-pHis (20 µg/mL) analysed by ^{31}P NMR. Error bars show the standard error of the mean (N = 2).

3.2.7.1: Use of π-pHis antibodies in Western blot

Several low molecular weight (< 32 kDa) proteins bands were detected on Western blot of HBE cell lysate probed with pHis antibodies 1-4(π) using the optimised condition identified from section 3.2.6.1. The protein bands detected between pHis antibodies 1-4(π) are similar, with 2(π) and 3 (π) giving the most intense bands. Assuming most of the pHis residues detected by pHis antibodies 1-4(π) are π-pHis, and those detected by pHis antibodies 1-5(τ) are τ-pHis; there is extensive His phosphorylation in HBE cells.

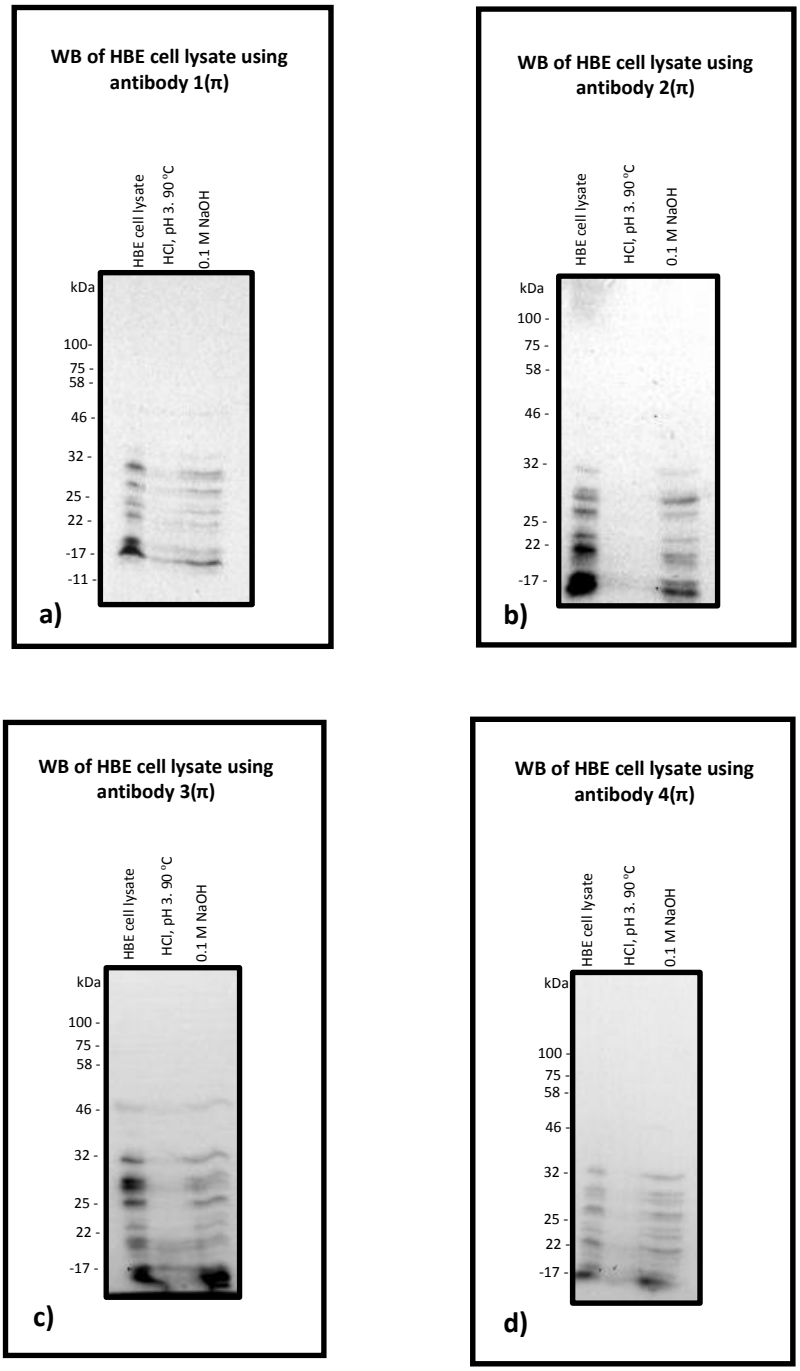

Figure 66: Western blot (WB) of 100 µg HBE protein cell lysate, treated with HCl to pH 3 at 90 °C for 15-45 min and with NaOH, (0.1 M final concentration) at room temp. in modified sample buffer. The membranes were visualised using Bio-Rad ChemiDoc™ XRS+, 3600 second exposure; **a**) 1(π), 1/5 (v/v) antibody dilution; **b**) 2(π), 1/5 (v/v) antibody dilution; **c**) 3(π), 1/40 (v/v) antibody dilution; **d**) 4(π), 1/50 (v/v) antibody dilution.

3.2.7.2: Immunoprecipitation using π-pHis antibody

As before (see section 3.2.6.2), pHis antibody 3(π) was used to pull down pHis protein from a HBE cell lysate and pyridine **141** (Figure 67) was used as the competitor. Unexpectedly, the colloidal gold and Western blots showed that most of the pHis proteins pulled down (Figure 68) were of high molecular weight (>32 kDa) and had immunoprecipitation profiles similar to those of pHis antibody 1(τ) (Figure 59, page 127). It is not clear if this was due to pHis isomer cross reactivity or other reasons as suggested in the immunoprecipitation using pHis antibody 1(τ) (see section 3.2.6.2). On the other hand, these proteins may be phosphorylated on multiple surface His residues, some being the τ-pHis isomer whilst others being π-pHis isomer. A less likely, but not inconceivable, explanation could be that mechanism of His phosphorylation in these proteins is not conserved, and phosphorylation gives rise to both isomers of pHis.

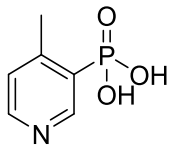

141

Figure 67: π-pHis competitor analogue, 4-methylpyridyl phosphonate **141** used in Figure 68.

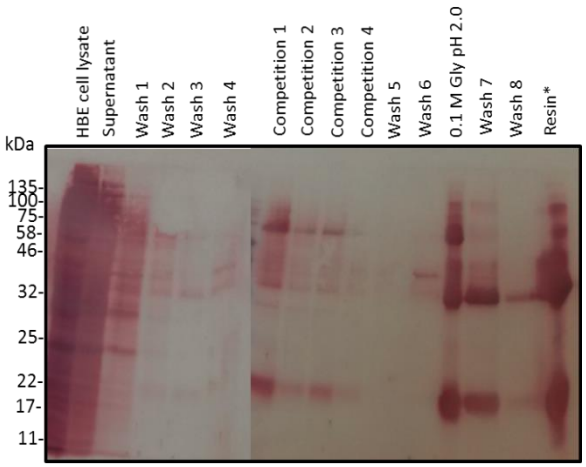

Colloidal gold stained PVDF membrane

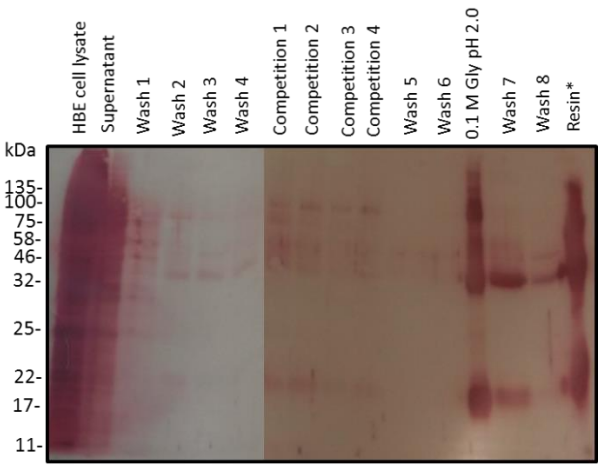

Colloidal gold stained PVDF membrane. Acid treated

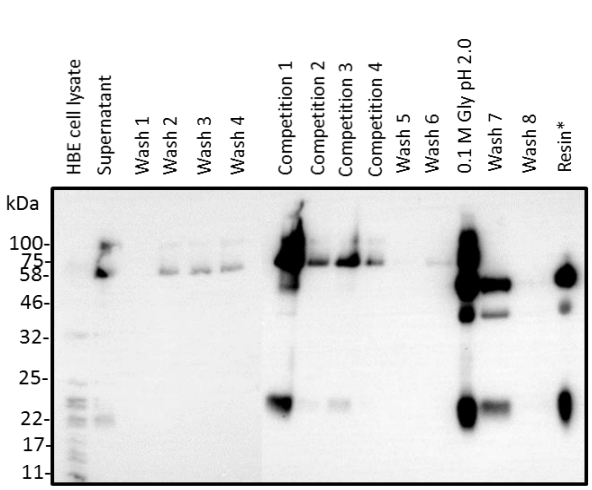

WB probed with pHis antibody 3(π)

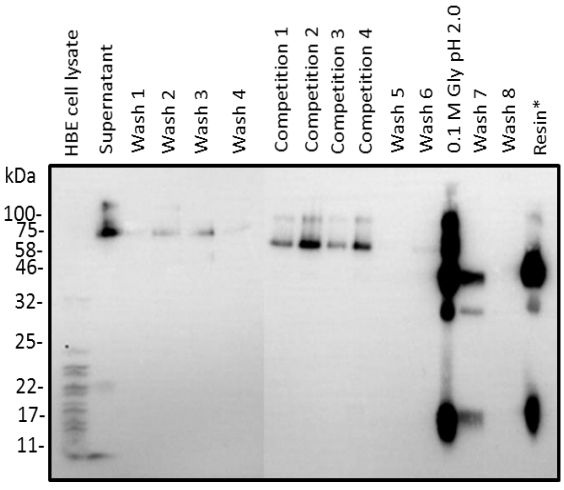

WB probed with pHis antibody 3(π). Acid treated

Figure 68: Immunoprecipitation of HBE cell lysate using pHis antibody 3(π) bound to protein G sepharose experiment samples. Upper membranes: proteins stained with colloidal gold. Lower membranes: Western blot (WB) with pHis antibody 3(π); the membranes were visualised using Bio-Rad ChemiDoc™ XRS+, 192 second exposures. Membranes on the left: HBE cells lysate untreated. Membranes on the right: HBE cell lysate pH reduced to 7.0 and heated at 60 ^{o}C for 30 min before immunoprecipitation. *Sepharose protein G after immunoprecipitation experiment.

4: Conclusion and Future Work

In conclusion, pyrazolylethylamine **61** and a new 3,4-disubstituted pyridine amino amide **130** proved to be excellent analogues of τ- and π-pHis respectively in polyclonal antibody generation (Figure 69). The purified antibodies could be used in biological techniques such as ELISA, Western blot and immunoprecipitation. Extensive His phosphorylation was detected on Western blots of HBE cell lysates using the pHis antibodies suggesting that pHis play a major role in many biological processes. The next phase of the study would be to identify what these proteins are, and the sites of His phosphorylation, using MS. Our preliminary MS data indicates considerable optimisation is required in the MS workflow, and exploring a peptide level immunoprecipitation is an alternative option to identify pHis sites in a protein.

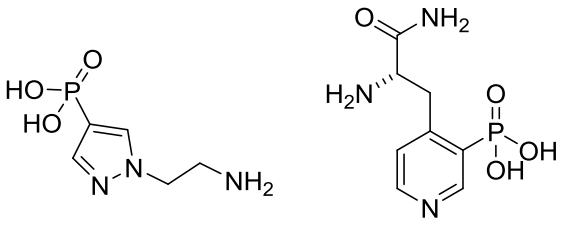

Figure 69: pHis analogues used in antibody generation.

For more quantitative studies on τ- and π-pHis, monoclonal antibodies are needed. Our study suggests pyrazolylethylamine **61** and the new 3,4-disubstituted pyridine amino amide **130** are two analogues that could be used to achieve this. The enormous genomic libraries that can be captured with a phage display would allow one to by-pass using potentially more optimal pHis analogues. The selective BSA-G-τ-pHis and BSA-G-π-pHis assays that have been developed will be essential in identifying isomer selective pHis monoclonals.

Demonstrating that the building block **91** can be incorporated into peptides using Fmoc SPPS will be important to unlock the full potential of the pyrazole τ-pHis analogue, in biological application such as peptide selective antibody generation, site specific protein mutations and protein crystallography. A full set of tools is required for the study of pHis so it will be necessary to prepare 3,4-disubstituted pyridine **154** with suitable protecting groups for Fmoc SPPS (Figure 70).

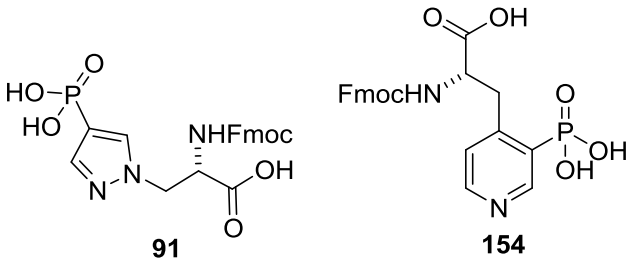

Figure 70: τ-pHis building block **91** synthesised in this study and proposed π-pHis building block **154**.

Finally, one of the original aims of the project, namely the synthesis of imidazole **94** and **95**, was not achieved and, it would be interesting to assess their performance as τ- and π-pHis analogues in polyclonal antibody generation (Figure 71).

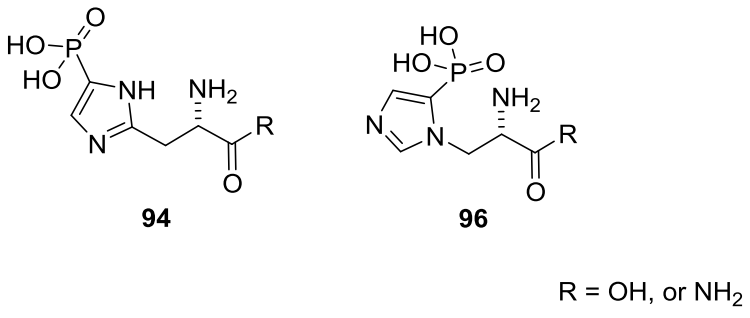

Figure 71: Proposed imidazole τ- and π-pHis analogue **94** and **96** respectively.

5: Experimental

5.1: Chemistry Experimental

All reagents used were purchased from Fluorochem, Sigma Aldrich, Alpha Aeser, Manchester Organics, VWR International, Fisher Scientific, and Acros Organics. Tert-butyl N-[(3S)-2-oxooxetan-3-yl]carbamate **50** was purchased from Clearsynth labs LTD. Distilled or ultrapure H_2O was used and all solvents were of HPLC grade or distilled. Pet ether refers to the fraction which boils in the range 40-60 °C. Dry dimethylformamide, tetrahydrofuran, toluene and dichloromethane was obtained from the in-house Grubbs system. Ethanol was dried by refluxing in iodine activated magnesium for 24 hours. The ethanol was then distilled and stored over 4 Å molecular sieves under nitrogen gas for up to 6 months. All reactions were stirred using a Teflon coated stirrer bar. N,N-diisopropylethylamine was distilled from calcium hydride and stored over nitrogen gas. All moisture/air sensitive reactions were performed under a positive pressure of nitrogen or argon gas in flame dried glassware. Tosyl chloride was recrystallized from chloroform/petroleum ether prior to use.[141] *p*-Toluenesulphonic acid monohydrate was dried by heating at 100 ^{o}C for 4 hours under vacuum and then recrystallizing from chloroform. All other reagents were used without further purification. Flash column chromatography was done manually under 0.34 atmospheres of pressure. Silica gel 40-60 µm from VWR International was used. Merck TLC Silcia gel 60 F_{254} TLC plates were used, and compounds were visualized by UV light (254 nm), 5 % (wt/v) ninhydrin in methanol, or basic potassium permanganate. Optical rotations were measured using an Optical Activity Ltd. AA-10 Series Automatic polarimeter at 589 nm. Specific rotations were measured to the nearest 0.1 degrees, and concentration are given to the nearest 0.1 mg/mL. The melting points were determined using Linkam HFs91 heating stage, used in conjunction with a TC92

controller and are uncorrected. The infrared spectra were taken using a Perkin Elmer Paragon 100 FTIR spectrophotometer as thin films using sodium chloride plates or attenuated total reflectance (ATR). Only selected peaks are reported were and the absorption maxima are given to the nearest wavenumber (cm^{-1}). All NMR spectra were recorded at room temperature. ^{1}H NMR spectra were recorded using a Bruker AVANCE 400 operating at 400.13 MHz, or Bruker AVANCE III HD 400 spectrometer operating at 400.23MHz. ^{13}C NMR spectra were recorded using a Bruker AVANCE 400 operating at 100.61 MHz, or Bruker AVANCE III HD 400 spectrometer operating at 100.64 MHz. ^{31}P NMR spectra were recorded using a Bruker AVANCE III HD 400 spectrometer operating at 162.02 MHz. Chemical shifts were measured relative to the residual solvent and expressed in parts per million (δ). The multiplicities are defined as s = singlet, d = doublet, t = triplet, q= quartet, quint. = quintet, sex. = sextet, m = multiplet, br = broad. Coupling constant (*J*) are given in Hertz and the measured values are rounded to the nearest 0.5 Hz and are rationalized. High-resolution mass spectra were measured using an Agilent Technologies 653 Accurate-Mass Q-TOF LC/MS operating in electrospray mode.

4-iodo-1H-pyrazole 51

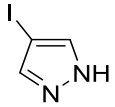

51

Iodine (0.152 g, 0.6 mmol, 0.6 equiv.), pyrazole (0.068 g, 1.0 mmol, 1.0 equiv.) and ammonium cerium (IV) nitrate (0.329 g, 0.6 mmol, 0.6 equiv.) were stirred in acetonitrile (3 mL) at room temperature for 5 hours. A precipitate was observed, and the solution changed from

red/brown to red/orange in colour. 10 % (w/w) sodium sulphite (3 mL) was added and the mixture stirred for 2 minutes. The aqueous phase was extracted with ethyl acetate (3 × 10 mL) and the combined organic fractions were washed with brine, dried over anhydrous magnesium sulphate, filtered and concentrated under reduced pressure. The solid left behind was purified by flash column chromatography over silica eluting with 4:6 ethyl acetate: petroleum ether. Compound **51** (0.187 g, 95 %) white crystals: R_F = 0.27 (2:3 EtOAc/pet. ether); m.p. = 106-108 °C (lit.[131] 106-108 °C); **ν_{max}**(ATR)/**cm^{-1}** 3116, 2879, 1361, 1321, 1139, 1031; **^{1}H NMR** (400 MHz, $CDCl_3$) 7.66 (s, 2H), 12.51 (br, 1H); **^{13}C NMR** (101 MHz, $CDCl_3$) 56.6, 138.8; **m/z** (ESI+): 194.9412 (MH+, 100 % $C_3H_4IN_2$ requires 194.9400).

The characterization data are similar to the literature.[131]

Dibenzyl (1H-pyrazol-4-yl)phosphonate 104

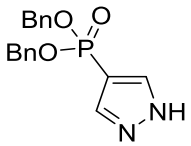

104

Palladium (II) acetate (0.022 g, 0.1 mmol, 0.1 equiv.), 4,5-bis(diphenylphosphino)-9,9-dimethylxanthene (0.116 g, 0.2 mmol, 0.2 equiv.), and sodium acetate (0.008 g, 0.1 mmol, 0.1 equiv.) were added to a microwave vial. A vacuum was applied followed by a positive pressure of nitrogen (× 3). Tetrahydrofuran (4 mL) was added followed by N,N-diisopropylethylamine (0.259 g, 0.35 mL, 2.0 mmol, 2.0 equiv.). The mixture was stirred in a microwave reactor at 70 °C for 20 minutes. To the now deep red solution dibenzyl phosphite (0.577 g, 0.49 mL, 2.2 mmol, 2.2 equiv.) and 4-iodo-1H-pyrazole **51** (0.194 g, 1.0 mmol, 1.0 equiv.) were added and

heated in a microwave reactor at 70 °C for 45 minutes. The mixture was immediately diluted with ethyl acetate (30 mL) and washed with saturated aqueous sodium bicarbonate (30 mL). The aqueous phase was extracted with ethyl acetate (3 × 30 mL), and the combined organic fractions were dried over anhydrous sodium sulphate, filtered and concentrated under reduced pressure. The residue was purified by flash column chromatography over silica eluting with ethyl acetate. Compound **104** (0.197 g, 60 %) a white crystalline solid: R_F = 0.35 (EtOAc); m.p. = 108-110 °C; **ν_{max}**(ATR)/**cm^{-1}** 3126, 3092, 3068, 2912, 2850, 1455, 1381, 1302, 1201, 1155; **^{1}H NMR** (400 MHz, $CDCl_3$) 5.03-5.12 (m, 4H), 7.30-7.35 (m, 10 H), 7.87 (d, *J* = 1.5 Hz, 2H), 11.98 (br, 1H); **^{13}C NMR** (101 MHz, $CDCl_3$) 67.8 (d, *J* = 5.5 Hz), 106.2 (d, *J* = 224.5 Hz), 127.9 (s), 128.5 (s), 128.6 (s), 135.9 (d, *J* = 7.0 Hz), 138.3 (br); **^{31}P NMR** (162 MHz, $CHCl_3$) 15.71; **m/z** (ESI+): 329.1048 (MH+, 100 % $C_{17}H_{18}N_2O_3P$ requires 329.1000).

(2S)-2-[(tert-butoxycarbonyl)amino]-3-[4-(dibenzyloxyphosphoryl)pyrazol-1-yl]propanoic acid 111

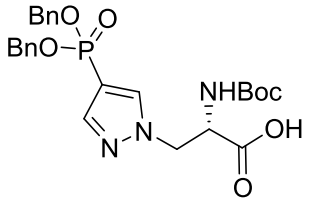

111

Tert-butyl N-[(3S)-2-oxooxetan-3-yl]carbamate **50** (0.187 g, 1.0 mmol, 1.0 equiv.), was added to a stirred solution of pyrazole **104** (0.394 g, 1.2 mmol, 1.2 equiv.), and 1,8-Diazabicyclo[5.4.0]undec-7-ene (0.304 g, 0.30 mL, 2.0 mmol, 2.0 equiv.) in acetonitrile (2.7 mL) at 50 °C overnight. The mixture was concentrated under reduced pressure and partitioned between water (25 mL) and diethyl ether (25 mL). The aqueous phase was washed

with diethyl ether (2 × 25 mL). The aqueous phase was carefully acidified to pH 5 with 1 molar aqueous hydrochloric acid and the extracted with ethyl acetate (25 mL), followed by further extraction of the aqueous phase with ethyl acetate (4 × 25 mL) whilst maintaining the pH. The combined ethyl acetate phases were dried over anhydrous magnesium sulphate, filtered and the solvent removed under reduced pressure. The crude was purified by column chromatography over silica eluting with a 99:1 to 95:5 ethyl acetate/acetic acid solvent gradient. Compound **111** (0.144 g, 28 % yield) a colourless oil: R_F = 0.23 (19:1 EtOAc/AcOH); $[\alpha]^{24}_D$ -2.0 (*c* 1.0, $CHCl_3$); ν_{max}(ATR)/**cm**$^{-1}$ 2978, 1703, 1525, 1497, 1456, 1363, 1202, 1158; **^{1}H NMR** (400 MHz, $CDCl_3$) 1.44 (s, 9H), 4.59 (dd, *J* = 4.0, 13.5 Hz, 1H), 4.63-4.77 (m, 2H), 4.97-5.10 (m, 4H), 5.60 (d, *J* = 7.5 Hz, 1Hz), 7.26-7.38 (m, 10H), 7.72 (s, 1H), 7.81 (s, 1H); **^{13}C NMR** (101 MHz, $CDCl_3$) 28.3 (s), 52.9 (s), 53.8 (s), 68.0 (d, *J* = 5.0 Hz), 80.5 (s), 106.9 (d, *J* = 227.0 Hz), 128.1 (d, *J* = 5.5 Hz), 128.6 (d, *J* = 5.5 Hz), 135.7 (d, *J* = 7.0 Hz), 136.7 (d, *J* = 24.5 Hz), 143.1 (d, *J* = 14.5 Hz), 155.4 (s), 170.7 (s); **^{31}P NMR** (162 MHz, $CHCl_3$) 14.87; **m/z** (ESI+): 516.1894 (MH+, 100 % $C_{25}H_{31}N_2O_7P$ requires 516.1900).

(2S)-3-[4-(dibenzyloxyphosphoryl)pyrazol-1-yl]-2-[[(9H-fluoren-9-ylmethoxy)carbonyl]amino]propanoic acid 91

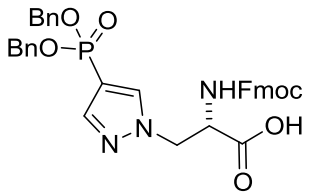

91

(2S)-2-[(tert-butoxycarbonyl)amino]-3-[4-(dibenzyloxyphosphoryl)pyrazol-1-yl]propanoic acid **111** (0.300 g, 0.58 mmol, 1.0 equiv.) was dissolved in dichloromethane (0.85 mL) under

nitrogen. Trifluoroacetic acid (1.27 g, 0.85 mL, 11.1 mmol, 19.2 equiv.) was added to the mixture which was stirred rapidly for 75 minutes. The solvent was then removed under reduced pressure and residual trifluoroacetic acid was azeotropically removed with toluene (× 3). The foam left behind was dissolved in 1,4-dioxane (0.77 mL) and cooled in an ice bath. 10 % (wt/v) aqueous sodium carbonate (1.58 mL) was added followed by dropwise addition of fluorenylmethyloxycarbonyl chloride (0.166 g, 0.64 mmol, 1.1 equiv.) dissolved in dioxane (1.54 mL), and the mixture was stirred at 0 °C for 10 minutes and then at room temperature overnight. The mixture was diluted with water (15 mL) and washed with diethyl ether (15 mL). The organic phase was washed with saturated aqueous sodium bicarbonate (15 mL) and the combined aqueous phases were acidified to pH 2 using 1 molar aqueous hydrochloric acid. The aqueous phase was extracted with ethyl acetate (4 × 30 mL) and the combined organic phases were dried over anhydrous sodium sulphate, filtered and concentrated under reduced pressure. The remaining residue was by column chromatography over silica eluting with 99:1 to 95:5 ethyl acetate/acetic acid solvent gradient. Compound **91** (0.229 g, 62 %) white crystals: R_F = 0.29 (19:1 EtOAc/AcOH); $[\alpha]^{24}_D$ -3.0 (*c* 1.0, $CHCl_3$); m.p. = 58-61 °C; **ν_{max}**(thin film)/**cm^{-1}** 3323, 3108, 3063, 3038, 2954, 2890, 1722, 1529, 1456, 1382, 1331, 1215, 1141; **^{1}H NMR** (400 MHz, $CDCl_3$) 4.19 (t, *J* = 7.0 Hz, 1H), 4.37 (d, *J* = 7.0 Hz, 2H), 4.53-4.63 (m, 1H), 4.73-4.83 (m, 2H), 4.94-5.10 (m, 4H), 6.16 (d, *J* = 7.0 Hz, 1H), 7.18-7.43 (m, 14H), 7.55-7.62 (m, 2H), 7.71-7.82 (m, 4H), 9.65 (br, 1H); **^{13}C NMR** (101 MHz, $CDCl_3$) 47.1 (s), 52.9 (s), 54.2 (s), 67.4 (s), 68.2 (d, *J* = 5.0 Hz), 106.7 (d, *J* =224.5 Hz), 120.0 (s), 125.3 (s), 127.1 (s), 127.8 (s),128.1 (s), 128.5 (s), 128.6 (s), 135.6 (br), 136.7 (d, *J* = 25.5 Hz), 141.3 (s), 143.01 (d, *J* = 14.0 Hz), 143.7 (d, *J* = 11.0 Hz), 156.0 (s), 170.3; **^{31}P NMR** (162 MHz, $CHCl_3$) 15.28; **m/z** (ESI+): 638.2051 (MH+, 100 % $C_{35}H_{33}N_3O_7P$ requires 638.2100).

(2S)-3-hydroxy-2-[(triphenylmethyl)amino]propanoic acid 118

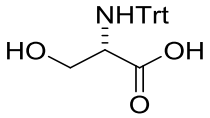

118

A two-necked round bottom flask containing L-Serine (4.20 g, 40.0 mmol, 1.0 equiv.) equipped with a condenser was evacuated and purged with nitrogen. Dichloromethane (70 mL) was added followed by trimethylsilylchloride (15.2 g, 17.8 mL, 140.0 mmol, 3.5 equiv.) and the mixture was refluxed for 20 minutes. The mixture was allowed to cool to room temperature and trimethylamine (14.2 g, 19.5 mL, 140.0 mmol, 3.5 equiv.) in dichloromethane (40 mL) was added. A white precipitate was observed. The mixture was refluxed for 45 minutes and then cooled to 0 ^{o}C. Methanol (1.92 g, 2.43 mL, 60.0 mmol, 1.5 equiv.) in dichloromethane (10 mL) was added dropwise. At room temperature, triethylamine (4.05 g, 5.58 mL, 40.0 mmol, 1.0 equiv.) was added followed by the addition of trityl chloride (11.2 g, 40.0 mmol, 1.0 equiv.) in two portions over 15 minutes. The mixture was stirred for 5 hours after which methanol (50 mL) was added, and the precipitate dissolved. The mixture was concentrated under reduced pressure. The residue was dissolved with ethyl acetate (50 mL) and sequentially washed with 5 % (wt/v) aqueous citric acid (50 mL), 1 molar aqueous sodium hydroxide (2 × 20 mL), and water (2 × 20 mL). The combined aqueous phases were extracted with ethyl acetate (20 mL) and neutralized at 0 ^{o}C with acetic acid; a precipitate was observed. The aqueous phase was extracted with ethyl acetate (2 × 30 mL), and the combined organic phases were washed with water (2 × 100 mL), dried over anhydrous magnesium sulphate, filtered and concentrated under reduced pressure. The crude solid was recrystallized from chloroform. Compound **108** (9.5 g, 68 %) a white powder: $[\alpha]^{22}_{D}$ +16.0 (*c* 1.0, MeOH) (lit.[137] $[\alpha]^{25}_{D}$ -29.0 (*c* 1.0, MeOH)); m.p. = 172 °C (lit.[159] ~180 °C); $\boldsymbol{\nu_{max}}$(thin film)/**cm^{-1}** 3162, 3061, 2931, 2900, 1629, 1554, 1487,

1448, 1393, 1349, 1311, 1080, 1061 **^{1}H NMR** (400 MHz, $CDCl_3$) 2.74 (dd, *J* = 4.5, 11.0 Hz, 1H), 3.52-3.55 (m, 2H), 3.77 (dd, *J* = 3.0, 11.0 Hz, 1H), 7.26-7.36 (m, 12H), 7.43-7.48 (m, 3H); **^{13}C NMR** (101 MHz, $CDCl_3$) 58.6 (s), 62.6 (s), 71.9 (s), 127.3 (s), 128.4 (s), 128.5 9 (s), 144.5 (s), 174.5 (s).

The characterization data are similar to the literature.[137,159]

(3S)-3-[(triphenylmethyl)amino]oxetan-2-one 119

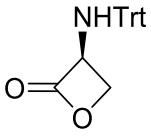

119

(2S)-3-hydroxy-2-[(triphenylmethyl)amino]propanoic acid **118** (1.75 g, 5.0 mmol, 1.0 equiv.), was dissolved in dichloromethane (25 mL), over nitrogen. Triethylamine (1.52 g, 2.0 mL, 14.0 mmol, 2.8 equiv.), was added followed by the addition of benzotriazol-1-yloxy)tris(dimethylamino)phosphonium hexafluorophosphate (3.12 g, 7.1 mmol, 1.4 equiv.) in two portions over 15 minutes. The mixture was stirred at room temperature for 1 hour. Water (25 mL) was added and the mixture was stirred for a further 20 minutes. The aqueous phase was separated and extracted with dichloromethane (3 × 25 mL). The combined organic phases were dried over anhydrous magnesium sulphate, filtered and concentrated under reduced pressure at room temperature. The crude was purified immediately by flash column chromatography over silica eluting with 3:17 ethyl acetate to pet ether. Compound **119** (1.37 g, 83 %) as a white solid: R_F = 0.26 (3:17 EtOAc/pet ether); **^{1}H NMR** (400 MHz, $CDCl_3$) 2.68 (d, *J* = 11.5 Hz, 1H), 3.12-3.17 (m, 1H), 3.55-3.59 (m, 1H), 4.60-4.67 (m, 1H), 7.25-7.30 (m, 3 H),

7.31-7.37 (m, 6H), 7.50-7.54 (m, 6H); **^{13}C NMR** (101 MHz, $CDCl_3$) 64.6 (s), 70.6 (s), 70.8 (s), 127.1 (s), 128.3 (s), 128.4 (s), 145.1 (s), 172.1 (s).

The characterization data are similar to the literature.[135,136]

(3S)-2-oxooxetan-3-aminium tosylate 112

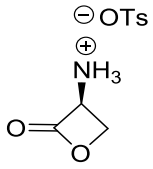

112

(2S)-3-hydroxy-2-[(triphenylmethyl)amino]propanoic acid **119** (1.40 g, 4.3 mmol, 1.0 equiv.), and *p*-toluenesulphonic acid (0.77 g, 4.5 mmol, 1.1 equiv.) were added to a round bottom flask purged in nitrogen and then cooled to 0 °C using an ice bath. Trifluoroacetic acid (12.8 mL) was added and the mixture was occasionally swirled by hand for 5 minutes upon which a yellow solution was observed, and the solids dissolved. The ice bath was removed, and the mixture was occasionally gently swirled for 5 minutes. The solvent was removed under reduced pressure with the help of a Kugelrohr apparatus, with the distilling flask at room temperature and collecting flask at -196 °C. The pale yellow solid left behind was triturated in diethyl ether (2 × 25 mL), and dried under reduced pressure. Compound **112** (1.00 g, 90 %) as a cream solid: $[\alpha]^{22}_D$ -5.5 (*c* 2.2, DMF) (lit.[134] $[\alpha]^{22}_D$ -15.9 (*c* 2.2, DMF)); m.p. = 155 °C (decomp.) (lit.[134] 173 °C (decomp.)); **ν_{max}**(thin film)/**cm^{-1}** 2946, 2859, 1831, 1752, 1162, 1121, 1029, 1008; **^{1}H NMR** (400 MHz, DMF-d_7) 2.51 (s, 3H), 4.86-4.94 (m, 2H), 5.74 (dd, *J* = 4.5, 6.5 Hz, 1H), 7.36 (d, *J* = 8.0 Hz, 2H), 7.86 (d, *J* = 8.0 Hz, 1H); **^{13}C NMR** (101 MHz, DMF-d_7) 20.6 (s),

52.5 (s), 61.5 (s), 128.3 (s), 130.6 (s), 138.5 (s), 146.0 (s),168.6 9 (s); **m/z** (ESI+): 260.0600 (MH+, 100 % $C_{10}H_{18}NO_5S$ requires 260.0600).

The characterization data are similar to the literature.[160]

(2S)-3-hydroxy-1-methoxy-1-oxopropan-2-aminium chloride 124

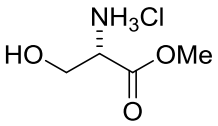

124

Acetyl chloride (25.4 g, 324.0 mmol, 23 mL, 2.8 equiv.) was added dropwise to methanol (150 mL) followed by the addition of L-serine (12.0 g, 114 mmol, 1.0 equiv.) at 0 ^{o}C. The mixture was stirred at reflux for 2 hours. The solvent was removed under reduced. Compound **124** (21.1 g, quantitative yield) white crystalline solid: $[\alpha]^{22}_{D}$ +9.3 (*c* 1.0 in MeOH); **^{1}H NMR** (MeOD, 400 MHz) 3.85 (s, 3H), 3.95 (dd, *J* = 3.4, 11.9 Hz, 1H), 4.02 (dd, *J* = 4.3, 11.9, Hz, 1H), 4.18-4.14 (m, 1H); **^{13}C NMR** (MeOD, 101 MHz) 53.7, 56.1, 60.7, 169.4.

The characterization data are similar to the literature.[145]

Methyl (2S)-3-hydroxy-2-[(triphenylmethyl)amino]propanoate 122

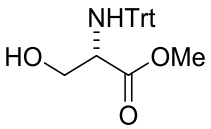

122

(2S)-3-Hydroxy-1-methoxy-1-oxopropan-2-aminium chloride **124** (7.51 g, 48.4 mmol, 1.0 equiv.) was stirred with dichloromethane (100 mL) at 0 ^{o} C. Triethylamine (10.0 g, 13.8 mL,

98.9 mmol, 2.0 equiv.) was added dropwise, followed by the dropwise addition of triphenyl methyl chloride (13.6 g, 48.7 mmol, 1.0 equiv.) dissolved in dichloromethane (30 mL). The resulting slurry was stirred at room temperature for 16 hours. The solvent was removed under reduced pressure. The residue was diluted in ethyl acetate (100 mL), and sequentially washed with saturated aqueous sodium bicarbonate (2 × 100 mL), 10 % (w/v) aqueous citric acid (2 × 100 mL) and then water (2 x 100 mL). The organic phase was dried over anhydrous sodium sulphate, filtered and the mixture was concentrated under reduced pressure. The solid was recrystallized by dissolving in a minimum volume of boiling ethyl acetate. Once crystallises were observed the mixture was cooled to 0 ^{o}C and petroleum ether was added in portions (1/5 total volume × 5) spaced over 2.5 hours. Compound **122** (7.29 g, 42 % yield) white crystalline solid; $[\alpha]^{25}_{D}$ + 3.0 (*c* 1.0, $CHCl_3$) (lit.[161] $[\alpha]^{20}_{D}$ + 3.0 (*c* 1.8, $CHCl_3$)); m.p. = 148-151 ^{o}C (lit.[162] 152-154 ^{o}C); $\mathbf{\nu_{max}}$(thin film)/**cm^{-1}** 3450, 3354, 3061, 3022, 2950, 2874, 1699, 1443, 1422, 1225, 1207, 1173; **^{1}H NMR** ($CDCl_3$, 400 MHz) 3.33 (s, 3H), 3.55-3.64 (m, 2H), 3.75 (dd, *J* = 4.0, 10.5 Hz, 1H), 7.20-7.36 (m, 9H), 7.51-7.57 (m, 6H); **^{13}C NMR** ($CDCl_3$, 400 MHz) 52.1, 57.9, 65.0, 71.0, 126.7, 128.0, 128.8, 145.7, 174.0; **m/z** (ESI+): 384.1575 (MNa+, 100 % $C_{23}H_{23}NNaO_3$ requires 384.1600).

The characterization data are similar to the literature.[161,162]

Methyl (2S)-3-[4-(dibenzyloxyphosphoryl)pyrazol-1-yl]-2 [(triphenylmethyl)amino]propanoate 125

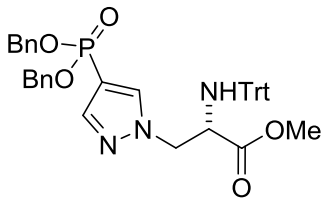

125

Dibenzyl (1H-pyrazol-4-yl)phosphonate **104** (0.197 g, 0.6 mmol, 1.2 equiv.), methyl (2s)-3-hydroxy 2-[(triphenyl methyl) amino] propanoate **122** (0.181 g, 0.5 mmol, 1.2 equiv.) and triphenyl phosphine (0.157 g, 0.6 mmol, 1.2 equiv.) were added to a round bottom flask under a argon atmosphere. Toluene (2 mL) was added followed by the addition of diethyl azodicarboxylate (0.104 g, 0.10 mL, 0.6 mmol, 1.2 equiv.) and the mixture was stirred at room temperature for 24 hours. The solution was diluted in ethyl acetate (10 mL) and washed sequentially with 1 molar aqueous hydrochloric acid (10 mL), saturated aqueous sodium bicarbonate (10 mL) and brine (10 mL). The combined organic layer was dried over anhydrous sodium sulphate, filtered and concentrated under reduced pressure. The residue was purified by flash column chromatography eluting with a 2:8 to 7:3 petroleum ether/ ethyl acetate solvent gradient. The solvent was removed from the combined product fractions under reduced pressure. Compound **125** (0.198 g, 59 %) colourless viscous oil: R_F = 0.35 (4:6 pet. ether/ EtOAc); $[\alpha]^{25}_D$ = + 20.0 (*c* 1.0, $CHCl_3$); $\boldsymbol{\nu_{max}}$(thin film)/**cm**$^{-1}$ 3059, 3032, 2950, 1734, 1530, 1491, 1448, 1214, 1136; **^{1}H NMR** ($CDCl_3$, 400 MHz) 2.86 (d, *J* = 10.5 Hz, 1H), 3.15 (s, 3H), 3.82 (dt, *J* = 10.5, 6.0 Hz, 1H), 4.19 (dd, *J* = 14.0, 6.0 Hz, 1H), 4.37 (dd, *J* = 14.0, 6.0 Hz, 1H), 5.03-5.14 (m, 4H), 7.15-7.29 (m, 9H), 7.31-7.35 (m, 10 H), 7.36-7.41 (m, 6H), 7.77 (s, 1H), 7.81 (d, *J* = 2.0 Hz, 1H); **^{13}C NMR** ($CDCl_3$, 400 MHz) 52.2, 56.1, 57.1, 67.6 (dd, *J* = 1.5, 5.0 Hz), 71.0, 107.8 (d, *J* = 223.5 Hz), 126.7, 127.9, 128.1, 128.4 (d, *J* = 1.5 Hz), 128.6, 128.6, 136.1 (d, *J* = 7.0 Hz),

136.2 (d, *J* =24.0 Hz), 142.8 (d, *J* = 13.5 Hz), 145.3, 172.9; **^{31}P NMR** ($CDCl_3$, 400 MHz) 14.64 ppm; **m/z** (ESI+): 694.2441 (MNa+, 100 % $C_{40}H_{38}N_3NaO_5P$ requires 694.2400).

Methyl (2S)-3-[4-(dibenzyloxyphosphoryl)pyrazol-1-yl]-2-[[(9H-fluoren-9-ylmethoxy)carbonyl]amino]propanoate 126

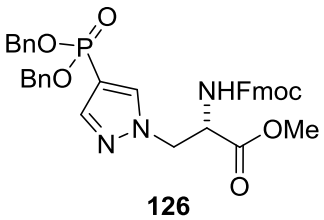

126

Methyl (2S)-3-[4-(dibenzyloxyphosphoryl)pyrazol-1-yl]-2-[(triphenylmethyl)amino]propanoate **125** (2.69 g, 4.0 mmol, 1.0 equiv.), was dissolved in dichloromethane (5.9 mL). Trifluoroacetic acid (8.76 g, 5.9 mL, 76.8 mmol, 19.2 equiv.) was added and the mixture was stirred at 0 ^{o} C for 10 minutes, and then at room temperature for 20 minutes. The solvent was removed under reduced pressure and residual trifluoroacetic acid was removed by forming an azeotrope with toluene (× 3) The residue was stirred with 10 % (w/v) aqueous sodium hydrogen carbonate (7.2 mL), and 1,4-dioxane (3.4 mL). Fluorenylmethyloxycarbonyl chloride (1.55 g, 6.0 mmol, 1.5 equiv.) dissolved in 1,4-dioxane (6.7 mL) was added dropwise at 0 ^{o}C. The mixture was stirred at room temperature overnight whilst maintaining a neutral pH with 10 % (w/v) aqueous sodium hydrogen carbonate. The mixture was diluted with water (55 mL) and extracted with ethyl acetate (3 × 50 mL). The combined organic phases were washed with brine, dried over anhydrous magnesium sulphate, filtered and concentrated under reduced pressure. The residue was purified by flash column chromatography eluting with 3:7 to 0:1 petroleum ether/ ethyl acetate solvent

gradient. Compound **125** (2.07 g, 79 %) colourless viscous oil: R_F = 0.39 (EtOAc); $[\alpha]^{19}_D$ = + 19.0 (*c* 1.0, $CHCl_3$); **ν_{max}**(thin film)/**cm^{-1}** 3407, 3262, 3062, 3036, 2951, 1724, 1528, 1451, 1223, 1138, 1035, 1006; **^{1}H NMR** ($CDCl_3$, 400 MHz) 3.77 (s, 1H), 4.23 (t, *J* = 7.0 Hz, 1H), 4.42 (d, *J* = 7.0 Hz, 2H), 4.54 (dd, *J* = 4.0, 14.0 Hz, 1H), 4.67 (dd, *J* = 4.0, 14.0 Hz, 1H), 4.72-4.79 (m, 1H), 5.01-5.12 (m, 4H), 7.29-7.44 (m, 14H), 7.60 (dd, *J* = 3.5, 7.5 Hz, 1H), 7.66 (d, *J* = 1.5 Hz, 1H), 7.73 (s, 1H), 7.77 (s, 1H), 7.79 (s, 1H); **^{13}C NMR** ($CDCl_3$, 400 MHz) 47.1, 52.8, 53.1, 54.1, 67.4, 67.6 (d, *J* = 5.0 Hz), 108.0 (d, *J* = 225.0 Hz), 120.1, 125.1 (d, *J* = 75 Hz), 127.2 (d, *J* = 4.5 Hz), 127.8, 128.0, 128.5, 128.6, 136.1, 136.1 (d, *J* = 24.0 Hz), 141.3, 143.3 (d, *J* = 13.5 Hz), 143.7, 155.8, 169.5; **^{31}P NMR** ($CDCl_3$, 400 MHz) 14.21; **m/z** (ESI+): 652.2207 (MH+, 100 % $C_{36}H_{35}N_3O_7P$ requires 652.2200).

Methyl (2R)-2-[(tert-butoxycarbonyl)amino]-3-iodopropanoate 131

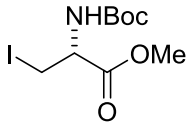

131

(2S)-3-hydroxy-1-methoxy-1-oxopropan-2-aminium chloride **124** (20.0 g, 128.6 mmol, 1.0 equiv.) was stirred into a flask containing tetrahydrofuran (400 mL) and triethylamine (28.0 g, 276 mmol, 38.6 mL, 2.1 equiv.) over nitrogen. The resulting white suspension was cooled to 0 ^{o}C and a solution of di-tert-butyl dicarbonate (28.6 g, 127.2 mmol, 1.0 equiv.) dissolved in tetrahydrofuran (200 mL) was added dropwise over a period of 1 hour. After 10 minutes of additional stirring, the suspension was stirred at room temperature overnight, and then warmed up to 50 °C and stirred for a further 3 hours. The solvent was removed under reduced pressure and the residue was partitioned between diethyl ether (400 mL) and saturated

aqueous bicarbonate solution (500 mL). The aqueous phase were extracted with diethyl ether (3 × 300 mL). The combined organic phases are dried with anhydrous sodium sulfate, filtered and concentrated under reduced pressure. The residue was dissolved dichloromethane (230 mL). The solution was cooled to 0 °C and 4-dimethylaminopyridine (0.830 g, 6.8 mmol, 0.05 equiv.), trimethylammonium chloride (1.30 g, 13.6 mmol, 1.1 equiv.), and *p*-toluenesulfonylchloride (25.9 g, 136.0 mmol, 1.1 equiv.) were added. Trimethylamine (13.7 g, 18.8 mL, 136 mmol, 1.1 equiv.) dissolved in dichloromethane (50 mL) and added dropwise to the mixture over 40 minutes. The resulting slurry was stirred at 0 °C for 2 hours and then poured into a mixture of ice (100 g), water (100 mL), and 2 molar aqueous hydrochloric acid (50 mL). The aqueous layer was extracted with dichloromethane (100 mL), and the combined organic layers were washed with brine (2 × 60 mL), dried over anhydrous magnesium sulfate, filtered and concentrated by under reduced pressure. The pale yellow solid was recrystallized by dissolving in hot diethyl ether (140 mL), and then immediately filtering and allowing the filtrate to cool to room temperature and then cooling to 0 °C. Once crystallises were observed petroleum ether was added in portions (5 × 50 mL) over 2.5 hours. Crystallisation was continued at -20 ^{o}C overnight. The crystals were collected and dissolved in acetone (150 mL). Sodium iodide (12.4 g, 82.8 mmol, 0.64 equiv.) was added and the mixture was stirred at room temperature in the dark for three days. Additional sodium iodide (3.1 g, 20.7 mmol, 0.16 equiv.) was added and the mixture was stirred for a further day. The mixture was filtered, and the solid was washed with acetone until colourless. The filtrate was concentrated under reduced pressure. The residue was dissolved in diethyl ether (150 mL) and washed with 1 molar aqueous sodium thiosulphate (2 × 50 mL), and brine (50 mL). The organic phase was dried over anhydrous magnesium sulphate, filtered and concentrated under reduced pressure. The crude product was recrystallized by dissolving in hot petroleum ether (30 mL),

before being allowed to cool to room temperature and then to 0 °C. Once crystallises were observed, the mixture was cooled to - 20 °C for 1 hour. The solid was filtered off and washed with cold petroleum ether. Compound **131** (20.3 g, 48 % yield) pale yellow soild: m.p.= 47-49 °C (lit.[141] 45-47 °C); $[\alpha]^{22}_{D}$ -3.7 (*c* 3.0, MeOH) (lit.[141] $[\alpha]^{22}_{D}$ -3.7 (*c* 3.0, MeOH)); $\boldsymbol{\nu_{max}}$(thin film)/**cm^{-1}** 3350, 2984, 2938, 1735, 1691, 1525, 1441, 1366, 1311, 1272, 1222, 1159, 1010, 1058; **^{1}H NMR** (400 MHz, $CHCl_3$) 1.48 (s, 9H), 3.78 (dd, *J* = 4.0, 10.5 Hz, 1H), 3.62 (dd, *J* = 3.5, 10.5 Hz), 3.82 (s, 3 H), 4.51-4.58 (m, 1H), 5.38 (d, *J* = 6.0 Hz, 1H); **^{13}C NMR** (101 MHz, $CHCl_3$) 7.8 (s), 28.3 (s), 53.0 (s), 53.7 (s), 80.5 (s), 154.8 (s), 170.2 (s); **m/z** (ESI+): 352.0016 (MNa+, 100 % $C_9H_{16}INNaO_4$ requires 352.0000).

The characterization data are similar to the literature.[141]

Diethyl (2-chloropyridin-4-yl)phosphonate 66

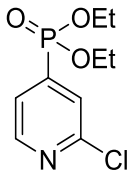

66

Palladium(II) acetate (0.067 g, 0.3 mmol, 0.03 equiv.), 1,1'-bis(diphenylphosphino)ferrocene (0.33 g, 0.6 mmol, 0.06 equiv.), and anhydrous sodium acetate (0.098 g, 0.12 mmol, 0.12 equiv.) were added to a round bottom flask equipped with a condenser. A vacuum was applied followed by a positive pressure of nitrogen (× 3). Tetrahydrofuran (20 mL) was added followed by N,N-diisopropylethylamine (1.55 g, 2.1 mL, 12.0 mmol, 1.2 equiv.) and the mixture was stirred at 60 °C for 30 minutes. 2-chloro-4-iodopyridine (2.39 g, 10.0 mmol, 1.0 equiv.) and diethyl phosphite (1.38 g, 1.3 mL, 10.0 mmol, 1.0 equiv.) were added and refluxed

for 24 hours. The mixture was allowed to cool to room temperature and then concentrated under reduced pressure. The remaining residue was purified by flash column chromatography over silica, eluting with ethyl acetate. Diethyl (2-chloropyridin-4-yl)phosphonate **66** (0.886 g, 36 % yield) yellow oil: R_F = 0.4 (EtOAc); $\boldsymbol{\nu_{max}}$(thin film)/**cm**$^{-1}$ 3541, 3485, 3057, 2991, 2938, 2907, 1581, 1529, 1455, 1393, 1358, 1260, 1163, 1089, 1048, 1020; ^{1}**H NMR** (400 MHz, $CDCl_3$) 1.35 (t, *J* = 7.5 Hz, 6H), 4.08-4.26 (m, 4H), 7.56 (dd, *J* = 5.0 Hz, 12.5 Hz, 1 H), 7.68 (d, *J* = 13.5 Hz, 1H), 8.50-8.55 (m, 1H); ^{13}**C NMR** (101 MHz, $CDCl_3$) 16.3 (d, *J* = 6.0 Hz), 63.1 (d, *J* = 5.5 Hz), 123.7 (d, *J* = 8.0), 126.3 (d, *J* = 9.5 Hz), 141.0 (d, *J* = 185.0 Hz), 150.1 (d, *J* = 14.0 Hz), 152.2 (d, *J* = 18.5 Hz); ^{31}**P NMR** (162 MHz, $CDCl_3$) 12.54; **m/z** (ESI+): 250.0394(MH+, 100 % $C_9H_{14}NO_3ClP$ requires 250.0400).

The characterization data are similar to what was reported in Lilley's thesis.[1]

Methyl (2S)-2-[(tert-butoxycarbonyl)amino]-3-[4-(diethoxyphosphoryl)pyridin-2-yl]propanoate 67

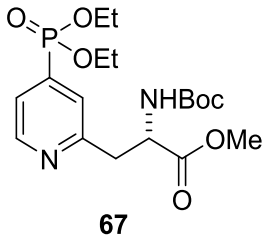

67

A round bottom flask containing zinc dust (0.550 g, 8.4 mmol, 3.0 equiv.) and a stirrer bar were flame dried under vacuum, which was followed by a positive pressure nitrogen (3 ×). Dimethylformamide (2.8 mL) was added followed by iodine (0.213 g, 0.84 mmol, 0.3 equiv.); the solution colour changed from yellow back to colourless again. With rapid stirring methyl (2R)-2-[(tert-butoxycarbonyl)amino]-3-iodopropanoate **131** (0.920 g, 2.8 mmol, 1.0 equiv.)

was added followed by the immediate addition of iodine (0.213 g, 0.84 mmol, 0.3 equiv.); a strong exotherm was observed. The reaction was stirred rapidly for 15 minutes. The supernatant was then withdrawn via a cotton wool filled syringe, and decanted in to a flask containing tris(dibenzylideneacetone)dipalladium (0) (0.064 g, 0.07 mmol, 0.025 equiv.), SPhos (0.057 g, 0.14 mmol, 0.05 equiv.), and diethyl (2-chloropyridin-4-yl) phosphonate **66** (0.699 g, 2.8 mmol, 1.0 equiv.) at 50 °C under nitrogen. The remaining zinc was washed with dimethylformamide (1.4 mL), and the supernatant transferred in the same way as above. After three hours a second equivalent of zinc reagent **13** was added and the mixture was stirred for a further 3 hours. The mixture was then diluted with ethyl acetate (60 mL) and filtered through a bed (1 cm) of Celite. The Celite was washed with ethyl acetate until the eluent was colourless. The filtrate was washed with water (250 mL), and then brine (250 mL) after which the organic phase was dried with anhydrous magnesium sulphate, filtered and concentrated under reduced pressure. The remaining residue was purified by flash column chromatography over silica eluting with solvent gradient 8:2 to 1:0 ethyl acetate/petroleum ether. Compound **67** (0.714 g, 61 % yield) pale yellow oil: R_F = 0.17 (EtOAc); $[\alpha]^{25}_D$ +28.0 (*c* 1.0, $CHCl_3$), (lit.[1] $[\alpha]^{22}_D$ +30.0 (*c* 1.0, $CHCl_3$); $\boldsymbol{\nu_{max}}$(thin film)/**cm^{-1}** 3293, 2984, 2935, 1744, 1717, 1595, 1514, 1393, 1361, 1160, 1125, 1020; **^{1}H NMR** (400 MHz, $CDCl_3$) 1.35 (t, *J* = 7.0 Hz, 6H), 1.42 (s, 9H), 3.34 (dd, *J* = 5.0, 15.0 Hz, 1H), 3.41 (dd, *J* = 6.0, 15.0 Hz, 1H), 3.70 (s, 3H), 4.06-4.24 (m, 4H), 4.69-4.77 (m, 1H), 5.74 (d, *J* = 8.5 Hz, 1H), 7.47-7.53 (m, 2H), 8.63-8.67 (m, 1H); **^{13}C NMR** (101 MHz, $CDCl_3$) 16.3 (d, *J* = 6.0 Hz), 28.3 (s), 52.3 (s), 52.7 (s), 62.7 (d, *J* = 5.5 Hz), 79.9 (s), 123.3 (d, *J* = 8.0 Hz), 124.4 (d, *J* = 8.5 Hz), 138.0 (d, *J* = 184.0 Hz), 149.5 (d, *J* = 13.0 Hz), 155.4 (s), 157.9 (d, *J* = 13.0 Hz), 172.2 (s); **^{31}P NMR** (162 MHz, $CDCl_3$) 14.6; **m/z** (ESI+): 417.1782 (MH+, 100 % $C_{18}H_{30}N_2O_7P$ requires 417.1800).

The characterization data are similar to what was reported in Lilley's thesis.[1]

(2S)-2-Amino-3-(4-phosphonopyridin-2-yl)propanoic acid 133

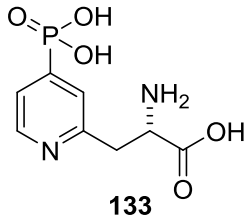

133

Methyl (2S)-2-[[tert-butoxy) carbonyl] amino]-3-[4-(diethoxyphosphoryl) pyridine-2-yl]propanoate **67** (0.180 g, 0.43 mmol, 1.0 equiv.) was dissolved in tetrahydrofuran (0.82 mL) and water (0.82 mL). Lithium hydroxide monohydrate (0.022 g, 0.52 mmol, 1.2 equiv.) was added and the mixture was stirred at room temperature for 100 minutes. The mixture was acidified to pH 4-5 using 1 molar aqueous hydrochloric acid and concentrated under reduced pressure. This brown oil was dissolved in acetonitrile (4.4 mL), over nitrogen. Bromotrimethylsilane (0.66 g, 0.56 mL, 4.3 mmol, 10.0 equiv.) was added and the mixture was stirred at 50 °C overnight. The mixture was allowed to cool to room temperature and the solvent was removed under reduced pressure The orange solid was triturated in isopropanol (15 mL), added to a centrifuge vile and centrifuged (3220 rcf, 4 °C, 5 min). The supernatant was discarded and the solid was loaded on to a pre-equilibrated (8:2 ethanol/water) flash chromatography silica gel column. The column was eluted with an 80:18:2 to 65:22:8; ethanol/water/32 % (wt/wt) aqueous ammonia gradient. The combined product fractions were concentrated under reduced pressure and then lyophilized. The remaining solid residue was dissolved in water (2.5 mL) and an aliquot was diluted in deuterated water for quantification by ^{1}H NMR using 1,4-dioxane as the internal standard. Compound **133** (0.036 g, 34 % yield) white solid: R_F = 0.30 (65:22:8 EtOH/H_2O/32 % (wt/wt) NH_3 (aq.)); $[\alpha]^{25}_{D}$ -4.0 (*c* 1.0, H_2O); m.p.= 234 °C (decomp.); $\boldsymbol{\nu_{max}}$(ATR)/**cm^{-1}** 3192, 2986, 2842, 1597, 1526, 1417, 1097; **^{1}H NMR** (400 MHz, D_2O) 3.18 (dd, *J* = 9.0, 15.0 Hz, 1H), 3.40 (dd, *J* = 4.5, 15.0 Hz, 1H), 4.05

(dd, *J* = 4.5, 9.0 Hz, 1H), 7.46-7.59 (m, 2H), 8.42 (t, J = 4.5 Hz, 1H); **^{13}C NMR** (101 MHz, D_2O) 37.3 (s), 54.5 (s), 123.8 (d, *J* = 7.5 Hz), 125.3 (d, *J* = 8.0 Hz), 148.4 (d, *J* = 11.0 Hz), 149.4 (d, *J* = 164.4 Hz), 155.8 (d, *J* = 11.0 Hz), 173.6 (s); **^{31}P NMR** (162 MHz, D_2O) 7.79; **m/z** (ESI+): 247.0482 (MH+, 100 % $C_8H_{12}N_2O_4P$ requires 247.0500).

(2S)-2-amino-3-(4-phosphonopyridin-2-yl)propanoic acid 132

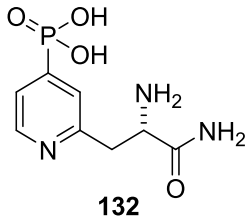

132

Methyl (2S)-2-[[tert-butoxy) carbonyl] amino]-3-[4-(diethoxyphosphoryl) pyridine-2-yl]propanoate **67** (0.200 g, 0.48 mmol, 1.0 equiv.) was dissolved in methanol (4 mL). 33 % (wt/wt) aqueous ammonia (1.9 mL) was added and the mixture which was stoppered and stirred at room temperature for 4 hours. After concentration under reduced pressure, the remaining residue was dissolved in acetonitrile (4.8 mL) over nitrogen. Bromotrimethylsilane (0.735 g, 0.63 mL, 4.8 mmol, 10.0 equiv.) was added and the mixture was stirred at 50 °C, overnight. The mixture was allowed to cool to room temperature and the solvent was removed under reduced pressure. The orange solid was triturated in isopropanol (15 mL), added to a centrifuge vile and centrifuged (3220 rcf, 4 °C, 5 min). The supernatant was discarded and the solid was loaded on to a pre-equilibrated (8:2 ethanol/water) flash chromatography silica gel column. The column was eluted an 80:18:2 to 65:22:8; ethanol/water/32 % (wt/wt) aqueous ammonia gradient. The combined product fractions were concentrated under reduced pressure and then lyophilized. The remaining solid residue

was dissolved in water (2.5 mL) and an aliquot was diluted in deuterated water for quantification by ^{1}H NMR using 1,4-dioxane as the internal standard. Compound **132** (0.057 g, 29 % yield) pale yellow sold: R_F = 0.37 (65:22:8 EtOH/H_2O/32 % (wt/wt) NH_3 (aq.)); $[\alpha]^{24}_D$ +12.0 (*c* 1.0, H_2O); m.p.= 210 °C (decomp.); $\boldsymbol{\nu_{max}}$(ATR)/**cm**$^{-1}$ 3049, 1682, 1415, 1068, 1004; **^{1}H NMR** (400 MHz, D_2O) 3.21 (dd, *J* = 8.0, 15.0 Hz, 1H), 3.30 (dd, *J* = 6.0, 15.0 Hz, 1H) 4.23-4.28 (m, 2 H), 7.40-7.48 (m, 2 H), 8.43 (t, *J* = 4.5 Hz, 1H); **^{13}C NMR** (101 MHz, D_2O) 38.1 (s), 53.0 (s), 124.2 (d, *J* = 7.5 Hz), 125.5 (d, *J* = 7.5 Hz), 148.6 (d, *J* = 11.0 Hz), 150.6 (d, *J* = 162.5 Hz), 153.6 (d, *J* = 11.1 Hz), 171.7 (s); **^{31}P NMR** (162 MHz, D_2O) 7.65; **m/z** (ESI+): 246.0641 (MH+, 100 % $C_8H_{13}N_2O_4P$ requires 246.0600).

Diethyl (5-bromopyridin-3-yl)phosphonate 135

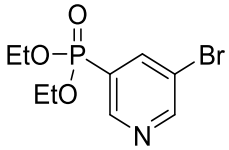

135

Palladium(II) acetate (0.067 g, 0.3 mmol, 0.03 equiv.), 1,1'-bis(diphenylphosphino)ferrocene (0.033 g, 0.6 mmol, 0.06 equiv.), and anhydrous sodium acetate (0.010 g, 0.012 mmol, 0.12 equiv.) were added to a round bottom flask equipped with a condenser. A vacuum was applied followed by a positive pressure of nitrogen (× 3). Tetrahydrofuran (2 mL) was added followed by N,N-diisopropylethylamine (0.155 g, 0.21 mL, 1.2 mmol, 1.2 equiv.) and the mixture was stirred at 60 °C for 30 minutes. 3,5-dibromopyridine (0.237 g, 1.0 mmol, 1.0 equiv.) and diethyl phosphite (0.138 g, 0.13 mL, 1.0 mmol, 1.0 equiv.) were added and the mixture was stirred at reflux for 24 hours. The mixture was concentrated under reduced

pressure and the residue was purified by flash column chromatography over silica, eluting with ethyl acetate. Compound **135** (0.133 g, 45 % yield) clear oil: R_F = 0.19 (2:3 pet. ether/EtOAc); ν_{max}(thin film)/**cm^{-1}** 3054, 2989, 2927, 2910, 1569, 1405, 1254, 1185, 1161, 1089, 1052, 1021; **^{1}H NMR** (400 MHz, $CDCl_3$) 1.36 (t, *J* = 7.0 Hz, 6H), 4.08-4.27 (m, 4H), 8.22 (dt, *J* = 13.5, 2.0 Hz, 1 H), 8.83 (d, *J* = 2.0 Hz, 1H), 8.86 (dd, *J* = 6.0, 2.0 Hz, 1H); **^{13}C NMR** (101 MHz, $CDCl_3$) 16.3 (d, *J* = 6.5 Hz), 62.9 (d, *J* = 5.5 Hz), 121.0 (d, *J* = 14.0), 126.9 (d, *J* = 187.0 Hz), 141.7 (d, *J* = 8.5 Hz), 150.1 (d, *J* = 11.5 Hz); 154.1 (d, *J* = 1.5 Hz); **^{31}P NMR** (162 MHz, $CDCl_3$) 13.32; **m/z** (ESI+): 293.9889 (MH+, 100 % $C_9H_{14}BrNO_3P$ requires 293.9900).

Methyl (2S)-2-[[(tert-butoxy)carbonyl]amino]-3-[5-(diethoxyphosphoryl)pyridin-3-yl]propanoate 136

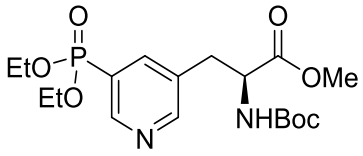

136

A round bottom flask containing zinc dust (0.850 g, 13.0 mmol, 3.0 equiv.) was rapidly stirred and the flask was flame dried under vacuum, which was followed by a positive pressure of nitrogen (× 3). Dimethylformamide (2.2 mL) was added followed by iodine (0.170 g, 0.70 mmol, 0.3 equiv.); the solution colour changed from yellow back to colourless again. Methyl (2R)-2-[(tert-butoxycarbonyl)amino]-3-iodopropanoate **131** (0.750 g, 2.3 mmol, 1.0 equiv.) was added followed by the immediate addition of iodine (0.170 g, 0.70 mmol, 0.3 equiv.). A strong exotherm was observed and the reaction was stirred at room temperature for 15 minutes. The supernatant was then withdrawn via a cotton wool filled syringe, and decanted in to a flask containing bis(triphenylphosphine)palladium(II) dichloride (0.052 g, 0.22 mmol,

0.1 equiv.), and diethyl 5-bromopyridin-3-ylphosphonate (0.64 g, 2.2 mmol, 1.0 equiv.) at 50 °C under nitrogen. The remaining zinc was washed with dimethylformamide (2.2 mL), and the supernatant was transferred as above. After 3 hours a second equivalent of zinc reagent **13** was added and the mixture was stirred for a further 3 hours. The mixture was diluted with ethyl acetate (60 mL) and filtered through a bed (1 cm) of celite. The celite was washed with ethyl acetate until the eluent was colourless. The filtrate was washed with water (250 mL), and then brine (250 mL). The organic phase was dried over anhydrous magnesium sulphate, filtered and concentrated under reduced pressure. The remaining residue was purified by flash column chromatography over silica eluting with ethyl acetate. Compound **136** (0.600 g, 66 % yield) pale yellow oil: R_F = 0.13 (EtOAc); $[\alpha]^{25}_D$ + 42.0 (*c* 1.0, $CHCl_3$); $\mathbf{\nu_{max}}$(ATR)/**cm**$^{-1}$ 3282, 2978, 1745, 1709, 1523, 1366, 1255, 1160, 1050, 1016; ^{1}**H NMR** (400 MHz, $CDCl_3$) 1.35 (t, *J* = 7.0, 6H), 1.42 (s, 9H), 3.09 (dd, *J* = 6.0, 14.0 Hz, 1H), 3.25 (dd, *J* = 5.5, 14.0 Hz, 1H), 3.76 (s, 3H), 4.07-4.25 (m, 4H), 4.58-4.66 (m, 1H), 5.12 (d, *J* = 7.5 Hz), 7.85-7.91 (m, 1H), 8.55 (s, 1H), 8.86 (dd, *J* = 2.0, 6.5 Hz, 1H); ^{13}**C NMR** (101 MHz, $CDCl_3$) 16.3 (d, *J* = 6.5 Hz), 28.2 (s), 35.5 (s), 52.6 (s), 54.0 (s), 62.6 (d, *J* = 5.5 Hz), 80.3 (s), 124.8 (d, *J* = 189.5 Hz), 131.8 (d, *J* = 11.5 Hz), 140.2 (d, *J* = 8.5 Hz), 150.8 (d, *J* = 12.0 Hz),153.8 (s), 154.9 (s), 171.5 (s); ^{31}**P NMR** (162 MHz, $CDCl_3$) 15.64; **m/z** (ESI+): 417.1785 (MH+, 100 % $C_{18}H_{30}N_2O_7P$ requires 417.1800).

(2S)-2-amino-3-(5-phosphonopyridin-3-yl)propanoic acid 127

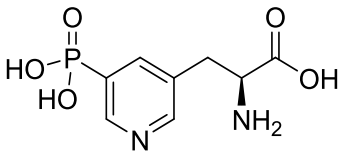

127

Methyl (2S)-2-[(tert-butoxycarbonyl)amino]-3-[5-(diethoxyphosphoryl)pyridin-3-yl]propanoate **136** (0.483 g, 1.16 mmol, 1.0 equiv.) was stirred at reflux in 6 molar aqueous hydrochloric acid (10 mL) overnight. After cooling to room temperature, the mixture was carefully neutralised with 2 molar aqueous sodium hydroxide. The residue was loaded on to a pre-equilibrated (8:2; ethanol/water) flash chromatography silica gel column. The column was eluted with an 80:18:2 to 65:22:8; ethanol/water/32 % (wt/wt) aqueous ammonia gradient. The combined product fractions were concentrated under reduced pressure and then lyophilized. The solid residue was dissolved in water (2.5 mL) and an aliquot was diluted in deuterated water for quantification by ^{1}H NMR using 1,4-dioxane as the internal standard. Compound **127** (0.034 g, 12 % yield): R_F = 0.25 (1:1 EtOH/H_2O); $[\alpha]^{24}_{D}$ -10.0 (*c* 1.0, H_2O); m.p. = 250 °C (decomp.); $\boldsymbol{\nu_{max}}$(ATR)/**cm^{-1}** 3338, 1625, 1530, 1415, 1122, 1099; **^{1}H NMR** (400 MHz, D_2O) 3.04 (dd, *J* = 8.0, 15.0 Hz, 1H), 3.21 (dd, *J* = 5.0, 15.0 Hz, 1H), 3.86-3.91 (m, 1H), 7.85-7.91 (m, 1H), 8.29 (s, 1H), 8.52-8.55 (m, 1 H); **^{13}C NMR** (101 MHz, D_2O) 33.6 (s), 55.5 (s), 131.2 (d, *J* = 10.0 Hz), 135.4 (d, *J* = 167.0 Hz), 140.3 (d, *J* = 7.5 Hz), 148.5 (d, *J* = 11.5 Hz), 149.2 (s), 173.4 (s); **^{31}P NMR** (162 MHz, D_2O) 7.67; **m/z** (ESI+): 247.0481 (MH+, 100 % $C_8H_{12}N_2O_4P$ requires 247.0500).

5-[(2S)-2-amino-2-carbamoylethyl]pyridin-3-ylphosphonic acid 128

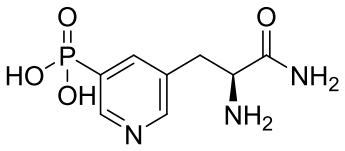

128

Methyl (2S)-2-[(tert-butoxycarbonyl)amino]-3-[5-(diethoxyphosphoryl)pyridin-3-yl]propanoate **136** (0.350 g, 0.84 mmol, 1.0 equiv.) was dissolved in methanol (6.7 mL). 32 % (wt/wt) aqueous ammonia (3.3 mL) was added and the mixture was stoppered and stirred at room temperature for 4 hours. The mixture was concentrated under reduced pressure. The residue was dissolved in acetonitrile (7 mL) under nitrogen. Bromotrimethylsilane (1.29 g, 1.11 mL, 8.4 mmol, 10 equiv.) was added the mixture was stirred at 50 °C overnight. The mixture was cooled to room temperature and the solvent was removed under reduced pressure. The orange solid was triturated in isopropanol (15 mL), added to a centrifuge vile and centrifuged (3220 relative centrifugal force, 4 °C, 5 minutes). The supernatant was discarded and the solid was loaded on to a pre-equilibrated (8:2 ethanol/water) flash chromatography silica gel column. The column was eluted with an 80:18:2 to 65:22:8; ethanol/water/32 % (wt/wt) aqueous ammonia gradient. The combined product fractions were concentrated under reduced pressure and then lyophilized. The remaining solid residue was dissolved in water (2.5 mL) and an aliquot was diluted in deuterated water for quantification by ^{1}H NMR using 1,4-dioxane as the internal standard. Compound **128** (0.086 g, 42 % yield): R_F = 0.75 (8:2 EtOH:H_2O); $[\alpha]^{23}_{D}$ -11.0 (*c* 1.0, H_2O); m.p. = 250 °C (decomp.); $\boldsymbol{\nu_{max}}$(ATR)/**cm^{-1}** 3022, 2842, 2324, 2118, 1681, 1577, 1540, 1420, 1284, 1043; **^{1}H NMR** (400 MHz, D_2O) 3.12-3.23 (m, 2H), 4.17 (t, *J* = 7.0 Hz, 1H), 7.92-7.97 (m, 1H), 8.34 (s, 1H), 8.59 (d, *J* = 6.0 Hz, 1H); **^{13}C NMR** (101 MHz, D_2O) 34.0 (s), 53.6 (s), 130.2 (d, *J* = 10.5 Hz), 134.9 (d, *J* =

168.0 Hz), 140.5 (d, *J* = 7.5 Hz), 148.7 (d, *J* = 12.0 Hz), 149.3 (s), 171.1 (s); **^{31}P NMR** (162 MHz, D_2O) 7.64; **m/z** (ESI+): 246.0638 (MH+, 100 % $C_8H_{13}N_2O_4P$ requires 246.0600).

Methyl (2S)-3-(3-bromopyridin-4-yl)-2-[(tert-butoxycarbonyl)amino]propanoate 138

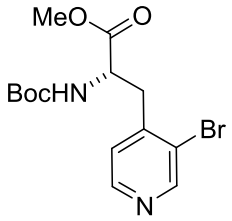

138

A round bottom flask containing zinc dust (0.990 g, 15.0 mmol, 3.0 equiv.) was rapidly stirred and the flask was flame dried under vacuum, which was followed by a positive pressure of nitrogen (× 3). Dimethylformamide (4.0 mL) was added followed by iodine (0.380 g, 1.5 mmol, 0.3 equiv.); the solution colour changed from yellow back to colourless again. Methyl (2R)-2-[(tert-butoxycarbonyl)amino]-3-iodopropanoate **131** (1.72 g, 5.2 mmol, 1.0 equiv.) was added followed by the immediate addition of iodine (0.38 g, 1.5 mmol, 0.3 equiv.). A strong exotherm was observed and the mixture was stirred at room temperature for 15 minutes. The supernatant was then withdrawn via a cotton wool filled syringe, and decanted in to a flask containing bis(triphenylphosphine)palladium(II) dichloride (0.350 g, 0.5 mmol, 0.1 equiv.), and 3,4-dibromopyridine (1.18 g, 5.0 mmol, 1.0 equiv.) at 50 °C under nitrogen. The remaining zinc was washed with dimethylformamide (2.0 mL), and the supernatant transferred as above. After 3 hours. a second equivalent of zinc reagent **13** was added and the mixture was stirred for a further 3 hours. The mixture was diluted with ethyl acetate (60 mL) and filtered through a bed (1 cm) of celite. The celite was washed with ethyl acetate until the eluent was colourless. The filtrate was washed with water (250 mL), and then brine (250

mL). The organic phase was dried over anhydrous magnesium sulphate, filtered and concentrated under reduced pressure. The remaining residue was purified by flash column chromatography over silica eluting with 3:7 ethyl acetate/petroleum ether. Compound **138** (0.895 g, 50 % yield) pale yellow oil: R_F = 0.33 (3:7 EtOAc/pet. ether); $[\alpha]^{25}_D$ +10.0 (*c* 1.0, $CHCl_3$); **ν_{max}**(ATR)/**cm^{-1}** 3350, 2978, 2952, 2936, 1745, 1705, 1588 1516, 1434, 1395, 1362, 1278, 1252, 1212, 1160, 1088, 1046, 1023; **^{1}H NMR** (400 MHz, $CDCl_3$) 1.39 (s, 9H), 3.10 (dd, *J* = 8.5, 14.0 Hz, 1H), 3.33 (dd, *J* = 5.5, 14.0 Hz, 1H), 3.76 (s, 3H), 4.65-4.74 (m, 1H), 5.18 (d, *J* = 8.0 Hz, 1H), 7.19 (d, *J* = 5.0 Hz, 1H), 8.44 (d, *J* = 5.0 Hz, 1H), 8.70 (s, 1H); **^{13}C NMR** (101 MHz, $CDCl_3$) 28.2 (s), 38.1 (s), 52.7 (s), 80.3 (s), 123.6 (s), 125.9 (s), 145.1 (s), 148.2 (s), 152.0 (s), 154.9 (s), 171.7 (s); **m/z** (ESI+): 359.0602 (MH+, 100 % $C_{14}H_{20}BrN_2O_4$ requires 359.0600).

Methyl (2S)-2-[(tert-butoxycarbonyl)amino]-3-[3-(diethoxyphosphoryl)pyridin-4-yl]propanoate 139

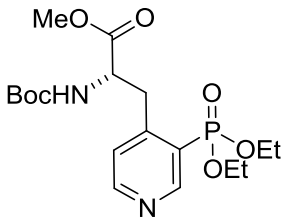

139

Palladium(II) acetate (0.024 g, 0.11 mmol, 0.1 equiv.), triphenylphosphine (0.084 g, 0.32 mmol, 0.3 equiv.), were added to a round bottom flask equipped with a condenser. A vacuum was applied followed by a positive pressure of nitrogen (× 3). Sequentially, ethanol (4 mL), triethylamine (0.162 g, 0.22 mL, 1.6 mmol, 1.2 equiv.), diethyl phosphite (0.220 g, 0.21 mL, 1.6 mmol, 1.2 equiv.) and methyl (2S)-3-(3-bromopyridin-4-yl)-2-[(tert-butoxycarbonyl)amino]propanoate **138** (0.449 g, 1.3 mmol, 1.0 equiv.) were added and the

mixture was stirred at reflux for 48 hours. The mixture was concentrated under reduced pressure and the residue was purified by flash column chromatography over silica, eluting with 15:85 petroleum ether/ethyl acetate. Compound **139** (0.295 g, 55 % yield) yellow oil: R_F = 0.20 (15:85 pet. ether/EtOAc); $[\alpha]^{25}_D$ +17.0 (*c* 1.0, $CHCl_3$); ν_{max}(ATR)/**cm**$^{-1}$ 2980, 2929, 2906, 1742, 1712, 1582, 1520, 1445, 1364, 1244, 1218, 1160, 1044, 1017; **^{1}H NMR** (400 MHz, $CDCl_3$) 1.33 (s, 9H), 1.38 (t, *J* =7.0 Hz, 3 H), 1.42 (t, *J* = 7.0 Hz, 3 H), 3.33 (dd, *J* = 4.5, 13.5 Hz, 1H), 3.45 (dd, *J* = 11.5, 13.5 Hz, 1 H), 3.78 (s, 3H), 4.15-4.34 (m, 4H), 4.50-4.58 (m, 1H), 6.21 (d, *J* = 8.5 Hz, 1H), 7.37 (t, *J* = 5.0 Hz, 1H), 8.70 (dd, *J* = 2.0, 5.0 Hz, 1H), 8.94 (d, *J* = 7.5 Hz, 1H); **^{13}C NMR** (101 MHz, $CDCl_3$) 16.3 (dd, *J* = 6.5, 8.0 Hz), 28.2 (s), 35.3 (s), 52.5 (s),54.8 (s), 62.8 (d, *J* = 6.0 Hz), 63.1 (d, *J* = 5.5 Hz), 79.7 (s), 124.4 (d, *J* = 186.0 Hz), 125.4 (d, *J* = 11.5 Hz), 150.6 (d, *J* = 10.5 Hz), 153.1 (s), 153.3 (d, *J* = 11.5 Hz), 155.6 (s), 172.2 (s); **^{31}P NMR** (162 MHz, $CDCl_3$) 16.48; **m/z** (ESI+): 417.1792 (MH+, 100 % $C_{18}H_{30}N_2O_7P$ requires 417.1800).

(2S)-2-amino-3-(3-phosphonopyridin-4-yl)propanoic acid 129

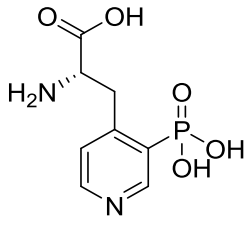

129

Methyl (2S)-2-[(tert-butoxycarbonyl)amino]-3-[3-(diethoxyphosphoryl)pyridin-4-yl]propanoate **129** (0.483 g, 1.16 mmol, 1.0 equiv.) was stirred at reflux in 6 molar aqueous hydrochloric acid (10 mL) overnight. The mixture was cooled to room temperature and carefully neutralized with 2 molar aqueous sodium hydroxide. The residue was loaded on to a pre-equilibrated (8:2; ethanol/water) flash chromatography silica gel column. The column

was eluted with an 80:18:2 to 65:22:8 ethanol/water/32 % (wt/wt) aqueous ammonia solvent gradient. The combined product fractions were concentrated under reduced pressure and then lyophilized. The solid residue was dissolved in water (2.5 mL) and an aliquot was diluted in deuterated water for quantification by ^{1}H NMR using 1,4-dioxane as the internal standard. Compound **129** (0.152 g, 54 % yield): R_F = 0.61 (8:2 EtOH:H_2O); $[\alpha]^{23}_{D}$ -16.0 (*c* 1.0, H_2O); m.p. = 260 °C (decomp.); $\boldsymbol{\nu_{max}}$(ATR)/**cm**$^{-1}$ 3165, 1624, 1590, 1511, 1401, 1128, 1105, 1055; ^{1}**H NMR** (400 MHz, D_2O) 3.51 (dd, *J* = 6.5, 14.0 Hz, 1H), 3.70 (dd, *J* = 5.5, 14.0 Hz, 1H), 3.70-3.98 (m, 1H), 7.44 (dd, *J* = 3.5, 5.5 Hz, 1H), 8.45 (d, *J* = 5.5 Hz, 1H), 8.76 (d, *J* = 7.0 Hz, 1 H); ^{13}**C NMR** (101 MHz, D_2O) 34.3 (d, *J* = 4.0 Hz), 54.6, 126.8 (d, *J* = 9.0 Hz), 136.5 (d, *J* = 159.0 Hz), 146.7, 148.4 (d, *J* = 11.5 Hz), 151.3 (d, *J* = 7.0 Hz), 173.7; ^{31}**P NMR** (162 MHz, D_2O) 4.47; **m/z** (ESI+): 247.0480 (MH+, 100 % $C_8H_{12}N_2O_5P$ requires 247.0500).

4-[(2S)-2-amino-2-carbamoylethyl]pyridin-3-ylphosphonic acid 130

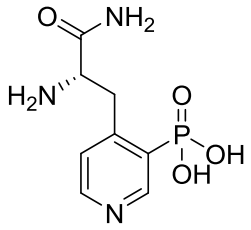

130

Methyl (2S)-2-[(tert-butoxycarbonyl)amino]-3-[5-(diethoxyphosphoryl)pyridin-3-yl]propanoate **139** (1.25 g, 2.90 mmol, 1.0 equiv.) was dissolved in methanol (24 mL). 32 % (wt/wt) ammonium hydroxide (12 mL) was added and the mixture was stoppered and stirred at room temperature for 4 hours. The mixture was concentrated under reduced pressure. The residue was dissolved in acetonitrile (28 mL) under nitrogen. Bromotrimethylsilane (4.24 g, 3.7 mL, 27.7 mmol, 10 equiv.) was added and the mixture was stirred at 50 °C overnight. The

solvent was removed under reduced pressure and the residue was loaded on to a pre-equilibrated (8:2; ethanol/water) flash chromatography silica gel column. The column was eluted an 80:18:2 to 65:22:8; ethanol/water/32 % (wt/wt) aqueous ammonium gradient. The combined product fractions were concentrated under reduced pressure and then lyophilized. The remaining solid residue was dissolved in water (2.5 mL) and an aliquot was diluted in deuterated water for quantification by ^{1}H NMR using 1,4-dioxane as the internal standard. Compound **130** (0.110 g, 15 % yield): R_F =0.58 (65:35 EtOH:H_2O); $[\alpha]^{23}_{D}$ -8.0 (*c* 1.0, H_2O); m.p. = 200 °C (decomp.); ν_{max}(ATR)/**cm^{-1}** 3011, 2970, 2285, 1741, 1667, 1587, 1439, 1399, 1370, 1218, 1130, 1040; **^{1}H NMR** (400 MHz, D_2O) 3.39 (dd, *J* = 7.0, 14.0 Hz, 1H), 3.55 (dd, *J* = 5.5, 14 Hz, 1H), 4.17-4.23 (m, 1H), 7.18-7.23 (m, 1H), 8.27-8.31 (m, 1H), 8.63 (d, *J* = 7.0 Hz, 1H); **^{13}C NMR** (101 MHz, D_2O) 34.9 (d, *J* = 4.0 Hz), 52.5, 126.3 (d, *J* = 9.0 Hz), 135.9 (d, *J* = 158.5 Hz), 147.7 (d, *J* = 7.0 Hz), 148.0, 149.9 (d, *J* = 11.0 Hz), 171.5; **^{31}P NMR** (162 MHz, D_2O) 4.86; **m/z** (ESI+): 246.0642 (MH+, 100 % $C_8H_{13}N_2O_4P$ requires 246.0600).

Diethyl (1H-pyrazol-4-yl)phosphonate 59

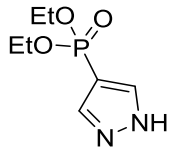

59

4-Iodopyrazole **51** (0.193 g, 1.0 mmol, 1.0 equiv.), triphenylphosphine (0.078 g, 0.3 mmol, 0.3 equiv.) and palladium(II) acetate (0.022 g, 0.1 mmol, 0.1 equiv.) were added to a round bottom flask equipped with a condenser. A vacuum was applied followed by a positive pressure of nitrogen (× 3). Ethanol (3.5 mL), triethylamine (0.202 g, 0.28 mL, 2.0 mmol, 2.0 equiv.) and diethyl phosphite (0.304 g, 0.28 mL, 2.2 mmol, 2.2 equiv.) were then added and

the mixture was stirred at reflux for 6 hours. The mixture was allowed to cool to room temperature and then diluted with saturated aqueous ammonium chloride (30 mL). The aqueous phase was extracted with ethyl acetate (3 × 80 mL) and the combined organic phases were washed with brine (80 mL), dried over anhydrous magnesium sulphate, filtered and concentrated under reduced pressure. The residue was purified by flash column chromatography over silica eluting with 1:9 ethyl acetate: pet ether. Compound **59** (0.203 g, 99 %), a white solid: R_F = 0.11 (EtOAc); m.p. = 57-59 °C (lit.[151] 85-87 °C); $\boldsymbol{\nu_{max}}$(ATR)/**cm**$^{-1}$ 3150, 2902, 1543, 1478, 1378, 1294, 1213, 1185, 1154, 1014, **^{1}H NMR** (400 MHz, $CDCl_3$) 1.34 (t, *J* = 7.0 Hz, 6H), 4.04-4.19 (m, 4 H), 7.92 (s, 2H), 12.65 (br, 1H); **^{13}C NMR** (101 MHz, $CDCl_3$) 16.2 (d, *J* = 6.5 Hz), 62.3 (d, *J* = 5.5 Hz), 106.5 (d, *J* = 222.5 Hz), 138.2 (br); **^{31}P NMR** (162 MHz, $CHCl_3$) 14.98; **m/z** (ESI+): 205.0737 (MH+, 100 % $C_7H_{14}N_2O_3P$ requires 205.0700).

The characterization data is similar to what was reported in Mukai's thesis.[151]

Tert-butyl N-(2-bromoethyl)carbamate 60

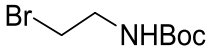

60

Di-tert-butyl dicarbonate (2.18 g, 10.0 mmol, 1.0 equiv.) dissolved in dichloromethane (130 mL) was cooled to 0 °C. 2-Bromoethylamine hydrobromide (2.27 g, 11.1 mmol, 1.1 equiv.) was added followed by the dropwise addition of triethylamine (1.52 g, 2.1 mL, 15.0 mmol, 1.5 equiv.). The mixture was stirred at room temperature overnight. The mixture was sequentially washed with saturated aqueous ammonium chloride (2 × 30 mL), saturated aqueous sodium bicarbonate (2 × 30 mL) and brine (2 × 30 mL). The organic layer was dried over anhydrous

sodium thiosulfate, filtered and concentrated under reduced pressure. The residue was purified by flash column chromatography over silica eluting with 2:8 ethyl acetate/petroleum ether. Compound **00** (1.61 g, 73 %) colour less oil: R_F = 0.51 (2:3 EtOAc/pet. ether); **^{1}H NMR** (400 MHz, $CDCl_3$) 1.47 (s, 9H), 3.42-3.59 (m, 4H), 4.99 (br, 1H); **^{13}C NMR** (101 MHz, $CDCl_3$); 28.3 (s), 32.9 (s), 42.3 (s), 79.8 (s), 155.6 (s).

The characterization data is similar to the literature.[163]

[1-(2-aminoethyl)-1H-pyrazol-4-yl]phosphonic acid 61

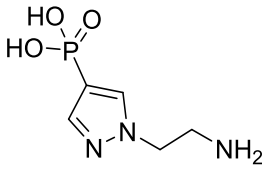

61

Diethyl 1H-pyrazol-4-ylphosphonate **59** (0.500 g, 2.45 mmol, 1.0 equiv.) tert-butyl N-(2-bromoethyl)carbamate **60** (0.75 g, 3.35 mmol, 1.4 equiv.) caesium carbonate (2.73 g, 8.37 mmol, 3.5 equiv.) and acetonitrile (9.6 mL) were stirred under nitrogen at room temperature for 6 hour. The mixture was diluted with ethyl acetate (50 mL) and the precipitate was filtered of through a silica plug (1 cm × 2 cm) which was washed with ethyl acetate (200 mL). The filtrate was concentrated under reduced pressure. The residue was dissolved in acetonitrile under nitrogen (24 mL). Bromotrimethylsilane (3.66 g, 3.2 mL, 23.9 mmol, 10 equiv.) was added and the mixture was stirred at 50 °C, overnight. After cooling cooling to room temperature the mixture was concentrated under reduced pressure. The residue was triturated in isopropanol (15 mL), added to a centrifuge vile and centrifuged (3220 relative centrifugal force, 4 °C, 5 minutes). The supernatant was discarded and the solid was loaded

on to a pre-equilibrated (8:2 ethanol/water) flash chromatography silica gel column. The column was eluted with an 80:18:2 to 65:22:8; ethanol/water/32 % (wt/wt) aqueous ammonia gradient. The combined product fractions were concentrated under reduced pressure and then lyophilized. The remaining residue was dissolved in water (2.5 mL) and an aliquot was diluted in deuterated water for quantification by ^{1}H NMR using 1,4-dioxane as the internal standard. Compound **61** (0.025 g, 5 %): R_F = 0.47 (65:22:8 EtOH/H_2O/32 % (wt/wt) NH_3 (aq.)); **^{1}H NMR** (400 MHz, D_2O) 3.40 (t, *J* = 5.5 Hz, 2H), 4.40 (t, *J* = 5.5 Hz, 2H), 7.62 (m, 1H), 7.72 (d, *J* = 2.5 Hz, 1 H); **^{13}C NMR** (101 MHz, D_2O) 39.3 (s), 48.3 (s), 117.5 (d, *J* = 197.0 Hz), 134.3 (d, *J* = 20.5 Hz), 142.6 (d, *J* = 13.0 Hz); **^{31}P NMR** (162 MHz, D_2O) 5.72; **m/z** (ESI+): 192.1000 (MH+, 100 % $C_5H_{11}N_3O_3P$ requires 192.0500).

The characterization data is similar to the literature.[111]

Diethyl 1-butylpyrazol-4-ylphosphonate 144

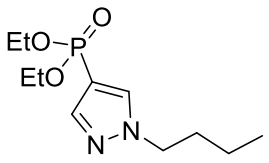

144

Diethyl 1H-pyrazol-4-ylphosphonate **59** (1.83 g, 9.0 mmol, 1.0 equiv.), 1-bromobutane (1.72 g, 1.35 mL, 12.6 mmol, 1.4 equiv.), cesium carbonate (10.2 g, 31.3 mmol, 3.5 equiv.) and acetonitrile (35 mL) were stirred under nitrogen at room temperature for 6 hours. The precipitate was filtered off and washed with ethyl acetate (2 × 50 mL). The filtrate was concentrated under reduced pressure. The residue was diluted with ethyl acetate (100 mL) and washed with saturated aqueous ammonium chloride (100 mL). The aqueous phase was

extracted with ethyl acetate (2 × 200 mL) and the combined organic phases were washed with brine (200 mL), dried over magnesium sulfate, filtered and concentrated under reduced pressure. Compound **144**, (1.76 g, 75 %) pale yellow oil; ν_{max}(ATR)/**cm**$^{-1}$ 3480, 3104, 2964, 2937, 2879, 1525, 1244, 1136, 1061, 1025; **^{1}H NMR** (400 MHz, $CDCl_3$) 0.91 (t, *J* = 7.5 Hz, 3H), 1.24-1.35 (m, 8H), 1.84 (quint., *J* = 7.5 Hz, 2H), 4.00-4.16 (m, 6H), 7.69 (s, 1H), 7.73 (d, *J* = 2.0 Hz, 1H); **^{13}C NMR** (101 MHz, $CDCl_3$) 13.5 (s), 16.3 (d, *J* = 6.5 Hz), 19.7 (s), 32.0 (s), 52.2 (s), 61.9 (d, *J* = 5.5 Hz), 107.3 (d, *J* = 221.0 Hz), 134.4 (d, *J* =23.5 Hz), 142.0 (d, *J* = 13.0 Hz); **^{31}P NMR** (162 MHz, $CDCl_3$) 14.95 (s); **m/z** (ESI+): 261.1366 (MH+, 100 % $C_{11}H_{22}N_2O_3P$ requires 261.1400).

1-butylpyrazol-4-ylphosphonic acid 140

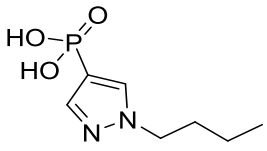

140

Diethyl 1-butylpyrazol-4-ylphosphonate **144** (1.63 g, 6.3 mmol, 1.0 equiv.), was dissolved in acetonitrile (63 mL) under nitrogen. Bromotrimethylsilane (9.65 g, 8.3 mL, 63 mmol, 10.0 equiv.) was added and the mixture was stirred at 50 °C overnight. After cooling to room temperature the mixture was concentrated under reduced pressure. The residue was purified by flash chromatography over silica eluting with a mixture of 75:4:10; ethanol/water/32 % (wt/wt) aqueous ammonia. The combined product fractions were concentrated under reduced pressure and then lyophilized. Compound **140** (1.00 g, 78 %) white solid: R_F = 0.51 (65:22:8, EtOH/H_2O/32 % (wt/wt) NH_3 (aq.)); m.p.= 135-137 °C; ν_{max}(ATR)/**cm**$^{-1}$ 3519, 3363, 2957, 2865, 1527, 1452, 1370, 1136, 1112, 1068, 1032; **^{1}H NMR** (400 MHz, D_2O) 0.72 (t, *J* =

7.5 Hz, 3H), 1.08 (sex., *J* = 7.5 Hz, 2H), 1.64 (quint., *J* = 7.0 Hz, 2H), 4.01 (t, *J* = 7.0 Hz, 2H), 7.51 (s, 1H), 7.65 (d, *J* = 2.5 Hz, 1H); **^{13}C NMR** (101 MHz, D_2O) 12.7 (s), 18.9 (s), 31.5 (s), 51.3 (s), 114.1 (d, *J* = 204.0 Hz), 133.8 (d, *J* = 21.5 Hz), 141.1 (d, *J* = 13.5 Hz); **^{31}P NMR** (162 MHz, D_2O) 7.22; **m/z** (ESI-): 203.0596 (M-H-, 100 % $C_7H_{12}N_2O_3P$ requires 203.0600).

Diethyl 4-methylpyridin-3-ylphosphonate 146

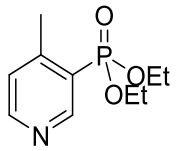

146

Palladium(II) acetate (0.269 g, 1.2 mmol, 0.1 equiv.), and triphenylphosphine (0.944 g, 3.6 mmol, 0.3 equiv.), were added to a round bottom flask equipped with a condenser. A vacuum was applied followed by a positive pressure of nitrogen (× 3). Ethanol (44 mL) followed by triethylamine (1.82 g, 2.51 mL, 18 mmol, 1.5 equiv.), diethyl phosphite (2.49 g, 2.32 mL, 18 mmol, 1.5 equiv.) and 3-bromo-4-methylpyridine (2.06 g, 1.33 mL, 12 mmol, 1.0 equiv.) were added and stirred at reflux for 48 hours. The mixture was concentrated under reduced pressure and the residue was purified by flash column chromatography over silica, eluting with ethyl acetate. Compound **146** (1.93 g, 70 % yield) yellow oil: R_F = 0.16 (EtOAc); **ν_{max}**(thin film)/**cm^{-1}** 3532, 2982, 2932, 2908, 1587, 1444, 1399, 1254, 1227, 1133, 1047, 1022; **^{1}H NMR** (400 MHz, $CDCl_3$) 1.34 (t, *J* = 7.0 Hz, 6H), 2.58 (s, 3H), 4.08-4.25 (m, 4H), 7.18 (t, *J* = 5.0 Hz, 1H), 8.59 (dd, *J* = 2.0, 5.0 Hz, 1H), 8.95 (d, *J* = 7.5 Hz, 1H); **^{13}C NMR** (101 MHz, $CDCl_3$) 16.3 (d, *J* = 6.0 Hz), 20.9 (d, *J* = 3.5 Hz), 62.3 (d, *J* = 5.5 Hz), 123.8 (d, *J* = 185.5 Hz), 125.9 (d, *J* = 11.5 Hz), 151.3 (d, *J* = 8.5 Hz), 152.9, 153.5 (d, *J* = 13.0 Hz); **^{31}P NMR** (162 MHz, $CDCl_3$) 16.37; **m/z** (ESI+): 230.1000 (MH+, 100 % $C_{10}H_{17}N_3P$ requires 230.0900).

4-methylpyridin-3-ylphosphonic acid 141

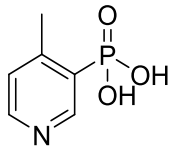

141

Diethyl 4-methylpyridin-3-ylphosphonate **146** (1.73 g, 7.54 mmol, 1.0 equiv.), was dissolved in acetonitrile (76 mL) under nitrogen. Bromotrimethylsilane (11.6 g, 10 mL, 10.0 mmol, 10.0 equiv.) was added and the mixture was stirred at 50 ^{o}C overnight. The solvent was removed under reduced pressure. The residue was purified by flash chromatography over silica eluting with a mixture of 70:4:10; ethanol/water/32 % (wt/wt) aqueous ammonia. The combined product fractions were concentrated under reduced pressure and then lyophilized. Compound **141** (1.15 g, 88 %) white solid: R_F = 0.09 (70:4:10, EtOH/H_2O/32 % (wt/wt) NH_3 (aq.); m.p. = 175-200 °C; $\boldsymbol{\nu_{max}}$(thin film)/**cm^{-1}** 2815, 2184, 1588, 1467, 1438, 1400, 1129, 1040; **^{1}H NMR** (400 MHz, D_2O) 2.60 (s, 3H), 7.46 (dd, *J* = 3.5, 5.5 Hz, 1H), 8.31 (dd, *J* = 1.0, 5.5 Hz, 1H), 8.60 (d, *J* = 7.5 Hz, 1H); **^{13}C NMR** (101 MHz, D_2O) 21.6 (d, *J* = 3.0 Hz), 127.5 (d, *J* = 9.5 Hz), 136.5 (d, *J* = 162.5 Hz), 143.4, 145.0 (d, *J* = 13.0 Hz), 158.4 (d, *J* = 7.0 Hz); **^{31}P NMR** (162 MHz, D_2O) 4.31; **m/z** (ESI-): 172.0170 (M-H-, 100 % $C_6H_7NO_3P$ requires 173.0200).

Amino(potassiooxy)phosphinic acid (Potassium phosphoramidate) 1

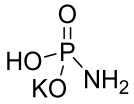

1

Ultra-pure water (100 mL), and 32 % (wt/wt) aqueous ammonia (50 mL) were cooled to 0 °C. Phosphorus(V) oxychloride (15.1 g, 9.2 mL, 98.5 mmol, 1.0 equiv.) cooled to 0 °C was added dropwise over 25 minutes to this mixture; effervescent was observed. The solution was stirred for a further 15 minutes. Acetone (500 mL) was added and the mixture was vigorously stirred for 5 minutes. The aqueous layer was partitioned and acidified with acetic acid to pH 6, a precipitate was observed. The mixture was kept at -20 °C for 60 minutes. The precipitate was filtered of and washed sequentially with ethanol (20 mL) and diethyl ether (20 mL). The air dried crystals were added in small portions to 50 % (wt/v) aqueous potassium hydroxide (23 mL), and then heated to 60 °C for 20 minutes. The mixture was allowed to cool to room temperature and then acidified with acetic acid to pH 6; a precipitate was observed. The suspension was poured into ethanol (1150 mL) and left to stand at room temperature for 60 minutes. The precipitate was collected on a sintered funnel, washed sequentially, with ethanol (2 × 30 mL) and then diethyl ether (2 × 30 mL) and dried under reduced pressure. Compound **1** (6.21 g, 47 %) white powder: m.p. = > 350 °C; $\boldsymbol{\nu_{max}}$(thin film)/**cm**$^{-1}$ 2849, 2473, 2175, 1614, 1462, 1413, 1150, 1073; ^{31}**P NMR** (162 MHz, D_2O) -3.33.

The characterization data are similar to the literature.[80]

2-amino-3-(3-phosphonoimidazol-4-yl)propanoic acid (π-pHis)

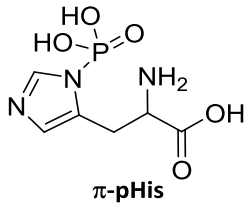

π-pHis

L-Histidine (0.251 g, 1.62 mmol, 1.0 equiv.), potassium phosphoramidate **1** and ultra pure water (4.5 mL) were stirred at 25 ° C for 40 minutes. The following chromatography procedure was carried out at 4 °C and 0.68 atmospheres as the solvent pressure. The sample was loaded on to a pre-equilibrated (85:4:1 ethanol/32 % (wt/wt) aqueous ammonia/water) silica gel column (4 cm diameter column with 27 cm of silica) and eluted with an ethanol, 32 % (wt/wt) aqueous ammonia and water gradient (Initially 300 mL of an 85:4:1 mixture was added, once 150 mL was eluted off, 150 mL of a 75:4:10 mixture was added. After a further 150 mL was eluted off and an additional 150 mL of this solvent was added. Subsequently the same cycle was repeated with a solvent mixture of 70:4:15, (300 mL), and 60:4:25, (300 mL) until the compound was eluted off). The first 750 mL was run off and 15 mL fractions were collected. The product fractions were collected such that 5 fractions between the product and the first co-eluted π- and τ-pHis mixture were discarded as analysed by TLC analysis. The combined product fractions were concentrated by rotary evaporation at 25 °C to approximately 4 mL whilst maintaining a pH between 10-12 using 2 molar aqueous sodium hydroxide and 1 molar aqueous hydrochloric acid. The remaining solution was aliquoted and snap frozen and stored at -80 °C. The concentration of τ-pHis was determined to be 2.2 mg/mL by ^{1}H NMR using 1,4-dioxane (0.001 g,1 µL, 0.012 mmol) as the standard. π-pHis (0.0084 g, 2 % yield): R_F = 0.44 (65:8:22 EtOH/32 % (wt/wt) NH_3 (aq.)/H_2O); **^{1}H NMR** (400 MHz, D_2O adjusted to ~pH 12 with 10 M KOH (aq.)) 2.96 (dd, *J* = 8.0, 15.5 Hz, 1H), 3.19 (dd, *J* = 5.0, 15.5 Hz, 1H), 3.84-3.90 (m,

1H), 6.72 (s, 1H), 7.73 (s, 1H); **^{13}C NMR** (101 MHz, D_2O adjusted to pH ~12 with 10 M NaOH (aq.)) 30.6 (s), 55.3 (s), 126.2 (d, *J* = 8.0 Hz), 130.4 (d, *J* = 3.5 Hz), 140.4 (d, *J* = 5.0 Hz), 181.9 (s); **^{31}P NMR** (162 MHz, D_2O adjusted to pH ~12 with 10 M KOH (aq.)) - 5.55; **m/z** (ESI+): 236.0431 (MH+, 100 % $C_6H_{11}N_3O_5P$ requires 236.0400).

The characterization data are similar to the literature.[153]

2-amino-3-(1-phosphonoimidazol-4-yl)propanoic acid (τ-pHis)

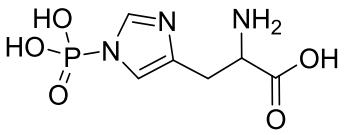

τ-pHis

L-Histidine (0.251 g, 1.62 mmol, 1.0 equiv.), potassium phosphoramidate **1** and ultra-pure water (4.5 mL) were stirred at 25 ° C for 16 hours. The following flash chromatography procedure was carried out at 4 °C and 0.68 atmospheres. The sample was loaded on to a pre-equilibrated (85:4:1 ethanol/32 % (wt/wt) aqueous ammonia/water) silica gel column (4 cm diameter column with 27 cm of silica) and with a mixture of ethanol, 32 % (wt/wt) aqueous ammonia and water gradient (Initially 300 mL of an 85:4:1 mixture was added, once 150 mL was eluted off, 150 mL of a 75:4:10 mixture was added. After a further 150 mL was eluted off an additional 150 mL of this solvent was added. Subsequently the same cycle was repeated with solvent mixture ratio of 70:4:15 (300 mL), and 60:4:25, (300 mL) in total until the compound was eluted off). The first 750 mL was run off and 15 mL fractions were collected. The product fractions were collected such that 5 fractions between the product and the first co-eluted π- and τ-pHis mixture were discarded as analysed by TLC analysis. The combined

product fractions were concentrated by rotary evaporation at 25 °C to approximately 8 mL whilst maintaining a pH between 10-12 using 2 molar aqueous sodium hydroxide and 1 molar aqueous hydrochloric acid. The remaining solution was aliquoted and snap frozen and stored at -80 °C. The concentration of τ-pHis was determined to be 4.9 mg/mL by ^{1}H NMR against 1,4-dioxane as the standard. τ-pHis (0.103 g, 27 % yield): R_F = 0.40 (65:8:22 EtOH/32 % (wt/wt) NH_3 (aq.)/H_2O); **^{1}H NMR** (400 MHz, D_2O adjusted to pH ~12 with 10 M KOH (aq.)) 2.53 (dd, *J* = 9.0, 14.5 Hz, 1H), 2.79 (dd, *J* = 4.5, 14.5 Hz, 1H), 3.32-3.3.38 (m, 1H), 6.86 (s, 1H), 7.56 (s, 1H); **^{13}C NMR** (101 MHz, D_2O adjusted to pH ~12 with 10 M NaOH (aq.)) 32.6 (s), 56.0 (s), 117.8 (d, *J* = 5.5 Hz), 137.0 (d, *J* = 8.5 Hz), 139.0 (d, *J* = 5.0 Hz), 181.2 (s); **^{31}P NMR** (162 MHz, D_2O adjusted to pH ~12 with 10 M KOH (aq.)) - 4.78; **m/z** (ESI+): 236.0431 (MH+, 100 % $C_6H_{11}N_3O_5P$ requires 236.0400).

The characterization data are similar to the literature.[153]

5.2: Biology Experimental

All reagents used were purchased from Fluorochem, MilliporeSigma, Alpha Aeser, VWR International, Thermo Scientific. Ultrapure water was used to make buffers and solutions unless stated otherwise. All solvents were of HPLC grade. Blue pre-stained protein standard, broad Range (11-190 kDa) was purchased from New England BioLabs. Sartorius Vivaspin 6/20's (3 and 10 kDa MWCO) were used for dialysis and protein concentration. Thermo Scientific Snakeskin dialysis tubing, 16 mm dry diameter (3.5 Da MWCO) was purchased from. NHS-Activated Sepharose 4 Fast Flow was purchased from GE health care life sciences. Sigma Protein G Sepharose®, Fast Flow recombinant, expressed in *E. coli*, 20 % (v/v) ethanol

suspension was used for immunoprecipitation experiments. Dako rabbit anti-goat immunoglobulins/ horseradish peroxidase was used as the secondary antibody. Dako mouse anti-rabbit immunoglobulins/ horseradish peroxidase was used as the secondary antibody. pHis monoclonal antibodies SC56-2 (0.26 mg/mL), SC50-3 (0.12 mg/mL), SC1-1 (0.15 mg/mL) were purchased from Millipore. Sigma Aldrich Hemocyanin from *Megathura crenulata* (keyhole limpet) PBS was used. Sigma Aldrich (BS3 linker) phosphotyrosine-BSA, phosphoserine-BSA, and phosphothreonine-BSA solution was used. Sigma Trypsin-EDTA solution (1 ×, sterile; sterile-filtered, BioReagent, suitable for cell culture, 0.5 g porcine trypsin and 0.2 g EDTA • 4Na per liter of Hanks' Balanced Salt Solution with phenol red) was used to trypsinize adhered HBE cells. SigmaAldrich Medium 199 with Earle's salts and sodium bicarbonate, without L-glutamine, liquid, sterile-filtered, suitable for cell culture was used. Gibco fetal bovine serum (FBS) was used to supplement medium 199. Human bronchial epithelial cell line between passage 46 and 53 was used. Corning® 96 Well EIA/RIA clear flat bottom polystyrene high bind microplate was used for ELISA assays. Easy flask 75 filt nunclon D si from Thermo Scientific were used as cell culture flasks. Pierce™ BCA protein assay kit was used to quantify proteins. Thermo Scientific SuperSignal™ West Pico PLUS chemiluminescent substrate was used to develop blotted membranes. ULTRA PURE AccuGel™ 29:1, 30 (w/v) 29:1 acrylamide: bis-acrylamide solution (gas stabilised) was used to make SDS-PAGE gels. Interchim TMB ELISA substrate standard solution was used to develop ELISA plates. Colloidal Gold Total Protein Stain purchased from Bio-Rad was used to stain electroblotted proteins. Western blotted membranes were visualised using a BIO-RAD ChemiDoc™ XRS+ with image Lab™ software. Absorbance was measured using a Varioskan flash spectrometer. ^{31}P spectra were acquired using a Bruker AVANCE III or AVANCE III HD spectrometer, operating at 162MHz or 202.5MHz respectively. Quantitative spectra were typically acquired using a 30

degree excitation pulse and a relaxation delay of 8s, which was determined as sufficiently long to enable full relaxation on one sample with internal standard early on in the study. Internal standard: 2 mM triphenylphosphine oxide, 20 mM chromium(III) acetylacetonate, in 150 µL of deuterated chloroform. Norell(tm) high throughput 3mm NMR sampling tubes length: 203 mm; inner diameter: 2.41 mm was used as the internal standard capillary. Norell® Standard Series™ 5 mm NMR tubes length, 7 inches; inner diameter: 4.2 mm was used. All other samples were assumed to have similar T1 relaxation profiles. Transients acquired typically ranged between 6k and 9k to obtain enough signal-to-noise in most cases. The concentration of the protein sample for ^{31}P NMR varied and required trial and error, proteins concentration between 20-40 mg/mL usually worked well. Acquisition windows ranged between 6.9KHz and 20kHz, using 32k acquisition points. Orygen Antibodies LTD immunized sheep with KLH immunogens (**149**-**153**) and supplied the post immune sheep antisera.

Conjugation of amino acids to BSA via glutaraldehyde

Coupling buffer: 0.1 M Na_2CO_3, 0.15 M NaCl, pH 8.5

Dialysis buffer: PBS, pH 7.4 or 0.1 M Na_2CO_3/$NaHCO_3$, pH 10.8 (for pHis conjugates)

Bovine serum albumin (50 mg, 0.0007 mmol, 1.0 equiv.) was added to a centrifuge tube (50 mL) and dissolved in coupling buffer (20 mL). The mixture was cooled on ice. The amino acid (0.03 mmol, 40 equiv.) was added followed by 50 wt. % (aq.) fresh glutaraldehyde solution (0.5 mL) so that the final concentration was 1 % (v/v). The solution was topped up with ice cold coupling buffer to 25 mL. The tube was sealed and left on the rotor at 4 °C for 3.5 hours. 1% (wt/v) sodium borohydride (0.25 g) was added to the mixture, and a small hole was

pierced in the lid before centrifugation (4 °C, 3220 RCF, 60 min). For rapid dialysis (especially for pHis conjugates; otherwise SnakeSkin dialysis tubing could be used (3 k MWCO)), the mixture was concentrated down to 2 mL using a Vivaspin 20 (10 kDa MWCO) by centrifugation (4 °C, 3220 RCF). The solution was diluted with ice cold dialysis buffer to 10 mL and concentrated down again to 2 mL (the solution was aspirated every 10 min). This cycle was repeated two more times. After a final concentration to approximately 1 mL, the sample was aliquoted, snap frozen and stored at -80 °C. The protein concentration was determined by bicinchoninic acid assay or NanoDrop with absorbance at 280 nm, 1 cm path length, BSA = 66.463 kDa and $\varepsilon = 43.824\ M^{-1}\ cm^{-1}$.

Conjugation of amino acids to KLH via glutaraldehyde for immunisation

Coupling buffer: 0.1 M Na_2CO_3, 0.15 M NaCl, pH 8.5

Dialysis buffer: PBS, pH 7.4.

Keyhole limpet hemocyanin (10 mg, 0.002 µM, 1.9 mL, 1.0 equiv.) in PBS solution was added to a centrifuge tube (15 mL) containing coupling buffer (3 mL) and the mixture was cooled on ice. The analogue (0.004 mmol, 2000 equiv.) was added followed by 50 wt. % (aq.) fresh glutaraldehyde solution (0.1 mL) so that the final concentration was 1 % (v/v). The tube was sealed and left on the rotor at 4 °C for 4 hours. 1% (wt/v) sodium borohydride (0.05 g) was added to the mixture, and a small hole was pierced in the lid before centrifugation (4 °C, 3220 RCF, 1.5 h.). The mixture was transferred to a Vivaspin 6 (10 kDa MWCO) concentrated down to 1 mL by centrifugation (4 °C, 3220 RCF). The solution was diluted with ice cold dialysis buffer to 2 mL and concentrated down again to 1 mL (the solution was aspirated every 10

min). This cycle was repeated four more times. The protein concentration was determined by NanoDrop with absorbance at 280 nm, 1 cm path length, and $\varepsilon_{1\%}$ = 15.7 M^{-1} cm^{-1}. The final KLH concentration was made up to 2 mg/mL using dialysis buffer and then aliquoted, snap frozen and stored at -80 °C before being shipped on dryice to Orygen Antibodies LTD.

Coupling of BSA-G-amino acid conjugates to NHS-Activated Sepharose 4 Fast Flow

Sepharose BSA-G-amino conjugate resins were synthesized following the manufacturer's instructions with modifications.

Wash solution: 1 mM HCl (aq.)

Coupling buffer: 0.2 M $NaHCO_3$, 0.5 M NaCl, pH 8.3.

Protein coupling solution: 3 mg/mL BSA-G-amino acid, 0.5 M NaCl, 0.2 M $NaHCO_3$, pH 8.3.

Fresh NHS activated sepharose 4 fast flow resin suspension was added to a column with a sintered frit and drained. The resin was washed with ice cold wash solution (3 × resin bed volume) and then with ice cold coupling buffer (2 × resin bed volume). The resin was suspended in protein coupling solution (1/2 × resin bed volume), transferred to a centrifuge vile and mixed end over end at room temperature for 1 hour. A second equivalent of protein coupling buffer solution was added, and the mixture was turned end over end for another 1 hour. The suspension was transferred back to the column. The solution was drained off and

the resin was washed with coupling buffer (3 × resin bed volume). When the resin was not immediately used it was stored in coupling buffer at 4 °C and used within 24 hours.

Dot blots

Wash buffer: 165 mM NaCl, 0.05 % (v/v) Tween 20, 10 mM Tris-HCl, pH 8.0.

Blocking buffer: 0.2 % (v/v) gelatin from cold water fish skin, 165 mM NaCl, 0.05 % (v/v) Tween 20, 10 mM Tris-HCl, pH 8.0.

BSA amino acid conjugates (1 µg; for equal phosphorus loadings, 0.7 µg BSA-G-pTyr, 0.9 µg BSA-G-π-pHis, 7.5 µg and BSA-G-τ-pHis was used) were blotted on to a polyvinylidene difluoride membrane and left to dry in the fume hood. The membrane was activated in methanol and blocked with 75 mL blocking buffer at room temperature for 1 hour. The following steps were carried out a room temp using an orbital shaker: 75 mL blocking buffer was added over the membrane in a tray (~10 cm × 14 cm) and left for 1 hour. The solution was discarded and pHis antiserum diluted 1/200 (v/v) in 10 mL blocking buffer, was added and left for 1 hour. The solution was discarded, and the membrane was washed with 50 mL wash buffer (6 × 5 min). Rabbit anti-goat IgG-HRP conjugate (1/2000) diluted in 10 mL blocking buffer was added over the membrane and left for 1 hour. The membrane was washed with 50 mL wash buffer (6 × 5 min), and incubated in chemiluminescence solution for 1 min. After draining of the excess chemiluminescence, the membrane was imaged using ChemiDoc XRS.

Crude antiserum serial dilution sandwich ELISA

Coating buffer: 0.1 M Na_2CO_3/$NaHCO_3$, pH 10.8.

Wash buffer: 0.05 % (v/v) Tween 20, PBS, pH 7.4.

Blocking buffer: 0.05 % (v/v) Tween 20, 0.2 % (w/v) gelatin, PBS, pH 7.4.

60 µL of blocking buffer was added to each well of a coaster 96 well plate (labelled plate one) except for the top row. 120 µL of sheep antiserum (1:50 (v/v) dilution blocking buffer) was added in duplicate to the top wells. 60 µL from the well was drawn and serially diluted (Figure 72). 60 µL of blocking buffer was added to each well. The plate was wrapped in foil and stored at 4 °C overnight. To a separate 96 well ELISA plate (labelled plate 2) 100 µL of BSA-G-τ-pHis or BSA-G-π-pHis (20 µg/mL) conjugate verified by ^{31}P NMR was diluted in coating buffer was added to each well. The plate was wrapped in foil and left at 4 °C overnight. The wells of plate two were emptied and washed with wash buffer (× 3). The wells were incubated with 150 µL of blocking buffer, wrapped in foil and left at 37 °C for 2 hours. The wells were emptied and washed with wash buffer (× 3). 100 µL from each well of plate one was added to the corresponding wells of plate two. The plate was wrapped in foil and left at 37 °C for 1.5 hours. The wells were emptied and washed with wash buffer (× 3). 100 µL of rabbit anti-goat IgG-HRP conjugate diluted 1/200 (v/v) in blocking buffer was added to each well, and the plate was wrapped in foil and left at 37°C for 1 hour. The wells were emptied and washed with wash buffer (× 3) and finally with distilled water. 50 µL of 3,3',5,5'-tetramethylbenzidine ELISA substrate was added to each well and incubated at room temperature between 0.5-5 min (until pale blue coloured solution was observed). 50 µL of 2 molar sulphuric acid was added to each well to quench the reaction. The absorbance was measured immediately at 450 nm.

	Pre-immune				Bleed 1			
A	1:100		1:25600		1:100		1:25600	
B	1:200		1:51200		1:200		1:51200	
C	1:400		1:102400		1:400		1:102400	
D	1:800		1:204800		1:800		1:204800	
E	1:1600		1:409600		1:1600-		1:409600	
F	1:3200		1:819200		1:3200		1:819200	
G	1:6400		1:1638400		1:6400		1:1638400	
H	1:12800		1:3276800		1:12800		1:3276800	
	1	**2**	**3**	**4**	**5**	**6**	**7**	**8**

	Bleed 3				Bleed 4			
A	1:100		1:25600		1:100		1:25600	
B	1:200		1:51200		1:200		1:51200	
C	1:400		1:102400		1:400		1:102400	
D	1:800		1:204800		1:800		1:204800	
E	1:1600		1:409600		1:1600		1:409600	
F	1:3200		1:819200		1:3200		1:819200	
G	1:6400		1:1638400		1:6400		1:1638400	
H	1:12800		1:3276800		1:12800		1:3276800	
	1	**2**	**3**	**4**	**5**	**6**	**7**	**8**

Figure 72: Serial dilution of sheep antiserum, pre-immune, bleed1, bleed 2, and bleed 3 on two 96 well ELISA plates. Note not all the wells are drawn here, columns 9-12 have been left out.

Sandwich ELISA

Coating buffer: 0.1 M Na_2CO_3/$NaHCO_3$, pH 10.8

Wash buffer: 0.05 % (v/v) Tween 20, PBS, pH 7.4.

Blocking buffer: 0.05 % (v/v) Tween 20, 0.2 % (w/v) gelatin, PBS, pH 7.4.

A solution of BSA-G-amino acid was diluted in coating buffer (1 µg/mL; for equal phosphorus loadings of 0.5 µg/mL BSA-G-pTyr, 0.7 µg/mL BSA-G-π-pHis, 4.4 µg/mL and BSA-G-τ-pHis was used). 100 µL of each sample was added to a 96 well ELISA plate, wrapped in foil and left at 4 °C overnight. The wells were emptied and washed with wash buffer (× 3). The wells were incubated with 150 µL of blocking buffer, wrapped in foil and left at 37 °C for 2 hours. The wells were emptied and washed with wash buffer (× 3). 100 µL of primary antibody diluted in blocking buffer (Table 7) was added to the wells. The plate was wrapped in foil and left at 37 °C for 1.5 hours. The wells were emptied and washed with wash buffer (x 3). 100 µL of rabbit anti-goat IgG-HRP conjugate diluted 1/2000 (v/v) in blocking buffer was added to each well, and the plate was wrapped in foil and left at 37 °C for 1 hour. The wells are emptied and washed with washed buffer (× 3) and finally with distilled water. 50 µL of 3,3',5,5'-tetramethylbenzidine ELISA substrate was added to each well and incubated at room temperature between 0.5-5 minutes (blue coloured solution). 50 µL of 2 molar sulphuric acid was added to well and the absorbance was measured immediately at 450 nm.

Table 7: Dilution of antiserum fractions.

Fraction	Dilution
Input (IN)	1/200
Flow through (FT)	1/100
Wash (W)	1/40
Elution (E)	1/20

Large scale sheep antiserum purification general procedure

Wash buffer: 25 mM Tris, 150 mM NaCl, pH 7.4.

Extraction buffer 1: 25 mM Tris, 150 mM NaCl, 200 µg/mL π-pHis, pH 7.4.

Extraction buffer 2: 25 mM Tris, 150 mM NaCl, 200 µg/mL τ-pHis, pH 7.4.

Extraction buffer 3: 0.1 M Gly, pH 2.0

Dialysis buffer: 25 mM Tris, 150 mM NaCl, 0.05 % (w/v) NaN_3, pH 7.4.

In a centrifuge vile the sheep antiserum was centrifuged (8960 RCF, 4 °C, 10 min) and the supernatant (half resin bed volume) was doubled in volume with 0.1 molar sodium chloride solution. The diluted sheep antiserum was poured over freshly prepared sepharose BSA-G-pTyr conjugate resin. The mixture was turned end over end at room temperature for 1 hour. The mixture was poured in to a column with a sintered frit and the flow through was collected. The resin was washed with wash buffer (6 × resin bed volume) and then extracted with

extraction buffer 1 (4 × double resin bed volume). The resin was washed with wash buffer (3 × resin bed volume) and then extracted with extraction buffer 2 (4 x double resin bed volume). The resin was then washed with wash buffer (2 × resin bed volume) and finally extracted with extraction buffer 3 (double resin bed volume) which was immediately neutralised with 1 molar Tris, pH 8.0 (1/10 volume of extraction buffer 3).

Large scale affinity depleted sheep antiserum S976D-B3: Affinity depleted sheep antiserum S976D-B3 fractions FT, W1-W2 were combined and further affinity depleted with sepharose conjugated to BSA-G-π-pHis (half the resin bed volume used in the first affinity depletion). The resin was washed with wash buffer (4 × resin bed volume). All pooled fractions were dialysed at 4^{o}C using SnakeSkin dialysis tubing (Table 8).

Table 8: S976D-B3 purified antibodies and concentrations, see Figure 51 and 52 pages 115-116. *Determined using NanoDrop 1000 Spectrophotometer with absorbance at 280 nm, 1 cm path length, and $\varepsilon_{1\%}$= 1.36.

Combined fractions	Antibody	Protein concentration (mg/mL)
FT2-W1’	1(τ)	10.8*
W2’-W4’	2(τ)	0.057*
W3-W6	3(τ)	0.192*
E1-E4 (π-pHis), W7-W9	4(τ)	0.12*
E1-E4 (τ-pHis), W7-W9	5(τ)	0.02*

Large scale affinity depleted sheep antiserum SA223-B3: Affinity depleted sheep antiserum S976D-B3 fraction FT was further affinity depleted with sepharose conjugated to BSA-G-τ-pHis (half the resin bed volume used in the first affinity depletion). The resin was washed with wash buffer (4 × resin bed volume) and then extracted with extraction buffer 1 (4 × resin bed volume). The resin was washed with wash buffer (2 × resin bed volume) and finally extracted with extraction buffer 3 (double resin bed volume). This extraction solution was immediately neutralised with 1 molar Tris, pH 8.0 (1/10 volume of eluent). All pooled fractions were dialysed at 4^{o}C using SnakeSkin dialysis tubing (Table 9).

Table 9: SA223-B3 purified antibodies and concentrations, see Figure 60 and 60 pages 130-131. *Determined using NanoDrop 1000 Spectrophotometer with absorbance at 280 nm, 1 cm path length, and $\varepsilon_{1\%}$= 1.36. (-) Protein concentration attempted with NanoDrop 1000 Spectrophotometer but the protein concentration to low.

Combined fractions	**Antibody**	**Protein concentration (mg/mL)**
FT2, W1'-W4'	1(π)	9.9*
E1-E4(π-pHis)	2(π)	-
W1-W4	3(π)	10.8*
W5-W6, E1-E4(τ-pHis)	4(π)	-

Small Scale: For small scale affinity purification of sheep antiserums, S976D-B3, SA220-B3, SA221-B3, SA222-B3, and SA223-B3 were affinity depleted as described above using a sepharose BSA-G-pTyr conjugate resin to but with no washes or elution. Subsequently the FT was immediately further affinity depleted with BSA-G-π-pHis or BSA-G-τ-pHis conjugated to sepharose. See Table 7 for dilutions.

Competitive ELISA

Coating buffer: 0.1 M Na_2CO_3/$NaHCO_3$, pH 10.8

Wash buffer: 0.05 % (v/v) Tween 20, PBS, pH 7.4.

Blocking buffer: 0.05 % (v/v) Tween 20, 0.2 % (w/v) gelatin, PBS, pH 7.4.

60 µL of blocking buffer was added to each well of a 96 well ELISA plate except for the top row. This plate was labelled plate one. 120 µL each amino acid (10 mM) was added in duplicate to the top wells. 60 µL from each top row well was drawn and serially diluted down the plate until the second last row (Figure 73). 60 µL of pHis antibody diluted (Table 10) in blocking buffer was added to each well. The plate was wrapped in foil and stored at 4 °C overnight. To a separate 96 well ELISA plate, labelled plate two; 100 µL of BSA-G-amino acid conjugate (20 µg/mL) diluted in coating buffer to each well. Plate two was wrapped in foil and left at 4 °C overnight. The wells of plate two were emptied and washed with wash buffer (× 3). The wells were incubated with 150 µL of blocking buffer, wrapped in foil and left at 37 °C for 2 hours. The wells were emptied and washed with wash buffer (× 3). 100 µL from each well of plate one was added to the corresponding wells of plate two. Plate two was wrapped in foil and left at 37 °C for 1.5 hours. The wells were emptied and washed with wash buffer (×

3). 100 µL of IgG-HRP conjugate diluted 1/2000 (v/v) in blocking buffer was added to each well. The plate was wrapped in foil and left at 37 °C for 1 hour. The wells were emptied and washed with

wash buffer (× 3) and finally with distilled water. 50 µL of 3,3',5,5'-tetramethylbenzidine ELISA substrate was added to each well and incubated at room temp. between 0.5-5 min until a blue coloured solution was observed. 50 µL of 2 molar sulphuric acid was added to quench

the reaction. The absorbance was measured immediately at 450 nm.

	His		pSer		pThr		pTyr		τ-pHis		π-pHis	
A	5 mM		5 mM		5 mM		5 mM		5 mM		5 mM	
B	2.5 mM		2.5 mM		2.5 mM		2.5 mM		2.5 mM		2.5 mM	
C	1.25 mM		1.25 mM		1.25 mM		1.25 mM		1.25 mM		1.25 mM	
D	0.625 mM		0.625 mM		0.625 mM		0.625 mM		0.625 mM		0.625 mM	
E	0.3125 mM		0.3125 mM		0.3125 mM		0.3125 mM		0.3125 mM		0.3125 mM	
F	0.15625 mM		0.15625 mM		0.15625 mM		0.15625 mM		0.15625 mM		0.15625 mM	
G	0.07812 mM		0.07812 mM		0.07812 mM		0.07812 mM		0.07812 mM		0.07812 mM	
H	0 mM		0 mM		0 mM		0 mM		0 mM		0 mM	
	1	**2**	**3**	**4**	**5**	**6**	**7**	**8**	**9**	**10**	**11**	**12**

Figure 73: Competitive ELISA plate serial dilution. The concentration given is the final concentration.

Table 10: pHis antibody dilution used for competitive ELISA.

Antibody	Competitive ELISA Dilution
1(τ)	1/18
2(τ)	1/4
3(τ)	1/8
4(τ)	1/12
5(τ)	1/8
1(π)	1/5
2(π)	1/5
3(π)	1/40
4(π)	1/50
SC56-2	1/500
SC50-3	1/1000
SC1-1	1/1000

Culturing Human Bronchial epithelial (HBE) cell line

Full serum medium: Medium 199 (including phenol red), supplemented with 10 % (v/v) FBS, 1.3 mM of L-glutamine, 80 μg/mL streptomycin, 80 units/mL penicillin.

Phosphate buffered saline (PBS): 1.8 mM KH_2PO_4, 10 mM Na_2HPO_4, 2.7 mM KCl, 137 mM NaCl, pH 7.4.

HBE cell line (between passage 49-60) was cultured in T75 flasks in full serum medium (12 mL) and incubated at 37 ^oC in a 5 % CO_2 atmosphere. The medium was changed every 2-3 days

by discarding the old medium, washing the cells with PBS (3 mL) and then adding full serum medium (12 mL). Once the HBE cells were between 70-90 % confluency they were split. The medium was discarded, and the cells were washed with PBS (3 mL). Cells were treated with porcine trypsin-EDTA solution (2 mL) and incubated at 37 ^{o}C in 5 % CO_2 atmosphere, for ~7 min. The cells were dislodged by tapping (a scrapper was also used if needed) and full serum medium (8 mL) was added. The cells were pelleted by centrifugation (room temp., 207 RCF, 5 minutes) and the supernatant was discarded. The cell pellet was suspended in full serum medium (12 mL), transferred to a T75 flash and incubated at 37 ^{o}C in 5 % CO_2 atmosphere.

Cell lysis

Phosphate buffered saline: 1.8 mM KH_2PO_4, 10 mM Na_2HPO_4, 2.7 mM KCl, 137 mM NaCl, pH 7.4.

Lysis buffers:

1. Modified radioimmunoprecipitation assay (RIPA) lysis buffer: 150 mM NaCl, 0.5 % (w/v) sodium deoxycholate, 1 % (w/v) Triton X-100, 0.1 % (w/v) SDS, 10 mM NaF, 5 mM Na_3VO_4, 10 mM $Na_4P_2O_7$, Roche complete protease inhibitor cocktail, 50 mM Tris, pH 9.0.
2. Denaturing lysis buffer: 6 M Urea, 30 mM octyl-β-D-glucopyranoside, Roche complete protease inhibitor cocktail, 0.1 M Na_2CO_3/$NaHCO_3$ pH 10.

The HBE cells were trypsinized as described in the cell culturing procedure up until pellet of the cells. The HBE cell pellet was suspended in phosphate buffered saline (1 mL), transferred

to a 1.5 mL centrifuge vile and centrifuged (4 ^{o}C, 90 RCF, 3 min). The supernatant was discarded the supernatant was discarded and this step was repeated two more times. The cells were cooled on ice and ice cold lysis buffer was added (350 µL for ~54 × 10^{6} cells or ~0.2 g cell pellet) and the cells were agitated with a pipette tip to assist lysis. When modified RIPA lysis buffer was used the lysate was left on ice for 10 minutes, and then centrifuged (4 ^{o}C, 8950 RCF, 3 min) and supernatant was used. When denaturing lysis buffer was used the lysate was sonicated on ice (45% amplitude 5 × 5 sec bursts, 59 sec rest between each burst).

Lysates were aliquoted, snap frozen using liquid nitrogen, and stored at -80 ^{o}C. Protein concentration was quantified by BSA assay (~10-15 mg/mL). For Western blot modified RIPA lusis buffer was used and denaturing buffer was used for immunoprecipitation experiments.

SDS-PAGE

Resolving gel: 12 % (v/v) acrylamide, 0.1 % (w/v) SDS, 0.1 % (w/v) ammonium persulphate, 0.001 % (v/v) tetramethylenediamine, 0.38 M Tris-HCl, pH 8.8.

Modified stacking gel: 4% (v/v) acrylamide, 0.1% (w/v) SDS, 0.1 % (w/v) ammonium persulphate, 0.001 % (v/v) tetramethylenediamine, 0.125 M Tris-HCl, pH 8.8.

Freshly prepared resolving gel solution was immediately poured between a 10 mm × 10 mm (1 mm spacers) and 10 mm × 10 mm (notched) glass plates. Isopropanol (~200 µL) was slowly added to the top. The gel was left to polymerise at room temperature for 30 minutes. The isopropanol was poured away, and the top of the gel was washed with water (× 3). Excess water was soaked up with a filter paper. Freshly prepared modified stacking gel solution was poured over the resolving gel to fill the cavity. A 10 well comb (~30 µL capacity per well) was

inserted and the gel was allowed to form at room temperature for two hours. Gels were used immediately or stored in plastic with a damp (running buffer) tissue for up to 3 days.

Coomassie gel staining

Fixer solution: 25 % (v/v) isopropanol (aq.), 10 % (v/v) acetic acid (aq.)

Coomassie blue stain solution: 0.1 % (w/v) Coomassie blue, 40 % (v/v) MeOH (aq.), 10% (v/v) acetic acid (aq.).

Destaining solution: 10 % (v/v) acetic acid (aq.)

The gel containing proteins were incubated with fixer solution at room temperature on an orbital shaker for 10 minutes. The fixer was discarded, and the gel was stained with Coomassie blue stain solution at room temperature. on an orbital shaker for 1 hour. Excess stain was discarded, and the stained gel was incubated in destaining solution at room temperature until minimal background stain remained. The destaining solution was changed several times.

Western blot

5× (concentrated) sample buffer: 10 % (w/v) LDS, 40 % (w/v) glycerol, 0.02 % (w/v) bromophenol blue, 50 mM EDTA, 500 mM DTT, 300 mM, Tris, pH 9.0. 1X sample buffer was made by diluting 5× sample buffer in water.

Resolving buffer: 0.1 % (w/v) SDS, 192 mM Gly, 25 mM Tris, pH 8.3.

Transfer buffer: 192 mM Gly, 25 mM Tris, pH 8.3.

Wash buffer: 165 mM NaCl, 0.05 % (v/v) Tween 20, 10 mM Tris-HCl, pH 8.0.

Blocking buffer: 0.2 % (v/v) gelatin from cold water fish skin, 165 mM NaCl, 0.05 % (v/v) Tween 20, 10 mM Tris-HCl, pH 8.0.

HBE cells lysates were treated with 5× sample buffer to give a 1× final concentration and then made up to 30 µL with 1× sample buffer. The samples were left at room temperature for 25 minutes. and then loaded on to SDS-PAGE gel. The samples were resolved using resolving buffer with the tank immersed in ice, at 120 V for the first 10 minutes and then 180 V for 50-60 minutes.

The resolved proteins were immediately electro blotted onto a methanol activated PVDF membrane using transfer buffer with the tank immersed in ice at 100 V for 1 hour. The following steps were carried out at room temperature using an orbital shaker: 75 mL blocking buffer was added over the membrane (~8 × 8 cm) in a covered tray (~10 cm × 14 cm) and left for 1 hour. The solution was discarded the pHis antibody diluted (Table 10) in 10 mL blocking buffer, was added and left for 1 hour. The solution was discarded, and the membrane was washed with 50 mL wash buffer (6 × 5 min). Secondary IgG-HRP conjugate (1/2000) diluted in 10 mL blocking buffer was added over the membrane and left for 1 hour. The membrane was washed with 50 mL wash buffer (6 × 5 min) and incubated in chemiluminescence solution for 1 minute. After draining of the excess chemiluminescence, the membrane was imaged using ChemiDoc XRS.

Table 11: Antibody dilution used in Western blots

Antibody	Western Blot Dilution
1(τ)	1/1000
2(τ)	1/100
3(τ)	1/300
4(τ)	1/200
5(τ)	1/100
1(π)	1/1000
2(π)	1/100
3(π)	1/500
4(π)	1/100
SC56-2	1/100
SC50-3	1/1000
SC1-1	1/1000

Colloidal gold stain

Wash buffer: 500 mM NaCl, 0.3% (v/v) Tween-20, 20 mM Tris pH 7.5.

The following steps were carried out at room temperature using an orbital shaker. The PVDF membrane with adhered proteins was washed with wash buffer (3 × 20 min) and then with water (3 × 2 min). The membrane was incubated in Colloidal Gold Total Protein stain for 1 hour or until protein were visible. The membrane was washed with water (3 × 1 min).

Immunoprecipitation of HBE cell lysate using purified pHis antibodies

Wash buffer 1: 165 mM NaCl, 10 mM Tris-HCl, pH 8.0.

Wash buffer 2: 165 mM NaCl, 0.05 % (v/v) Tween 20, 10 mM Tris-HCl, pH 8.0.

Wash buffer 3: 500 mM NaCl, pH 7.4, 0.3 % (v/v), Tween 20, 20 mM Tris-HCl pH 8.0.

Extraction buffer 1: 165 mM NaCl, 0.05 % (v/v) Tween 20, 40 mM competitor **140** or **141**, 10 mM Tris-HCl, pH 8.0.

Extraction buffer 2: 0.1 M Gly, pH 2.0

Centrifugation conditions: 1000 RCF, 2 mins, 4 °C.

Protein G sepharose slurry (~80 µL bed volume) was added to a 1.5 mL centrifuge vile and washed with wash buffer 1 (4 × 400 µL) (note: all washes herein were followed by centrifugation to pellet the resin and remove the supernatant). Wash buffer 1 (960 µL) and pHis antibody 1 (40 µL) was added to the resin. The vile was added to 50 mL centrifuge tube and left on the roller mixture at 4 °C for 2 hours. The suspension was centrifuged, and the supernatant was discarded. The resin wash washed with wash buffer 2 (3 × 1000 µL) and then suspended in wash buffer 2 (600 µL). The mixture was aspirated, partitioned equally, centrifuged and the supernatant was discarded. Freshly prepared HBE (0.42 mg) cell lysate, lysed in denaturing lysis buffer was diluted using wash buffer 2 to a final urea concentration of 0.5 molar and added to the resin. The vile was added to a 50 mL centrifuge tube and left on the roller mixture at 4 °C for 45 minutes. The resin was centrifuged, and the supernatant was removed and kept for later analysis. The resin was then washed with wash buffer 3 (4 × 1000 µL). The suspension was treated with extraction buffer 1 (80 µL) and left on a thermomixer (550 rpm) at room temperature for 15 minutes. The resin was pelleted and 60 µL of the supernatant was removed using loading tips. The extraction step was repeated three

more times. The resin was then washed with wash buffer 3 (2 × 1000 µL). The resin was then treated with extraction buffer 2 and left on the thermomixer (550 rpm) at room temperature for 15 minutes. The resin was pelleted, and the supernatant was immediately neutralised with 1 molar Tris, pH 8.0 (1/10 volume of extraction buffer 2). An aliquot of the fractions was analysed by Western blot and colloidal gold stain (Table 12)

Table 12: Volumes used from immunoprecipitation experiment samples for Western blot and colloidal gold staining

Sample	**Volume (µL)**
HBE cell lysate	5
Supernatant	5
Wash	25
Extraction	25
0.1 M Gly, pH 2.0	5
Beads	5

6: References

(1) Lilley, M. PhD Thesis, The University of Sheffield, 2013.

(2) Lad, C.; Williams, N. H.; Wolfenden, R. *Proc. Natl. Acad. Sci. U.S.A.* **2003**, *100*, 5607.

(3) Hunter, T. *Philos. Trans. R. Soc. Lond., Ser. B: Biol. Sci.* **2012**, *367*, 2513.

(4) Zetterqvist, O. *Biochim. Biophys. Acta* **1967**, *136*, 279.

(5) Zetterqvist, O. *Biochim. Biophys. Acta* **1967**, *141*, 540.

(6) Khorchid, A.; Ikura, M. *Int. J. Biochem. Cell Biol.* **2006**, *38*, 307.

(7) Santos, J. L.; Shiozaki, K. *Science's STKE* **2001**, *2001*, re1.

(8) Perry, J.; Koteva, K.; Wright, G. *Mol. Biosyst.* **2011**, *7*, 1388.

(9) Besant, P. G.; Attwood, P. V. *Biochim. Biophys. Acta: Proteins Proteomics* **2005**, *1754*, 281.

(10) Wadhams, G. H.; Armitage, J. P. *Nat. Rev. Mol. Cell Biol.* **2004**, *5*, 1024.

(11) Boissan, M.; Dabernat, S.; Peuchant, E.; Schlattner, U.; Lascu, I.; Lacombe, M.-L. *Mol. Cell. Biochem.* **2009**, *329*, 51.

(12) Muimo, R.; Alothaid, H. M. M.; Mehta, A. *Lab. Invest.* **2017**, *98*, 272.

(13) Desvignes, T.; Pontarotti, P.; Fauvel, C.; Bobe, J. *BMC Evol. Biol.* **2009**, *9*, 256.

(14) Wagner, P. D.; Vu, N. D. *J. Biol. Chem.* **1995**, *270*, 21758.

(15) Wagner, P. D.; Steeg, P. S.; Vu, N. D. *Proc. Natl. Acad. Sci. U.S.A.* **1997**, *94*, 9000.

(16) Freije, J. M. P.; Blay, P.; MacDonald, N. J.; Manrow, R. E.; Steeg, P. S. *J. Biol. Chem.* **1997**, *272*, 5525.

(17) Wagner, P. D.; Vu, N. D. *Biochem. J.* **2000**, *346*, 623.

(18) Hartsough, M. T.; Steeg, P. S. *J. Bioenerg. Biomembr.* **2000**, *32*, 301.

(19) Klinker, J. F.; Seifert, R. *Eur. J. Biochem.* **1999**, *261*, 72.

(20) Cuello, F.; Schulze, R. A.; Heemeyer, F.; Meyer, H. E.; Lutz, S.; Jakobs, K. H.; Niroomand, F.; Wieland, T. *J. Biol. Chem.* **2003**, *278*, 7220.

(21) Hippe, H. J.; Lutz, S.; Cuello, F.; Knorr, K.; Vogt, A.; Jakobs, K. H.; Wieland, T.; Niroomand, F. *J. Biol. Chem.* **2003**, *278*, 7227.

(22) Cai, X.; Srivastava, S.; Surindran, S.; Li, Z.; Skolnik, E. Y. *Mol. Biol. Cell* **2014**, *25*, 1244.

(23) Srivastava, S.; Li, Z.; Ko, K.; Choudhury, P.; Albaqumi, M.; Johnson, A. K.; Yan, Y.; Backer, J. M.; Unutmaz, D.; Coetzee, W. A.; Skolnik, E. Y. *Mol. Cell* **2006**, *24*, 665.

(24) Srivastava, S.; Panda, S.; Li, Z.; Fuhs, S. R.; Hunter, T.; Thiele, D. J.; Hubbard, S. R.; Skolnik, E. Y. *eLife* **2016**, *5*.

(25) Smith, D. L.; Bruegger, B. B.; Halpern, R. M.; Smith, R. A. *Nature* **1973**, *246*, 103.

(26) Chen, C. C.; Smith, D. L.; Bruegger, B. B.; Halpern, R. M.; Smith, R. A. *Biochemistry* **1974**, *13*, 3785.

(27) Chen, C. C.; Bruegger, B. B.; Kern, C. W.; Lin, Y. C.; Halpern, R. M.; Smith, R. A. *Biochemistry* **1977**, *16*, 4852.

(28) Tan, E. L.; Besant, P. G.; Zu, X. L.; Turck, C. W.; Bogoyevitch, M. A.; Lim, S. G.; Attwood, P. V.; Yeoh, G. C. *Carcinogenesis* **2004**, *25*, 2083.

(29) Kowluru, A. *Biochem. Pharmacol.* **2002**, *63*, 2091.

(30) Kowluru, A. *Am. J. Physiol. Endocrinol. Metabol.* **2003**, *285*, 498.

(31) Besant, P. G.; Attwood, P. V. *Int. J. Biochem. Cell Biol.* **2000**, *32*, 243.

(32) Smith, D. L.; Chen, C. C.; Bruegger, B. B.; Holtz, S. L.; Halpern, R. M.; Smith, R. A. *Biochemistry* **1974**, *13*, 3780.

(33) Fujitaki, J. M.; Fung, G.; Oh, E. Y.; Smith, R. A. *Biochemistry* **1981**, *20*, 3658.

(34) Ek, P.; Pettersson, G.; Ek, B.; Gong, F.; Li, J. P.; Zetterqvist, O. *Eur. J. Biochem.* **2002**, *269*, 5016.

(35) Klumpp, S.; Bechmann, G.; Maurer, A.; Selke, D.; Krieglstein, J. *Biochem. Biophys. Res. Commun.* **2003**, *306*, 110.

(36) Srivastava, S.; Zhdanova, O.; Di, L.; Li, Z.; Albaqumi, M.; Wulff, H.; Skolnik, E. Y. *Proc. Natl. Acad. Sci. U.S.A.* **2008**, *105*, 14442.

(37) Xu, A.; Hao, J.; Zhang, Z.; Tian, T.; Jiang, S.; Hao, J.; Liu, C.; Huang, L.; Xiao, X.; He, D. *Lung Cancer* **2010**, *67*, 48.

(38) Busam, R. D.; Thorsell, A.-G.; Flores, A.; Hammarstrom, M.; Persson, C.; Hallberg, B. M. *J. Biol. Chem.* **2006**, *281*, 33830.

(39) Ma, R. X.; Kanders, E.; Sundh, U. B.; Geng, M. Y.; Ek, P.; Zetterqvist, O.; Li, J. P. *Biochem. Biophys. Res. Commun.* **2005**, *337*, 887.

(40) Hiraishi, H.; Yokoi, F.; Kumon, A. *Arch. Biochem. Biophys.* **1998**, *349*, 381.

(41) Hiraishi, H.; Yokoi, F.; Kumon, A. *J. Biochem.* **1999**, *126*, 368.

(42) Matthews, H. R.; Pesis, K.; Kim, Y. K. *FASEB J.* **1995**, *9*, A1347.

(43) Kim, Y. H.; Huang, J. M.; Cohen, P.; Matthews, H. R. *J. Biol. Chem.* **1993**, *268*, 18513.

(44) Back, S. H.; Adapala, N. S.; Barbe, M. F.; Carpino, N. C.; Tsygankov, A. Y.; Sanjay, A. *Cell. Mol. Life Sci.* **2013**, *70*, 1269.

(45) Thomas, D. H.; Getz, T. M.; Newman, T. N.; Dangelmaier, C. A.; Carpino, N.; Kunapuli, S. P.; Tsygankov, A. Y.; Daniel, J. L. *Blood* **2010**, *116*, 2570.

(46) Panda, S.; Srivastava, S.; Li, Z.; Vaeth, M.; Fuhs, S. R.; Hunter, T.; Skolnik, E. Y. *Mol. Cell* **2016**, *63*, 457.

(47) Wong, C.; Faiola, B.; Wu, W.; Kennelly, P. J. *Biochem. J.* **1993**, *296*, 293.

(48) Ohmori, H.; Kuba, M.; Kumon, A. *J. Biochem.* **1994**, *116*, 380.

(49) Matthews, H. R.; Mackintosh, C. *FEBS Lett.* **1995**, *364*, 51.

(50) Motojima, K.; Goto, S. *J. Biol. Chem.* **1994**, *269*, 9030.

(51) Matthews, H. R. *Pharmacol. Ther.* **1995**, *67*, 323.

(52) Wieland, T.; Nurnberg, B.; Ulibarri, I.; Kaldenbergstasch, S.; Schultz, G.; Jakobs, K. H. *J. Biol. Chem.* **1993**, *268*, 18111.

(53) Hippe, H.-J.; Wolf, N. M.; Abu-Taha, I.; Mehringer, R.; Just, S.; Lutz, S.; Niroomand, F.; Postel, E. H.; Katus, H. A.; Rottbauer, W.; Wieland, T. *Proc. Natl. Acad. Sci. U.S.A.* **2009**, *106*, 16269.

(54) Srivastava, S.; Choudhury, P.; Li, Z.; Liu, G. X.; Nadkarni, V.; Ko, K.; Coetzee, W. A.; Skolnik, E. Y. *Mol. Biol. Cell* **2006**, *17*, 146.

(55) Rose, Z. B. *Arch. Biochem. Biophys.* **1970**, *140*, 508.

(56) Han, C. H.; Rose, Z. B. *J. Biol. Chem.* **1979**, *254*, 8836.

(57) Rose, Z. B. *Adv. Enzymol. Relat. Areas Mol. Biol.* **1980**, *51*, 211.

(58) Heiden, M. G. V.; Locasale, J. W.; Swanson, K. D.; Sharfi, H.; Heffron, G. J.; Amador-Noguez, D.; Christofk, H. R.; Wagner, G.; Rabinowitz, J. D.; Asara, J. M.; Cantley, L. C. *Science* **2010**, *329*, 1492.

(59) Crovello, C. S.; Furie, B. C.; Furie, B. *Cell* **1995**, *82*, 279.

(60) Muimo, R.; Hornickova, Z.; Riemen, C. E.; Gerke, V.; Matthews, H.; Mehta, A. *J. Biol. Chem.* **2000**, *275*, 36632.

(61) Fraczyk, T.; Ruman, T.; Rut, D.; Dabrowska-Mas, E.; Ciesla, J.; Zielinski, Z.; Sieczka, K.; Debski, J.; Golos, B.; Winska, P.; Walajtys-Rode, E.; Shugar, D.; Rode, W. *Pteridines* **2009**, *20*, 137.

(62) Ghosh, A.; Shieh, J. J.; Pan, C. J.; Sun, M. S.; Chou, J. Y. *J. Biol. Chem.* **2002**, *277*, 32837.

(63) Ghosh, A.; Shieh, J. J.; Pan, C. J.; Chou, J. Y. *J. Biol. Chem.* **2004**, *279*, 12479.

(64) Burgos, E. S.; Ho, M.-C.; Almo, S. C.; Schramm, V. L. *Proc. Natl. Acad. Sci. U.S.A.* **2009**, *106*, 13748.

(65) Ostrowski, W. *Biochim. Biophys. Acta* **1978**, *526*, 147.

(66) Muniyan, S.; Chaturvedi, N. K.; Dwyer, J. G.; LaGrange, C. A.; Chaney, W. G.; Lin, M.-F. *IJMS* **2013**, *14*, 10438.

(67) Hultquist, D. E.; Moyer, R. W.; Boyer, P. D. *Biochemistry* **1966**, *5*, 322.

(68) Hultquist, D. E. *Biochim. Biophys. Acta* **1968**, *153*, 329.

(69) Attwood, P. V.; Piggott, M. J.; Zu, X. L.; Besant, P. G. *Amino Acids* **2007**, *32*, 145.

(70) Gassner, M.; Stehlik, D.; Schrecker, O.; Hengstenberg, W.; Maurer, W.; Ruterjans, H. *Eur. J. Biochem.* **1977**, *75*, 287.

(71) Lecroisey, A.; Lascu, I.; Bominaar, A.; Veron, M.; Delepierre, M. *Biochemistry* **1995**, *34*, 12445.

(72) Wolodko, W. T.; Fraser, M. E.; James, M. N. G.; Bridger, W. A. *J. Biol. Chem.* **1994**, *269*, 10883.

(73) Cherfils, J.; Morera, S.; Lascu, I.; Veron, M.; Janin, J. *Biochemistry* **1994**, *33*, 9062.

(74) Morera, S.; Lascu, I.; Dumas, C.; Lebras, G.; Briozzo, P.; Veron, M.; Janin, J. *Biochemistry* **1994**, *33*, 459.

(75) Roberts, J. D.; Yu, C.; Flanagan, C.; Birdseye, T. R. *J. Am. Chem. Soc.* **1982**, *104*, 3945.

(76) Gonzalez-Sanchez, M.-B.; Lanucara, F.; Helm, M.; Eyers, Claire E. *Biochem. Soc. Trans.* **2013**, *41*, 1089.

(77) Fuhs, S. R.; Meisenhelder, J.; Aslanian, A.; Ma, L.; Zagorska, A.; Stankova, M.; Binnie, A.; Al-Obeidi, F.; Mauger, J.; Lemke, G.; Yates, J. R., 3rd; Hunter, T. *Cell* **2015**, *162*, 198.

(78) Fuhs, S. R.; Hunter, T. *Curr. Opin. Cell Biol.* **2017**, *45*, 8.

(79) Kee, J.-M.; Muir, T. W. *ACS Chem. Biol.* **2012**, *7*, 44.

(80) Kee, J. M.; Oslund, R. C.; Perlman, D. H.; Muir, T. W. *Nat. Chem. Biol.* **2013**, *9*, 416.

(81) Williams, S. P.; Sykes, B. D.; Bridger, W. A. *Biochemistry* **1985**, *24*, 5527.

(82) Walinder, O. *J. Biol. Chem.* **1968**, *243*, 3947.

(83) Mardh, S.; Ljungstorm, O.; Hogstedt, S.; Zetterqvist, O. *Biochim. Biophys. Acta* **1971**, *251*, 419.

(84) Jencks, W. P.; Gilchris.M *J. Am. Chem. Soc.* **1965**, *87*, 3199.

(85) Duclos, B.; Marcandier, S.; Cozzone, A. J. *Methods Enzymol.* **1991**, *201*, 10.

(86) Besant, P. G.; Attwood, P. V. *Mol. Cell. Biochem.* **2009**, *329*, 93.

(87) Huebner, V. D.; Matthews, H. R. *J. Biol. Chem.* **1985**, *260*, 6106.

(88) Lapek, J. D., Jr.; Tombline, G.; Kellersberger, K. A.; Friedman, M. R.; Friedman, A. E. *Naunyn-Schmiedeberg's Arch. Pharmacol.* **2015**, *388*, 161.

(89) Kleinnijenhuis, A. J.; Kjeldsen, F.; Kallipolitis, B.; Haselmann, K. F.; Jensen, O. N. *Anal. Chem.* **2007**, *79*, 7450.

(90) Hardman, G.; Perkins, S.; Ruan, Z.; Kannan, N.; Brownridge, P.; Byrne, D. P.; Eyers, P. A.; Jones, A. R.; Eyers, C. E. *bioRxiv* **2017**.

(91) Oslund, R. C.; Kee, J.-M.; Couvillon, A. D.; Bhatia, V. N.; Perlman, D. H.; Muir, T. W. *J. Am. Chem. Soc.* **2014**, *136*, 12899.

(92) Gonzalez-Sanchez, M.-B.; Lanucara, F.; Hardman, G. E.; Eyers, C. E. *Int. J. Mass Spectrom.* **2014**, *367*, 28.

(93) Potel, C. M.; Lin, M.-H.; Heck, A. J. R.; Lemeer, S. *Nat. Methods* **2018**.

(94) Potel, C. M.; Lin, M.-H.; Prust, N.; van den Toorn, H. W. P.; Heck, A. J. R.; Lemeer, S. *Anal. Chem.* **2019**, *91*, 5542.

(95) Fíla, J.; Honys, D. *Amino Acids* **2012**, *43*, 1025.

(96) Reinders, J.; Sickmann, A. *Proteomics* **2005**, *5*, 4052.

(97) Napper, S.; Kindrachuk, J.; Olson, D. J. H.; Ambrose, S. J.; Dereniwsky, C.; Ross, A. R. S. *Anal. Chem.* **2003**, *75*, 1741.

(98) Druker, B. J. *Oncologist* **2004**, *9*, 357.

(99) Cohen, P. *Nat. Rev. Drug Discov.* **2002**, *1*, 309.

(100) Hunter, T. *Curr. Opin. Cell Biol.* **2009**, *21*, 140.

(101) Kaufmann, H.; Bailey, J. E.; Fussenegger, M. *Proteomics* **2001**, *1*, 194.

(102) Pandey, A.; Podtelejnikov, A. V.; Blagoev, B.; Bustelo, X. R.; Mann, M.; Lodish, H. F. *Proc. Natl. Acad. Sci. U.S.A.* **2000**, *97*, 179.

(103) Pirrung, M. C.; James, K. D.; Rana, V. S. *J. Org. Chem.* **2000**, *65*, 8448.

(104) Allen, J. J.; Li, M.; Brinkworth, C. S.; Paulson, J. L.; Wang, D.; Hubner, A.; Chou, W.-H.; Davis, R. J.; Burlingame, A. L.; Messing, R. O.; Katayama, C. D.; Hedrick, S. M.; Shokat, K. M. *Nat. Methods* **2007**, *4*, 511.

(105) Carlson, H. K.; Plate, L.; Price, M. S.; Allen, J. J.; Shokat, K. M.; Marletta, M. A. *Anal. Biochem.* **2010**, *397*, 139.

(106) Pirrung, M. C.; Pei, T.; Drabik, S. J.; Gothelf, K. V. *Abstr. Pap. Am. Chem. S.* **1999**, *218*, U139.

(107) Schenkels, C.; Erni, B.; Reymond, J. L. *Bioorg. Med. Chem. Lett.* **1999**, *9*, 1443.

(108) Schenkels, C. PhD Thesis, University of Bern, 2001.

(109) Lilley, M.; Mambwe, B.; Jackson, R. F. W.; Muimo, R. *Chem. Commun.* **2014**, *50*, 9343.

(110) Kee, J.-M.; Villani, B.; Carpenter, L. R.; Muir, T. W. *J. Am. Chem. Soc.* **2010**, *132*, 14327.

(111) Kee, J.-M.; Oslund, R. C.; Couvillon, A. D.; Muir, T. W. *Org. Lett.* **2015**, *17*, 187.

(112) Frackelton, A. R.; Posner, M.; Kannan, B.; Mermelstein, F. *Methods Enzymol.* **1991**, *201*, 79.

(113) Frackelton, A. R.; Ross, A. H.; Eisen, H. N. *Mol. Cell. Biol.* **1983**, *3*, 1343.

(114) Behrendt, R.; White, P.; Offer, J. *J. Pept. Sci.* **2016**, *22*, 4.

(115) McAllister, T. E.; Webb, M. E. *Org. Biomol. Chem.* **2012**, *10*, 4043.

(116) McAllister, T. E.; Horner, K. A.; Webb, M. E. *ChemBioChem* **2014**, *15*, 1088.

(117) Senderowicz, L.; Wang, J. X.; Wang, L. Y.; Yoshizawa, S.; Kavanaugh, W. M.; Turck, C. W. *Biochemistry* **1997**, *36*, 10538.

(118) Vliet, B. V. PhD Thesis, Technical University of Dortmund, 2012.

(119) Eerland, M. F.; Hedberg, C. *J. Org. Chem.* **2012**, *77*, 2047.

(120) Tabanella, S.; Valancogne, I.; Jackson, R. F. W. *Org. Biomol. Chem.* **2003**, *1*, 4254.

(121) Eerland, M. PhD Thesis, Technical University of Dortmund, 2015.

(122) Lilley, M.; Mambwe, B.; Thompson, M. J.; Jackson, R. F. W.; Muimo, R. *Chem. Commun.* **2015**, *51*, 7305.

(123) Niesobski, P. “The Synthesis of Phosphopyrazolylethylamine ” The University of Sheffield, 2014.

(124) Naray-Szabo, G.; Ferenczy, G. G. *Chem. Rev.* **1995**, *95*, 829.

(125) Connolly, M. L. *J. Appl. Crystallogr.* **1983**, *16*, 548.

(126) Schwan, A. L. *Chem. Soc. Rev.* **2004**, *33*, 218.

(127) Kalek, M.; Ziadi, A.; Stawinski, J. *Org. Lett.* **2008**, *10*, 4637.

(128) Tran, G.; Gomez Pardo, D.; Tsuchiya, T.; Hillebrand, S.; Vors, J.-P.; Cossy, J. *Org. Lett.* **2013**, *15*, 5550.

(129) Birkholz, M.-N.; Freixa, Z.; van Leeuwen, P. W. N. M. *Chem. Soc. Rev.* **2009**, *38*, 1099.

(130) Krenk, O.; Kratochvil, J.; Spulak, M.; Buchta, V.; Kunes, J.; Novakova, L.; Ghavre, M.; Pour, M. *Eur. J. Org. Chem.* **2015**, *2015*, 5414.

(131) Rodriguez-Franco, M. I.; Dorronsoro, I.; Hernandez-Higueras, A. I.; Antequera, G. *Tetrahedron Lett.* **2001**, *42*, 863.

(132) Hartwig, S.; Nguyen, M. M.; Hecht, S. *Polym. Chem.* **2010**, *1*, 69.

(133) Singh, S. P.; Michaelides, A.; Merrill, A. R.; Schwan, A. L. *J. Org. Chem.* **2011**, *76*, 6825.

(134) Arnold, L. D.; May, R. G.; Vederas, J. C. *J. Am. Chem. Soc.* **1988**, *110*, 2237.

(135) Blauvelt, M. L.; Howell, A. R. *J. Org. Chem.* **2008**, *73*, 517.

(136) Sliedregt, K. M.; Schouten, A.; Kroon, J.; Liskamp, R. M. J. *Tetrahedron Lett.* **1996**, *37*, 4237.

(137) Barlos, K.; Papaioannou, D.; Theodoropoulos, D. *J. Org. Chem.* **1982**, *47*, 1324.

(138) Arnold, L. D.; Kalantar, T. H.; Vederas, J. C. *J. Am. Chem. Soc.* **1985**, *107*, 7105.

(139) Fletcher, A. R.; Jones, J. H.; Ramage, W. I.; Stachulski, A. V. *J. Chem. Soc., Perkin Trans. 1* **1979**, 2261.

(140) Attaryan, O. S.; Baltayan, A. O.; Badalyan, K. S.; Minasyan, G. G.; Matsoyan, S. G. *Russ. J. Gen. Chem.* **2006**, *76*, 1131.

(141) Jackson, R. F. W.; Perez-Gonzalez, M. *Org. Synth.* **2005**, *81*, 77.

(142) Liu, H.; Pattabiraman, V. R.; Vederas, J. C. *Org. Lett.* **2007**, *9*, 4211.

(143) Nicolaou, K. C.; Estrada, A. A.; Zak, M.; Lee, S. H.; Safina, B. S. *Angew. Chem., Int. Ed.* **2005**, *44*, 1378.

(144) Ouyang, H.; Fu, C.; Fu, S.; Ji, Z.; Sun, Y.; Deng, P.; Zhao, Y. *Org. Biomol. Chem.* **2016**, *14*, 1925.

(145) Dondoni, A.; Perrone, D. *Org. Synth.* **2000**, *77*, 64.

(146) Huo, S. Q. *Org. Lett.* **2003**, *5*, 423.

(147) Ross, A. J.; Lang, H. L.; Jackson, R. F. W. *J. Org. Chem.* **2010**, *75*, 245.

(148) Zon, J.; Videnova-Adrabinska, V.; Janczak, J.; Wilk, M.; Samoc, A.; Gancarz, R.; Samoc, M. *CrystEngComm* **2011**, *13*, 3474.

(149) Ritter, S.; Nordhoff, S.; Voss, F.; Wachten, S.; Oberboersch, S.; Gruenenthal GmbH, Germany . 2015, p 73pp.

(150) Bessmertnykh, A.; Douaihy, C. M.; Muniappan, S.; Guilard, R. *Synthesis-Stuttgart* **2008**, 1575.

(151) Mukai, S. PhD Thesis, The University of Western Australia, 2011.

(152) Wei, Y. F.; Matthews, H. R. *Methods Enzymol.* **1991**, *200*, 388.

(153) Besant, P. G.; Byrne, L.; Thomas, G.; Attwood, P. V. *Anal. Biochem.* **1998**, *258*, 372.

(154) Hermanson, G. T. *Bioconjugate Techniques, 2nd Edition*, 2008.

(155) Josephy, P. D.; Eling, T.; Mason, R. P. *J. Biol. Chem.* **1982**, *257*, 3669.

(156) Lichtner, R.; Wolf, H. U. *Biochem. J.* **1979**, *181*, 759.

(157) Sjobring, U.; Bjorck, L.; Kastern, W. *J. Biol. Chem.* **1991**, *266*, 399.

(158) Moeremans, M.; Daneels, G.; De Mey, J. *Anal. Biochem.* **1985**, *145*, 315.

(159) Amiard, G.; Heymes, R.; Velluz, L. *Bull. Soc. Chim. Fr.* **1955**, 191.

(160) Pu, Y.; Martin, F. M.; Vederas, J. C. *J. Org. Chem.* **1991**, *56*, 1280.

(161) Liu, F.; Thomas, J.; Burke, T. R., Jr. *Synthesis* **2008**, 2432.

(162) Foley, D.; Pieri, M.; Pettecrew, R.; Price, R.; Miles, S.; Lam, H. K.; Bailey, P.; Meredith, D. *Org. Biomol. Chem.* **2009**, *7*, 3652.

(163) Luescher, M. U.; Vo, C.-V. T.; Bode, J. W. *Org. Lett.* **2014**, *16*, 1236.

7: Appendix

Sep 26, 2019

This Agreement between University of Sheffield -- Mehul Makwana ("You") and Elsevier ("Elsevier") consists of your license details and the conditions provided by Elsevier and Copyright Clearance Center.

License Number	4570950975354
License date	Apr 16, 2019
Licensed Content Publisher	Elsevier
Licensed Content Publication	Biochimica Biophysica (BBA) Bioenergetics
Licensed Content Title	The preparation and characterization of phosphorylated derivatives of histidine
Licensed Content Author	D.E. Hultquist
Licensed Content Date	Feb 12, 1968
Licensed Content Volume	153
Licensed Content Issue	2
Licensed Content Pages	12
Start Page	329
End Page	340
Type of Use	reuse in a thesis/dissertation
Portion	figures/tables/illustrations
Number of figures/tables /illustrations	1
Format	both print and electronic
Are you the author of this Elsevier article?	No
Will you be translating?	No
Original figure numbers	Fig 7
Title of your	New chemical tools in the study of phosphohistidine
Expected completion date	Apr
Estimated size (number of pages)	230
Requestor Location	University of 20 Canon Street Leice ter, LE4 6NG United Kingdom Attn: University of Sheffield
Publisher Tax ID	GB 494 6272 12
Total	0.00 GBP
Terms and Conditions	

INTRODUCTION

1. The publisher for this copyrighted material is Elsevier. By clicking "accept" in connection with completing this licensing transaction, you the following terms and conditions apply to this transaction (along with the Billing Payment terms and

http://myaccount.copyright.com).

2. Elsevier hereby grants you permission to reproduce the aforementioned material subject to the terms and conditions indicated.

3. Acknowledgement: If any part of the material be used (for example, figures) has appeared in our publication with credit or acknowledgement to another source, permission must also be sought from that source. If such permission is obtained then that material may not be included in your publication/copies. Suitable acknowledgement to the source must be made, either as a footnote or in reference list at the end of your publication, as follows:

"Reprinted from Publication title, Vol /edition number, Author(s), Title of article / title of chapter, Pages No., Copyright (Year), with permission from Elsevier [OR APPLICABLE SOCIETY COPYRIGHT OWNER]." Also Lancet special credit - "Reprinted from The

permission is hereby given.

5. Altering/Modifying Material: Not Permitted. However figures and illustrations may be

Ltd. (Please contact Elsevier at permissions@elsevier.com). No modifications can be made

6. If the permission fee for the requested use of our material is waived in this instance, please be advised that your future requests for Elsevier materials may attract a fee.

7. Reservation of Rights: Publisher reserves all rights not specifically granted in the combination of (i) the license details provided by you and accepted in the course of this licensing transaction, (ii) these terms and conditions and (iii) CCC's Billing and Payment terms and conditions.

8. License Contingent Upon Payment: While you may exercise the rights licensed immediately upon issuance of the license the end of the licensing process for the transaction, provided that you have disclosed complete and details of your proposed

by publisher or by CCC) as provided in CCC's Billing and Payment terms and conditions. If full payment is not received on a timely basis, then any license preliminarily granted shall be deemed automatically revoked and shall be void as if never granted. Further, in the event

terms and conditions, the license is automatically revoked and be void as if never

and publisher reserves the right to take any all action to protect its copyright in the materials.

material.

pursuant to this license.

12. No Amendment Except in Writing: This license may not be amended except in a writing signed by both parties (or, in the case of publisher, by CCC on publisher's behalf).
13. Objection to Contrary Terms: Publisher hereby objects to any terms contained in any purchase order, acknowledgment, check endorsement or other writing prepared by you, which terms are inconsistent with these terms and conditions or CCC's Billing and Payment terms and conditions. These terms and conditions, together with CCC's Billing and Payment

shall control.

to you. Notice of such denial will be made using the contact information provided by you.

permissions.

LIMITED LICENSE

The following terms and conditions apply only to specific license types:
15. **Translation**: This permission is granted for non-exclusive world **English** rights only

16. **Posting licensed content on any Website**: The following terms and conditions apply as

http://www.sciencedirect.com/science/journal/xxxxx or the Elsevier homepage for books at http://www.elsevier.com; Central Storage: This license does not include permission for a

Heron/XanEdu.

homepage at http://www.elsevier.com . All content posted to the web site must maintain the

licensed content on **reserve**: In addition to the above the following

17. **For journal** the following clauses are applicable in addition to the above:
Preprints:

If accepted for publication, we encourage authors to link from the preprint to their formal publication via its DOI. Millions of researchers have access formal publications on ScienceDirect, and so links will help users to find, access, cite use the best available

preprint policies. Information on these policies is available the journal homepage.
Accepted Author Manuscripts: An accepted author manuscript is the manuscript of an article that has been accepted for publication and which typically includes author incorporated changes suggested during submission, peer review and editor-author communications.
Authors can share their accepted author manuscript·

- immediately
  - via their no
  - by updating a preprint in arXiv or RePEc with the accepted manuscript
  - directly by providing copies to their students or to research collaborators for their personal use
  - for private scholarly sharing as part of an invitation-only work group on commercial sites with which Elsevier has an agreement
- After the embargo period

In all cases accepted manuscripts should:

-
- bear a CC-BY NC-ND license - this is easy to do
- if aggregated with other manuscripts, for example in a repository or other site, be shared in alignment with our hosting policy not be to or enhanced in any way to appear more like, or to substitute for, the published journal article.

Published journal article (JPA): A published journal article (PJA) is the definitive final record of published research that appears or will appear in the journal and embodies all value-adding publishing activities including peer review co ordination, copy editing, formatting, (if relevant) pagination and online enrichment.
Policies for sharing publishing journal articles differ for subscription and gold open access articles:
Subscription Articles:
full-text. Millions of re
and so links will help your users to find, access, cite, and use the best available version.
Theses and dissertations which contain embedded PJAs as part of the formal submission can be posted publicly by the awarding institution with DOI links back to the formal publications on ScienceDirect.

license and should contain a CrossMark logo, the end user license, and a DOI link to the formal publication on ScienceDirect.
Please refer to Elsevier's posting policy for further information.
18. **For book authors** the following clauses are applicable in addition to the above:

If accepted for publication, we encourage authors to link from the preprint to their formal publication via its DOI. Millions of researchers have access formal publications on ScienceDirect, and so links will help users to find, access, cite use the best available

preprint policies. Information on these policies is available the journal homepage.
Accepted Author Manuscripts: An accepted author manuscript is the manuscript of an article that has been accepted for publication and which typically includes author incorporated changes suggested during submission, peer review and editor-author communications.
Authors can share their accepted author manuscript·

- immediately
  - via their no
  - by updating a preprint in arXiv or RePEc with the accepted manuscript
  - directly by providing copies to their students or to research collaborators for their personal use
  - for private scholarly sharing as part of an invitation-only work group on commercial sites with which Elsevier has an agreement
- After the embargo period

In all cases accepted manuscripts should:

- bear a CC-BY NC-ND license - this is easy to do
- if aggregated with other manuscripts, for example in a repository or other site, be shared in alignment with our hosting policy not be to or enhanced in any way to appear more like, or to substitute for, the published journal article.

Published journal article (JPA): A published journal article (PJA) is the definitive final record of published research that appears or will appear in the journal and embodies all value-adding publishing activities including peer review co ordination, copy editing, formatting, (if relevant) pagination and online enrichment.
Policies for sharing publishing journal articles differ for subscription and gold open access articles:
Subscription Articles:
full-text. Millions of re
and so links will help your users to find, access, cite, and use the best available version.
Theses and dissertations which contain embedded PJAs as part of the formal submission can be posted publicly by the awarding institution with DOI links back to the formal publications on ScienceDirect.

license and should contain a CrossMark logo, the end user license, and a DOI link to the formal publication on ScienceDirect.
Please refer to Elsevier's posting policy for further information.
18. **For book authors** the following clauses are applicable in addition to the above:

allowed to download and post the published electronic version of your chapter, nor may you scan the printed edition to create an electronic version. **Posting to a repository:** Authors are

19. **Thesis/Dissertation**: If your license is for use in a thesis/dissertation your thesis may be

Terms and Conditions

Commons user license. See our open access license policy for more information.
Terms & Conditions applicable to all Open Access articles published with Elsevier:

If any part of the material to be used (for example, figures) has appeared in our publication

Additional Terms & Conditions applicable to each Creative Commons user license:

available at http://creativecommons.org/licenses/by/4.0.
CC BY SA: The CC BY-NC SA license allows users to copy, to create extracts,

details of the license are available at http://creativecommons.org/licenses/by-nc-sa/4.0.
CC BY NC The CC BY-NC-ND license allows users to copy and distribute the Article,

full details of the license are available at http://creativecommons.org/licenses/by-nc-nd/4.0.

Commercial reuse includes:

- Associating advertising with the full text of the Article
- Charging fees for
- Article aggregation
- Systematic distribution via e mail lists or share buttons

Posting or linking by commercial companies for use by customers of those companies.

v1.9

customercare@copyright.com or (toll in the +1-978-646-2777.